In-depth immunological analysis of prototypic adjuvants for vaccine formulations

Dissertation

zur Erlangung des Grades

Doktor der Naturwissenschaften

am Fachbereich Biologie

der Johannes Gutenberg-Universität Mainz

Laura Roßmann

geb. am 21.02.1991 in Rüsselsheim am Main

Mainz, 2020

Dekan:

1. Berichterstatter:

2. Berichterstatter:

Tag der mündlichen Prüfung: 04.11.2020

Table of contents

List of figures

List of tables

Abbreviations

°C	Degree Celsius
µg	Microgram
µl	Microliter
µM	Micrometer
2B4	CD244
ADX	Addavax
AE	Adverse event
Al(OH)3	Aluminium hydroxide
APC	Antigen presenting cell
AS01/04	Adjuvant system 01/04
BCG	Bacillus Calmette–Guérin
BCR	B cell receptor
CAF01	cationic liposome vehicle including TDB
CCR7	C-C chemokine receptor type 7
CD	Cluster of differentiation
cDC	conventional DC
CFSE	Carboxyfluorescein succinimidyl ester
CMV	Cytomegalovirus
DAMP	Danger associated molecular pattern
DC	Dendritic cell
DNA	Deoxyribonucleic acid
ELISA	Enzyme-linked immunosorbent assay
EU/ml	Euopean Units/ milliliter
FACS	Fluorescence activated cell sorting
FasL	Fas ligand
FCS	Fetal calf serum
FDR	False discovery rate
FluM1	Influenza matrix protein 1
FSC	Forward scatter
g	Gram
g	Gravitational force
GARD	Gardiquimod
Geo. MFI	Geometric mean fluorescence intensity
G-CSF	Granulocyte colony-stimulating factor
GLA	Glucopyranosyl Lipid Adjuvant
GM-CSF	Granulocyte macrophage colony-stimulating factor
h	hour
HBV	Hepatitis B virus
HEPES	4-(2-hydroxyethyl)-1-piperazineethanesulfonic acid)
HIV	Human immunodeficieny virus
HLA	Human leukocyte antigen
HLA-DR	Human Leukocyte Antigen – DR isotype
HPV	Human papillomavirus
ICAM	Intracellular adhesion molecule

iDC	immature DC
IFN	Interferon
IgG/ IgM	Immunoglobulin G/ M
IkB	Inhibitor of κB
IL-	Interleukin
IMQ	Imiquimod (R837)
IP-10	Interferon gamma-induced protein 10; CXCL10
kDA	Kilo Dalton
LAG-3	Lymphocyte-activation gene 3, CD223
LAV	Live-attenuated vaccine
LCMV	*lymphocytic choriomeningitis mammarenavirus*
LPS	Lipopolysaccharide
MACS	Magnetic activated cell sorting
MAT	Monocyte activation test
MCP-1	Monocyte chemotactic protein-1; CCL2
MF59	Oil-in-water emulsion adjuvant
mg	Milligram
MHC	Major histocompatibility complex
MIG	Monokine induced by gamma interferon; CXCL9
min	Minute
min/ max	Minimum/ maximum
ml	Milliliter
MoA	Mode of action
moDC	monocyte-derived DC
MPL	Monophosphoryl lipid A
MPL-s	synthetic monophosphoryl lipid A
MPL-SM	Monophosphoryl lipid A derived from Salmonella minnesota R595
MyD88	Myeloid differentiation primary response 88
n	Number of donors
NFkB	Nuclear factor 'kappa-light-chain-enhancer' of activated B-cells
ng	Nanogram
NK cell	Natural killer cell
NKT cell	Natural killer T cell
NOD	Nucleotide-binding oligomerization domain
Pam	Pam3CSK4
PAMP	Pattern associated molecular pattern
PBL	Peripheral blood lymphocyte
PBMC	Peripheral blood mononuclear cells
PBS	Phosphate buffered saline
PCA	Principal component analysisi
pDC	plasmacytoid DC
PD-L1	Programmed death ligand 1
PFA	Paraformaldehyde
PHA	Phytohemagglutinin
PI	Propidium iodid
PRR	Pattern recognition receptor

PSM	Phenol-soluble modulin
QS-21	Saponin adjuvant; purified fraction of the tree *Quillaja saponaria*
Quil	Quil-A
R848	Resiquimod
RIG-I	Retinoic acid-inducible gene I
RESTORE	Resetting T cells to original reactivity
RNA	Ribonucleic acid
RT	Room temperature (22°C)
SAE	Serious adverse event
SCC	Side scatter
SCF	Stem cell factor
SD	Standard deviation
SDS-PAGE	Sodium dodecyl sulfate polyacrylamide gel electrophoresis
SNP	Single nucleotide polymorphism
TCM	Central memory T cell
TCR	T cell receptor
TDB	Trehalose-6,6-dibehenate
TEM	Effector memory T cell
TFH	T follicular helper cell
TFH	Follicular T helper cell
Th cell	T helper cell
TIMP	Tissue inhibitor of metalloproteinases
TLR	Toll-like receptor
TNF	Tumor necrosis factor
TRIF	Toll/IL-1R domain-containing adaptor molecule 1
TRM	Resident memory T cell
TT	Tetanus toxoid
v/v	volume per volume
w/v	weight per volume
WBA	Whole blood assay
WHO	World Health Organization
XCL	Chemokine ligand
XCR	Chemokine receptor

1 Summary

Vaccine adjuvants have the potential to initiate, amplify and shape the immune response against the vaccine antigen depending on their inherent mode of action (MoA). Thus, the appropriate selection of the adjuvant is of pivotal importance for vaccine efficacy. In order to control newly emerging or existing pathogens such as SARS-CoV-2, HIV or *M. tuberculosis,* effective adjuvants eliciting a specific immune response will have a critical role within next generation vaccine formulations. However, even for the best-known adjuvants, such as aluminium hydroxide ($Al(OH)_3$), some aspects of their modes of action (MoAs) still remain elusive, making the corresponding immune response difficult to predict.

In this study, we systematically assessed the adjuvants' immunomodulatory MoAs on human monocyte-derived dendritic cells (DCs) and their effect on the arising adaptive immune response. To this end, we compared ten structurally and functionally different single component adjuvants in an *in vitro* human primary immune cell-based assay composed of DCs co-cultured with autologous peripheral blood lymphocytes (PBLs).

By investigating maturation markers and endocytosis capacity by flow cytometry, we observed that the adjuvants TDB, $Al(OH)_3$, AddaVax^{TM} and Quil-A exert only weak effects on DCs, whereas the other adjuvants tested induce a strong DC maturation. We further analyzed 25 secreted cytokines and chemokines from the DC:PBL culture supernatant using a Luminex multiplex assay and revealed adjuvant-specific protein patterns even for adjuvants targeting the same receptor. To assess the effect on the adaptive immune response, we examined the ability of the adjuvants to induce antigen-independent proliferation of PBLs co-cultured with the DCs. We found that Pam3CSK4, Gardiquimod, Resiquimod, and two variants of monophosphoryl lipid A (MPL-s and MPL-SM) induced antigen-independent proliferation of PBLs to varying degrees, with Resiquimod being the strongest stimulator. A detailed examination of B-, NK-, NKT-, $CD4^+$ and $CD8^+$ T cells within the proliferated PBL population demonstrated that each adjuvant promoted the proliferation of different lymphocyte subsets. When testing the adjuvants' immunostimulating potential in an antigen-specific context, we found that Pam3CSK4, MPL-s and $Al(OH)_3$ increased the proportion of FluM1-specific $CD8^+$ T cells significantly. These adjuvant-expanded T cells were still polyfunctional as determined by their secretion of pro-inflammatory cytokines as well as their degranulation upon re-stimulation with the FluM1 peptide.

Taken together, our results provide a comprehensive overview of the immunogenic effects of prototypic candidate or established adjuvants on primary human immune cells. The detailed data obtained on their distinct immune signatures will contribute to facilitate the selection of suitable adjuvants for the development of tailored vaccines.

2 Zusammenfassung

Adjuvanzien sind den meisten Impfstoffen zugesetzt, um eine gerichtete Immunantwort gegen das Antigen anzuregen, zu verbreiten und zu formen. Jedes Adjuvans besitzt hierfür eine spezifische Wirkweise. Deshalb ist die Wahl des Adjuvans von größter Bedeutung für die Wirksamkeit des Impfstoffs. Besonders in Impfstoffen der nächsten Generation werden neuartige oder kombinierte Adjuvanzien eine wichtige Rolle spielen, denn die Bekämpfung neu auftretender und bereits existierender Pathogene, wie SARS-CoV-2, HIV oder *M. tuberculosis* erfordern eine effektive Immunantwort. Jedoch ist die Wirkweise von sogar langjährig bekannten Adjuvanzien, wie Aluminiumhydroxid ($Al(OH)_3$), bisher noch nicht vollständig aufgedeckt, weshalb die Vorhersage der entstehenden Immunantwort schwierig ist.

In dieser Studie untersuchten wir die immunmodulatorische Wirkweise der Adjuvanzien auf humane dendritischen Zellen (DCs) und die daraus resultierenden Folgen für die aufkommende adaptive Immunantwort. Zu diesem Zweck verglichen wir zehn strukturell und funktional unterschiedliche Adjuvanzien in einem *in vitro* Assay, welcher auf humanen primären Immunzellen basiert. Diese setzen sich aus einer Kokultur, bestehend aus DCs und autologen peripheren Blutlymphozyten (PBLs) zusammen.

Bei der Analyse von Reifungs-Markern und der Endozytosekapazität von DCs mittels Durchflusszytometrie beobachteten wir, dass die Adjuvanzien TDB, AddaVax und Quil-A nur geringe Auswirkungen auf DCs zeigten, während die anderen Adjuvanzien eine starke DC-Reifung erzeugten. Mithilfe der Luminex-Techologie maßen wir 25 sekretierte Zytokine und Chemokine im Überstand der DC:PBL Kultur und konnten somit Adjuvans-spezifische Proteinmuster auch für solche Adjuvanzien ermitteln, die an den gleichen Rezeptor binden. Weiterhin prüften wir die Auswirkung der Adjuvanzien auf die adaptive Immunantwort, indem wir die Antigen-unabhängige Zellproliferation der PBLs untersuchten. Wir fanden heraus, dass Pam3CSK4, Gardiquimod, Resiquimod, sowie zwei Varianten des Monophosphoryl Lipid A (MPL-s and MPL-SM) die Zellproliferation der PBLs in unterschiedlichem Ausmaß induzierten. Die Identifikation von B-, NK-, NKT-, $CD4^+$ und $CD8^+$ T-Zellen innerhalb der proliferierenden Population ergab, dass jedes Adjuvans unterschiedliche Zellpopulationen aktiviert. In einer folgenden, Antigen-spezifischen Versuchsreihe erhöhten Pam3CSK4, MPL-s und $Al(OH)_3$ den Anteil der FluM1-spezifischen $CD8^+$ T-Zellen signifikant. Diese Antigen-spezifischen T-Zellen demonstrierten auch nach erneuter Stimulation, ihre gerichtete Polyfunktionalität als Antwort auf das FluM1-Peptid mittels Degranulation und Zytokinsekretion.

Zusammenfassend bieten diese Ergebnisse einen umfangreichen und detaillierten Überblick über die immunogene Wirkung von prototypischen und etablierten Adjuvanzien auf primäre humane Immunzellen. Die Erkenntnisse zu den individuellen Immunsignaturen der

Adjuvanzien werden zu einer erleichterten Wahl des geeigneten Adjuvans für die Entwicklung eines maßgeschneiderten Impfstoffs beitragen.

3 Introduction

3.1 Vaccination

Vaccination is the most fundamental achievement of the past century to mitigate human mortality and morbidity. Many infectious diseases such as smallpox, measles and polio could be controlled or even eradicated in industrialized countries with an effective vaccination campaign (Fenner et al., 1988; Aylward and Tangermann, 2011; Holzmann et al., 2016). The term of vaccination was first defined by Edward Jenner in 1769. His demonstration that the inoculation of cowpox protected the recipient against the fatal disease smallpox, remains the underlying basis of vaccination until today (Murphy and Weaver, 2017, p. 1). The overall goal of vaccination is the generation of a protective immune response against the pathogen without arousing a disease outbreak from the vaccine itself. Therefore, traditional prophylactic vaccines are based on the principles of attenuation or inactivation of the pathogen against which an immune response should be generated. Empirically, live-attenuated vaccines (LAV) rely on a reduced pathogenicity to the human host, which is acquired by adapting the pathogen to several non-human cell lines through repeated passaging. The process of adaptation to different hosts led to mutated clones, which are still able to replicate, but have a weak virulence and thus will cause no or only a mild disease in humans (Plotkin, 2014; Mort et al., 2020, Module 2: Types of vaccines and adverse reactions). LAV simulate a natural infection with consistence antigenic stimulation, leading to a protective memory cell generation of the humoral and cellular immune response. Although LAVs provide long-term protection, they bear several safety and stability concerns such as the reversion of the pathogen to its pathogenic form, the inability of immunocompromised persons to control the pathogen, contamination of cell cultures during production or sensitivity to wrong storage and reconstitution. This all led to the unattractiveness of LAVs for prophylactic vaccination (Vetter et al., 2018; Mort et al., 2020, Module 2: Types of vaccines and adverse reactions). The class of inactivated vaccines harbors different design approaches: Whole pathogen vaccines use inactivation methods such as fixation, heat and radiation to make the pathogen replication-incapable (Plotkin, 2014; Sabbaghi et al., 2019). Inactivated vaccines have a better safety and stability record compared to LAVs but they require several immunizations at the beginning and possibly a booster immunization after several years to maintain protection. Split vaccines consist of pathogen fragments which were disrupted by detergent treatment (Soema et al., 2015). While split vaccines contain most of the pathogen’s proteins, toxoid vaccines comprise only the purified and by fixation inactivated toxoid of pathogens.

3.1.1 Design of modern subunit vaccines

The main idea driving the progress of vaccine development is the improvement of vaccine efficacy while reducing potential risks and vaccine-related adverse events. The latter is of special importance due to the fact that prophylactic vaccination is mainly given to healthy and young people (Di Pasquale et al., 2015). Safety concerns, including the reversion of a low-virulent pathogen mutant into the wildtype strain, potential infection of immunocompromised persons as well as the incomplete inactivation of the pathogen paired with the disillusion that approaches of attenuation or inactivation could be employed for dangerous pathogens such as human immunodeficiency virus (HIV) (Whitney and Ruprecht, 2004), led to the development of so-called subunit vaccines, consisting of antigenic fragments of the pathogen and an immunostimulating compound, the adjuvant (**Figure 1**).

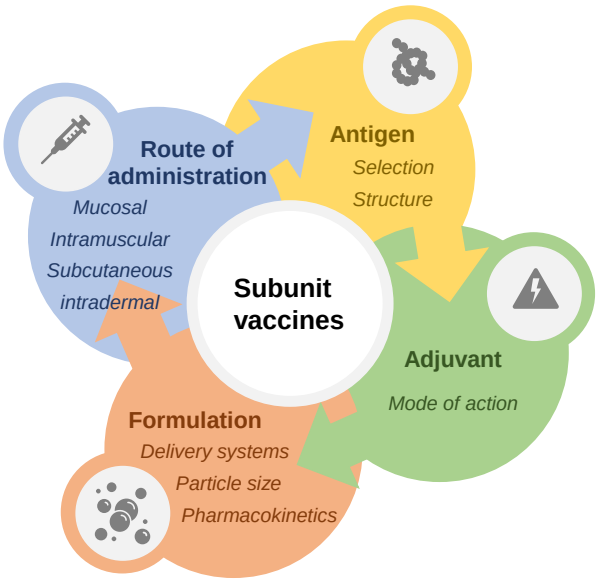

Figure 1: The rational design of subunit vaccines.
The aim of achieving a directed immune response to ensure long-term protection is dependent on the interplay of four categories: Antigen, adjuvant, formulation and the route of administration.

3.1.1.1 Antigen

Traditionally, vaccines were developed empirically following a standard procedure of pathogen isolation, its attenuation or inactivation and finally the immunization of the recipient (Rappuoli, 2014). Today, a new wave of technologies, such as genomics, high-throughput protein expression, B cell repertoire deep sequencing, proteomics, epitope mapping and structure-based antigen design have revolutionized the field of vaccine development (Rappuoli et al., 2016). The convergence of genetics, structural biology, immunology and computational approaches enabled “reverse vaccinology”. This term means that the use of the mentioned technologies accompanied by a deeper understanding starts with the prediction of a

pathogen's antigens rather than the pathogen's cultural growth conditions (Rappuoli, 2000). Recombinant technologies allowed for the first time the generation of antigens of pathogens that were unable to grow *in vitro* as well as the combination of antigens from several disease-causing strains in a single dose (Di Pasquale et al., 2015). Depending on the desired immune response, the *in silico* selection process of the candidate antigen considers that the antigen harbors B cell receptor (BCR) epitopes and peptide sequences which are recognized by the T cell receptor (TCR). The restriction of the immune response to defined antigenic regions accompanied by the exclusion of allergens, toxins and other stimulatory domains of the pathogens, reduces the potential reactogenicity of the vaccine (Rueckert and Guzmán, 2012).

3.1.1.2 Adjuvant

Although rationally designed purified antigens, recombinant proteins or peptides increase vaccine tolerability, they have low intrinsic immunogenicity compared to live-attenuated or inactivated vaccines. While pathogen-associated molecular patterns (PAMPs) in attenuated and inactivated vaccines are present to stimulate the innate immune system, subunit vaccines necessitate the combined application of the antigen with a potent immunostimulatory compound, an adjuvant. The term 'adjuvant' is derived from the latin word 'adjuvare', which means 'to help'. Adjuvants comprise a heterogenous group of compounds, some of them with intrinsic immunomodulatory activity, such as pattern recognition receptor (PRR) ligands, host-derived cytokines and chemokines, plant-derived substances as well as toxins, while others function as carrier protein for the antigen (Guy, 2007). The latter were earlier thought to act as passive antigen delivery system (Reed et al., 2009), generating a depot effect or increase the uptake of the antigen by antigen presenting cells (APCs). However, latest research has evaluated that they exert their adjuvant activity by triggering innate immune responses as well (Coffman et al., 2010). The modes of action (MoA) of adjuvants orchestrate the immune response and thus, adjuvants are the responsible key players for vaccine efficacy.

Alum was the first adjuvant employed in several vaccines from 1926 on and MF59 followed 70 years later. Although adjuvant investigation comprises decades with hundreds of described potent candidates, only a few adjuvants are included in licensed vaccines today: Beside $Al(OH)_3$ and MF59, there are the adjuvant system (AS) 04, consisting of $Al(OH)_3$ and monophosphoryl lipid A (MPL), AS03, a squalene-based oil-in-water emulsion adjuvant as well as liposomes (O'Hagan and Gregorio, 2009; O'Hagan et al., 2013). Failures in the manufacturing process, such as the negative impact on antigen stability or difficulties in large scale production as well as safety concerns due to adverse effects including short and long-term reactions prevented the further development. Especially the aspect of safety and the associated 'acceptable level of tolerability' is a challenging issue, which means that the benefit/

risk analysis for an adjuvant in a therapeutic vaccine is different to an adjuvant used in prophylactic vaccines applied to children (O'Hagan and Gregorio, 2009). To address the issue of safety, a detailed knowledge of the adjuvants' MoA is necessary to predict adjuvant effectiveness and estimate its reactogenicity. However, even the MoA of $Al(OH)_3$ has not been completely elucidated so far (Reed et al., 2013).

A new generation of adjuvants is needed since the few adjuvants being included in licensed vaccines do not induce a protective and sustained immune response against every pathogen of interest (Mbow et al., 2010). Furthermore, the potential of new generation adjuvants might also address several of the unmet needs in vaccine development (Coffman et al., 2010; Reed et al., 2013) (Figure 2). The first priority is an adjuvant-induced potent and protective T cell-mediated response to control intracellular pathogens such as *Mycobacterium tuberculosis* or *Plasmodium falciparum*. Furthermore, adjuvants mediating an antibody response broadening are necessary to react to pathogenic strain variations and evasion strategies (Reed et al., 2013). However, besides the demands on the immune response itself, there are further needs a new generation adjuvant can accomplish. As demonstrated in the current SARS-CoV-2 pandemic, vaccines which induce a fast protection against the virus are required. Adjuvants can have beneficial influence on the immunization regimen as demonstrated by the AS04-adjuvanted HBV vaccine Fendrix (GlaxoSmithKline, GSK), which reduced the vaccinations from three to two doses (Levie et al., 2002) and thus, ensured a quicker protection. Another point which is also especially highlighted during pandemics, is the sparing use of antigen per vaccine dose to cover the supply for the worldwide population. The large-scale production of recombinant proteins has an advantage over growing pathogens in culture, but the pairing with the appropriate adjuvant is essential for the reduction of antigen amount (Boyle et al., 2007; Banzhoff et al., 2009; Schwarz et al., 2009). And lastly, groups with increased risk of a severe course of the disease due to a weak immune function, including elderly, infants and immunocompromised persons are often unresponsive in inducing a protective immune response to vaccination, which in contrast stimulate an efficient immune response in healthy adults. The aim of the new-generation of adjuvants is, to overcome this reduced responsiveness. A higher antibody response against influenza was achieved in infants and elderly persons with an MF59 adjuvanted vaccines in contrast to a non-adjuvanted vaccine (Frey et al., 2014; Nolan et al., 2014).

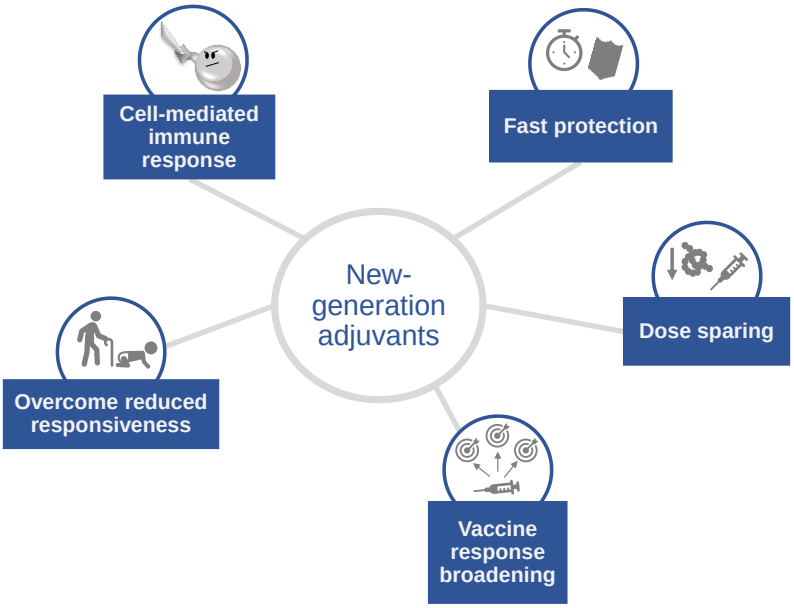

Figure 2: Unmet needs in vaccine development may be addressed by appropriate adjuvant selection.
New-generation adjuvants are aimed to favor a cell-mediated immune response, provide protection by a fast seroconversion, reduce the amount of antigen per dose to increase the global vaccine supply, broaden the antibody response and overcome the poor responsiveness to immunization in elderly persons and infants.

3.1.1.3 Formulation

The optimization of vaccines' safety and potency resulted in novel formulation strategies to ensure a controlled biodistribution of the vaccine. For the induction of an effective adaptive immune response, the antigen must reach the lymph node, being either transported by APCs or via the lymphatic drainage. Traditional intramuscular application induces a potent humoral response, but only small quantities of antigen reach the lymph node, which might limit the induction of a cell-mediated response (Dupuis, 1999). To increase the effectiveness of the vaccine, strategies include the co-delivery of antigen and adjuvant, enhanced delivery to the lymph nodes, targeting of APCs and the programming of vaccine kinetics (Moyer et al., 2016). Particulate delivery systems are promising tools to implement these strategies. They include immune stimulating complexes (ISCOMs), nanoparticles, liposomes, mineral salts and emulsions ranging from 20 nm to 20 µM in size (Bachmann and Jennings, 2010). The particle size is critical for efficient uptake in the lymphatics. Large molecules, which were not cleared from tissues by blood, traffic to the lymph (up to 45 kDa; Supersaxo et al., 1990). This phenomenon may explain, why low-molecular-weight adjuvants provide the risk of systemic distribution. Thus, the incorporation of antigen and adjuvant into particulate delivery system increases adjuvant safety and antigen delivery to the lymph nodes.

3.1.1.4 Route of administration

As already mentioned, the route of vaccination can have fundamental consequences on the induced immune response. Most vaccines are applied through parenteral routes, which includes intramuscular, subcutaneous and intradermal administration. Intradermal application

induces a more potent immune response compared to intramuscular and subcutaneous application, which both show similar effects (Zhang et al., 2015). Despite demonstrated dose sparing upon intradermal application (Zehrung et al., 2013), the intramuscular vaccine delivery showed the least local adverse events (Ikeno et al., 2010; Enama et al., 2014). Alternative routes of administration such as mucosal and cutaneous have gotten more attention during the last years. Application of the vaccine through the mucosal route generates a front-line defense, enabling the control of the pathogen directly, when crossing the barrier (Shakya et al., 2016). The skin is a promising targeting site due to the dense network of Langerhans cells and dendritic cells and increased lymphatic drainage, which allows an efficient antigen transportation to the local lymph nodes (Teunissen and Zehrung, 2015).

The design strategy of subunit vaccines demonstrates that multiple components of the vaccine including antigen, adjuvant, formulation and route of administration can be adjusted to gain a synergistic-acting composition to generate the desired immune response. This flexibility in assembly of vaccine components is simultaneously a big challenge. To cope with this difficult task, a deep understanding of every of the four parts is required.

3.2 Immunology of immunization

The ability to recognize a pathogen and to remember how to fight it for several decades or even life-long is given by the memory cells of our adaptive immune system. Innate immune cells, such as dendritic cells (DCs), initiate the development of a potent memory response upon the first encounter with the pathogen (Figure 3). While the primary response against the pathogen takes several days to establish effector functions needed to fight the infection, memory cells, which differentiate from these effector cells after pathogen clearance, can react directly upon re-exposure to the pathogen (Akondy et al., 2017). Here, clonal expansion and differentiation of the cells, results in a greater magnitude of effector memory cells and antibody levels with a higher affinity to ensure a fast control of infection (Murphy and Weaver, 2017, pp. 473).

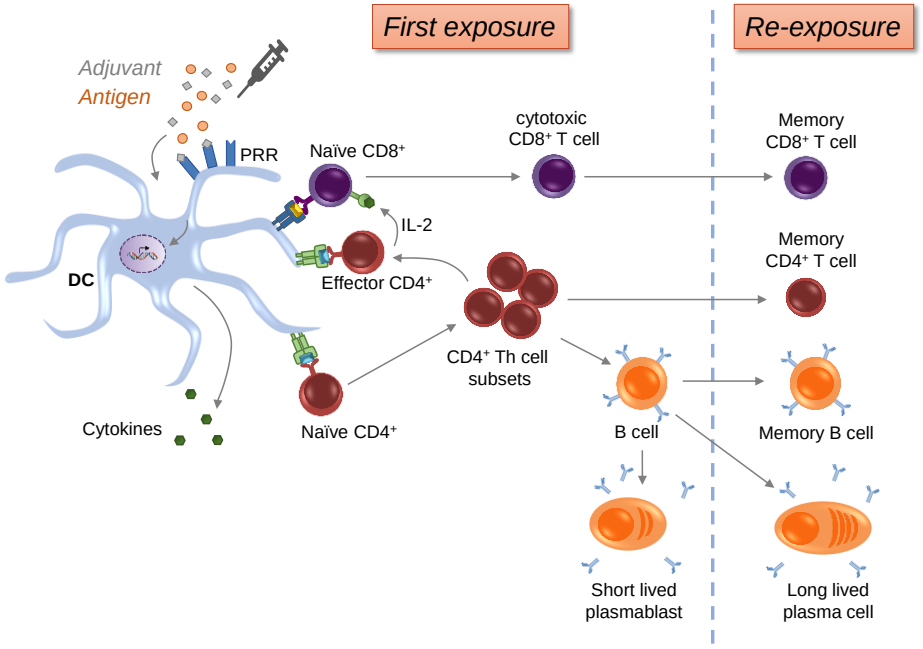

Figure 3: Immune response after vaccination.
Adjuvant binding to PRR receptors induce the maturation of the DC. Internalized antigen is processed, loaded on MHC-complexes and presented to naïve T cells. The priming requires co-stimulation and a defined cytokine milieu. Priming of naïve $CD8^+$ T cells requires additional help by $CD4^+$ T cells. Subsequently, naïve $CD8^+$ T cells develop to cytotoxic effector T cells. Naïve $CD4^+$ T cells are biased by DCs into a distinct Th cell subset. The interaction of $CD4^+$ T_{FH} cells and B cells induces the formation of short-lived plasmablasts. While most of the effector cells undergo apoptosis after clearance of the infection, some differentiate to memory cells, which are able to respond quickly upon a re-exposure to the pathogen.

3.2.1 Dendritic cells bridge innate and adaptive immune responses

Professional APC such as DC, macrophages and B cells interact with T cells by presenting antigens on their major histocompatibility complexes (MHCs) along with co-stimulation through CD80/CD86 and CD40. In contrast to macrophages and B cells, DCs have the unique ability to migrate to draining lymph nodes and prime naïve T cells (Steinman et al., 1997). Thus, DCs have the key role in initiating and directing the adaptive immune response, which makes them an attractive target of vaccination.

DCs are sentinels of the immune system and equipped with a variety of PRR, (Gordon, 2002) which allow them to detect PAMPs or danger-associated patterns (DAMPs; (Matzinger, 1994). Besides NOD-like, RIG-I-like and C-type-lectin receptors, toll-like receptors (TLR) belong to the group of PRRs. Their specificity in binding of a diverse but highly conserved pathogenic structure and the consequent activation of immune cells upon ligation, is exploited in today's vaccine development (Duthie et al., 2011). The expression of the ten known TLRs in humans varies between cell types but is generally prevalent in innate and adaptive immune cells as well as resident cells, including epithelial cells and fibroblasts (Takeuchi and Akira, 2010).

Immature DCs surveil their surrounding and continuously take up antigen by phagocytosis (Reis e Sousa et al., 1993), receptor-mediated endocytosis (Jiang et al., 1995) or

macropinocytosis (Sallusto et al., 1995). In combination with a pathogenic signal, DCs transform into a mature phenotype to be able to initiate the adaptive immune response (Banchereau and Steinman, 1998). During the maturation process, they reduce their capacity to acquire new antigen and start to degrade the incorporated ones in endosomal compartments. The resulting antigenic peptides are loaded on MHC molecules and are transported to the cell surface, where they are presented to T and B cells (Trombetta and Mellman, 2005). Furthermore, DCs increase the expression of the co-stimulatory molecules of the B7 and TNF family (Fujii et al., 2004) and alter their chemokine receptor expression e.g. by increasing CCR7 expression for migration to the lymph nodes (Sallusto et al., 1998).

DCs can present antigen on MHC class II to naïve $CD4^+$ T cells or by cross-presentation on MHC class I to $CD8^+$ T cells (Figure 3). While antigenic display on MHC class I is normally restricted to peptides from within the cell (self or in the case of non-self, derived from an intracellular infection), DCs are capable to present internalized extracellular peptides on MHC class I molecules to prime naïve $CD8^+$ T cells (Jung et al., 2002). The process of cross priming is of great importance for peptide and protein-based vaccines desiring to stimulate a cytotoxic $CD8^+$ T cell response with vaccine-derived exogenous antigen (Figure 3, (Joffre et al., 2012). Engagement of the TCR with its specific antigen presented on the MHC complex initiates the priming process (Figure 4). Besides the MHC-peptide-mediated TCR triggering (signal 1), co-stimulation through CD80/ CD86 - CD28 and CD40 - CD40L interaction (signal 2) is required to promote T cell survival and expansion. The expression of CD40 on DCs is essential for competent APCs. Studies have shown that the interruption of the CD40-CD40L axis negatively influences $CD4^+$ and $CD8^+$ T cell priming (Stuber et al., 1996; Schoenberger et al., 1998). However, there are several other co-stimulatory receptor-ligand pairs, some of them having regulatory function such as T cell's CTLA-4, which controls the proliferative phase upon binding to CD80/CD86 (Tivol et al., 1995). For guiding naïve CD4 T cells into certain Th cell subsets, DCs determine this polarization by the secretion of distinct cytokines (signal 3). The critical signal is elicited by the class of the pathogen, and it consequently promotes the development of a certain Th cell subset that will most efficiently destroy the pathogen (Walsh and Mills, 2013).

Priming of naïve $CD8^+$ T cells by DCs most often requires the help of $CD4^+$ effector T cells recognizing the related antigen. This two-step interaction functions as safety control mechanism due to the $CD8^+$ T cells' detrimental cytotoxic effector functions (Figure 3). Certain viruses might already sufficiently activate DCs to induce the secretion of IL-2, otherwise, $CD4^+$ effector T cells have to 'license' DCs through a CD40 dependent process to boost DCs' stimulatory potential (Laidlaw et al., 2016). The activation of the immature DCs and the resulting degree of maturation are crucial for the delivery of the three signals to T cells, their activation and polarization (Kapsenberg, 2003). Thus, vaccines aiming to induce a T cell-

mediated immune response have to efficiently mature DCs to ensure the development of a potent adaptive T cell response.

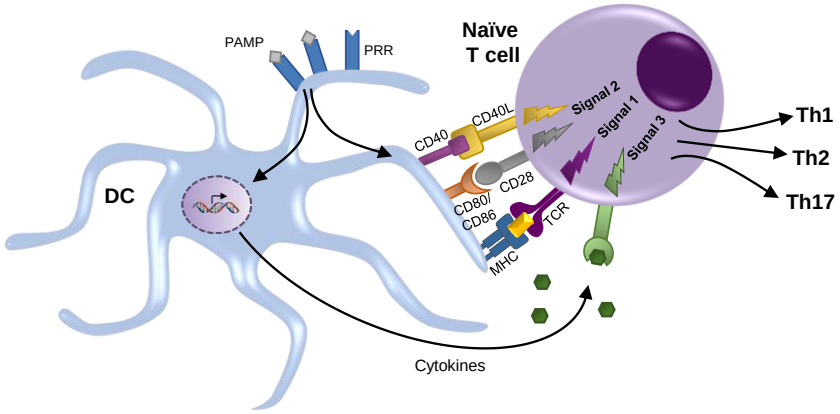

Figure 4: T cell priming by DCs.
Maturation induced by PAMPs through binding to its PRR enable DCs to initiate and direct the adaptive immune response. Upon interaction with a naïve T cell, MHC-peptide-TCR interaction (signal 1), ligation of CD80/CD86-CD28 and CD40-CD40L (signal 2) and a defined cytokine milieu, activates and polarizes naïve T cells to a distinct T helper (Th) cell subset. Figure is adapted from (Kapsenberg, 2003).

Most vaccines (e.g. diphteria-tetanus-pertussis, hepatitis B) are applied intramuscularly. Common DC types being present within the muscle include conventional (cDC) and monocyte-derived DCs (Langlet et al., 2012). cDCs comprise two subsets, cDC1 and cDC2. cDC1 (or $CD141^+$ cDCs) are equipped with TLR1, TLR2, TLR6, TLR8 and express high levels of TLR3 and TLR10 (Hémont et al., 2013). Additionally, they sense necrotic cells with their key marker CLEC9A (Zhang et al., 2012) and are specialized to perform cross-presentation to $CD8^+$ T cells. This function is linked to XCR1 expression due to their recruitment via XCL1 by activated $CD8^+$ T cells (Brewitz et al., 2017). In contrast, cDC2 (or $CD1c^+$ cDCs) express a variety of TLR, NOD and RIG-I receptors and induce preferentially potent Th1, Th2 and Th17 responses (Nizzoli et al., 2013; Sittig et al., 2016). MoDCs develop from monocytes upon their recruitment to inflamed tissue. Here, their main function is to support pathogen clearance, to produce cytokines and to present antigen to effector T cells (Collin and Bigley, 2018). Another important DC subset are plasmacytoid DCs (pDCs), due to their efficient sensing of viruses. pDCs recognize the viruses' unmethylated CpG-rich DNA motifs or double-stranded RNA through TLR7 and TLR9 (Gilliet et al., 2008). Consequently, they respond quickly with a pronounced type I interferon secretion (Villadangos and Young, 2008; Swiecki and Colonna, 2015).

3.2.2 T cells provide cell-mediated protection against pathogens

Following naïve T cell priming, T cells proliferate and differentiate into effector T cells (Figure 3). Upon encountering a target cell, which present the effector T cells' specific antigen on its MHC complex, the effector mechanisms are being activated. The TCR forms a supramolecular activation complex (immunological synapse) with the target cell's MHC molecules and associated co-receptors. This mechanism increases target cell selectivity for directed release and efficient concentration of effector molecules by reorganization of the microtubule skeleton and by narrowing the gap between both cells (Huppa and Davis, 2003; Stinchcombe et al., 2006). Effector molecules can include perforin and the serin protease granzyme, which are synergistically acting cytolytic molecules. Perforin multimerizes at the target cell's membrane and form pores through which granzyme is delivered to induce apoptosis by activating caspases within the target cell (Lieberman, 2003). Additionally, effector cytokines such as IFNγ and TNFα are secreted with the intention to control infection. While IFNγ inhibits viral replication and recruits as well as activate other immune cells such as macrophages (Kang et al., 2018), TNFα additionally triggers the apoptotic signaling cascade by binding to TNF receptor or supports the control of bacterial infection (Allie et al., 2013). While cytolytic activity performed by perforin or granzymes was solely attributed to $CD8^+$ effector T cells, studies in recent years demonstrate that cytotoxic $CD4^+$ T cells exist (Lund and Randall, 2010). Cytotoxic T cells and Th1 $CD4^+$ T cells possess another killing mechanism which is mediated by the expression of FasL on the T cells' surface. The binding to Fas, expressed on the target cell's membrane, induces the activation of caspases, leading to apoptosis of the target cell (Alderson et al., 1995). Further effector functions of $CD4^+$ T cells include the support of B cell activation (Figure 3) as well as the secretion of B cell's growth factors (Th2) and the promotion of acute inflammation by secretion of IL-17 for neutrophil recruitment (Th17) (Murphy and Weaver, 2017, pp. 402).

As soon as the infection is cleared, most effector T cells undergo apoptosis, due to the loss of antigenic stimulation and the associated secretion of the pro-survival cytokine IL-2 and its receptor (Krammer et al., 2007). A fraction of effector T cells differentiates into memory T cells (Akondy et al., 2017), comprising central (T_{CM}), effector (T_{EM}) and resident (T_{RM}) memory T cells (Mueller et al., 2013). T_{CM} cells express the lymph node homing receptor CCR7 and are thus able to traffic between lymph nodes and blood. In contrast to T_{EM}, they have a higher proliferative potential. However, T_{CM} are slower in activating effector functions after early re-exposure with their cognate antigen, while T_{EM} rapidly mature into effector cells. T_{EM} are equipped with receptors to enter inflamed tissue and can be found in blood, spleen and non-lymphoid tissue. Comparable to T_{EM}, T_{RM} cells lack CCR7 expression but reside primarily in epithelial sites including skin, lung, intestine and vaginal mucosa (Farber et al., 2014). The

T cell memory heterogeneity enables the protection against a wide range of pathogens and different routes of exposure. It is assumed that T_{RM} cells provide first-line defense as residents of barrier tissues, followed by migrated T_{EM} cells, which rapidly support with their effector functions. In the meanwhile, T_{CM} provide a self-renewing source of T_{EM} cells, expanding and developing effector functions after encounter with APCs in the lymph nodes, followed by their migration to sites of infection (Youngblood et al., 2013).

As already mentioned, a T cell-mediated immune response is especially important for a directed killing of intracellular pathogens as it is needed in e.g. malaria, tuberculosis and leishmaniasis. The only way to control these infections is the induction of $CD4^+$ and $CD8^+$ T cells to a sufficient magnitude as well as their development into the required effector phenotype, which allows the clearance of the pathogen by cell-mediated effector mechanisms such as pro-inflammatory cytokine production or contact-dependent cell lysis (Foged et al., 2012). So far, a T cell-mediated immune response was only induced using the LAV with Bacille Calmette–Guérin (BCG; Ryan et al., 2009), varicella zoster virus (Smith et al., 2003) and influenza (He et al., 2006). In contrast, inactivated vaccines favor a humoral response as demonstrated by increasing IgG antibodies after e.g. measles, tetanus or diptheria vaccination (Rappuoli, 2007). Thus, adjuvants are necessary which effectively engage T memory cell responses.

Since vaccination has the goal to induce protective memory T cells without having experienced an actual infection, vaccine developers have a big interest to track memory T cell generation for the prediction of potential vaccine efficacy (Jameson and Masopust, 2018).

3.2.3 Antibody-mediated protection upon vaccination

Antibodies support the clearance of the pathogen or pathogen-derived products such as toxins by neutralisation or masking for recognition by other immune cells such as phagocytes. Antibodies are produced by plasma or memory B cells. On their cell surface B cells express immunoglobulins with a distinct specificity for an antigen, which serves as B cell receptor (BCR). Upon recognition of their cognate antigen, this antigen is internalized, processed and loaded onto the B cell's MHC complex to be presented to specialized $CD4^+$ T cells, T follicular helper cells (T_{FH}) at the boundary of the B cell - T cell zone in secondary lymphoid tissue (Okada et al., 2005; Kerfoot et al., 2011). The interaction is intensified by CD40 – CD40L co-stimulation and IL-21, secreted by T_{FH} cells (Vogelzang et al., 2008), leading to the activation and proliferation of the B cell (Coffey et al., 2009). The strength of B cell interaction with T_{FH} cell determines whether B cells develop into IgM-secreting short-lived plasmablasts or whether they form a germinal center to differentiate into memory B cells or long-lived plasma cells (Figure 3; (Schwickert et al., 2011). B cells have to undergo processes such as somatic

hypermutation and antibody class switch to be able to produce high affinity antibodies with various effector functions (Berek and Ziegner, 1993). After antibody affinity maturation, memory B cells and long-lived plasma cells leave the germinal center with a broad antibody repertoire. While plasma cells constitutively secrete low levels of antibodies, serving as a first-line defense upon re-infection, memory B cells are able to rapidly respond with a greater magnitude of antibodies if necessary (Kurosaki et al., 2015).

Many pathogens can be controlled with an antibody-mediated immune response. However, pathogen strain specific variations and evasion strategies such as antigenic drift could lead to the pathogen's escape and the failure of vaccine protection (Reed et al., 2013). By mediating the expansion of B cell diversity, adjuvants drive the broadening of the antibody response as counter-strategy. This tactic was observed after influenza (Khurana et al., 2011) and HPV vaccination (Draper et al., 2013) adjuvanted with MF59 and AS04 respectively.

3.3 Adjuvants – diverse targets and distinct MoAs

As already mentioned above, purified antigens in vaccine formulations exhibit poor immunogenicity and have to be adjuvanted. Perspectively, rather than relying on the still insufficiently understood effects of the traditional adjuvants, the use of next-generation adjuvants is preferred, leading to a very specific adaptive immune response to protect against a certain infection or disease. Therefore, adjuvant candidates are studied with regard to their ability to provide effective signals in priming, amplifying and directing the immune response (Coffman et al., 2010). After setting the basis, the 'ideal' vaccine adjuvant should support the generation of cytotoxic T cells, specific antibodies in a high magnitude, antigen-specific clonal expansion and a long-lasting adaptive immune response (Bonam et al., 2017; Figure 5).

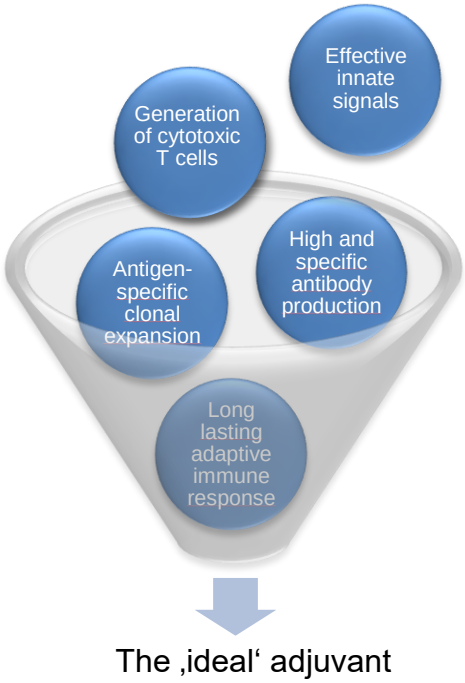

Figure 5: The characteristics of the 'ideal' adjuvant.
An adjuvant comprising all the highlighted characteristics could be useful for protection against pathogens such as HIV.

3.3.1 Adjuvants' potential modes of action

The adjuvants' modes of action are distinct for every adjuvant and the mechanistic details, even for the ones already used in the clinic, are far from being completely understood. DCs have a central role as APCs with exclusive T cell priming function and as orchestrators of the immune response. Thus, they are of special interest to be targeted and activated by adjuvants. In Figure 6, an overview of putative modes of action of adjuvants is illustrated (Awate et al., 2013; Reed et al., 2013). Once applied to the human body as part of a vaccine, adjuvants have the potential to enhance antigen uptake and antigen presentation by MHC molecules. In combination with an increase of co-stimulatory molecules, the contact to T cells is intensified. Additionally, the activation of cell surface and endosomal PRRs and their signaling pathways, result in production and secretion of defined cytokines and chemokines. Hence, other immune cells get recruited to the site of vaccination. Furthermore, the engagement of the inflammasome and the resulting secretion of the pro-inflammatory cytokines IL-18 and IL-1β initiates the amplification of the signal by activating further immune cells (Jo et al., 2016).

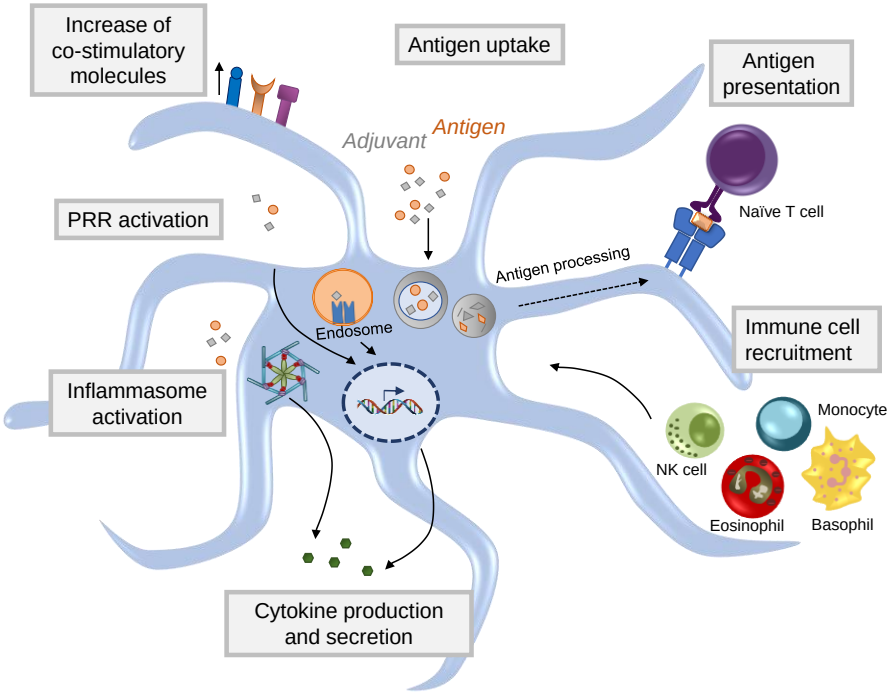

Figure 6: Adjuvants' potential immunomodulatory properties to initiate and polarize the immune response. The mode of action is different for every adjuvant but might include one or more of the following mechanisms: Enhancing antigen uptake and presentation, recruitment of other immune cells, activation of cell surface or endosomal PRR's signaling pathways, increase of co-stimulatory molecules, engagement of the inflammasome and defining a specific cytokine and chemokine milieu. The illustration is adapted from (Reed et al., 2013).

A more detailed introduction into the described modes of actions of the adjuvants used in this study (Figure 7), is given in the following chapters. We analyzed a panel of ten adjuvants comprising single component adjuvants (PRR ligands and Quil), one emulsion (AddaVax) and an aluminium hydroxide wet gel suspension.

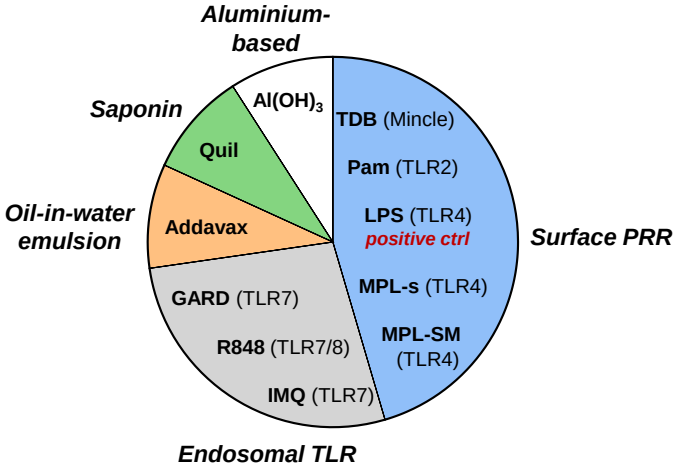

Figure 7: Adjuvants being investigated in this thesis for their immunogenic properties.

3.3.2 Classes of adjuvants

3.3.2.1 Pattern recognition receptor ligands

The first steps using pattern recognition receptor (PRR) ligands as adjuvants and potentiators of a strong immune response were made by Charles Janeway. He observed that the activation of B and T cells in culture was only triggered when the antigen was paired with a microbial constituent, which he called “the immunologist’s dirty little secret” (Janeway, 1989). Beside C-type lectin receptors (CLR), NOD-like receptors (NLR) and RIG-I-like receptors (RLR) - Toll-like receptors (TLR) belong to the multifaceted class of PRRs and were the first PRR to be identified (Kawai and Akira, 2011). TLRs detect a wide range of PAMPs with each TLR detecting distinct PAMPs derived from viruses, bacteria, fungi or parasites such as lipoproteins (TLR1, TLR2, TLR6), double stranded RNA (TLR3) lipopolysaccharide (LPS; TLR4), flagellin (TLR5), single stranded RNA (TLR7, TLR8) or DNA (TLR9) (Akira et al., 2006; Kawai and Akira, 2011). PRRs are transmembrane proteins with their receptor moiety facing either the extracellular space (TLR1, 2, 4) or the endosome lumen (TLR7, 8, 9). Upon TLR engagement, adapter molecules with a Toll/interleukin-1 receptor domain such as MyD88 or TRIF, are recruited to the TLR and initiate a downstream signaling process, resulting in the expression of proinflammatory cytokines, type I interferons, chemokines, and antimicrobial peptides to combat intruding pathogens (Kawai and Akira, 2010, 2011). The function of TLRs as important pathogen sensors of the immune system was discovered in 1996, when Lemaitre and colleagues showed in *Drosophila* that mutations in the Toll signaling pathway led to a reduced survival of after fungal infection (Lemaitre et al., 1996). Since then the development of a wide range of potential TLR-targeting immunomodulators began. So far, only the TLR4 ligand monophosphoryl lipid A (MPL; GlaxoSmithKline) as part of the AS04 formulation is approved in vaccines against HBV and HPV. However, several TLR ligands are in an advanced stage of preclinical or clinical testing. In this thesis, we have analyzed the immunogenic properties of natural or synthetic PRR ligands targeting the C-type lectin receptor Mincle, TLR1/2, TLR4, TLR7 or TLR8.

Trehalose-6,6’-dibehenate (***TDB***) is a Mincle ligand (C-type lectin receptor) and a synthetic equivalent of the immunogenic mycobacterial cell wall component trehalose-6,6’-dimycolate (TDM). TDB stimulation of human primary DCs and macrophages lead to the upregulation of CD86 and the secretion of IL-6, IL-8, IL-1β, MCP-1 and MIP-1α (Ostrop et al., 2015). Similar innate activation profiles were found in mice, resulting in a Th1/Th17-mediated adaptive immune response, which however protected only partially against mycobacterium tuberculosis challenge (Werninghaus et al., 2009; Desel et al., 2013). TDB formulated within cationic

liposomes (CAF01 adjuvant) was already used in phase I clinical studies for a prophylactic vaccine against tuberculosis (NCT00922363; (van Dissel et al., 2014), which generated a potent and long-lived antigen-specific $CD4^+$ T cell response.

The synthetic analogue Pam3CSK4 (***Pam***) of the triacyl lipopeptide, a bacterial cell wall component, stimulates through the heterodimer TLR1/2 (Ozinsky et al., 2000; Takeda et al., 2002). Pam is able to potently stimulate innate immune responses by NFκB activation (Brandt et al., 2013) and the consequent expression of IL-6, TNFα, IL-12 and IL-10 in murine DCs (Welters et al., 2007). Furthermore, Pam favors the development of $CD4^+$ T cells into a Th1 response (Lombardi et al., 2008) as well as the generation of antigen-specific $CD8^+$ T cells in a DNA-based vaccine against Leishmania in mice (Jayakumar et al., 2011).

The only PRR agonist being part of licensed vaccine formulation is a TLR4 ligand. Although, the natural bacterial ligand to TLR4 is ***LPS***, TLR4 adjuvants are detoxified derivatives of LPS, which maintain biologic activity but have a reduced toxicity profile (Takayama et al., 1981; Qureshi et al., 1982). These monophosphoryl lipid A (MPL) TLR4 ligands can be either extracted from LPS produced from *Salmonella minnesota* R595 (***MPL-SM***) or are synthetic lipid A analogues from *E. coli* serotype R515 (***MPL-s***, GLA). In contrast to MPL-SM, consisting of a mixture of 5 to 7 fatty acyl chains, MPL-s is 3-acylated and contains a defined number of 6 fatty acyl groups (Coler et al., 2011). While LPS signals through the TLR4 adapter proteins MyD88 and TRIF, MPL has a bias towards TRIF signaling, resulting in a reduced proinflammatory cytokine profile indicated by lower levels of TNFα and IL-1β (Mata-Haro et al., 2007). Although IL-12p70 is a MyD88-dependent cytokine, Ismaili and colleagues showed IL-12p70 secretion upon stimulation with MPL by human moDCs accompanied with phenotypical maturation and T cell activating function (Ismaili et al., 2002). MPL-SM is used in licensed vaccines within an adjuvant formulation including Alum (AS04) against HBV (Fendrix®) and HPV (Cervarix). AS04 induces local and transient cytokine production, leading to an increased number of activated antigen-loaded APCs in the draining lymph nodes. Consequently, a cell-mediated immune response is generated having a pronounced Th1 profile. Moreover, AS04 promote high and persistent antibody titers. While MPL is responsible for the immune reaction, Alum rather reduces the magnitude and prolongs the response (Garçon and Tavares Da Silva, 2017). The natural and the synthetic MPL are both phase II-III candidates (against influenza, cancer or malaria) within adjuvant mixtures AS01 (consisting of: liposomes, MPL and the saponin QS-21; Agnandji et al., 2011), AS02 (an oil in water emulsion including MPL and QS-21; Kruit et al., 2013), AS15 (comprising liposomes, MPL, QS-21 and the TLR9 ligand CpG oligonucleotide; Pujol et al., 2015) and GLA-SE (glucopyranosyl lipid adjuvant formulated in a stable emulsion; Coler et al., 2018).

TLR7 and TLR8 sense single-stranded RNA of viruses, such as influenza, within endosomes. Adjuvants targeting TLR7 and TLR8 include gardiquimod (***GARD),*** imiquimod (***IMQ)*** and ***R848*** (or resiquimod), which are small synthetic molecules and guanosine derivates of the imidazoquinoline family (Gorden et al., 2005). TLR7 ligands enter the endosome via endocytosis (Blasius and Beutler, 2010; Petes et al., 2017). GARD and IMQ selectively target TLR7, whereas R848 is a dual ligand for TLR7 and TLR8 (Jurk et al., 2002). IMQ and R848 both showed to have substantial influence on the adaptive immune response in mice by enhancing antibody levels and mediating a Th1 response with cytokines such as TNFα, IFNγ and IL-2, while suppressing a Th2 immune response (Vasilakos et al., 2000; Brugnolo et al., 2003). Similar results were obtained *in vitro,* using human PBMCs. Here, IFNα, IL-12, IL-1 and IL-6 were identified as the leading cytokines of the innate immune response (Weeks and Gibson, 1994; Wagner et al., 1999). Despite these promising immunomodulatory effects of R848, comparisons to other TLR ligands revealed, that R848 is not as effective in inducing protection (Johnson et al., 2009; Caproni et al., 2012) and safety concerns arose due to its reactogenicity (Pockros et al., 2007). Due to the small size of imidazoquinolines, they distribute very quickly throughout the body and do not retain at the application site, which might be the reason for the observed systemic immune activation and their reduced efficacy in past pre-clinical studies. However, new approaches regarding their formulation, such as the encapsulation in nanoparticles or inclusion within a gel for topical application, enhanced adjuvant activities while limiting reactogenicity (Ilyinskii et al., 2014). So far, IMQ is formulated within a gel (Aldara®) for topical application. Aldara® provides local immune activation is already approved and prescribed against genital warts and basal cell carcinoma. Furthermore, it is used in many clinical trials as vaccine adjuvant against cancer or influenza (NCT00899574, NCT02103023). R848 was applied as adjuvant in a phase I clinical anti-tumor study (NCT00821652) and in an influenza vaccine for seniors (NCT01737580). GARD can be ranked in-between IMQ and R848 regarding its potency, and it also exhibits potential benefits in cancer therapy (Ma et al., 2010a; Zou et al., 2015).

3.3.2.2 Oil in water emulsion

AddaVax™ (***ADX***) is a squalene-based oil-in-water nano-emulsion with a formulation similar to MF59®. MF59® has been licensed for the use in a several influenza vaccines (Fluad, Aflunov (H5N1), Focetria (H1N1)). It consists of squalene oil droplets stabilized by the addition of two non-ionic surfactants (Span85, Tween-80) in citrate buffer (Kommareddy et al., 2017). None of the single components, only the formulated emulsion has adjuvant activity (Calabro et al., 2013). Upon injection, the release of ATP (Vono et al., 2013) and the secretion of

chemokines (MCP-1, MIP-1α and CCL4; (Seubert et al., 2008) stimulate the influx of phagocytic cells, resulting in an increased antigen uptake and transport to the draining lymph nodes (Cantisani et al., 2015). It has been shown that MF59 engages a strong T cell-dependent B cell response, which provides antibody-mediated protection (Lofano et al., 2015). Since its first approval in 1997, it has reached a good safety profile with over 150 million administered doses (O'Hagan et al., 2013). Recently, an HIV-vaccine candidate of the HIV Vaccine Trials Network (HVTN100) adjuvanted with MF59 qualified for phase 2b/3 efficacy testing (NCT02404311; (Bekker et al., 2018).

3.3.2.3 Saponin

Quil-A (***Quil***) is a triterpenoid saponin and isolated from the bark of Quillaja saponaria Molina. It is a potent inducer of the humoral, Th1 and cytotoxic $CD8^+$ T cell response and hence, has been used in a veterinary vaccine against hand-and-foot disease (Dalsgaard, 1974). Its interaction with membrane cholesterol and the associated toxicity prevented the use in human vaccines. QS-21 is a purified fraction of the enriched heterogenous saponin mixture Quil-A with similar adjuvant activity (Kensil et al., 1991; Newman et al., 1992; Kensil et al., 1995) and has been included in the adjuvant formulation AS01 together with MPL. The formulation was enriched with cholesterol to inhibit the saponin-induced pore formation (Garçon et al., 2007). Until today, a specific receptor for QS-21 has not been discovered. However, its adjuvanticity has recently been described to be mediated by inflammasome activation when co-stimulated with LPS (Marty-Roix et al., 2016), as well as by cholesterol-dependent endocytosis with cathepsin B (Welsby et al., 2016) in human primary APCs *in vitro.* The most promising vaccine candidates, that already reach the clinical trial phase III, are against malaria (RTS,S: (RTS, 2015) or herpes zoster (HZ/su: (Lal et al., 2015).

3.3.2.4 Aluminium-based adjuvant

Aluminium hydroxide ($Al(OH)_3$, Alum) belongs to the 2^{nd} generation of aluminium-based adjuvants and led to the preparation of aluminium-adsorbed vaccines, which are in use for more than 60 years. These include a variety of prophylactic vaccines against bacterial (e.g. diphteria, tetanus) and viral (e.g. HBV) antigens and therapeutic vaccines for hyposenitization of allergies (Lindblad and Duroux, 2017). The mechanism of action is still not fully understood (Marrack et al., 2009; Hogenesch, 2012; Ghimire, 2015). Conflicting *in vivo* and *in vitro* data complicate this enlightenment. It is assumed that chemokines and cytokines trigger APC recruitment upon injection (Kool et al., 2008a; McKee et al., 2009; Calabro et al., 2011), followed by the antigen uptake, which is enhanced due to the particulate form of aluminium salts and antigen as a result of adsorption (Morefield et al., 2005; Ghimire et al., 2012). Within

the draining lymph node, an IL-4-induced cytokine milieu polarizes a Th2 cell response (Serre et al., 2009), which favors the priming and expansion of antigen-specific B cells and antibody production (Jordan et al., 2004).

4 Hypothesis and Objectives

Vaccination is the most successful medical invention of the past century to protect against infectious diseases. By generating a pathogen-specific memory immune response, the immune system is able to rapidly control the infection upon a rechallenge. The use of purified antigens with low intrinsic immunogenicity in today's subunit vaccines, requires the addition of an adjuvant within the vaccine formulation. Adjuvants are the key inducers, amplifier and guides of a directed immune response against the antigen. Thus, the selection of an appropriate adjuvant has pivotal influence on vaccine efficacy. So far, licensed adjuvants are limited, but many new adjuvants are in clinical development to fulfill the need of inducing a strong cell mediated immune response against intracellular and viral pathogens. However, our understanding of the adjuvants' modes of action, even for the most commonly used adjuvant aluminium hydroxide, is far from being comprehensive. In this study, we aim to systematically evaluate the immunogenic profile of ten single component adjuvants to predict their potential to shape the immune response.

We hypothesize that:

'Specific innate and adaptive immune responses can be linked to the adjuvant's immunomodulatory mode of action, revealing an immunogenic profile, which facilitates the selection of candidate adjuvants for novel vaccines.'

To examine this hypothesis, we formulated the following objectives (Figure 8):

1) Evaluation of the phenotypical and functional maturation of DCs upon stimulation with the different immunomodulators by assessing DC's expression levels of cell surface maturation markers and endocytic uptake capacity.

2) Analysis of the adjuvant-induced cytokine and chemokine profile defined by an immune-stimulatory milieu of DCs and autologous lymphocytes.

3) Comparison of the adjuvants to activate different lymphocyte sub-populations to proliferate in an antigen-independent manner.

4) Investigating the adjuvant's capacity to boost antigen-specific $CD4^+$ and $CD8^+$ T cell responses including antigen-directed effector functions.

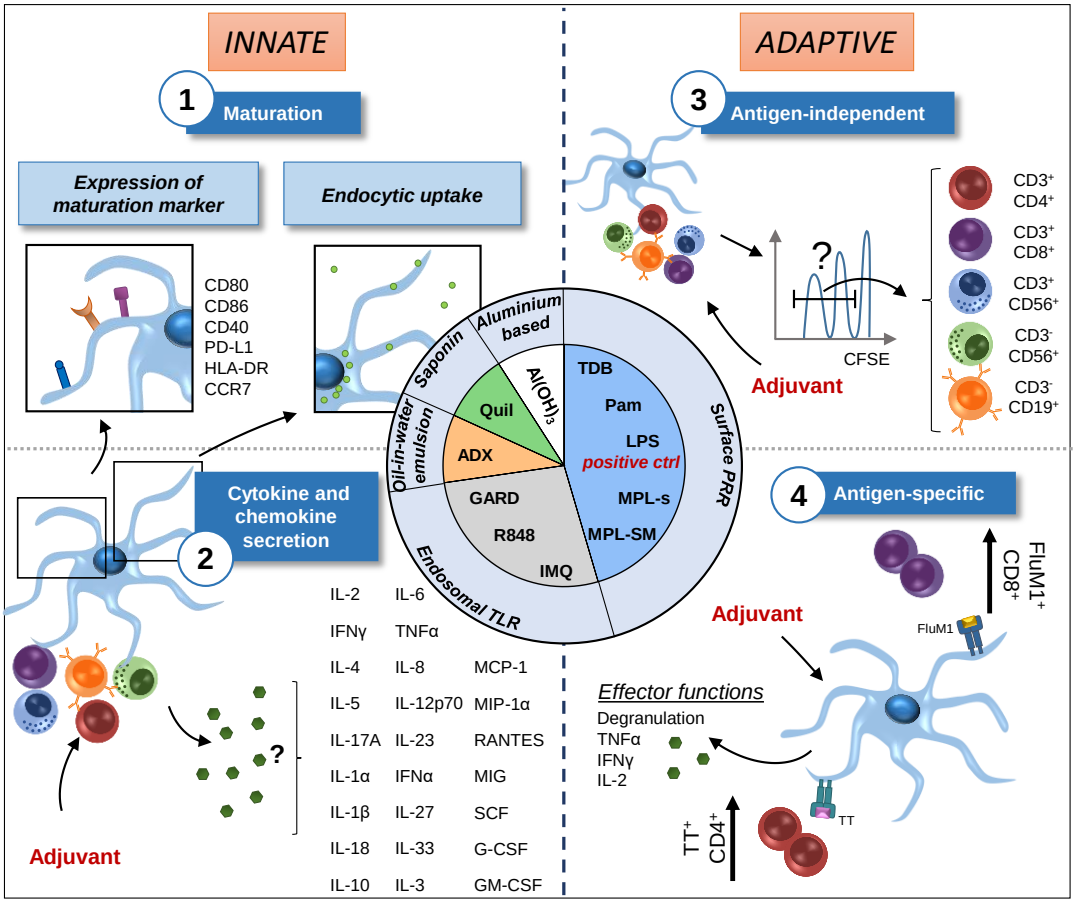

Figure 8: Schematic representation of the objectives of this study.
The immunomodulatory modes of action of ten single component adjuvants will be addressed using a human primary immune cell-based assay, which is composed of monocyte-derived DCs and autologous PBLs. (1) We investigate the adjuvant's capacity to mature DCs by phenotypical and functional assessment of their maturation marker expression and endocytic activity. (2) The resulting cytokine and chemokine milieu after adjuvant stimulation will be defined using a multiplex analysis. (3) We compare the adjuvant-induced activation of lymphocyte subpopulations by analyzing their proliferation in an antigen-independent context. (4) Lastly, we investigate the influence of adjuvants on antigen-specific T cell responses and directed effector functions.

5 Material and Methods

5.1 Material

5.1.1 Devices

Device	Manufacturer/ Distributor
Analytical balance KB BA 100	Sartorius Göttingen, GER
CASY® Cell Counter Model TT	Roche Innovatis AG, Bielefeld, GER
Centrifuge 5430 and 5430R	Eppendorf, Hamburg, GER
Centrifuge Megafuge 40R with BIOLiner swinging bucket rotor and buckets (75003670, 75003668)	Thermo Fisher Scientific, Dreieich, GER
CO_2 Incubator Heracell™ VIOS 160i	Thermo Fisher Scientific, Dreieich, GER
Cytocentrifuge Cellspin II Universal 320 R	Tharmac, Waldsoms, GER
ECL and Fluorescence Imager Chemostar	Intas, Göttingen, GER
Electrophoresesis chamber for SDS-PAGE mini-Protean Tetra cell	Bio-Rad, München, GER
Freezer U725-G, -80°C	Eppendorf, Hamburg, GER
Freezer, -20°C	Liebherr, Biberach a. d. Riß, GER
Fridge FKS 3600	Liebherr, Biberach a. d. Riß, GER
Laminar Flow Workbench MSC-Advantage	Thermo Fisher Scientific, Dreieich, GER
LSR Fortessa	BD Bioscience, Heidelberg, GER
LSR II	BD Bioscience, Heidelberg, GER
LSR II SORP (special order research product)	BD Bioscience, Heidelberg, GER
Magnetic stirrer C-MAG HS7	IKA, Staufe, GER
Microscope AxioVert A1	Carl Zeiss Microscopy, Jena, GER
Microscope Primo Star	Carl Zeiss Microscopy, Jena, GER
Microscope Z.1 Fluorescence equipped with AxioCam MRm and light source HXP120C	Carl Zeiss Microscopy, Jena, GER
MidiMACS Separator	Miltenyi Biotec, Bergisch Gladbach, GER
Mini centrifuge Sprout	Biozym Scientific GmbH, Hessisch Odendorf, GER
pH meter PB -11	Sartorius, Göttingen, GER
Power Supply 'PowerPac™ HC'	Bio-Rad, München, GER
Precision balance PFB 600-1M	Kern & Sohn GmbH, Balingen, GER
Semi-dry transfer unit OWL HEP-1	Thermo Fisher Scientific, Dreieich, GER

Device	Manufacturer/ Distributor
Sonifier Branson 450 II Classic	Branson Ultrasonic, Danbury, USA
Spectrophotometer NanoDrop 2000c	Thermo Fisher Scientific, Dreieich, GER
Thermomixer™ comfort with thermoblock	Eppendorf, Hamburg, GER
Vortex mixer VV3	VWR, Darmstadt, GER
Waterbath	Köttermann, Darmstadt, GER

5.1.2 Laboratory equipment and consumables

Equipment/ Consumable	Manufacturer/ Distributor
CASY cups	OLS OMNI Life Science, Bremen, GER
Cell culture flasks with filter: 25cm^2, 75cm^2	Sarstedt, Nürnbrecht, GER
Cell culture petri dish, 10cm	Sarstedt, Nürnbrecht, GER
Microplate, 96 well, PP, U-bottom, sterile	Greiner Bio-One, Frickenhausen, GER
Cell culture plates: 6 well flat bottom, 24 well flat bottom, 48 well flat bottom, 96 well round/ V shaped bottom	Sarstedt, Nürnbrecht, GER
Centrifuge tubes, 15ml, 50ml	Greiner Bio-One, Frickenhausen, GER
Cryo.s™ Freezing Tube, 2 ml, round bottom	Greiner Bio-One, Frickenhausen, GER
EasySep™ Magnet	Stemcell Technologies, Cologne, GER
FACS micronic tubes, 1.4 ml, U-bottom	Micronic, Lelystad, NLD
FACS tube, no cap, 5 ml	BD labware, Le Point de Claix, FRA
FACS tube, snap cap, 5 ml, sterile	BD labware, Le Point de Claix, FRA
Filter card for cytospins	Tharmac, Waldsolms, GER
Filter paper, Whatman	VWR, Darmstadt, GER
Hemocytometer Neubauer improved, depth 0.1mm, 0.0025 mm^3	VWR, Darmstadt, GER
Multiwell plate lid with condensation rings, high profile, sterile	Greiner Bio-One, Frickenhausen, GER
MACS Chill Rack	Miltenyi Biotech, Bergisch Gladbach, GER
MACS column, LS	Miltenyi Biotec, Bergisch Gladbach, GER
MACS Multistand	Miltenyi Biotech, Bergisch Gladbach, GER
Microcentrifuge tubes, 1.5ml, 2ml	Eppendorf, Hamburg, GER
Microscope slide for cytospins, uncoated	Tharmac, Waldsolms, GER
MidiMACS Magnet	Miltenyi Biotec, Bergisch Gladbach, GER

Equipment/ Consumable	Manufacturer/ Distributor
Multichannel pipette Research® plus, 8 channel: 10-100 µl	Eppendorf, Hamburg, GER
Multichannel pipette, Transferpette® S-8, 10-100 µl, 20-200 µl, 30-300 µl	Brand GmbH & Co. KG, Wertheim, GER
Nalgene™ Mr. Frosty Freezing Container	Thermo Fisher Scientific, Dreieich, GER
Nitril gloves	Sued-Laborbedarf, Gauting, GER
Pipette controller accu-jet® pro	Brand GmbH & Co. KG, Wertheim, GER
Pipette filter tips: 0.5-10µl, 10-200µl, 100-1000µl	Nerbe plus, Winsen/Luhe, GER
Pipette tips SurPhob SafeSeal®: 0.1-10µl, 10-200µl, 100-1000µl	Biozym Scientific GmbH, Hessisch Oldendorf, GER
Pipettes Research® plus: 0.1-2.5µl, 0.5-10µl, 10-100µl, 20-200µl, 100-100µl	Eppendorf, Hamburg, GER
Polyvinylidene difluoride (PVDF) membrane	GE Healthcare, Buckinghamsgure, UK
Pre-Separation Filter, 30µM	Miltenyi Biotec, Bergisch Gladbach, GER
Serological pipettes, sterile, 5ml, 10ml, 25ml	Greiner Bio-One, Frickenhausen, GER
Tharmac® Cellclip®	Tharmac, Waldsoms, GER
Tharmac® Cellfunnel®	Tharmac, Waldsoms, GER
S-Monovette®, 10 ml, Citrate 3.2% (1:10)	Sarstedt, Nürnbrecht, GER
Safety-Multifly® 20G tube	Sarstedt, Nürnbrecht, GER

5.1.3 Chemicals and reagents

Reagents that were obtained from the in-house facility, being responsible for the manufacturing of ultra-pure H_2O, solutions and growing media, are marked with 'Paul-Ehrlich-Institut'.

Chemical/ Reagent	Manufacturer/ Distributor
(L)-glutamine, 200 mM	Biochrom, Berlin, GER
Acrylamide/ Bisacrylamide solution 30%	Roth, Karlsruhe, GER
Agarose, LE	Biozym Scientific, Hessisch Oldendorf, GER
Ammonium chloride (0.15 M)	Pau-Ehrlich-Institute
Ammonium persulfate (APS)	SERVA Electrophoresis, Heidelberg, GER
Aqua bidest. (ddH_2O)	Paul-Ehrlich-Institut
Blasticidin	InvivoGen, Toulouse, FR

Chemical/ Reagent	Manufacturer/ Distributor
Bovine Serum Albumin (BSA)	Applichem, Darmstadt, GER
Bromophenol blue	Merck, Darmstadt, GER
CASYclean	OLS OMNI Life Sciences, Bremen, GER
CASYton	OLS OMNI Life Sciences, Bremen, GER
Dimethyl sulfoxide (DMSO)	Sigma-Aldrich, Steinheim, GER
Dimethyl sulfoxide for cell culture	Applichem, Darmstadt, GER
Dithiothreitol (DTT)	Sigma-Aldrich, Steinheim, GER
Dithiothreitol (DTT)	Sigma-Aldrich, Steinheim, GER
Amersham™ ECL™ Prime Western Blotting Detection Reagents	GE Healthcare, Buckinghamshire, UK
ECL Western Blotting Detection Reagents	GE Healthcare, Buckinghamshire, UK
Ethanol (EtOH, 96%)	Paul-Ehrlich-Institut
Ethylenediaminetetraacetic acid (EDTA)	Paul-Ehrlich-Institut
FACS Clean	BD Biosciences, Heidelberg, GER
FACS Flow (Sheath Solution)	Paul-Ehrlich-Institute
FACS Rinse	BD Biosciences, Heidelberg, GER
Fetal Calf Serum (FCS)	Sigma-Aldrich, Steinheim, GER
Fluorescein isothiocyanate (FITC)-dextran (MW 40,000)	Sigma-Aldrich, Steinheim, GER
Glycerol (99%)	Citifluor, London, UK
Golgiplug™ Protein Transport Inhibitor (containing Brefeldin-A)	BD Biosciences, Heidelberg, GER
Golgistop™ Protein Transport Inhibitor (containing Monensin)	BD Biosciences, Heidelberg, GER
HEPES, 1 M	Merck, Darmstadt, GER
High-purity water	Paul-Ehrlich-Institut
Histopaque 1.077 g/ml	Sigma-Aldrich, Steinheim, GER
Human Serum Type AB	Sigma-Aldrich, Steinheim, GER
Hydrochloric acid 37%	Roth, Karlsruhe, GER
Luminata™ Forte Western HRP Substrate	Merck, Darmstadt, GER
MEM Non-Essential Amino Acids Solution (Gibco™,10 mM, 100x)	Thermo Fisher Scientific, Dreieich, GER
MEM Sodium Pyruvate (Gibco™,100 mM)	Thermo Fisher Scientific, Dreieich, GER
MEM Vitamin Solution (Gibco™, 100x)	Thermo Fisher Scientific, Dreieich, GER
Methanol (MeOH)	Paul-Ehrlich-Institut

Chemical/ Reagent	Manufacturer/ Distributor
Paraformaldehyde (PFA)	Sigma-Aldrich, Steinheim, GER
Penicillin, 10000 U/ml/ Streptomycin, 10 mg/ml	Biochrom, Berlin, GER
Puromycin	InvivoGen, Toulouse, FR
Ringer's solution	B. Braun, Melsungen, GER
Roswell Park Memorial Institute (RPMI) 1640 w/o L-glutamine	Biowest, Nuaillé, FR
Skim-milk powder	EDEKA, Hamburg, GER
Sodium azide (NaN_3)	Sigma-Aldrich, Steinheim, GER
TEMED (Tetramethylethylendiamine)	Roth, Karlsruhe, GER
Tris solutions	Paul-Ehrlich-Institute
Trypsin 0.25%/ EDTA 1%/ PBS w/o Ca^{2+}, Mg^{2+}	Paul-Ehrlich-Institut
β-Mercaptoethanol	Sigma-Aldrich, Steinheim, GER
123count eBeads™ Counting Beads, Invitrogen™	Thermo Fisher Scientific, Dreieich, GER
UltraComp eBeads™ Compensation Beads, Invitrogen™	Thermo Fisher Scientific, Dreieich, GER
PageRuler™ Plus Prestained Protein Ladder, 10 to 250 kDa	Thermo Fisher Scientific, Dreieich, GER

5.1.4 Commercial Kits

Commercial Kit	Manufacturer/ Distributor
Annexin V-FITC Kit	Miltenyi Biotec, Bergisch Gladbach, GER
BD Cytofix/Cytoperm™, Fixation/Permeabilization Solution Kit	BD Biosciences, Heidelberg, GER
CD14 MicroBeads, human	Miltenyi Biotec, Bergisch Gladbach, GER
EasySep™ Human $CD4^+$ T cell isolation	StemCell Technologies, Cologne, GER
EasySep™ Human $CD8^+$ T cell isolation	StemCell Technologies, Cologne, GER
eBiosciene™ Foxp3 Transcription Factor Staining Buffer Set	Thermo Fisher Scientific, Dreieich, GER

5.1.5 Dyes

Dye	Manufacturer/ Distributor
Carboxyfluorescein succinimidyl ester (CFSE)	Sigma-Aldrich Chemie, Steinheim, GER
CellTrace™ Far Red Cell Proliferation Kit	Thermo Fisher Scientific, Dreieich, GER
Fixable Viability Dye, Zombie Yellow	Biolegend, San Diego, USA
Hoechst 33342 fluorescent nucleic acid stain	ImmunoChemistry Technologies, LLC, USA
Trypan Blue	Lonza, Basel, CH

5.1.6 Antibodies

If not otherwise specified, all listed antibodies are directed against human target molecules.

Target molecule	Clone	Isotype	Manufacturer
Anti-284 (TLR4) PE	HTA125	Mouse IgG2a, κ	BioLegend, San Diego, USA
Anti-2B4 APC	C1.7	Mouse IgG1, κ	BioLegend, San Diego, USA
Anti-CCR7 APC-Cy7	G043H7	Mouse IgG1, κ	BioLegend, San Diego, USA
Anti-CD107a	H4A3	Mouse IgG1, κ	BioLegend, San Diego, USA
Anti-CD14 PB	M5E2	Mouse IgG2a,κ	BioLegend, San Diego, USA
Anti-CD19 APC	HIB19	Mouse IgG1, κ	BioLegend, San Diego, USA
Anti-CD19 APC/Fire 750	HIB19	Mouse IgG1, κ	BioLegend, San Diego, USA
Anti-CD1a FITC	HI149	Mouse IgG1, κ	BD Biosciences, Heidelberg, GER
Anti-CD1a PerCP-Cy5.5	HI149	Mouse IgG1, κ	BioLegend, San Diego, USA
Anti-CD209 APC	DCN46	Mouse IgG2b, κ	BD Biosciences, Heidelberg, GER
Anti-CD25 APC	M-A251	Mouse IgG1, κ	BioLegend, San Diego, USA
Anti-CD28/CD49d (BD FastImmune™)	L293/ L25	Mouse IgG1, κ/ IgG2b, κ	BD Biosciences, Heidelberg, GER
Anti-CD282/ TLR2 AF488	T2.5	Mouse IgG1, κ	BioLegend, San Diego, USA

Target molecule	Clone	Isotype	Manufacturer
Anti-CD283/TLR3 PE	TLR-104	Mouse IgG2a, κ	BioLegend, San Diego, USA
Anti-CD3 PB	UCHT1	Mouse IgG1,κ	BioLegend, San Diego, USA
Anti-CD4 APC/Fire 750	RPA-T4	Mouse IgG1, κ	BioLegend, San Diego, USA
Anti-CD4 PE-Cy7	RPA-T4	Mouse IgG1, κ	BioLegend, San Diego, USA
Anti-CD40 AF647	5C3	Mouse IgG1, κ	BioLegend, San Diego, USA
Anti-CD45RA PerCP-Cy5.5	HI100	Mouse IgG2b, κ	BioLegend, San Diego, USA
Anti-CD45RO APC	UCHL1	Mouse IgG2a, κ	BD Biosciences, Heidelberg, GER
Anti-CD56 (NCAM) PE	HCD56	Mouse IgG1, κ	BioLegend, San Diego, USA
Anti-CD56 (NCAM) PerCP-Cy5.5	HCD56	Mouse IgG1, κ	BioLegend, San Diego, USA
Anti-CD62L PE-Vio770	145/15	Mouse IgG1, κ	Miltenyi Biotec, Bergisch Gladbach, GER
Anti-CD8 APC/Fire 750	SK1	Mouse IgG1, κ	BioLegend, San Diego, USA
Anti-CD8 APC-Cy7	SK1	Mouse IgG1, κ	BioLegend, San Diego, USA
Anti-CD8 PB	RPA-T8	Mouse IgG1, κ	BioLegend, San Diego, USA
Anti-CD80 PE-Cy7	2D10	Mouse IgG1, κ	BioLegend, San Diego, USA
Anti-CD86 FITC	2331	Mouse IgG1, κ	BD Biosciences, Heidelberg, GER
Anti-CTLA-4 PE-Cy7	L3D10	Mouse IgG1, κ	BioLegend, San Diego, USA
Anti-HLA-A2 FITC	BB7.2	Mouse IgG2b, κ	BioLegend, San Diego, USA
Anti-HLA-DR PB	L243	Mouse IgG2a, κ	BioLegend, San Diego, USA
Anti-IFNγ APC	4S.B3	Mouse IgG1, κ	BioLegend, San Diego, USA
Anti-IL-2	MQ1-17H12		BioLegend, San Diego, USA
Anti-LAG-3 PE-Cy7	11C3C65	Mouse IgG1, κ	BioLegend, San Diego, USA
Anti-MyD88 AF488	316628	Rat IgG2b	R&D Systems, minneapolis, USA

Target molecule	Clone	Isotype	Manufacturer
Anti-PD-1 PerCP-Cy5.5	EH12.2H7	Mouse IgG1, κ	BioLegend, San Diego, USA
Anti-PD-L1 APC	29E.2A3	Mouse IgG2b, κ	BioLegend, San Diego, USA
Anti-PD-L1 PE	29E.2A3	Mouse IgG2b, κ	BioLegend, San Diego, USA
Anti-Tim-3 PerCP-Cy5.5	F38-2E2	Mouse IgG1, κ	BioLegend, San Diego, USA
Anti-TLR7	533707	Mouse IgG2a	R&D Systems, minneapolis, USA
Anti-TLR8	935166	Mouse IgG2b	R&D Systems, minneapolis, USA
Anti-TNFα PE-Cy7	Mab11	Mouse IgG1, κ	BioLegend, San Diego, USA
Isotype Ctrl APC	MPC-21	Mouse IgG2b, κ	BioLegend, San Diego, USA
Isotype Ctrl APC	MOPC-21	Mouse IgG1, κ	BioLegend, San Diego, USA
Isotype Ctrl APC	27-35	Mouse IgG2b, κ	BD Biosciences, Heidelberg, GER
Isotype Ctrl APC-Cy7	MOPC-173	Mouse IgG2a, κ	BioLegend, San Diego, USA
Isotype Ctrl FITC	MOPC-21	Mouse IgG1, κ	BD Biosciences, Heidelberg, GER
Isotype Ctrl FITC	27-35	Mouse IgG2b, κ	BD Biosciences, Heidelberg, GER
Isotype Ctrl FITC	A95-1	Rat IgG2b	BD Biosciences, Heidelberg, GER
Isotype Ctrl PB	MOPC-173	Mouse IgG2a, κ	BioLegend, San Diego, USA
Isotype Ctrl PE	MOPC-173	Mouse IgG2a, κ	BioLegend, San Diego, USA
Isotype Ctrl PE	MPC-11	Mouse IgG2b, κ	BioLegend, San Diego, USA
Isotype Ctrl PE-Cy7	MOPC-21	Mouse IgG1, κ	BioLegend, San Diego, USA
Isotype Ctrl PerCP-Cy5.5	MOPC-21	Mouse IgG1, κ	BioLegend, San Diego, USA

Target molecule	Clone	Isotype	Manufacturer
Anti-α-Tubulin (#3873)	DM1a	Mouse IgG1	Cell Signaling Technology, Leiden, NLD
Anti-IκBα (#9242)		Rabbit	Cell Signaling Technology, Leiden, NLD
Anti-mouse IgG1κ binding protein-HRP	-	Binding Protein	Santa Cruz Biotechnology, Heidelberg, GER
Anti-rabbit IgG, HRP linked (#7074)		Goat	Cell Signaling Technology, Leiden, NLD

5.1.7 Peptides and tetramers

Peptides and tetramers	Manufacturer
Influenza matrix protein 1, $FluM1_{58-66}$, GILGFVFTL, HLA-A*02:01 restricted	Innovagen AB, Lund, SWE
Tetanus toxoid, TT $p2_{829-844}$, MQYIKANSKFIGITEL, HLA-DRB*11:01 restricted	MBL® International Corporation, Woburn, USA
NY-ESO-1, SLLMWITQV, HLA-A*02:01 restricted	Iba, Goettingen, GER
iTAg™ MHC Tetramer, HLA-A*02:01, Influenza M1, GILGFVFTL, PE	MBL® International Corporation, Woburn, USA
T-select HLA-DRB*11:01 Tetramer, TT p2 829-844 MQYIKANSKFIGITEL, PE	MBL® International Corporation, Woburn, USA

5.1.8 Cell culture media and buffers

Buffers that were obtained from the in-house facility, being responsible for the manufacturing of ultra-pure H_2O, solutions and growing media, are marked with 'Paul-Ehrlich-Institut'.

Cell culture medium/ Buffer	Components
A'Medium	M'Medium
	5% human AB serum (v/v)
B'Medium	M'Medium
	10% FCS (v/v)
Blocking solution (Western Blot)	TBST
	5% skim-milk powder (w/v)

Cell culture medium/ Buffer	**Components**
Blotting buffer (Western Blot, Paul-Ehrlich-Institut)	ddH_2O
	50 mM Tris
	40 mM Glycine
	0.0375% SDS (w/v)
	2.5% MeOH (v/v)
Complete medium	RPMI 1640
	10% FCS (v/v)
	2 mM L-glutamine
	100 U/ml Penicillin
	100 µg/ml Streptomycin
	10 mM HEPES buffer
	50 µM β-Mercaptoethanol
EasySep™ Recommended buffer	PBS
	2% FCS
	1 mM EDTA
FACS blocking buffer	PBS pH 7.1
	10% FCS (v/v)
	10% human AB Serum (v/v)
Freezing medium	CM
	40% FCS (v/v)
Intracellular FACS blocking buffer	1x BD Perm/Wash™ solution (BD Cytofix/Cytoperm™ kit) **or**
	1x Permeabilization Buffer (eBioscienceTM Foxp3/ Transcription factor buffer staining kit)
	10% FCS (v/v)
	10% human AB serum (v/v)
Laemmli buffer (6x)	ddH_2O
	500 mM Tris-HCl pH 6.8
	38% Glycerol (v/v)
	10% SDS (w/v)
	600 mM DTT
	0.01% Bromophenol blue

Cell culture medium/ Buffer	Components
M' Medium	RPM1 1640
	2 mM L-glutamine
	1x MEM Vitamin Solution
	1 mM MEM Sodium Pyruvate
	1x MEM Non-essential amino acids
	100 U/ml Penicillin
	100 µg/ml Streptomycin
	50 µM β-Mercaptoethanol
MACS buffer (Paul-Ehrlich-Institut)	PBS pH 7.2
	0.5% BSA (w/v)
	0.5 mM EDTA
HEK293T/TLR7 Medium	DMEM
	10% FCS
	2 mM L-glutamine
	100 U/ml Penicillin
	100 µg/ml Streptomycin
	+ 5 µg/ml Blasticidin (added freshly)
	+ 2 µg/ml Puromycin (added freshly)
Paraformaldehyde solution (4%)	PBS pH 7.1
	4% Formaldehyde (w/v)
Phosphate-buffered saline (PBS) w/o Ca^{2+}/Mg^{2+} (Paul-Ehrlich-Institut)	ddH_2O
	140 mM NaCl (w/v)
	10 mM Na_2HPO_4 x 2 H_2O
	2.7 mM KCl (w/v)
	1.8 mM KH_2PO_4
Raji Medium	10% FCS (heat-inactivated)
	2 mM L-glutamine
	100 U/ml Penicillin
	100 µg/ml Streptomycin
	0.05 mM β-Mercaptoethanol
SDS-PAGE Running buffer (5x, Paul-Ehrlich-Institut)	ddH_2O
	125 mM Tris
	1.25 M Glycine
	0.5% SDS (w/v)

Cell culture medium/ Buffer	Components
Separation gel buffer	ddH_2O
	0.5 M Tris-HCl pH 8.8
	0.4% SDS (w/v)
Stacking gel buffer	ddH_2O
	1.5 M Tris-HCl pH 6.8
	0.4% SDS (w/v)
TAE buffer (TAE, 20x, Paul-Ehrlich-Institut)	ddH_2O
	0.8 M Tris (w/v)
	2.25% acetic acid (v/v)
	20 mM EDTA
Tris-buffered saline + Tween-20 (TBST, Paul-Ehrlich-Institut)	ddH2O
	50 mM Tris-HCl pH 7.4
	150 mM NaCl
Wash buffer (PBMC isolation)	PBS pH 7.1
	5% CM (v/v)

5.1.9 Cytokines and immunomodulators

Cytokine/ Immunomodulators	Manufacturer/ Distributor
Interleukin 4 Recombinant Human Protein, Gibco™	Thermo Fisher Scientific, Dreieich, GER
Human Recombinant Granulocyte Macrophage Colony Stimulation Factor (GM-CSF), Leukine®	Bayer Healthcare Pharmaceutical, Leverkusen (GER)
Interleukin 2 Recombinant Human Protein, PROLEUKIN® S	Novartis AG, Basel, CHE
Phytohemagglutinin-L (PHA-L)	Sigma-Aldrich, Steinheim, GER
Cell Activation Cocktail (without Brefeldin A, containing PMA/ Ionomycin)	BioLegend, San Diego, USA
Addavax™	InvivoGen, Toulouse, FRA
Alhydrogel® adjuvant 2%, Brenntag Biosector A/S	InvivoGen, Toulouse, FRA
Quil-A® adjuvant, Brenntag Biosector A/S	InvivoGen, Toulouse, FRA
Trehalose-6,6-dibehenate (TDB) Vaccigrade™	InvivoGen, Toulouse, FRA
Pam3CSK4 Vaccigrade™	InvivoGen, Toulouse, FRA

Cytokine/ Immunomodulators	Manufacturer/ Distributor
Lipopolysaccharide from Escherichia coli 0111:B4 (LPS-EB) Ultrapure	InvivoGen, Toulouse, FRA
Monophosphoryl Lipid A (MPLA) Synthetic Vaccigrade™	InvivoGen, Toulouse, FRA
Monophosphoryl Lipid A from S. minnesota R595 (MPLA-SM) Vaccigrade™	InvivoGen, Toulouse, FRA
Gardiquimod™ Vaccigrade™	InvivoGen, Toulouse, FRA
Imiquimod (R837) Vaccigrade™	InvivoGen, Toulouse, FRA
Resiquimod (R848) Vaccigrade™	InvivoGen, Toulouse, FRA

5.1.10 Cells

Cells/ Cell line	Source
Peripheral blood mononuclear cells	Buffy Coat, DRK-Blood donation centre Baden-Wuerttemberg-Hessen, Frankfurt, GER
Peripheral blood mononuclear cells with HLA-DRB1*11:01 characteristic	Whole Blood, Donors of the Paul-Ehrlich-Institute
HEK 293/TLR7-NF-kB luciferase	Generously gifted by Prof. S. Chanda, Sanford-Burnham Medical Research Institute
Raji (human B cell lymphoma cells)	Generously gifted by Prof. J.P. Schneck, Johns Hopkins School of Medicine ATCC: CCL-86 ™
HLA-A*02:01–positive, TAP-deficient 174xCEM.T2 (T2) cells	Generously gifted by Prof. J.P. Schneck, Johns Hopkins School of Medicine ATCC: CRL-1992™

5.1.11 Softwares

Softwares	Manufacturer
BD FACSDiva™ Software v8.0.1	BD Biosciences, Heidelberg, GER
Citavi v6.3	Swiss Academic Software, Waedenswil, CHE
FlowJo v10.6.1	BD Biosciences, Heidelberg, GER
GraphPad Prism v8.3.1	GraphPad Software Inc., La Jolla, USA
LabImage1D – Gel and Blot Analysis Software	Intas, Göttingen, GER

Softwares	Manufacturer
Microsoft Office (2016, 2019)	Microsoft Corporation, Redmond, USA
Qlucore Omnics Explorer v3.5	Qlucore, Lund, SWE
Zeiss AxioVision Rel. Imaging v4.8	Carl Zeiss Microscopy, Jena, GER

5.2 Methods

5.2.1 Cell culture methods

All cell culture procedures were carried out under sterile conditions provided by a laminar flow workbench. Human cells were incubated at 37°C with 5% CO_2.

5.2.1.1 Counting of cells

Peripheral blood mononuclear cells (PBMCs), peripheral blood lymphocytes (PBL), $CD14^+$ monocytes and dendritic cells (DCs) were counted with a CASY cell counter model TT using a 150 µM capillary. The sample was prepared by 1:10,000 dilution in CASYton. The cell concentration was determined by three subsequent automatic measurements of the sample. Additionally, cell size, cell viability and cell aggregation were specified. The calculation of the final cell concentration is based on the viable cell count and furthermore takes cell aggregation into account.
T cells and cell lines were counted using a Neubauer improved hemocytometer (depth: 0.1 mm). Cells were diluted in Trypan Blue for exclusion of apoptotic cells. The mean of cell number counted in four squares was multiplied by the chamber factor (10^4) and the dilution factor.

5.2.1.2 Cultivation of cell lines

HLA-A*02:01–positive, TAP-deficient 174xCEM.T2 (T2) cells consist of T and B lymphoblast and remain in suspension. This cell line is suitable for efficient external loading of peptides given to the culture. Since T2 cells are TAP-deficient and thus have a low level of peptides for presentation on MHC class I, most molecules remain empty or associate with low affinity peptides. The addition of high-affinity peptides to the T2 culture lead either to the binding of the peptide to empty MHC class I molecules and consequently to their stabilization or to the replacement of bound low-affinity peptides (Cerundolo et al., 1990; Wei and Cresswell, 1992). T2 cells were cultivated in B'medium in a 25 or 75 cm^2 T-culture flasks in standing position. They were splitted twice a week to a concentration of 0.25 x 10^6 cells/ml. Therefor, cells were centrifuged at 500 x g for

5 min at RT and resuspended to the final concentration by addition of fresh B'medium (T25: 10 ml, T75: 30 ml).
The Raji cell line consists of B cell lymphoma cells, which remain in suspension. Cells were cultivated in Raji medium in T25 flasks (standing position) and splitted twice a week to a concentration of 0.04 x 10^6 cells/ml (T25: 6 ml) as described above.
The HEK 293/TLR7-NF-kB luciferase cell line was generated by (Chiang et al., 2012) by transfecting HEK293T with TLR7 expression vectors and a 5x NF-κB luciferase reporter construct. For splitting of this adherent cell line, supernatant was discarded, cells were washed with pre-warmed PBS and incubated with Trypsin-EDTA for 5 min at 37°C. Enzymatic reaction was stopped by addition of sufficient HEK293T/TLR7 culture medium. Cells were counted and adjusted to 0.13 x 10^6 cells/ml and transferred to a culture flask (T25: 5 ml). Blasticidin (5 µg/ml) and Puromycin (2 µg/ml) were added freshly to each passage.

5.2.1.3 Isolation of human PBMCs from buffy coat

PBMCs were isolated from buffy coats obtained from blood donations of healthy and anonymous donors (DRK Blood donation centre Baden-Wuerttemberg-Hessen, Frankfurt, ethical approval #329/10.). The buffy coat was disinfected, then opened under sterile conditions and filled into a bottle. The 30 to 50 ml buffy coat was diluted with prewarmed PBS to a final volume of 100 ml and divided onto four 50 ml falcons as followed: 25 ml of the diluted buffy coat was carefully layered on top of 15 ml prewarmed Histopaque 1077 without perturbing the Histopaque-phase. Subsequently, the tubes were centrifuged at 537 x g for 30 min with acceleration and deceleration at its lowest level to separate red blood cells, PBMCs and plasma. The PBMC-containing interphase was harvested and evenly distributed to six 50 ml falcon tubes and filled up with prewarmed wash buffer. Several washing steps at different rotation speeds (1084, 573, 143 x g; 8 min, RT) followed, to remove cell debris and thrombocytes. Contaminating erythrocytes were lysed with cold 0.15 M ammonium chloride for 10 min at RT. Cells were washed again (143 x g, 8 min, RT) and pooled in one falcon tube. PBMCs were counted and further processed in 5.2.1.5.

5.2.1.4 Isolation of PBMCs from whole blood

For antigen-specific $CD4^+$ T cell experiments (5.2.2.6), donors with the HLA characteristic DRB*11:01 were required. HLA characteristics were identified by HLA typing performed at the DRK Blood donation center, Frankfurt and at the DKMS, Tübingen. Blood sampling of donors (up to 100 ml blood/ donor), HLA-typing and the

experimental procedure was approved by the local ethics committee (Identification no. 19-226; Department of Medicine, Goethe University, Frankfurt) and informed, written consents were obtained from all donors. Blood was collected in tubes containing 3.2% citrate using a multifly needle set. Whole blood was collected in a glas bottle diluted with PBS to a final volume of 200 ml. 25 ml of diluted blood was layered over a histopaque (1.077 g/ml, 15 ml) phase, followed by a density gradient centrifugation (537 x g for 30 min with acceleration and deceleration at its lowest level). PBMCs were isolated as described in 5.2.1.3.

5.2.1.5 Isolation of CD14$^+$ monocytes from PBMCs

PBMCs were isolated as described in 5.2.1.3 and 5.2.1.4. All steps required for Magnetic Cell Separation (MACS) were performed at 4°C. Cells were washed in cold MACS buffer and centrifuged at 322 x g for 6 min. Subsequently, cells were resuspended in 95 µl MACS buffer/ 10x10^6 cells. For the positive isolation of CD14$^+$ monocytes, CD14 microbeads were given at a concentration of 5 µl/ 10x10^6 cells to the cell solution. The sample was incubated for 20 min at 4°C followed by a washing step with MACS buffer (322 x g, 6 min). Subsequently, the supernatant was discarded and the cell pellet resuspended in 3 ml MACS buffer. LS columns were placed in the magnetic field of a Midi-MACS separator and equilibrated by rinsing the column with 5 ml MACS buffer. The bead-labeled cell suspension was applied to the column. Unlabeled cells (CD14$^-$, PBLs) that passed through were collected. The column was washed three times with 3 ml MACS buffer to remove residual CD14$^-$ cells. Then, the column was removed from the separator and placed on a new falcon. The column was filled with 5 ml MACS buffer and CD14$^+$ cells were flushed out of the column by using the plunger. Eluted CD14$^+$ monocytes were counted and the required amount was differentiated to monocyte-derived DCs (5.2.1.6). The collected flow-through (CD14$^-$ PBLs) was centrifuged (322 x g, 6 min) and frozen as described in 5.2.1.7 for the isolation of T cells (5.2.1.8) at a later time point.

5.2.1.6 Generation of monocyte-derived DCs

CD14$^+$ monocytes were isolated by MACS (5.2.1.5), spun down (322 x g, 6 min) and resuspended in CM. Cells were seeded at a density of 1.5x10^6 monocytes/ well in 2 ml CM supplemented with 10 ng/ml IL-4 and 5 ng/ ml GM-CSF. Cells were differentiated for 5-6 days with a medium refresh on day 3. For that, 1 ml CM with 30 ng/ml IL-4 and 15 ng/ml GM-CSF was added to each well.

Immature DCs do not adhere to the plate surface and thus can be harvested by gently flushing the cells. All wells were collected in a tube and centrifuged at 322 x g for 6 min at RT. DCs were resuspended in an appropriate amount of medium and counted (5.2.1.1). The phenotype of immature DCs was randomly controlled by flow cytometry. Fully differentiated immature DCs are $CD14^-$, $CD1a^+$ and $CD209^+$ (Sallusto and Lanzavecchia, 1994; Geijtenbeek et al., 2000).

5.2.1.7 Freezing and thawing of cells

PBMCs, which remained after isolation (5.2.1.3) and collected $CD14^-$ after $CD14^+$ MACS isolation (5.2.1.5) were counted and afterwards centrifuged at 322 x g for 6 min. The supernatant was completely removed and the cell pellet was resuspended in the appropriate amount of freezing medium (900 µl/ $100x10^6$ cells) containing FCS in a final concentration of 40%. Up to $100x10^6$ cells/ml were frozen in a volume of 1 ml (corresponds to one cyro vial), containing 900 µl cell solution and 100 µl dimethyl sulfoxide (DMSO). A Nalgene™ Mr. Frosty Freezing container served for consistent freezing (-1°C/min) to -80°C. Frozen cells were stored at -80°C until use.

The T2 and HEK 293/TLR7-NF-kB luciferase cell line (5.2.1.2; 5.1.10) were both expanded in a low passage number to generate several aliquots for freezing. These cells were frozen at a density of $5x10^6$ cells/ml in freezing medium supplemented with 10% DMSO. Cells were frozen in a Nalgene™ Mr. Frosty Freezing container at -80°C and transferred on the next day to liquid nitrogen.

Aliquots with frozen cells were thawed in the water bath at 37°C. As soon as the cell suspension was ice crystal free, cells were slowly dropped into pre-warmed culture medium. Cells were centrifuged at 143 x g for 8 min at RT. Supernatant was discarded and the pellet carefully resuspended in the respective culture medium. Cell lines were directly seeded in T25 culture flasks. PBMCs and $CD14^-$ PBLs were counted (5.2.1.1) and used for the isolation of T cells (5.2.1.8) or directly applied in an experimental setting (5.2.2.5.1, 5.2.2.5.2, 5.2.2.5.3).

5.2.1.8 Isolation of $CD4^+$ and $CD8^+$ T cells from PBMCs or $CD14^-$ PBL

$CD4^+$ and $CD8^+$ T cells were isolated using an untouched (negative) selection procedure (EasySep™) from StemCell Technologies to prevent stress-mediated activation of T cells through the interaction with antibodies and beads or the passaging through a column.

Cryo vials with PBMCs or $CD14^-$ PBLs were thawed (5.2.1.7) and cell solution was directly dropped into EasySep™'s recommended buffer, which was warmed to RT. Cells were centrifuged at 143 x g for 8 min, resuspended in EasySep™ buffer and passed

through a 30 µM filter mesh to remove cell clumps. After cell counting (5.2.1.1), cells were adjusted to $50x10^6$ cells/ml and transferred to sterile 5 ml FACS tubes with cap. In contrast to the MACS isolation protocol, EasySep™ separates at RT. Due to limitations of the EasySep™ magnet, only up to $100x10^6$ cells per isolation can be used. A higher number of cells required several rounds of isolation. In brief, isolation cocktail (50 µl/ml of sample) was added to the cell solution. During the incubation of 5 min at RT, RapidSpheres™ were vortexed and subsequently given to the sample. Then, the sample volume was adjusted to 2.5 ml with EasySep™ buffer and the FACS tube (without cap) was placed into the magnet. After 3 min incubation, the magnet with the tube was picked up and inverted in one continuous motion to pour the enriched cell suspension into a new tube. Isolated cells were counted and used in antigen-specific experiments (5.2.2.6).

5.2.2 Experimental assays

5.2.2.1 Endotoxicity test: Limulus amebocyte lysate test

Bacterial endotoxin testing is described in the Pharmacopoeia of Europe and the United States to detect and quantify endotoxin within a sample. The limulus amebocyte lysate test is the golden standard of bacterial endotoxin tests. It is based on the aqueous extract from amebocytes of the North American Horseshoe Crab (*Limulus polyphemus*), which generates a coagulation cascade triggered by endotoxin. This enzymatic reaction leads to the formation of a gel clot. The developing turbidity can be measured (Sandle, 2016). The LAL test was performed by P. Windecker and I. Spreitzer at the Paul-Ehrlich-Institut at the department of Microbiology (Microbiological Safety). Adjuvants were prepared in CM at the concentrations defined for this project (Table 1). Except for LPS, MPL-s and MPL-SM, only the high concentration of the adjuvant was applied for testing. In addition, the solvents CM and CM+0.1%DMSO were also analyzed for endotoxin contamination. The LAL test used here, is based on the kinetic-turbimetric method using Pyrotell®- T lysate, which was solved in Pyrosol® buffer. Each sample underwent a product positivity test (spike) with 0.5 EU/ml LPS to exclude possible confounding factors within the sample. The determination of endotoxin amount was valid, if 50-200 % of the spiked endotoxin was recovered. Turbidity was measured with the ELx808™ microplate reader at 340nm. Endotoxin concentrations were calculated using the endotoxin European pharmacopoeia reference standard generated standard curve.

5.2.2.2 Pyrogenicity test: Monocyte activation test

The monocyte activation test (MAT) is an *in vitro* test to detect and quantify pryogenic substances that activate human monocytes, leading to the release of fever-inducing mediators such as the inflammatory cytokines TNFα, IL-1β and IL-6, which are then detected by Enzyme-linked Immunosorbent Assay (ELISA). The MAT was developed to replace the rabbit pyrogen test. In Europe, the MAT was accepted as alternative endotoxin test method in 2010 (European Pharmacopoeia, 10th edition, English, 2019, monograph 2.10; Sandle, 2016).

The pyrogenicity of the adjuvant solutions at the indicated concentrations (Table 1) was analyzed using the MAT, which was performed by P. Windecker and I. Spreitzer at the Paul-Ehrlich-Institut (Department of Microbiology; Microbiological Safety).

The monocyte activation test was carried out as previously described (Schindler et al., 2006; Montag et al., 2007). In brief, 20 µl cryopreserved human whole blood and adjuvant solution was added to 200 µl RPMI. Samples were tested in triplicates. The standard curve was prepared using the endotoxin European pharmacopoeia reference standard. The spiking with 0.5 EU/ml LPS of each sample served as control. Plates were incubated at 37°C, 5% CO_2 overnight. A volume of 100 µl per well was used for the IL-β cytokine ELISA.

5.2.2.3 Stimulation of cells with adjuvants

The adjuvants used in this study have a specific purity grad (VacciGrade™) for preclinical studies: They are prepared under strict aseptic conditions and guaranteed sterile. Quil and $Al(OH)_3$ were produced according to GMP guidelines by Brenntag Biosector A/S. Lyophilized adjuvants were solved according to InvivoGen's instructions and aliquoted to limit thawing and freezing to a maximum of 5 cycles. Furthermore, a single batch of adjuvants was used throughout the study. The concentrations (Table 1) were determined at the beginning of this project by analyzing cytotoxicity and proliferation-inducing capacity of the adjuvants (5.2.2.5.1; 6.2).

Table 1: Adjuvants and their respective concentrations used throughout this study.

Immunomodulator	Abbr.	Information	Low conc.	High conc.
Trehalose-6,6-dibehenate VacciGrade™	TDB	Mincle ligand	1 µg/ml	10 µg/ml
Pam3CSK4 VacciGrade™	Pam	TLR1/2 ligand	100 pg/ml	1 µg/ml
Gardiquimod VacciGrade™	GARD	TLR7 ligand	0.35 µM	3 µM
Imiquimod VacciGrade™	IMQ	TLR7 ligand	3.6 µM	36 µM

Immunomodulator	Abbr.	Information	Low conc.	High conc.
Resiquimod VacciGrade™	R848	TLR7/8 ligand	0.15 µM	1 µM
Positive control (LPS-EB, ultrapure)	LPS	TLR4 ligand	38.4 pg/ml	0.1 µg/ml
Synthetic monophosphoryl lipid A VacciGrade™	MPL-s	TLR4 ligand	0.01 µg/ml	1 µg/ml
Monophosphoryl lipid A (*S. minnesota R595)* VacciGrade™	MPL-SM	TLR4 ligand	0.01 µg/ml	1 µg/ml
Addavax™ VacciGrade™	ADX	squalene-based oil-in-water nano-emulsion	15 µg/ml	150 µg/ml
Quil-A® adjuvant	Quil	saponin adjuvant	0.15 µg/ml	1.5 µg/ml
Alhydrogel® 2%	$Al(OH)_3$	aluminum hydroxide wet gel suspension	1 µg/ml	10 µg/ml

For the stimulation of the cells with adjuvants, a x-fold concentrated working solution was prepared before each experiment by diluting the adjuvants in CM or A'M (antigen-specific assays). The concentrated working solution was diluted to the final concentration (Table 1) upon addition to the cell solution present within the well.

5.2.2.4 Fluorescent labeling of cells with proliferation dyes

Proliferation of lymphocytes can be studied by labeling of the cells with fluorescent dyes, which enter the cell by diffusion through the cell membrane. They bind intracellularly to proteins, which result in retention of the dye within the cell. Particularly, dyes such as 6-Carboxyfluorescein N-succinimidyl ester (CFSE) and CellTrace™ FarRed contain a cell-permeant nonfluorescent ester of an amine-reactive fluorescent molecule, which gets cleaved by the cell's esterases, leading to the conversion into a fluorescent derivative. Upon division of the cell, daughter cells receive half of the fluorescent label of their parent cells, allowing the analysis of proliferation by flow cytometry.

DCs and PBLs or T cells were stained with 4 µM CFSE in CM for 12 min at 37°C. Staining with CellTrace™ FarRed required a protein-free environment. Therefore, cells were washed with PBS and subsequently labeled with 1 µM CellTrace™ FarRed in a volume of 1 ml PBS for 20 min at 37°C. The excess of both dyes was quenched with the addition of sufficient CM. Cells were washed (322 x g, 6 min, RT), resuspended in CM or A'M (antigen-specific assays) and counted (5.2.1.1).

5.2.2.5 Antigen-independent experiments

To assess the adjuvant-specific reaction, the following assays were carried out without the addition of antigen.

5.2.2.5.1 Cytotoxicity test: Annexin-V/ Propidium iodide staining

To determine the concentration of the adjuvants, concentration-dependent cytotoxicity was analyzed with Annexin-V/PI staining by flow cytometry. Annexin-V binds to phosphatidylserine, which gets flipped to the extracellular surface of the cell membrane, when the cell undergoes apoptosis (Vermes et al., 1995). Propidium iodide (PI) is used as a marker for cell membrane permeability (Belloc et al., 1994), which is seen in late apoptosis or necrosis.

The proliferation-inducing capacity was also examined in this assay. Therefore, DCs were harvested (5.2.1.6), autologous $CD14^-$ PBLs were thawed (5.2.1.7), cells were counted (5.2.1.1) and both were labeled with 1 µM CellTrace™ FarRed (5.2.2.4). After washing and another counting, cells were seeded in 96-well U-shape plates. DCs were plated first at $2x10^4$ cells/ well and were rested for 30 min at 37°C in the incubator. Afterwards, $1x10^5$ PBLs were added to each well to achieve a 1:5 ratio of DCs:PBLs. As a last step, the adjuvant working solutions were prepared and added to the wells. Nine serial diluted concentrations were tested of each adjuvant in duplicates.. The negative control was left untreated. Here, CM was added to the wells at the same volume as the adjuvant working solution. After 6 days of incubation (37°C, 5% CO_2), cells were prepared for flow cytometric analysis. To detach all cells, the plate was put on ice for 30 min. Subsequently, supernatant was discarded, cells were washed with PBS and Trypsin/ EDTA solution was given to the cells for 7 min at 37°C. Reaction was stopped with CM, duplicates were pooled, cells were washed and resuspended in Ringer solution, which is required for the Ca^{2+}-dependent binding of Annexin-V to phosphatidyl serine. The master mix of Annexin-V/ PI was prepared and given to the sample. After a 10 min incubation, flow cytometry analysis should then be accomplished within the next 45 min to prevent PI-induced cytotoxicity. A control for Annexin-V/ PI positivity was generated with a heat-shock of left-over cells. Therefore, cells were heated at 65°C for 4 min and afterwards put directly on ice. Around half of the cells were then Annexin- V/ PI positive.

5.2.2.5.2 Investigation of DC maturation following adjuvant stimulation

Dendritic cells were harvested on day 5 or 6 of culture (5.2.1.6), counted (5.2.1.1) and seeded at a density of $4x10^5$ DCs/ well in 24-well culture plates. Autologous PBLs were

thawed (5.2.1.7), counted and $2x10^6$ PBLs were added to each well (1:5 ratio of DC:PBL). When the adjuvant-induced effect on DC maturation was investigated on DCs only (DC_{solo}), autologous PBLs were replaced by the equal amount of volume. The adjuvant working solutions were prepared (5.2.2.3) and added to achieve the final adjuvant concentration as indicated in Table 1. CM was given to the unstimulated control instead of the adjuvant working solution. The volume of each well was adjusted to $1x10^5$ DCs/ 100 µl. Cells were incubated overnight (20 hours) at 37°C and 5% CO_2.

5.2.2.5.2.1 Expression of surface maturation marker

On the next day, cells were harvested and collected in 1.5 ml microcentrifuge tubes. After centrifugation (300 x g, 6 min, 4°C), cells were resuspended in FACS blocking buffer and incubated for 10 min at 4°C. Subsequently, the cell solution of each condition was splitted equally in two wells of a 96-well V-bottom plate for antibody-specific and isotype control-staining. Adjuvant-induced expression of the co-stimulatory molecules CD80, CD86 and CD40, the co-inhibitory molecule PD-L1, MHC-class II (HLA-DR) and the migration-mediating CCR7 molecule was analyzed by flow cytometry. The preparation of the staining solution as well as the staining procedure is described in 5.2.3.1.

5.2.2.5.2.2 Endocytic capacity

The assay procedure was performed in principle as described in 5.2.2.5.2.2. However, for the following assay, a second culture plate with a replicate of each condition has to be prepared. To have enough cells for each condition, cell numbers were reduced to $0.2x10^6$ DCs and $1x10^6$ PBLs per well (total well volume: 200 µl in 48-well plates). After stimulating the cells with the adjuvants for 20 hours, one of both assay plates was cooled to 4°C for 30 min in the fridge. These cells served as control for non-specific binding of FITC-dextran, since uptake activity is reduced at low temperatures. Subsequently, 50 µg/ml FITC-dextran was given to the cells for 1 hour and incubated either at 37°C or 4°C. Then, cells were harvested, transferred to 96-well V-bottom plates and washed 3-times with cold MACS buffer. Cells were stained with a viability dye and DC-identifying markers (CD14 and CD1a) for analysis by flow cytometry.

5.2.2.5.3 Adjuvant stimulation of the DC: PBL co-culture in a 96-well U-bottom culture plate

For Luminex multianalyte profiling (5.2.2.5.3.1; Figure 9) and adjuvant-induced antigen-independent proliferation (5.2.2.5.3.2), donors were selected by stratification, since a

consistence in gender and age distribution was necessary. The inclusion criteria were defined before donor enrollment for four groups (female/ male; <40/ >40 years of age) with 7-8 corresponding donors each. The selection of the buffy coats for both experiments was performed by the DRK Blood donation center.

DCs were harvested on day 5 of culture (5.2.1.6), autologous PBLs were thawed (5.2.1.7) and both cell types counted (5.2.1.1). To study antigen-independent proliferation (5.2.2.5.3.2) DCs and PBLs were labeled with 4 µM CFSE (5.2.2.4). To study adjuvant-induced cytokine and chemokine profiles (5.2.2.5.3.1), cells remained unlabeled. Cells were adjusted to $0.4x10^6$ DCs/ml and $2x10^6$ PBLs/ml. DCs were seeded with a multichannel pipette in a 96-well U-bottom plate ($2x10^4$ DCs/ well) and rested for at least 30 min at 37°C and 5% CO_2. Due to a higher evaporation in the outer rows and columns of the plate, they were left cell-free and filled with PBS. Meanwhile, adjuvant working solutions were prepared (5.2.2.3) and added to the indicated wells. Biological replicates were performed for each condition. Subsequently, $1x10^5$ PBLs were added to each well with the help of a multichannel pipette. The well volume amounts to 150 µl. The DC:PBL co-culture, stimulated with the different adjuvants at low and high concentration, was incubated for 24 hours (5.2.2.5.3.1) or 6 days (5.2.2.5.3.2) at 37°C and 5%CO_2.

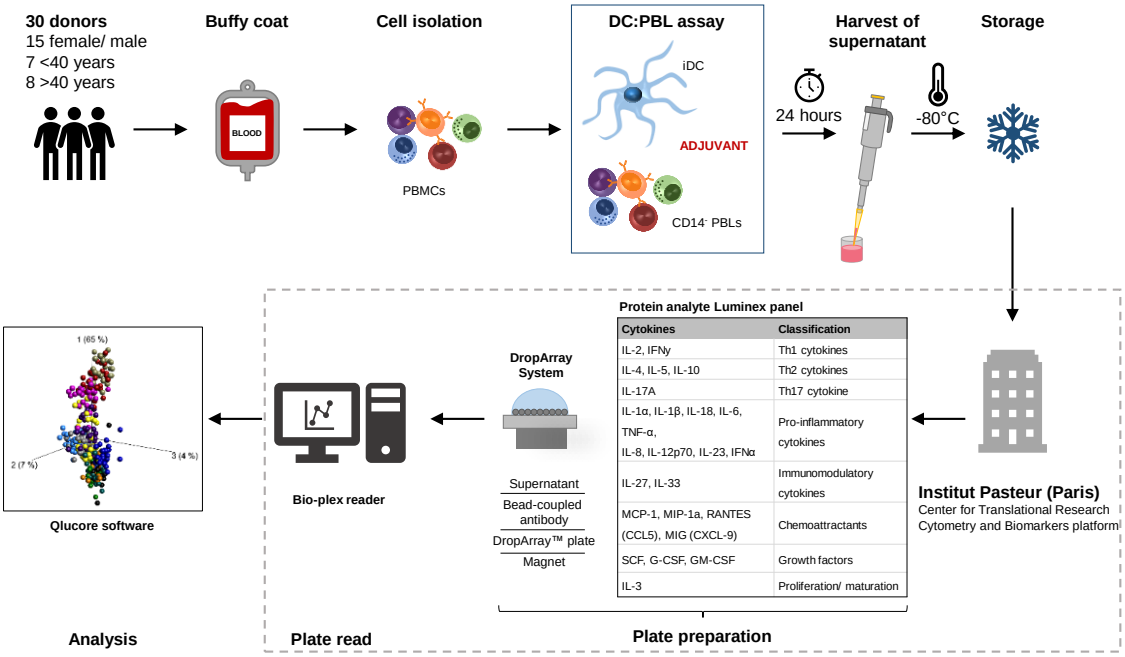

Figure 9: Experimental and analysis procedure of the cytokine and chemokine multiplex profiling. Buffy coats of donors with defined criteria were selected and PBMCs were isolated. The human primary immune cell-based assay (DC:PBL co-culture) was set up as indicated and stimulated with the different adjuvants for 24 hours. Subsequently, supernatant was harvested and immediately stored at -80°C. Plates with supernatants were sent to M. Hasan and T. Stephen at the Institut Pasteur (Center for Translational

Research; Cytometry and Biomarker platform), who performed the 25 analyte Luminex analysis using the DropArray System and a Bioplex reader. Data analysis was conducted with Qlucore Omnics Explorer.

5.2.2.5.3.1 Cytokine and chemokine analysis

After incubation, plate was centrifuged at 440 x g for 6 min. 120 µl of supernatant (75% of the well volume) was harvested carefully without touching the cell pellet and collected in 96-well U-bottom plates (polypropylene plates). Half of the supernatants were transferred to another 96-well U-bottom plate. This plate was sent later to M. Hasan and T. Stephen at the Institut Pasteur (Center for Translational Research, Cytometry and Biomarkers platform) for cytokine and chemokine analysis of the adjuvant-stimulated DC:PBL co-culture (5.2.3.2). Plates were tightly sealed and frozen at -80°C immediately (Figure 9).

5.2.2.5.3.2 Antigen-independent proliferation of lymphocytes

After 6 days of incubation, plates were centrifuged at 440 x g for 6 min (4°C). Supernatant was collected and stored immediately at -80°C for potential cytokine analysis. Replicates were pooled and transferred to 96-well V-bottom plates for the staining procedure before flow cytometry analysis (5.2.3.1). Cells were stained for CD3, CD4, CD8, CD56 and CD19 to analyze $CD4^+$ T cells ($CD3^+CD4^+$), $CD8^+$ T cells ($CD3^+CD8^+$), NKT cells ($CD3^+CD56^+$), B cells ($CD3^-CD19^+$) and NK cells ($CD3^-CD56^+$). Fluorescence minus one (FMO) controls helped to identify target populations. Proliferating cells were identified by exhibiting a lower intensity of CFSE. Moreover, 123count eBeads™ Counting Beads were spiked in and acquired during sample analysis, allowing the calculation of the absolute cell count of proliferating lymphocytes within the respective sample. The volume of counting beads amounted to 10% of the total sample volume. During sample acquisition, at least 1000 beads were collected to ensure statistically significant results. Absolute cell counts were calculated according to the manufacturer's instruction with the following formula:

$$Absolute\ cell\ count\ (cells/ml) = \frac{(Cell\ count\ \times eBead\ volume)}{(eBead\ count\ \times cell\ volume)} \times eBead\ concentration$$

5.2.2.6 Antigen-specific experiments

To investigate if the adjuvants are able to boost the expansion of antigen-specific $CD4^+$ and $CD8^+$ T cells, we performed an antigen-recall assay using immunodominant peptide sequences of the model antigens influenza matrix protein 1 (FluM1; 58-66) and tetanus toxin (TT p2; 829-844). For both antigens we assume that most of the donors were either

already infected with an influenza virus or vaccinated against influenza and/or TT. Antigen-specific T cells were detected with MHC/peptide-tetramers, which bind to the T cell receptor (TCR) recognizing the specific peptide. The peptide sequences and the tetramers are restricted to certain HLA-characteristics. Therefore, donors carrying HLA- A*02:01 (FluM1) and HLA- DRB1*11:01 (TT) are required for these antigen-specific T cell assays.

5.2.2.6.1 Selection of blood donors with HLA-A*02:01 or HLA-DRB1*11:01 characteristic

HLA-A*02:01 positive donors were identified with an antibody staining against HLA- A*02 (Figure 10:Figure 10). Therefore, six to eight buffy coats were tested. The antibody staining was performed for 15 min at 4°C using 100 µl buffy coat after erythrocyte lysis (10 min). Cells were washed in MACS buffer and directly acquired using a flow cytometer. Unstained cells of the same donor served as control. HLA-A*02 positivity was detected with a shift in fluorescence intensity of two log decades. Around 50% of the tested buffy coats were from donors carrying the HLA-A*02 characteristic. HLA-A*02 positive PBMCs were isolated from buffy coats as described in 5.2.1.3.

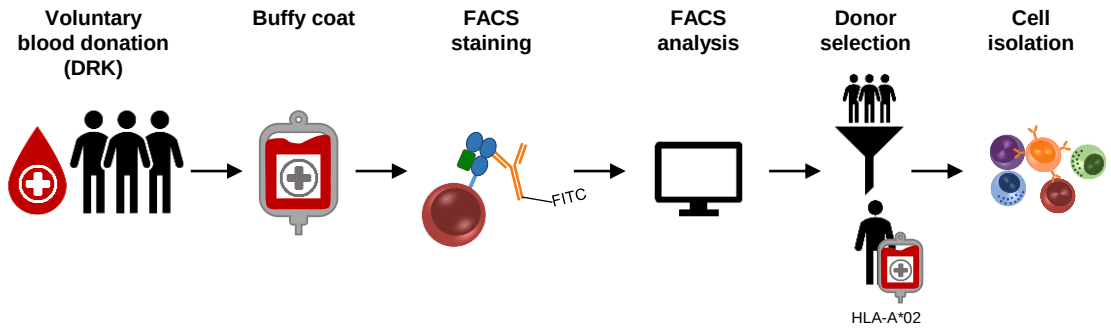

Figure 10: Selection procedure of HLA-A*02-positive donors for the antigen-specific CD8⁺ T cell assay.
Buffy coats from healthy donors were obtained from the DRK blood donation center. HLA-A*02 positive donors were detected with an antibody staining. After flow cytometric analysis, PBMCs from HLA-A*02 positive donors were isolated.

Due to the fact that no antibody against HLA-DRB1*11:01 exists, donors have to be haplotyped before their cells can be used for this experiment (Figure 11). Blood sampling of donors, HLA-typing and the experimental procedure was approved by the local ethics committee (Identification-no. 19-226; Department of Medicine der Goethe-University Frankfurt) and informed, written consents were obtained from all donors. HLA-typing was performed at the DRK blood donation center Baden-Wuerttemberg/ Hessia and the DKMS. Five employees of the Paul-Ehrlich-Institut, who voluntarily registered for the

study, were HLA-DRB1*11:01 positive and donated blood for the antigen specific $CD4^+$ T cell experiments. Blood sampling and isolation of PBMCs from whole blood was performed as described in 5.2.1.4.

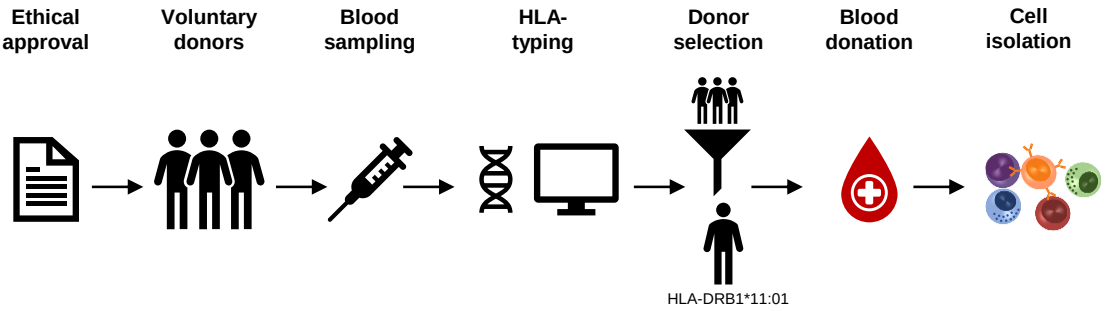

Figure 11: Selection procedure of HLA-DRB1*11:01-positive donors for antigen-specific $CD4^+$ T cell experiments.
After approval by the local ethics committee, voluntary donors were taken blood for HLA-typing. Donors having the HLA-DRB1*11:01 haplotype were asked to donate blood for the experiments. PBMCs were isolated as described.

5.2.2.6.2 Loading of DCs with peptides for T cell stimulation

DCs were harvested (5.2.1.6), counted (5.2.1.1) and stained with 4 µM CFSE (5.2.2.4). Subsequently, DCs were washed in serum-free media (M'medium)and resuspended in M'medium before separating on two falcons. For efficient peptide loading, cells were pulsed in a small volume (1 ml) with a cell number less than $10x10^6$ DCs. DCs within falcon 1 were loaded with 10 µg/ml peptide, whereas DCs in falcon 2 served as control cells. After incubation for 2 hours at 37°C with 5% CO_2, DCs were washed extensively to remove unbound peptide (3 times with a volume of at least 30 ml, 322 x g for 8 min). Subsequently, DCs were counted and adjusted to $0.4x10^6$ DCs/ml with A'medium.

5.2.2.6.3 Co-cultivation of peptide-pulsed DCs and T cells

Autologous $CD14^-$ PBLs or PBMCs were thawed (5.2.1.7), counted (5.2.1.1) and subsequently $CD4^+$ or $CD8^+$ T cells were selected using EasySep™ isolation kits (5.2.1.8). T cells were labeled with 4 µM CFSE (5.2.2.4), again counted and adjusted to $2x10^6$ T cells/ml in A'medium. Peptide-loaded and Ctrl-DCs (5.2.2.6.2) were seeded in 96-well U-bottom plates with the help of a multichannel pipette at a density of $2x10^4$ DCs/ well and rested for 30 min at 37°C and 5% CO_2. Afterwards, $1x10^5$ $CD4^+$ or $CD8^+$ T cells were added to each well. The outer rows and columns of the plate remained cell free and were just filled with PBS. Adjuvant working solutions were prepared in A'medium (5.2.2.3) and given to the corresponding wells to obtain the final adjuvant concentration (Table 1). For each condition several replicates were prepared. The co-culture of DC and

$CD8^+$ T cells additionally received 20 IU/ml IL-2. Cells were incubated for 6-7 days at 37°C with 5% CO_2.

5.2.2.6.4 Analysis of antigen-specific T cells with MHC/peptide tetramers

Antigen-specific T cells can be detected with MHC/peptide tetramers. These MHC/peptide tetramers bind only to matching TCRs. This means that the peptide sequence as well as the MHC molecule has to be recognized by the TCR. The MHC/ peptide complexes are tetramerized to maintain a stable binding to four TCRs. A fluorophore attached to the complex allows the analysis by flow cytometry. We used MHC/peptide tetramers with the identical peptide sequence as used for loading on DCs. The staining was performed as recommended by the manufacturer. In brief, T cells were washed in PBS, resuspended in PBS and the MHC/peptide tetramer was given to the wells (1 µl/ $8x10^5$ T cells). Cells were stained for 45 min in the dark at 4°C. T cell identifying antibodies were added for another 15 min. Subsequently, cells were washed and analyzed using flow cytometry. For the detection of $FluM1^+CD8^+$ T cells at least 20,000 cells and for TT^+CD4^+ T cells 200,000 cells per sample were acquired.

5.2.2.6.5 Cytokine-secretion after peptide re-stimulation

For the re-stimulation of antigen-specific $CD8^+$ T cells, T2 cells were used as target cells. T2 cells were harvested, washed two times with PBS (573 x g, 5 min), resuspended in M'medium and counted in trypan blue with a Neubauer hemocytometer (5.2.1.1). $10x10^6$ T2 cells were prepared for loading of the FluM1 and NY-ESO-1 peptide. NY-ESO-1 is a tumor antigen and here used as control peptide. T2 cells were pulsed with 1 µM peptide and incubated for at least 1 hour at 37°C with 5% CO_2. Afterwards, T2 cells were washed several times, resuspended in A'M and counted.

T cells were harvested from the 96-well plate after 6-7 days of co-culture with DCs and adjuvant stimulation (5.2.2.6.3). T cells were counted in trypan blue with a Neubauer hemocytometer. Subsequently, T cells were seeded in a 96-well V-bottom plate at a density of $2x10^5$ T cells/ well. T2 target cells were added at a 1:1 ratio in the presence of monensin/ brefeldin A, anti-CD28/CD49d co-stimulus and CD107A antibody. The same setting, but without target cells and CD28/CD49d co-stimulus, was used for the negative (unstimulated) and positive control (PMA/ Ionomycin). Here, equal volumes of A'medium were given to the wells. Cells were resuspended carefully and centrifuged at 503 x g for 5 min. Cells were incubated for 6 hours at 37°C with 5% CO_2 with a short interruption after 2 hours to add PMA/ Ionomycin to the positive control (Cell activation cocktail: 1 µl/ $1x10^6$ cells). After the incubation, cells were pelleted at 503 x g for 5 min and

resuspended in PBS. Subsequently, MHC/FluM1-tetramer was added to each well for 45 min (5.2.2.6.4) at 4°C, followed by live/dead and extracellular antibody staining for additional 15 min. Subsequently, cells were washed two times with MACS buffer and resuspended in Cytofix/ Cytoperm™ buffer for fixation overnight at 4°C in the dark. On the next day, cells were stained against TNFα, IL-2 and IFNγ for 1 hour in 1x Perm/ Wash™ (5.2.3.1). After washing, cells were resuspended in MACS buffer and acquired immediately by flow cytometry.

5.2.3 Analyzing methods

5.2.3.1 Flow cytometry

The expression of specific markers, cytokine production, detection of antigen-specific T cells as well as the proliferation of lymphocytes was assessed by flow cytometry. For this purpose, cells and conditions of interest were collected in 96-well V-bottom plates at a density of at least $1.5x10^5$ cells/ well. After centrifugation (440 x g, 5 min), cells were resuspended in FACS blocking buffer and incubated for 10 min at 4°C. Subsequently, cells were washed once with PBS and the antibody staining solution against cell surface antigens was added. The antibody staining solution was prepared in PBS and contained the fixable viability dye Zombie Yellow (1:1000) and the antibodies of interest or their respective isotype controls. After incubation of 30 min at 4°C, cells were washed two times with MACS buffer and resuspended in 75-100 µl MACS buffer for sample acquisition. When sample analysis was performed on the next day, cells were fixed with 0.25% PFA, without any further washing. For intracellular protein analysis, the Cytofix/Cytoperm™ Fixation/Permeabilization Solution Kit or eBioscience™ Foxp3/ Transcription Factor Staining Buffer Set was used according to manufacturers' instructions. In brief, cells were fixed in 100 µl Cytofix/Cytoperm™ buffer or 1x Fixation/ Permeabilization diluent and incubated for 20 min to 12 hours in the dark at 4°C. Cells were washed with 1x Perm/ Wash™ or 1x Permeabilization buffer, followed by blocking of unspecific binding with intracellular FACS blocking buffer for 20 min at 4°C. After another wash with 1x Perm/ Wash™ or 1x Permeabilization buffer, cells were incubated with the antibodies of interest, reconstituted in 1x Perm/ Wash™ or 1x Permeabilization buffer for 1 hour at 4°C. Samples were recorded using an BD LSR II, BD LSR SORP or LSR Fortessa and analyzed by FlowJo software. The geometric mean fluorescence intensity (geo. MFI) values of the isotype controls were subtracted from the geo. MFI values of the specific antibody staining. Proliferation of lymphocytes was assessed by a decline in CFSE fluorescence intensity.

5.2.3.2 Luminex Multiplex assay

Luminex Multiplex assays allows the detection of multiple proteins within a given sample and thus is a big advantage over conventional ELISAs regarding the saving of resources such as sample and kit material or time. The capturing antibodies are linked to color-coded magnetic beads. Analytes within the sample material attach to the capturing antibodies. The antibody-antigen-antibody sandwich is established by binding of the detection antibody to its specific antigen. In a next step, streptavidin tagged with PE attach to the biotinylated detection antibody. The read-out is performed using a dual-laser detection instrument. One laser identifies the bead and thus the corresponding analyte, whereas the other laser detects the magnitude of PE-derived signal, which is proportional to the amount of analyte bound.

The protein analysis of 25 cytokines and chemokines in the supernatant (5.2.2.5.3; Figure 9; p. 64) was performed at the Institut Pasteur in the Center for Translational Research (Cytometry and Biomarkers platform) by M. Hasan and T. Stephen. The protein analysis with Luminex xMAP technology was carried out using the DropArray system (Curiox) and a Bio-Plex reader (Biorad). The 25 analytes (ProCartaplex custom panel 25-plex, Invitrogen) were organized on one multiplex array and a single batch of reagents was used for testing all samples. The least detectable dose (LDD) was derived by averaging the values obtained with sample diluent of 169 blank reads and adding three standard deviations of the mean. The lower limit of quantification (LLOQ) is the lowest concentration of an analyte that can be reliably detected, corresponding to the lowest point of the standard curve. LDD and LLOQ of the tested analytes are displayed in Table 2. Undetected values (OOR <) were replaced by 10% of the least detectable dose, whereas saturated values (OOR >) were replaced by 10x of the upper limit of quantification. The subsequent cytokine analysis is based on the mean of biological duplicates.

Table 2: Parameters of the Luminex xMAP immunoassay.

Analytes	Abbreviation	Units	mean LDD	[min;max] - std	mean LLOQ	[min;max] - std
Granulocyte Colony-Stimulating Factor	G-CSF	pg/mL	159.2	[5.73 ; 648.40] - 194.26	30	[2.56 ; 186.92] - 46.49
Granulocyte-Macrophage Colony-Stimulating Factor	GM-CSF	pg/mL	11.6	[0.01 ; 28.77] - 6.64	8.1	[2.40 ; 14.65] - 5.45
Interferon alpha	IFNα	pg/mL	1.6	[0.55 ; 3.43] - 0.79	0.4	[0.12 ; 0.59] - 0.18
Interferon gamma	IFNγ	pg/mL	21.5	[7.20 ; 77.40] - 13.01	6.41	[2.62 ; 11.98] - 4.47
Interleukin-1 alpha	IL-1α	pg/mL	6.3	[0.01 ; 13.08] - 3.55	1.7	[0.18 ; 2.98] - 1.10
Interleukin-1 beta	IL-1β	pg/mL	4.1	[1.72 ; 7.55] - 1.26	1.8	[0.49 ; 2.26] - 0.61
Interleukin-10	IL-10	pg/mL	1.3	[0.005 ; 4.41] - 0.93	0.9	[0.48 ; 1.99] - 0.65
Interleukin-12 Subunit p70	IL-12p70	pg/mL	3.4	[0.01 ; 27.16] - 5.44	3.5	[2.68 ; 11.90] - 2.28
Interleukin-17A	IL-17A	pg/mL	9.7	[0.07 ; 29.06] - 8.04	5.3	[0.53 ; 7.75] - 2.68
Interleukin-18	IL-18	pg/mL	6.3	[0.17 ; 30.94] - 5.76	5.6	[3.39 ; 14.45] - 4.20
Interleukin-2	IL-2	pg/mL	16.9	[3.30 ; 39.92] - 7.98	13.2	[5.65 ; 25.83] - 9.46
Interleukin-23	IL-23	pg/mL	56.5	[20.33 ; 133.38] - 26.61	21.9	[0.34 ; 68.55] - 21.39
Interleukin-27	IL-27	pg/mL	239.8	[42.52 ; 2142.96] - 505.76	58.2	[6.88 ; 240.45] - 39.58

Analytes	Abbreviation	Units	mean LDD	[min;max] - std	mean LLOQ	[min;max] - std
Interleukin-3	IL-3	pg/mL	305.3	[62.18 ; 1343.36] - 298.48	58.6	[7.56 ; 261.10] - 60.17
Interleukin-33	IL-33	pg/mL	8.1	[1.11 ; 32.05] - 8.20	3.9	[0.18 ; 12.26] - 4.00
Interleukin-4	IL-4	pg/mL	26.6	[1.88 ; 165.82] - 30.98	10.6	[2.22 ; 39.77] - 9.54
Interleukin-5	IL-5	pg/mL	32.5	[0.68 ; 93.72] - 22.25	19.6	[2.51 ; 41.23] - 15.41
Interleukin-6	IL-6	pg/mL	13.2	[0.11 ; 35.22] - 8.68	3.3	[1.68 ; 7.41] - 2.42
Interleukin-8	IL-8	pg/mL	26.3	[0.05 ; 202.20] - 36.35	5.6	[0.56 ; 9.99] - 4.19
Monocyte Chemotactic Protein 1	MCP-1	pg/mL	8.0	[2.13 ; 24.16] - 5.92	4.3	[0.90 ; 14.94] - 4.07
C-X-C motif chemokine 9	MIG (CXCL9)	pg/mL	27.9	[0.53 ; 74.06] - 20.51	9.6	[1.71 ; 46.11] - 11.67
Macrophage Inflammatory Protein-1 alpha	MIP-1α	pg/mL	8.0	[1.15 ; 25.95] - 4.92	2.1	[0.31 ; 7.10] - 2.11
C-C motif chemokine 5	RANTES (CCL5)	pg/mL	4.3	[0.47 ; 17.81] - 4.34	1.5	[0.27 ; 3.57] - 1.18
Stem Cell Factor	SCF	pg/mL	2.9	[0.01 ; 6.90] - 1.66	2.2	[0.27 ; 6.22] - 2.04
Tumor Necrosis Factor alpha	TNF-A	pg/mL	15.2	[6.31 ; 41.61] - 8.24	5.3	[1.51 ; 9.93] - 3.63

5.2.3.3 Microscopy

For representative microscopic pictures of the endocytic uptake of FITC-dextran in DCs (5.2.2.5.2.2), DCs were labelled with CellTrace™ Far Red Cell Proliferation Kit (Thermo Fisher Scientific) before adjuvant stimulation. Apart from that, the assay was performed as described. After incubation with FITC-dextran, cells were harvested and washed several times with PBS. The following steps were carried out at room temperature. The cell nucleus was stained for 30 min in the dark with Hoechst 33342 (2.5 µg/ml) diluted in PBS. After another wash with PBS, cells were sedimented on glass slides using a CellSpin II cytocentrifuge (Tharmac) and were shortly air-dried. The IMAGEN™ Chlamydia detection kit's mounting medium (glycerol solution, pH 10 with an anti-fading agent) was added and the cover slip was applied. Cells were analyzed with a Zeiss Axio Observer Z1 fluorescence microscope using the 63x objective magnification.

5.2.3.4 Western Blot

Cells ($2x10^5$ DCs, $2x10^6$ $CD14^-$ PBLs) were pelleted at 1100 x g for 6 min (RT) and lysed in 20 µl 1x Laemmli buffer by resuspension and subsequent heating at 95°C for 10 min. Samples were stored at -20°C for further processing. Proteins were separated on a 10% SDS polyacrylamide gel (Table 3) by SDS-PAGE according to their molecular weight in an electric field. In addition to the samples loaded onto the gel, a pre-stained molecular weight marker was applied.

Table 3: Components of a 10% SDS-polyacrylamide gel

Chemicals	Separation gel (10%)	Stacking gel
Aqua bidest	2.5 ml	0.625 µl
Separation gel buffer	1.5 ml	-
Stacking gel buffer	-	250 µl
Polyacrylamide (30%)	2 ml	125 µl

TEMED	12.5 µl	2.5 µl
APS (10%)	60 µl	10 µl

The electrophoresis was carried out in a tank containing 1x SDS-PAGE Running buffer at 70 and 110 Volt for passage through the stacking and separation gel, respectively. In a next step, the proteins were blotted onto a PVDF membrane at 1.5 mA per cm^2 for 1 hour using a semi-dry blotting apparatus. Subsequently, the membrane was blocked in TBST + 5% skimmed milk powder for 1 hour at RT. Next, the membrane was incubated with the first antibody IκB or α-tubulin, which both were diluted 1:2000 in TBST + 5% skimmed milk powder. Antibody incubation was performed with gentle agitation either overnight at 4°C (anti-IκB), or for 1 hour at RT (anti-α-tubulin). After washing three times in TBST for 10 min, the HRP coupled-secondary antibody was added for 1 hour at RT. Both antibodies were diluted in TBST + 5% skimmed milk powder (goat anti-rabbit (1:1000); goat anti-mouse (1:10,000)). After three washing steps with TBST, HRP activity was detected with chemiluminescence using ECL- or Luminate Forte-substrate. The membrane was incubated for 1 minute with the substrate, followed by the detection of the signal detected with a chemiluminescence imager device. Densitometry analysis was performed with the imager-corresponding software (LabImage 1D). Signals of IκB were normalized to the loading control α-tubulin. Furthermore, adjuvant-induced reduction of IκB was determined by normalizing to the respective unstimulated control, which was set to 100%.

5.2.4 Statistical analysis and data visualization

Principal component analysis (PCA), agglomerative hierarchical clustering and heat maps were performed with Qlucore Omnics Explorer v3.5. Here, false discovery rate (FDR)-adjusted ANOVA p-values, called q-values were used to define the cytokine cut-off of the data visualizations and to discriminate the most differentially induced proteins. Data were transformed prior to analysis by the software: logarithmized, mean-centered and scaled to unit variance. The mean centering is in accordance with the paired structure of the data. Data was corrected for donor variation to observe adjuvant-specific effects.

Dot plot/ bar graphs, box plots, whisker plots and two-way correlations were compiled using GraphPad Prism v8 or R v3.6.1 using the functions kruskal.test(), cor() and cor.test() as well as the package corrplot for plotting correlation matrices v0.84. Graphical illustration with R was carried out by T. Stephens (Institut Pasteur) and C. Kamp

(Department of Microbiology, Biostatistics, PEI). Radar plots and part-of-whole diagrams were drafted with Excel 2016.

Statistical significance of antigen-specific experiments was determined by Wilcoxon matched-pairs signed rank test or Friedman test with Dunn's correction. Spearman non-parametric ranks were used for correlation analysis. All other statistical analyses were performed using the Kruskal-Wallis test with Dunn's multiple comparison correction. Every statistical analysis was conducted as two-sided test with alpha=0.05. P-values $p<0.05$ (*), $p<0.01$ (**), $p<0.001$ (***) and $p<0.0001$ (****) were considered to be statistically significant

6 Results

6.1 Cell composition of the human primary immune cell *in vitro* assay

In the beginning of the study, three *in vitro* assays were tested for their suitability to investigate the immunogenic properties of the adjuvants. These included a PBMC assay, the RESTORE assay (Römer et al., 2011) with pre-cultured PBMCs at a high density and DC:PBL co-culture assay with monocyte-derived DCs and autologous PBLs. Under supervision of Dr. Anja Ullrich, Katharina Lindt analyzed in her bachelor thesis (Lindt, 2017) the lymphocyte proliferation-inducing capacity of the adjuvants Pam, GARD, R848 and the antigen TT in these three *in vitro* assays. They found that all three assays mimic the same adjuvant-induced lymphocyte proliferation, but the DC:PBL assay enabled the strongest proliferation response compared to the PBMC or RESTORE assay. Since the additive effect of the adjuvant/ antigen combination was higher in the DC:PBL assay, this assay was chosen for the following experiments of this project. Hence, immature DCs were differentiated from monocytes using IL-4 and GM-CSF. After 5 days of culture, they presented a $CD14^-CD1a^+CD209^+$ phenotype (Figure 12A). The autologous PBL population corresponds to the $CD14^-$ fraction, which was obtained after MACS separation, and reached a purity of approximately 95%, with 5.00 ± 5.50% remaining $CD14^+$ monocytes. The PBL populations consisted of $CD3^+CD4^+$ T cells (mean ± SD [%]: 38.21 ± 10.37), $CD3^+CD8^+$ T cells (23.12 ± 9,428), $CD3^-CD56^+$ NK cells (11.98 ± 5.79), $CD3^-CD19^+$ B cells (7.83 ± 3.49) and $CD3^+CD56^+$ NKT cells (5.83 ± 5.20) (Figure 12B). Existing donor variances in cell populations (Figure 12B) were not adjusted to a consistent cell subset number to keep the naturally occurring variation of the immune response between donors.

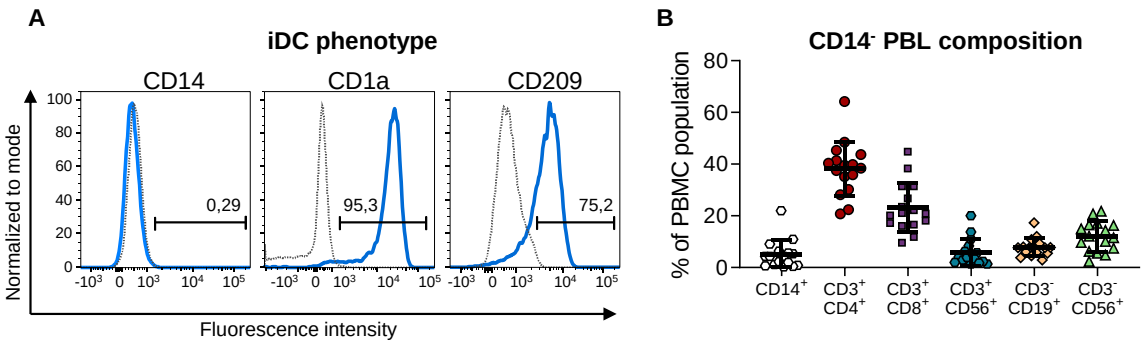

Figure 12: Cell composition of the DC:PBL co-culture assay.
The DC:PBL co-culture consists of human monocyte-derived DCs and autologous PBL at a ratio of 1:5. (A) Immature dendritic cells (iDC) were differentiated from human monocytes with IL-4 and GM-CSF over 5 days. Upon full differentiation, iDCs can be characterized as $CD14^-CD1a^+CD209^+$ cells by flow cytometry. Histogram overlays of antibody (blue solid line) and respective isotype control (grey dashed line) for a representative donor is shown. (B) The composition of different lymphocyte populations within the autologous PBLs was determined using flow

cytometry. Each data point represents one donor (n=16). Data are shown as mean ± SD and were obtained in at least three independent experiments.

6.2 Exclusion of cytotoxic, endotoxic and pyrogenic side-effects allows for an adjuvant-specific immune response

6.2.1 Determination of adjuvants' concentrations

Next, we aimed to determine a suitable concentration for each of the ten adjuvants as well as the positive control LPS to be used throughout this study. Therefore, we analyzed the proliferation-inducing capacity and the cytotoxicity of the adjuvants' concentrations on PBLs within the chosen *in vitro* assay. To study the proliferation of lymphocytes, they were labeled with CellTrace™ FarRed fluorescent dye before co-culturing with DCs. Adjuvants were serially diluted and given to the DC:PBL culture. After 7 days of culture, the latest time-point of data analysis, cells were harvested and prepared for flow cytometry assessment. A decline of the CellTrace™ FarRed's fluorescent intensity indicates cell division and thus cell proliferation. Non-proliferating cells maintain the CellTrace™ FarRed fluorescent intensity and thus proliferating and non-proliferating cells can be separated. Cytotoxicity was investigated using fluorescently labeled Annexin-V and the DNA-intercalating dye propidium iodide (PI) to detect apoptosis and necrosis-related hallmarks through the exposition of phosphatidylserine on the cell surface and the loss of cell membrane integrity, respectively. Figure 13 shows the concentration-dependent proliferation of lymphocytes as well as cytotoxic effects (Annexin- V^+/PI^+ cells) induced by the ten adjuvants and the positive control LPS. Based on the following criteria, we selected two concentrations for each adjuvant, which hereafter are termed 'low' and 'high'. Concentrations, which induced an increase of cell death (Annexin-V^+/PI^+ cells) to more than 25% compared to the unstimulated control were defined as non-suitable for this study. For Pam, LPS, MPL-s, MPL-SM, GARD and R848, which induced the proliferation of lymphocytes, their stimulating capacity was additionally taken into account: A lower concentration that stimulates only minor proliferation and a higher concentration that was well in the range of inducing proliferation but did not show any cytotoxicity (Table 1).

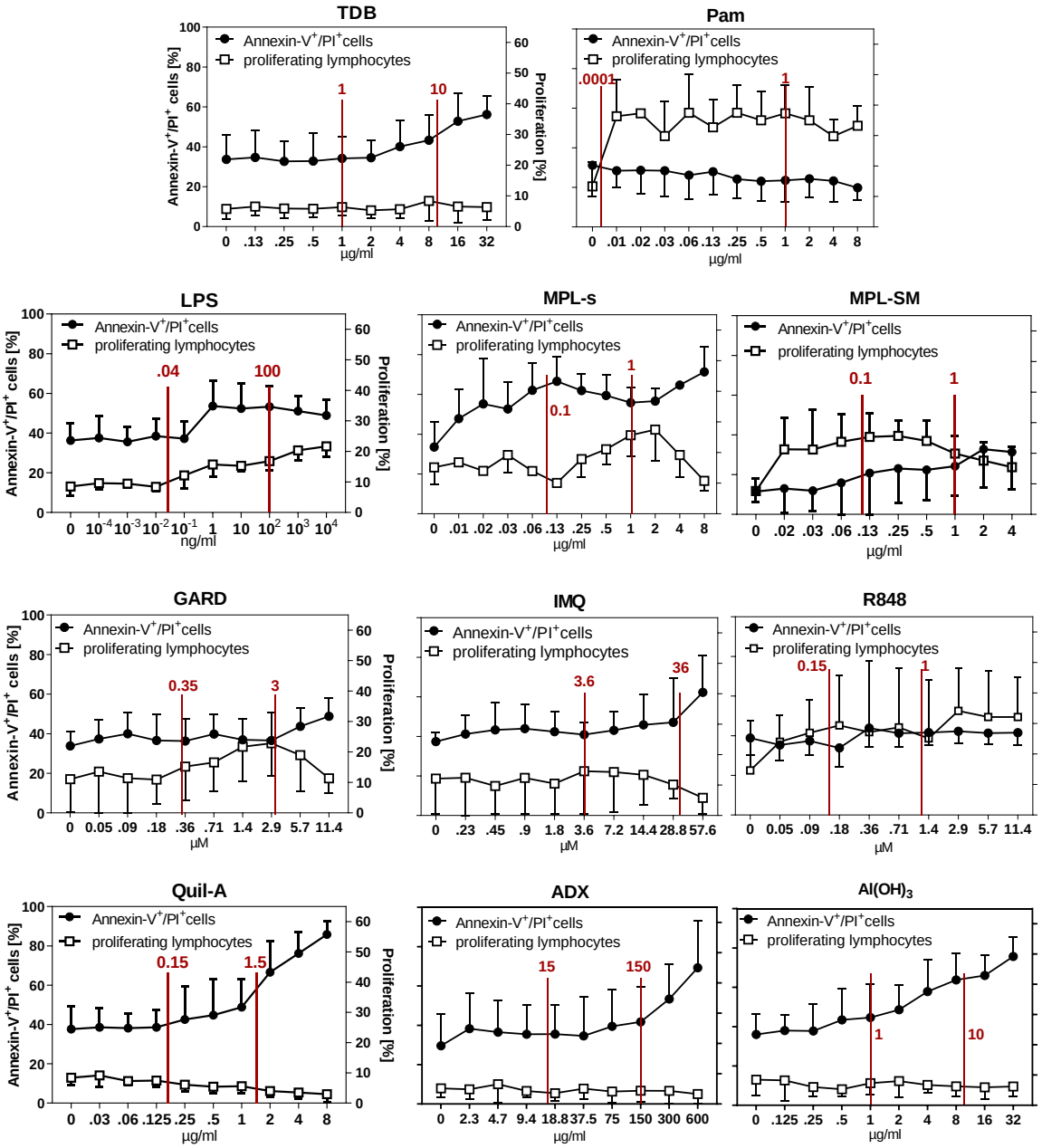

Figure 13: Determination of adjuvants' concentrations.
Immature DCs and autologous PBLs were co-cultured at a 1:5 ratio and stimulated with serial diluted adjuvants' concentrations for 7 days. Subsequently, cells were harvested and prepared for flow cytometry analysis. Adjuvants' concentrations were defined by assessing cytotoxicity with an annexin-V/ PI staining (filled black dots) and the induction of lymphocyte proliferation (white squares). On the basis of these results, the low and high concentration of each adjuvants was defined (indicated by the red vertical lines). Data are representative for at least 2 independent experiments (n=4-9 donors). Data points are shown as mean ± SD.

6.2.2 The chosen adjuvants' concentrations show no endotoxic or pyrogenic side- effects in specific pyrogenicity tests

Pyrogenicity testing is an important measure to detect the presence and concentration of endotoxins (LPS) and non-endotoxins, e.g. components of viruses and fungi, within medicinal or biological products and hence, to guarantee product sterility. Exogenous pyrogens can

induce the production of endogenous pyrogens, such as IL-1β, IL-6 and TNFα, leading to a fever reaction or in the case of a strong release, to a cytokine storm and multiple organ failure. Using a bacterial endotoxin test, e.g. limulus amebocyte lysate (LAL) assay, the concentration of the present endotoxin can be determined. On the other hand, the monocyte-activation test (MAT) displays the effect of the test substance on the immune system. Pyrogens within the test substance stimulate the secretion of fever-inducing cytokines, which can then be assessed with an ELISA. With the help of both assays, we did not only address product sterility, but also if the chosen concentrations might cause a fever reaction. These tests were crucial to demonstrate that the further results obtained in this project are adjuvant-specific.

For both assays, LAL and MAT, adjuvants were diluted in CM to their chosen high concentration or in the case of lipid-A containing adjuvants (MPL-s, MPL-SM, LPS) to both concentrations (Table 1). The analyses were performed in the department for microbiological safety at the Paul-Ehrlich-Institut. The LAL assay is based on an enzymatic coagulation cascade, which is triggered by endotoxin. The developing turbidity can then be measured. The LAL assay demonstrated that all adjuvants were negative for endotoxin (<0.02 EU/ml), except for Lipid A-containing adjuvants such as MPLs, MPL-SM as well as LPS (Figure 14A), as expected. All tests were counted as valid, when the endotoxin spike-in was detected in a range of 50-200%.

The MAT was performed with cryopreserved human whole blood as previously described (Schindler et al., 2009). After 24 hours of incubation with the samples or standards, the supernatant was harvested and an IL-1β ELISA was carried out. The MAT declared that the stimulation with the high concentrations of TDB, Pam, GARD, IMQ, R848 and $Al(OH)_3$ did not induce IL-1β levels higher than the fever-inducing threshold of 0.5 EU/ml LPS) (Figure 14B). For MPL-s, MPL-SM and LPS, IL-1β secretion was only below the threshold, when stimulating with the low concentration.

Taken together, endotoxicity and pyrogenicity tests demonstrated that the chosen adjuvant concentrations, defined by considering the cytotoxicity (Annexin-V^+/PI^+) and proliferation-inducing capacity (Figure 13), were suitable to investigate adjuvant-specific effects and thus, they were used in the following experiments.

A

Adjuvant	Conc.	Endotoxin [EU/ml]	Spike recovery [%]
TDB	10 µg/ml	< 0.02	135
Pam	1 µg/ml	< 0.02	111
LPS	38.4 pg/ml	0.04	100
LPS	100 ng/ml	> 10	N/A
MPL-s	0.01 µg/ml	2.31	83
MPL-s	1 µg/ml	> 10	N/A
MPL-SM	0.01 µg/ml	> 10	N/A
MPL-SM	1 µg/ml	> 10	N/A
GARD	3 µM	< 0.02	122
IMQ	36 µM	< 0.02	144
R848	1 µM	< 0.02	109
ADX	150 µg/ml	< 0.02	146
Quil	1.5 µg/ml	< 0.02	165
$Al(OH)_3$	10 µg/ml	< 0.02	145
Complete Media (CM)	-	< 0.02	133
CM+1% DMSO	-	< 0.02	137

B

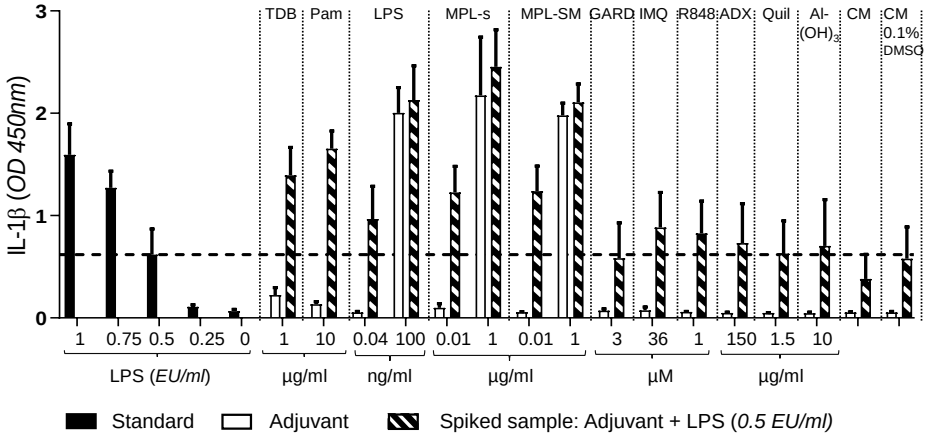

Figure 14: Chosen adjuvants' concentrations show no endotoxic and pyrogenic side-effects in specific pyrogenicity tests.
Adjuvants were prepared in culture medium at the chosen concentrations and analyzed in the department for microbiological safety at the Paul-Ehrlich-Institut. A) Adjuvants were tested for endotoxin contamination using the Limulus amaebocyte lysate (LAL; turbidimetric method) assay with an endotoxin spike-in of 0.5 EU/ml LPS as positive control. For a valid test, the spike recovery must be within the range of 50-200% (defined by the coefficient of variation). B) Pyrogenicity of the adjuvants was analyzed by the monocyte activation test (MAT) on cryopreserved human blood pooled from several donors. After 24 hour- incubation with the controls, adjuvants or standards, IL-1β concentrations in cell supernatants were analyzed by ELISA. Data are representative of at least three independent experiments.

6.3 Immunomodulatory effects of adjuvants on DC maturation

The maturation of DCs is an important process to orchestrate the adaptive immune response. Mature DCs are able to prime T cells and thus enable the generation of memory cells, which are necessary for a protective immune response. The process of maturation includes the phenotypical and functional differentiation of the DCs, such as the expression of co-stimulatory

markers on the cell surface, increased presentation of peptides within MHC-complexes, secretion of cytokine and chemokines and a reduced antigen uptake capacity (Banchereau and Steinman, 1998; Kapsenberg, 2003).

Subunit vaccine formulations containing purified antigens are not per se immunogenic and the addition of an adjuvant is needed to promote the activation and maturation of APCs such as DCs upon vaccination. Hence, within the first set of experiments shown here, we want to address the general effects of adjuvants on DCs or DCs co-cultured with PBLs in the absence of an antigen.

6.3.1 TLR ligand adjuvants increase the expression of maturation markers on DCs

To explore the capacity of the adjuvants to induce the maturation of monocyte-derived DCs, we first analyzed the expression of the maturation markers CD80, CD86, CD40, PD-L1, CCR7 and HLA-DR on the cell surface of DCs after being stimulated with the different adjuvants for 24 hours. The geometric mean fluorescence intensity (geo. MFI) of the different markers was assessed on viable $CD14^{-}CD1a^{+}$ DCs (Figure 15A) when cultured either alone (DC_{solo}) or in the co-culture with PBLs (DC_{PBL}). For DC_{solo}, we observed a significantly increased and concentration-dependent expression of two or more maturation markers upon stimulation with Pam, LPS, MPLs or R848 compared to the unstimulated control (Figure 15B). The expression of the maturation markers on DC_{PBL} was even more pronounced after Pam or R848 treatment (Figure 15C). In contrast, the marker expression profiles induced by the TLR4 ligands MPLs, MPL-SM and LPS were either constant or decreasing, except for PD-L1. The TLR7 ligands GARD and IMQ induced high expression levels of CD80, CD86 and PD-L1 only when DC were co-incubated and stimulated together with PBL but not solo stimulated DC (Figure 15B, C). This finding is illustrated in representative histogram overlays showing the expression of CD86, CD80 and PD-L1 on unstimulated and adjuvant-stimulated DC_{solo} and DC_{PBL} (Figure 16). In addition, we noted that R848, a dual TLR7/8 ligand, admittedly enhanced the expression of CD40, CD80, CD86 and PD-L1 significantly on DC_{solo} (Figure 15B), but to a much higher degree on DC_{PBL} (Figure 15C). Since we did not observe an TLR7-mediated expression of maturation markers when stimulating with GARD and IMQ, we assume that the observed elevated levels of CD40, CD80, CD86 and PD-L1 on DC_{solo} upon stimulation with the TLR7/8 ligand R848 are TLR8-specific.

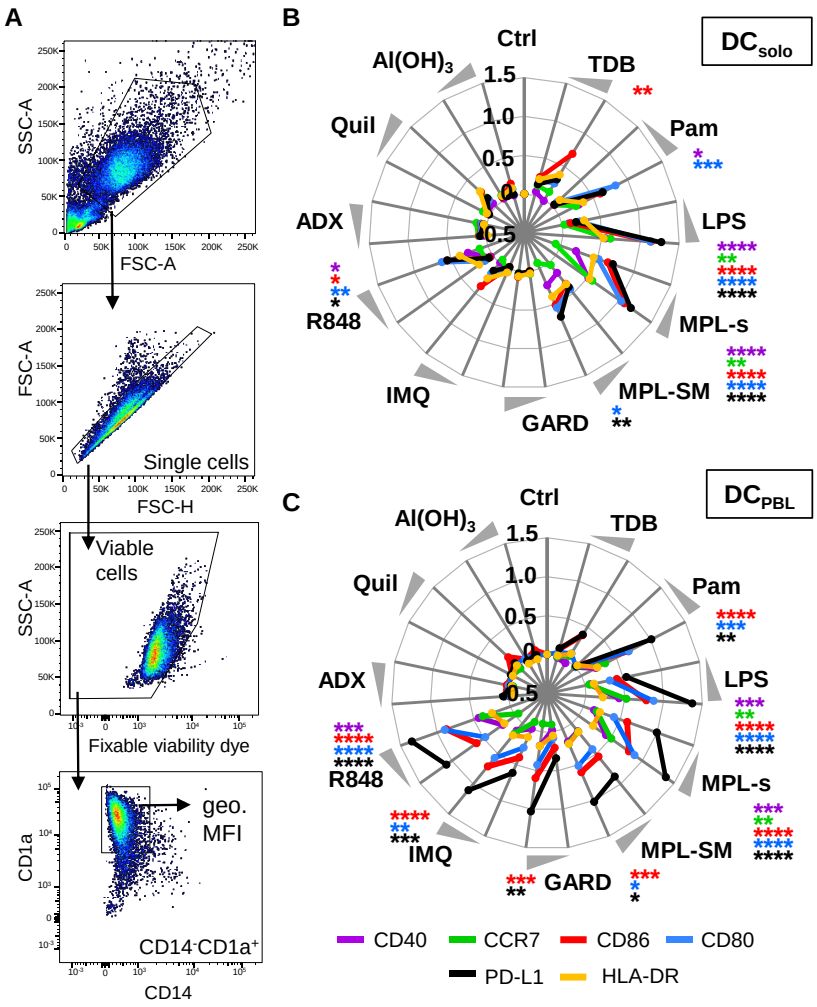

Figure 15: TLR ligand adjuvants increase the expression of maturation markers on DCs.
DC_{solo} and DC_{PBL} cultures were stimulated with the different adjuvants for 24 hours or were left untreated. The expression of the maturation markers CD40, CCR7, CD86, CD80, PD-L1 and HLA-DR was analyzed by flow cytometry. (A) Gating strategy to identify $CD14^-$ $CD1a^+$ DCs. The geometric mean fluorescence intensity (geo. MFI) of the different markers was analyzed on single, viable $CD14^-$ $CD1a^+$ DCs. Respective isotype antibodies were used to determine the background staining. (B), (C) Radar plots showing the adjuvant-induced expression of maturation markers on DC_{solo} or DC_{PBL}, respectively. Obtained geo. MFI values are displayed as fold change (compared to the respective unstimulated control) and transformed to log scale. Each maturation marker is represented as mean (n=9-15 donors) in a colored line. Significant differences between the adjuvant-induced expression and the unstimulated control were analyzed using the Kruskal-Wallis test with Dunn's correction for multiple comparisons on the non-normalized data (* $p<0.05$, ** $p<0.01$, *** $p<0.001$, **** $p<0.0001$). Statistics are depicted only for the high concentration of the adjuvant.

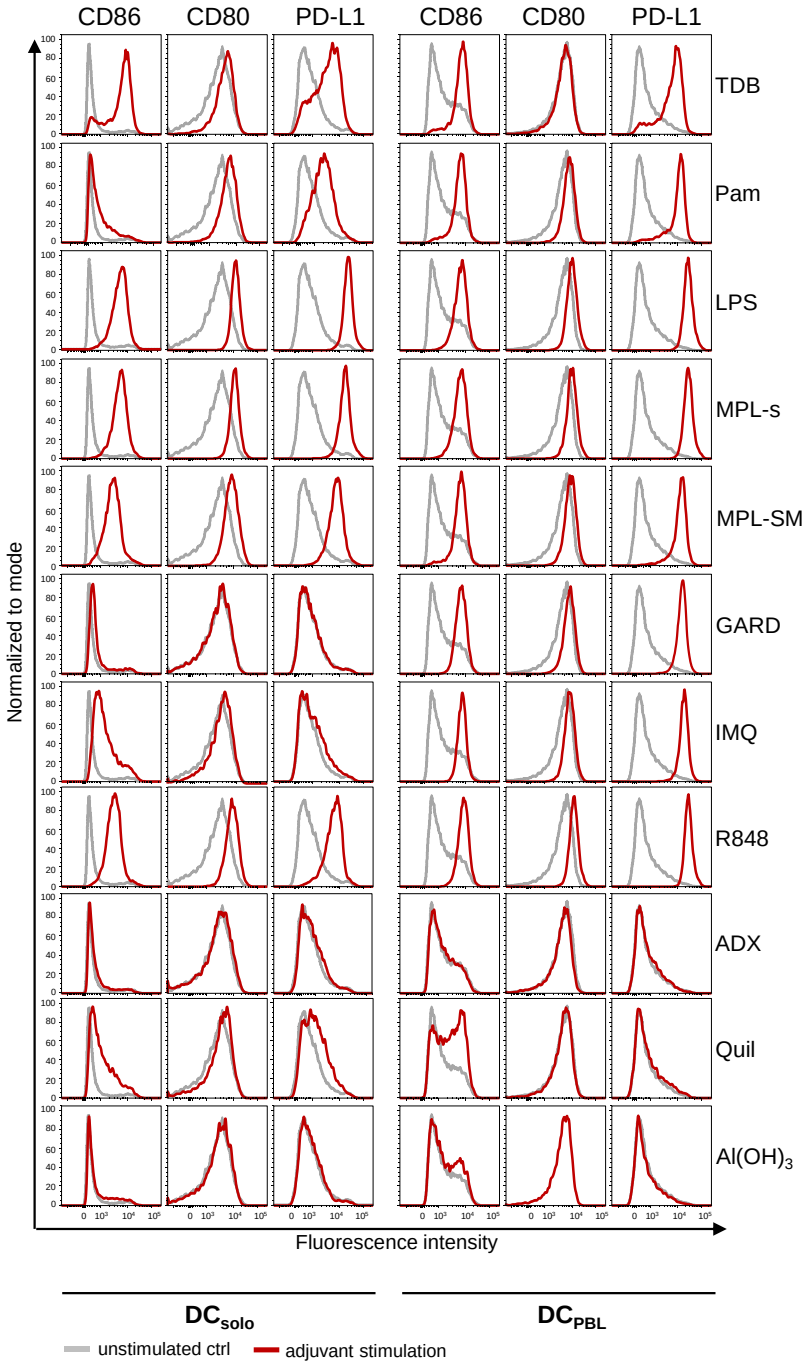

Figure 16: The TLR7 ligands GARD and IMQ increased the expression of CD80, CD86 and PD-L1 on DC_{PBL}, but not on DC_{solo}.
Representative histogram overlays of the maturation markers CD80, CD86 and PD-L1 showing the differences in fluorescence intensity between DC_{solo} and DC_{PBL} when stimulated with the adjuvants GARD or IMQ. The solid grey line represents the fluorescence intensity of the unstimulated control of the respective culture, whereas the solid red line represents the fluorescence intensity of the respective adjuvant stimulation.

The unresponsiveness of moDCs to TLR7 stimulation indicates that TLR7 is not expressed on moDCs, which is in accordance with the literature (Hackstein et al., 2011). However, as TLR7 is described to be expressed on $CD4^+$ T cells (Dominguez-Villar et al., 2015), $CD8^+$ T cells (Li et al., 2019), NK cells (Hornung et al., 2002) and B cells (Månsson et al., 2006), we analyzed

the expression of TLR7 on iDCs and different lymphocyte populations of PBLs with an intracellular flow cytometry staining to confirm that different handling and differentiation protocols did not affect the TLR7 expression. The flow cytometry staining was performed on unstimulated cells directly after harvest (DCs, Raji, HEK293/TLR7) or thawing (PBLs). In accordance with the literature, we found no expression of TLR7 on iDCs (mean geo. MFI ± SD; 84.9 ± 72.3) and a clear but generally low expression of TLR7 on $CD8^+$ T cells (144 ± 69.0) and B cells (170 ± 75.9) (Figure 17A, B). We detected similar expression levels for $CD4^+$ T cells (134 ± 68.7) and NK cells (171.6 ± 78), though they were not significantly elevated, when compared to the expression levels of iDCs. Raji (450.7 ± 216.3) and HEK293/TLR7 cells (953.9 ± 664.1) served as positive controls and demonstrated the highest TLR7 expression levels. Thus, the expression of maturation markers on DC_{PBL} after TLR7 ligand stimulation indicates an adjuvant-indirect activation of DCs that is likely due to the presence of PBLs and probably their adjuvant-induced activation.

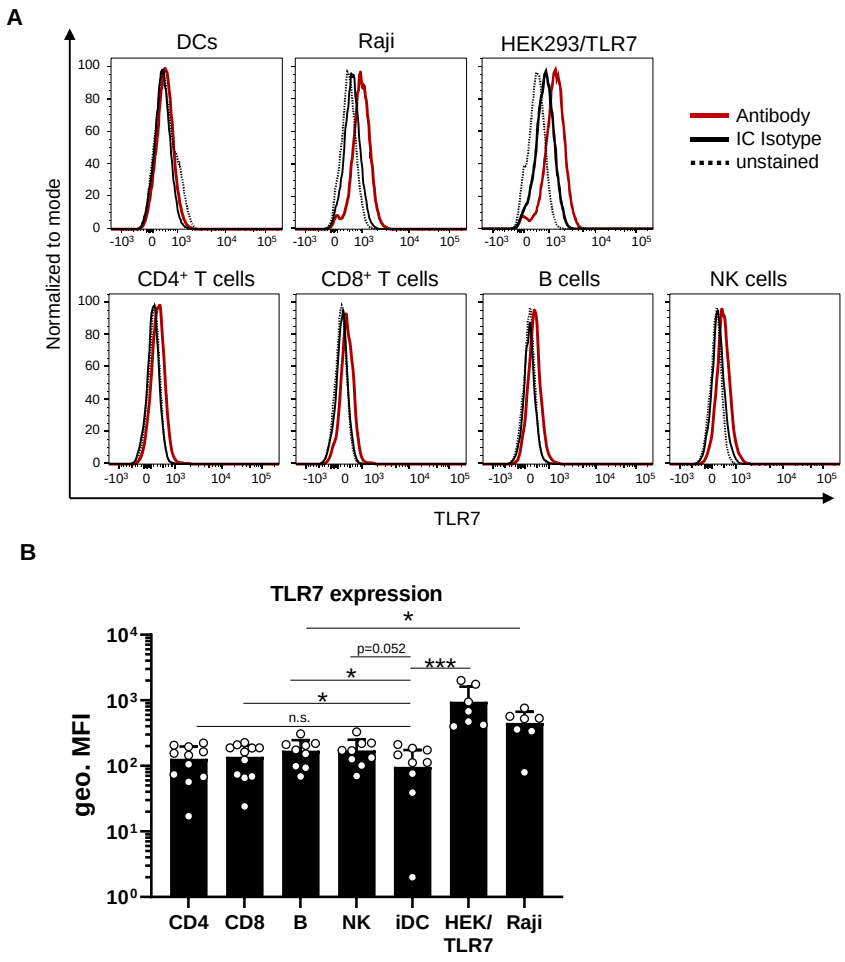

Figure 17: TLR7 is expressed on PBLs but not on DCs.
The expression levels of TLR7 were analyzed as geometric MFI by flow cytometry. The intracellular antibody staining was carried out on unstimulated cells directly after harvest (DC, Raji, HEK293/TLR7) or thawing ($CD14^-$ PBL). The different lymphocyte populations were identified with cell type specific antibodies. Raji and HEK293/TLR7 cells served as positive controls for TLR7 expression. (A) Representative histogram overlays of one experiment show the expression of TLR7 (red solid line) in comparison to the intracellular isotype (black solid line) and the unstained control (black dashed line). (B) Expression levels of TLR7 were specified as geo. MFIs. At least 3 independent experiments were performed. Data are presented as mean ± SD (n=7-9). Statistical significance was determined using the Mann-Whitney test (* p<0.05, ** p<0.01, *** p<0.001).

6.3.2 Endocytic activity negatively correlates with the expression of maturation markers after adjuvant stimulation

The down-regulation of endocytosis is a hallmark of DC maturation, occurring during the terminal differentiation program. Hence, we investigated here the functional maturation of the DCs by analyzing the endocytic uptake of FITC-labeled dextran at 37°C after adjuvant stimulation, in comparison to the unstimulated condition (negative control) or the 4°C control (Figure 18). Endocytic processes are strongly reduced at 4°C and thus, this condition served as control for potential binding of FITC-dextran on the cell surface. The endocytic capacity was examined as geo. MFI by flow cytometry. A representative histogram demonstrates the decrease of FITC fluorescence intensity when DCs were stimulated with LPS (positive control) in contrast to the unstimulated control (Figure 18A). The decrease of FITC fluorescence intensity indicated a diminished FITC-dextran uptake, which was significant for LPS-stimulated DC_{solo} in comparison to the unstimulated control (Figure 18B). Stimulation of DC_{solo} with all other adjuvants showed an uptake of FITC-dextran which was similar to the unstimulated control or tended to be even higher.

In contrast to DC_{solo}, we found that DC_{PBL} diminished their endocytic uptake of FITC-dextran after being stimulated with Pam, LPS, MPL-s, MPL-SM, IMQ and R848 (Figure 18C, D). In contrast, stimulation with ADX, Quil and $Al(OH)_3$ did not lead to a difference in endocytic uptake of FITC-dextran in DC_{PBL} compared to the unstimulated control (Figure 18C, D). As we assumed that the expression of DC maturation markers is functionally linked to the endocytic capacity of DCs, we assessed the relationship between both datasets for all immunomodulators. Here, we found that the expression levels of all maturation markers negatively correlated with the endocytic uptake of FITC-dextran (Spearman correlation) (Figure 18E). Expression of CD86 ($r = - 0.89$), CD80 ($r = - 0.88$), HLA-DR ($r = - 0.91$) and PD-L1 ($r = - 0.88$) showed the strongest inverse correlation to the endocytic uptake of FITC-dextran with r-values close to - 1. The data demonstrate that the adjuvants PAM, MPL-s, MPL-SM, IMQ and R848 induced not only a phenotypical, but also a functional maturation of the DC_{PBL}.

Summarizing, in response to Pam, LPS, MPL-s, MPL-SM, GARD, IMQ and R848 DC_{PBL} represented phenotypically and functionally matured DCs by pronounced expression of maturation markers and a reduced endocytic capacity. Strikingly, the immunogenic effects of GARD and IMQ on DC maturation revealed only, when DCs were co-cultured with PBLs.

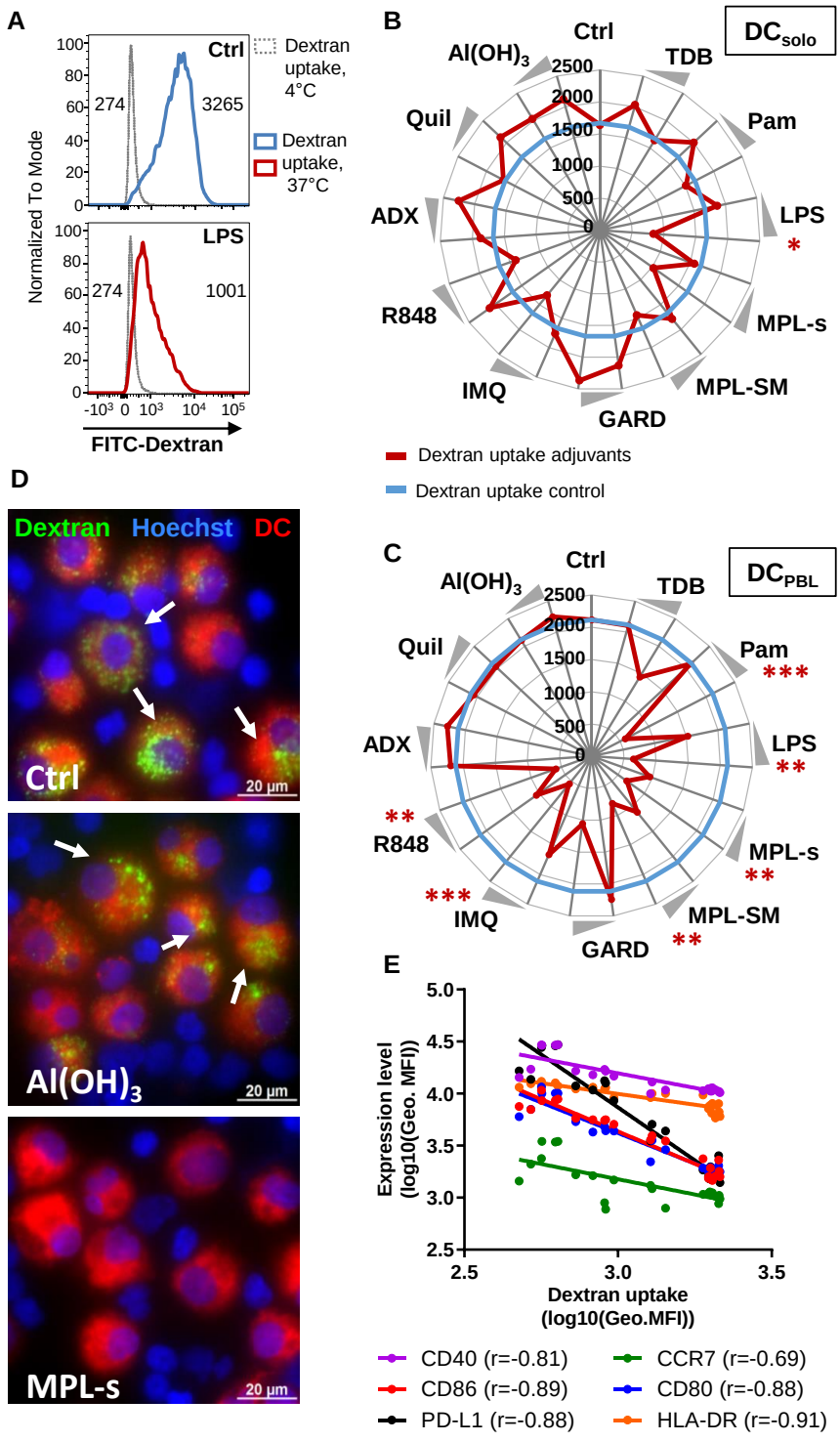

Figure 18: Endocytic activity negatively correlates with the expression of maturation markers after adjuvant stimulation.

DC_{solo} or DC_{PBL} cultures were stimulated with the different adjuvants for 24 hours. Subsequently, 50µg/ml FITC-dextran was given to the culture for an additional hour. After thorough washing, uptake of FITC-dextran in $CD14^{-}$ $CD1a^{+}$DCs was measured as geo. MFI in the unstimulated control or when stimulated with LPS. (A) Non-specific binding of FITC-dextran at 4°C served as control (dotted grey line). DC's endocytic capacity of FITC-dextran was analyzed at 37°C. Values within the histograms indicate the geo. MFI of the respective condition at 4°C and 37°C. (B), (C) Radar plots showing the endocytic uptake of FITC-dextran in DC_{solo} or DC_{PBL}, respectively. The blue solid line indicates the geo. MFI of FITC in the unstimulated controls. Adjuvant-induced changes of the endocytic capacity (geo. MFI of FITC) are shown in red. Both lines are represented as mean (n=12) from at least 3 independent experiments. Statistical comparisons of the unstimulated control and the adjuvants was performed using the Kruskal-Wallis test with Dunn's correction (* $p<0.05$, ** $p<0.01$, *** $p<0.001$). D) Representative fluorescent microscopic pictures are shown for the unstimulated, $Al(OH)_3$- and MPL-s stimulated DC:PBL co-cultures (green: FITC-dextran, blue: Hoechst, red: DCs; scale bar: 20µM). E) Expression of the different maturation markers (geo. MFI) on DC_{PBL} was correlated with the uptake of FITC-dextran (geo. MFI) using spearman's nonparametric rank correlation.

6.4 Cytokine and chemokine expression patterns after adjuvant stimulation

In a next step, we sought to investigate the adjuvant-induced cytokine and chemokine expression of DC:PBL cultures after 24 hours of stimulation as this innate immune response could impact a subsequently elicited adaptive immune response. To this end, we performed a multianalyte protein profiling in which we analyzed 25 cytokines and chemokines using the Luminex xMAP technology (Figure 9, p. 64). We collected the supernatant of DC:PBL cultures from 30 healthy donors, separated equally in age and sex (15 male/ female; 7-8 >40/ <40 years of age), after stimulation with the adjuvants for 24 hours. We especially focused on the DC:PBL co-culture assay system, rather than on DCs alone, to further elaborate the complex interplay within this immunological network.

6.4.1 Induction of cytokine and chemokine expression varies between adjuvants

To assess the overall adjuvant-induced signature of the 25 proteins, we plotted the concentration of the measured analytes (raw data) across all donors. The cytokine and chemokine expression profiles of six immunomodulators LPS, TDB, Pam, MPL-s, GARD and $Al(OH)_3$, examples of each adjuvant class, are shown in Figure 19. Expression profiles of all immunomodulators in low and high concentration can be found in the appendix (8; p. 135).

When the DC:PBL co-culture was stimulated with the positive control LPS, we observed a broad range of cytokine expression levels spanning up to 1000-fold compared to the unstimulated control (e.g. IL-12p70, IL-6). Moreover, we found LPS to cause the strongest expression induction for most of the protein analytes, confirming that LPS was a good positive control for inducing a potent immune response. Herein, the only cytokine being close to the upper limit of detection (5 out of 30 donors were OOR >) was IL-6 while all other protein analytes remained within the standard range. Strikingly, the expression profile of MPL-s was very similar compared to that of LPS, although MPL-s is a detoxified variant of LPS, lacking the polysaccharide chain and the core region.

In contrast to LPS and MPL-s, which induced the expression of all 25 protein analytes, the other in Figure 19 depicted immunomodulators (TDB, Pam, GARD, $Al(OH)_3$), showed selective protein expressions. TDB stimulated most prominently the secretion of IL-6, IL-8, MIP-1α and TNFα, whereas GARD evoked the expression of IFNα, IFNγ, IL-10, IL-6, MCP-1, MIP-1α, RANTES and TNFα. When comparing Pam and $Al(OH)_3$, we observed that the expression of certain protein analytes strongly varied between donors, which is indicated by the length of the quartiles. Nevertheless, we noted a distinct upregulation of IL- 10, IL-1β, IL-6, IL-8, MCP-1, MIP-1α and TNFα upon Pam stimulation. In contrast to all other expression profiles, cytokine

and chemokine levels after $Al(OH)_3$ stimulation led to only minor differences in expression levels compared to the unstimulated control. Except for an enhanced MCP-1 expression, we found generally reduced protein levels compared to the unstimulated control with the most remarkable being IL-12p70 and MIP-1α.

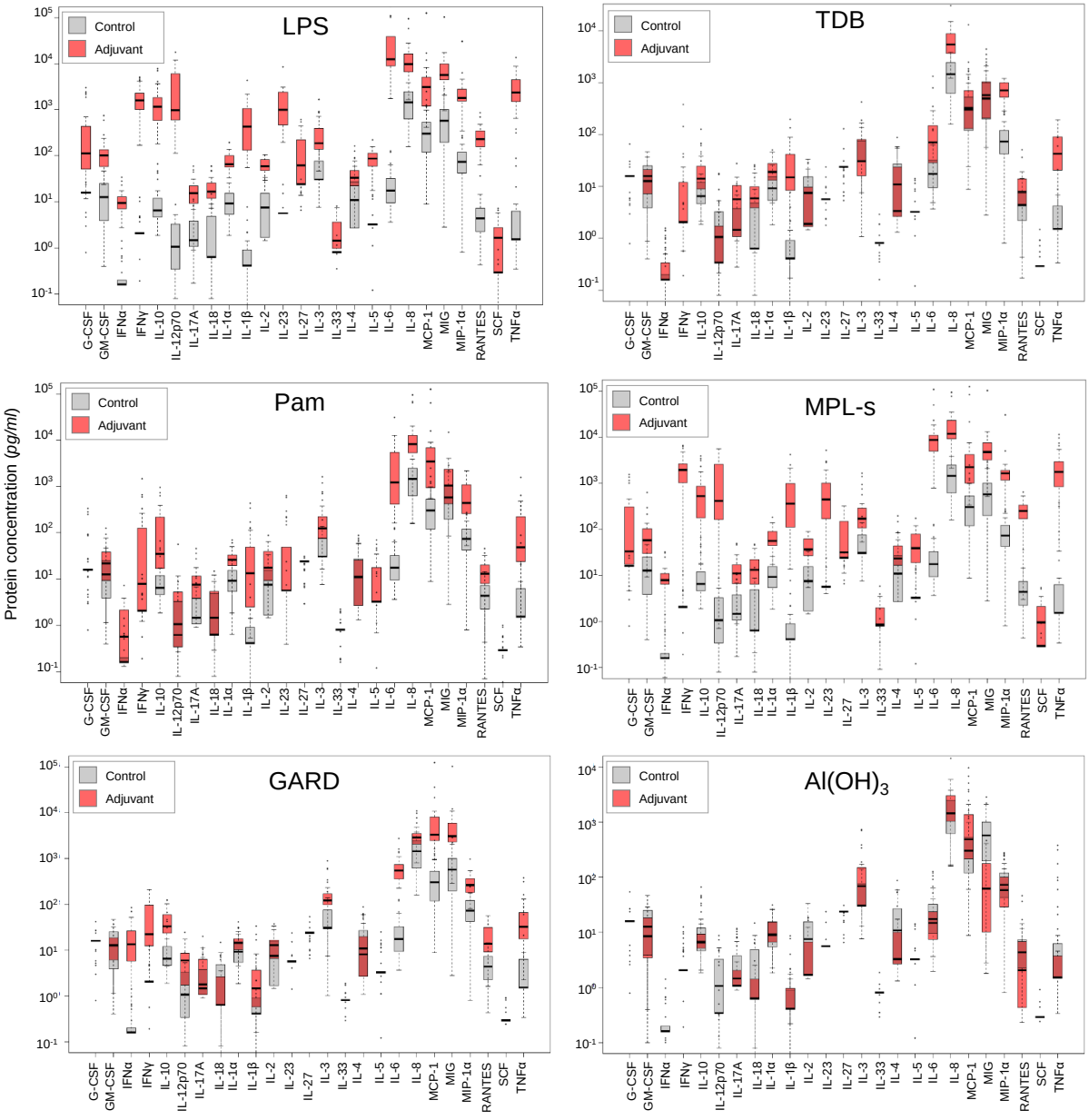

Figure 19: Induction of cytokine and chemokine expression varies between adjuvants.
The DC:PBL co-culture was stimulated with the different adjuvants or left untreated (null response). After 24 hours, supernatant was harvested and analyzed for cytokine and chemokine secretion (25 proteins in total) using the Luminex xMAP technology. Box-whisker plots (Tukey) represents the induced cytokine and chemokine response of six exemplified stimuli (high concentration). Induced responses of alphabetically listed analytes are colored in red; the null response is overlaid in grey. Data are generated from 15 independent experiments with n=30 donors. Data points beyond the whiskers are outliers.

6.4.2 Adjuvants are characterized by their differential cytokine and chemokine expression profiles

Next, we employed principal component analysis (PCA) with the help of Qlucore omnics explorer 3.5 to identify specific patterns of cytokine and chemokine expression that are induced by certain groups of adjuvants, or to separate the effects of adjuvants with the same target receptor. Therefore, the data were normalized (5.2.4) by the software using z-score normalization. This is necessary so that every datapoint has the same scale and that all variables contribute equally. Thus, variables with larger scales will not dominate others and we are able to distinguish all patterns (codecademy, 2020). In addition, donor-related corrections enabled to analyze adjuvant-specific effects.

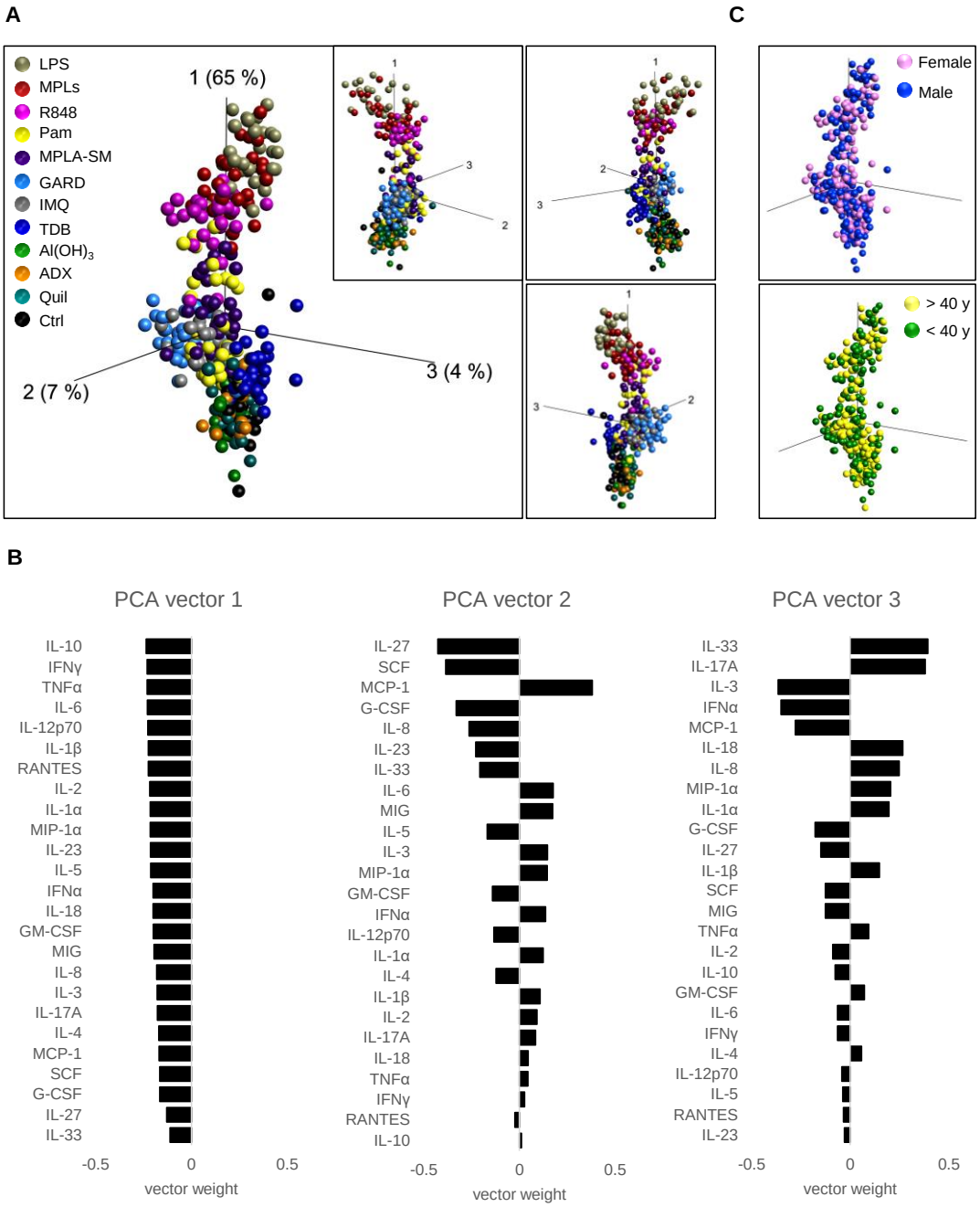

Figure 20: Adjuvants are characterized by their differential cytokine and chemokine expression profiles. The DC:PBL co-culture was stimulated with the different adjuvants or left untreated (control) for 24 hours. Subsequently, the supernatant was analyzed for cytokine and chemokine secretion (25 proteins in total) using the Luminex xMAP technology. A) Principal component analysis with each dot representing one donor (n=30) and each color one of the 12 different conditions (Ctrl or high adjuvant concentrations). The PCA plot captures 76 % of the total variance within the selected data set (PCA-1: 65%, PCA-2: 4%, PCA-3: 7%). Each variable was centered to have a mean of zero, scaled to have unit variance (v=1) and logarithmized before performing the PCA. The q-value was not adjusted here (q-value=1). B) The graphs show the contribution of each protein analyte to the 3 principal component axes. The positioning of the bars is not considered positive or negative, except in relation to the other analytes. C) PCA plots showing the distribution of induced cytokine and chemokine expression within donors of different age or sex.

Without applying any variance or statistical filtering (q- and p-value=1), the PCA revealed stimuli-specific clustering with the first three PC vectors, depicted in a PCA plot, explaining

75 % of the total variance (Figure 20A). Thereof, PC vector 1 represents solely already 65 % of the total variance, indicating that the adjuvants are mainly segregated by the emphasis of cytokines related to this axis. In more detail, the cytokines IL-10, IFNγ, TNFα, IL-6 and IL- 12p70 have the strongest influence on the separation of the adjuvants on PC vector 1 (Figure 20B). The similarity of the cytokine and chemokine expression profile upon LPS and MPL- s stimulation, we mentioned before (Figure 19), becomes even more obvious in the PCA plot by their merged data points. Furthermore, the PCA revealed that both LPS and MPL-s induce the most differential expression protein profiles of all immunomodulators in relation to the unstimulated control. By focusing on the expression profiles of donors (data points) after Pam stimulation, we noticed that the donor variation, we observed in Figure 19, is due to the separation of the donors into low and high responders. Further analysis revealed no sex- or age-related responses upon stimulation, as indicated by the absence of specific clustering (Figure 20C).

6.4.3 Adjuvants can be classified into strong, intermediate and weak immunomodulators based on their induced cytokine and chemokine expression pattern

To characterize the patterns of protein analytes induced by the different adjuvants, we performed hierarchical clustering with the focus on the 17 most differentially expressed proteins (Figure 21). This approach separated the adjuvants into 3 classes, strong, intermediate and weak-stimulating immunomodulators, which is indicated by the branches of the heatmap. The group of strong-stimulating immunomodulators comprised the positive control LPS, MPLs and R848. To the group of intermediate-stimulating immunomodulators belonged Pam, MPL-SM, GARD, IMQ and TDB and the group of weak-stimulating immunomodulators included ADX, $Al(OH)_3$, Quil. The branches of the hierarchical clustering indicated that the weak and intermediate-stimulating modulators were more similar in their expression profile compared to the strong modulators. We observed that the expression profiles of donors stimulated with one of the weak immunomodulators could not be separated by means of these 17 protein analytes. Moreover, only the adjuvants R848, GARD and TDB induced a distinct expression profile of all 30 donors, causing their segregation from all other expression profiles induced by the other adjuvants.

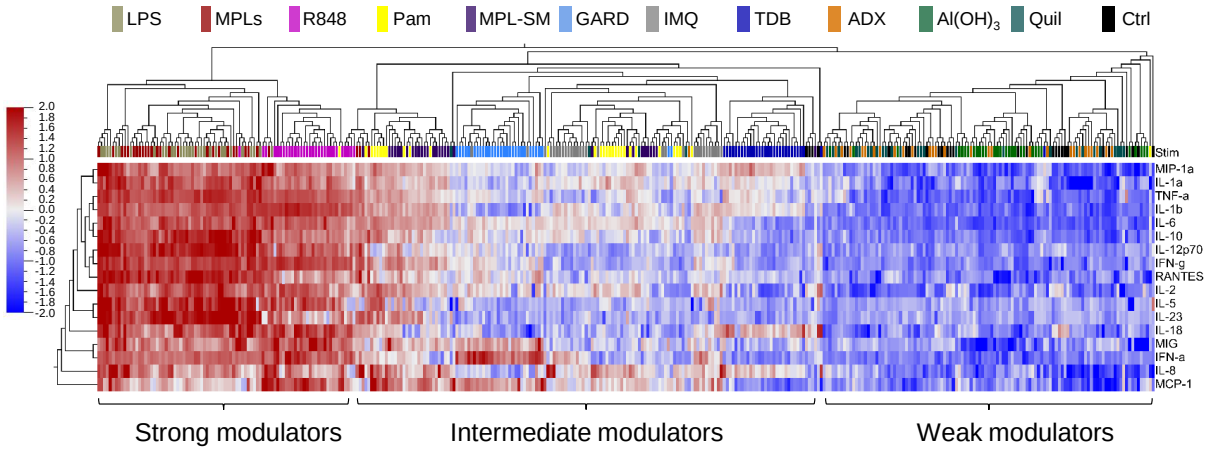

Figure 21: Adjuvants are classified into strong, intermediate and weak immunomodulators based on their induced cytokine and chemokine expression pattern.
24 hours after stimulating DC:PBL co-cultures with the different adjuvants, supernatant was harvested and analyzed for cytokine and chemokine secretion (25 proteins in total) using the Luminex xMAP technology. A data set obtained from 30 donors stimulated with the high concentration of the adjuvants was used for the following analysis. The dendrogram, including all adjuvants (color code on top of the heat map), shows the hierarchical clustering of the protein expression data. Each box within the color code on top of the heat map stands for one donor. The expression of the proteins is illustrated as a color graduation ranging between red (high expression) and blue (low expression). The analysis is based on the 17 most differentially induced proteins (cut off value was determined by ANOVA, q-value < $1x10^{-50}$).

6.4.3.1 The strong immunomodulators MPL-s, R848 and LPS

The strong immunomodulators grouped together in the heat-map on the basis of their high induction of all 17 cytokines (Figure 21) and are comprised of MPLs, R848 and the positive control LPS. By performing PCA with these strong immunomodulators (Figure 22A), we again observed that MPL-s and LPS cluster together, even if variance and statistical filtering (q-value < $1x10^{35}$) was applied, which led to the removal of variables (protein analytes) with the lowest variance (Fontes and Soneson, 2011). This indicated that LPS and MPL- s were indeed very similar in their cytokine and chemokine response in relation to R848 and the unstimulated control. Except for lower levels of IL-10, IL-12p70 and IL-23 in MPL-s-treated samples, all other protein levels were comparable to LPS (Figure 22C). Although low-variance variables were removed, the PCA explained 97% of the total variance. This indicates that almost all 25 proteins had a high variance, which matched their classification into strong modulators. PC vector 1 covers 91% of the total variance with the proteins TNFα, IL-10 and IL-6 contributing the most to this axis (Figure 22C). R848 separated on PC axis 2 due to a reduced expression induction of IL-23 and RANTES as well as higher protein induction of IFNα and IL- 1β compared to LPS and MPL-s (Figure 22A, B;C).

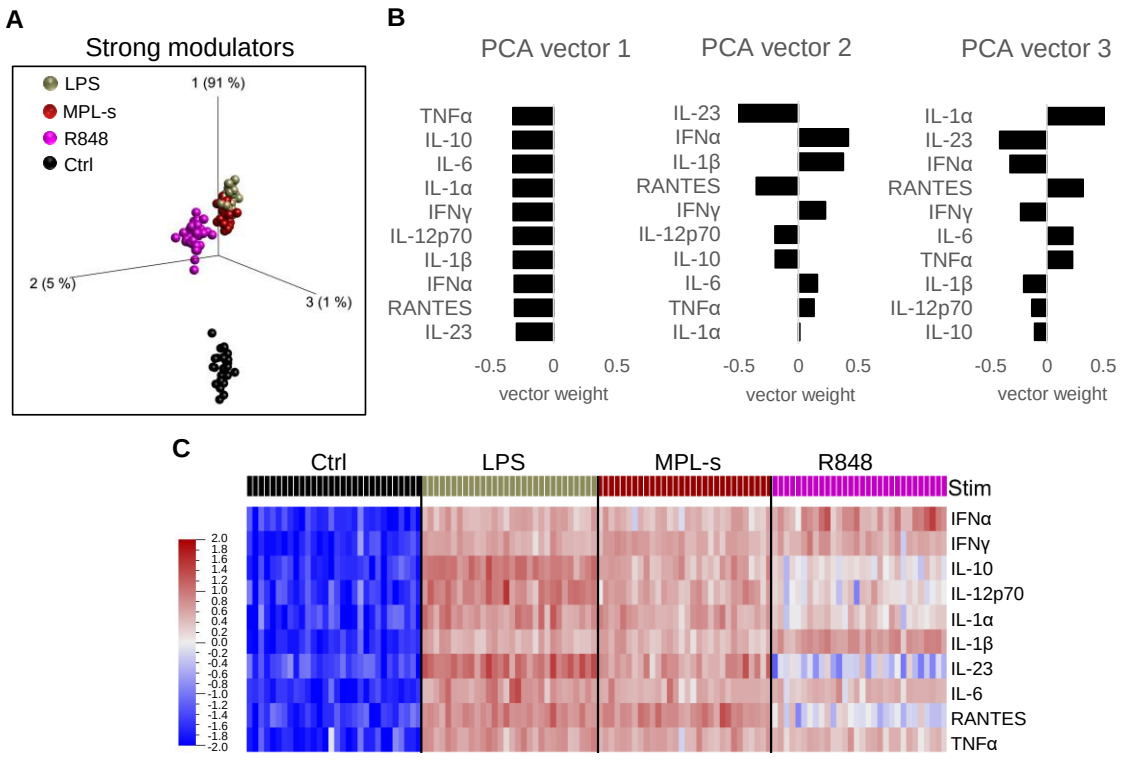

Figure 22: LPS, MPL-s and R848 are strong-immunomodulating adjuvants.
(A) Principal component analysis was performed on the same data set as described in Figure 21, but restricted to the strong immunomodulators LPS, MPL-s and R848. The unstimulated control served as base line. (B) The 10 protein analytes contributed with diverse emphasis to the first three PC vectors. The vector weight does not indicate positive or negative, except in relation to each other. (C) Cytokine and chemokine expression profiles induced by the strong immunomodulators are illustrated as heat-map (high expression: red; low expression: blue). (A)-(C) The cut off q-value < $1x10^{-35}$ was defined by ANOVA and included the 10 most differentially induced proteins.

6.4.3.2 The intermediate immunomodulators MPL-SM, Pam, GARD, IMQ and TDB

The group of intermediate immunomodulators comprised Pam, MPL-SM, GARD, IMQ and TDB. In the PCA plot (Figure 23A), the three PC axes illustrated 93% of the total variance (PC1: 63%, PC2: 23%, PC3:7%). The separation of the different expression profiles induced by the adjuvants was possible by applying variance and statistical filtering ($q \leq 1x10^{-30}$). We found that the differential expression of IL-6, MCP-1, MIP-1α, IL-1β and IFNα caused the cluster formation of the intermediate immunomodulators (Figure 23 B, C). As already noted in the heatmap (Figure 21), the distinct expression profiles following GARD and TDB stimulation led to their clustering from the grouping of MPL-SM, IMQ and Pam. GARD, which is directed to PC vector 2 (Figure 23A), segregated due to a distinct high expression induction of IFNα and low levels of IL-1β induction (Figure 23B, C). TDB was isolated on PC vector 2 (Figure 23A) by causing a low expression of IFNα, IL-6 and MCP-1 but the highest MIP- 1α expression initiation within the group of intermediate immunomodulators (Figure 23B, C). Although Pam, IMQ and MPL- SM are grouped closely together within the PCA, small differences in the expression of these 5 cytokines and chemokines were noticed in the heat map (Figure 23).

MPLA-SM induced a low expression of IFNα, but strong expression of IL-β, IL- 6, MCP-1 and MIP-1α. In contrast, IMQ stimulation results in low levels of MIP-1α, but higher levels of IFNα, while IL-6 and IL-1β expressions are comparable to MPL-SM. Considering the donor-dependent variation in expression after Pam stimulation, we noticed a similar expression of IL-6 compared to MPL-SM and IMQ, as well as a trend of elevated MCP- 1 and MIP-1α expression.

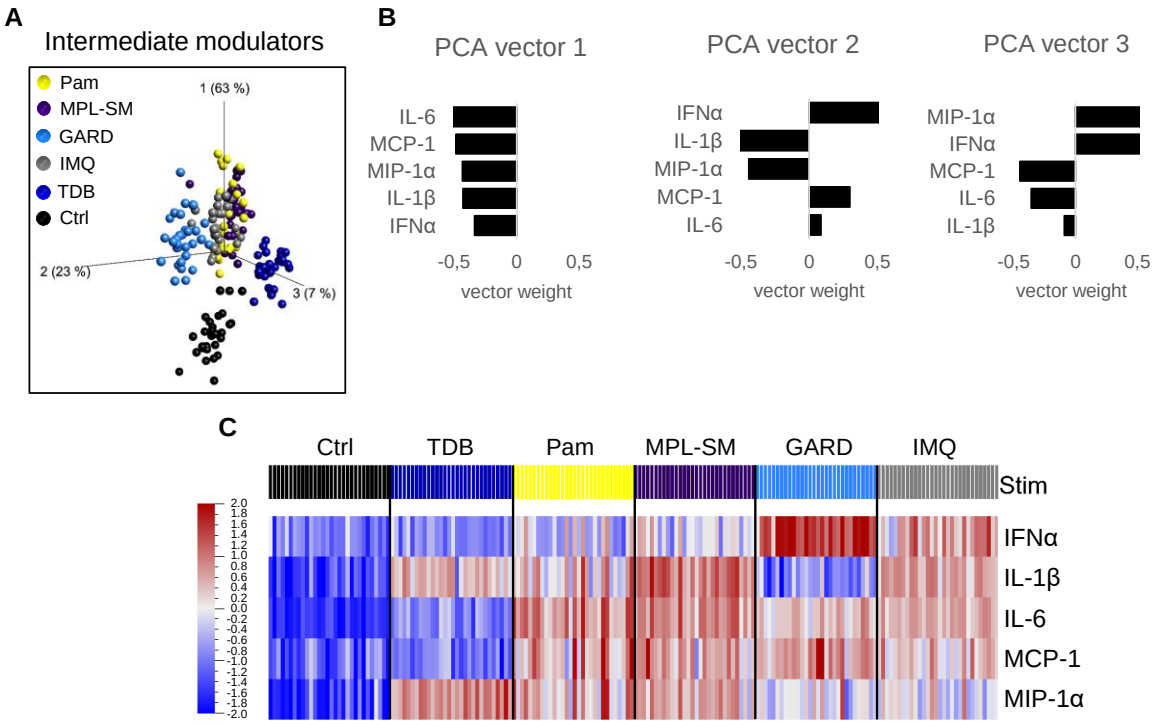

Figure 23: MPL-SM, Pam, GARD, IMQ and TDB are intermediate-immunomodulating adjuvants.
The cytokine and chemokine expression data set obtained from the 30 donors was used for (A) PCA, but restricted to the adjuvants of intermediate modulators MPL-SM, Pam, GARD, IMQ, TDB as well as the unstimulated control. (B) The graphs show the contribution of the protein analytes to each PCA vector. (C) Expression levels of the adjuvant-induced cytokines and chemokines in relation to the unstimulated control are displayed as heat map. Red indicates high protein expression, whereas blue indicates a low protein expression. A)-(C) The cut off q-value ≤ $1x10^{-30}$ was defined by ANOVA and included the 5 most differentially induced proteins.

6.4.3.3 The weak immunomodulators ADX, Quil and Al(OH)₃

The group of weak immunomodulators enclosed the adjuvants ADX, Quil and $Al(OH)_3$. Using variance and statistical filtering, we found only 3 out of 25 protein analytes, namely MIG, MCP- 1 and IL-6, which were the most differentially expressed proteins within this group of immunomodulators. However, when performing PCA, these cytokines and chemokines did not lead to a clear separation of ADX- and Quil-treated cells from the unstimulated control, although the PCA plot covered 100% of the total variance with its three vectors (Figure 24A). While this aggregation of ADX, Quil-A and the unstimulated control indicated a similar expression of cytokines, the heat map emphasized elevated IL-6 levels after Quil stimulation,

whereas an equal expression profile compared to the unstimulated control became apparent for ADX (Figure 24C). For $Al(OH)_3$-treated cells, we found lower levels of MIG and IL-6 and the highest induction of MCP-1 in this group (Figure 24C), which led to the separated clustering on PC axis 2 (Figure 24A, C).

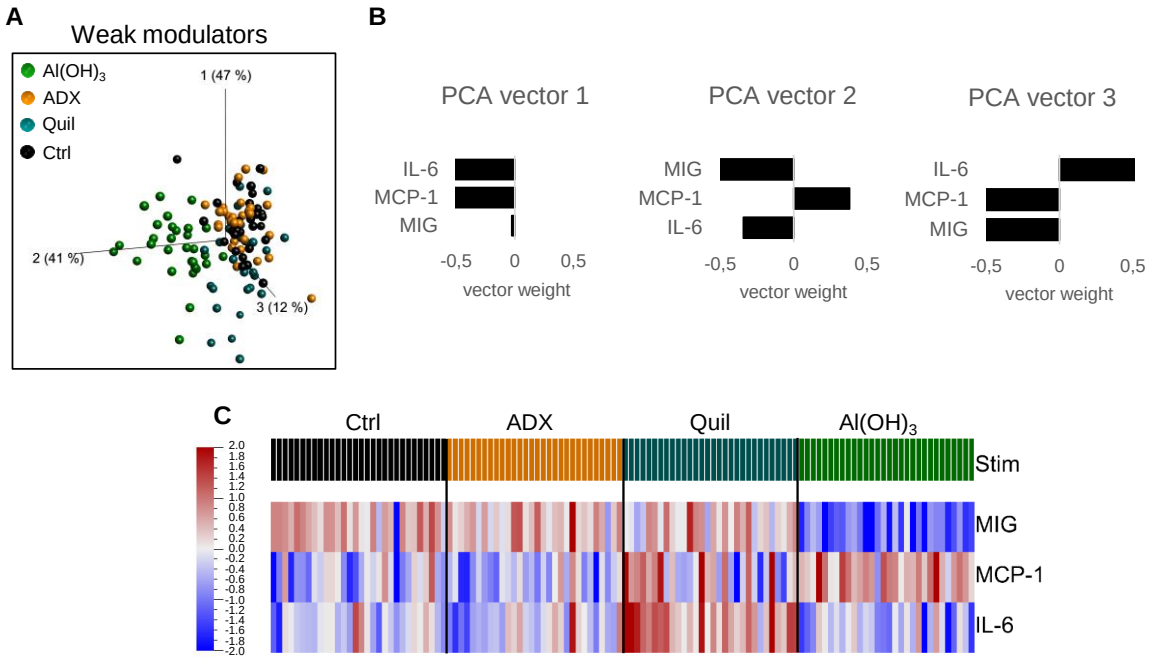

Figure 24: The weak immunomodulators ADX, Quil and $Al(OH)_3$.
(A) ADX-, Quil- and $Al(OH)_3$-induced expression profiles of 30 donors were analyzed for cluster formation by PCA. Three protein analytes were identified to contribute to the separation of the weak immunomodulators by variance and statistical filtering ($q \leq 1x10^{-4}$). The contribution of these three cytokines and chemokines to each axis is shown in (B). The positioning of the bars is not considered positive or negative, except in relation to the other analytes. (C) The heat map illustrates the expression levels for the protein analytes of each donor and adjuvant stimulation.

6.4.4 Adjuvants targeting the same receptor can induce distinct cytokine and chemokine responses

6.4.4.1 TLR4 ligands MPLs, MPL-SM and LPS

Since we observed differences in the expression levels of maturation markers between MPLs, MPL-SM and LPS, we aimed to assess their cytokine and chemokine expression signatures more closely. Thus, we compared the TLR4 ligands LPS, MPL-s and MPL-SM by applying PCA (Figure 25A) with variance and statistical filtering (q-value $\leq 1x10^{-34}$), which allowed us to capture 95% of the measured variance in response to TLR4 stimulation. The resulting 12 out of 25 protein analytes contributed almost equally to the PCA vector 1 (Figure 25B), on which all TLR4 ligands are strongly aligned and which explained 91% of the variance. The separation of MPL-SM in opposite direction to MPL-s and LPS on that axis pointed to a generally lower expression of these 12 cytokines upon MPL-SM stimulation with regard to MPLs or LPS. To

further dissect the differences in protein expression level between MPL-SM, MPLs and LPS, we selected the 6 most differentially induced proteins, which were identified by ANOVA (Figure 25C), and compared the absolute protein concentrations of RANTES, IL- 10, IL-12p70, IFNα, TNFα and IL-23 between the TLR4 ligands. The cluster formation of LPS and MPLs in the PCA was confirmed by the representation of their absolute protein concentrations (Figure 25C), which demonstrated overlapping concentration levels. More specifically, significant differences between LPS and MPLs were not identified by Kruskal-Wallis test. Nevertheless, MPL-s tended to induce less protein expression compared to LPS, which is additionally illustrated in a heat-map (Figure 25D). All listed cytokines, except for IL- 8, were expressed at lower levels upon MPLs stimulation compared to LPS. In contrast, IL-8 is the only cytokine, which was induced in more elevated levels in MPLs-treated cells than in LPS-treated cells.
Compared with MPL-s and LPS, MPL-SM-stimulated cells exhibited significantly lower protein levels for all 6 proteins shown here (Figure 25C).

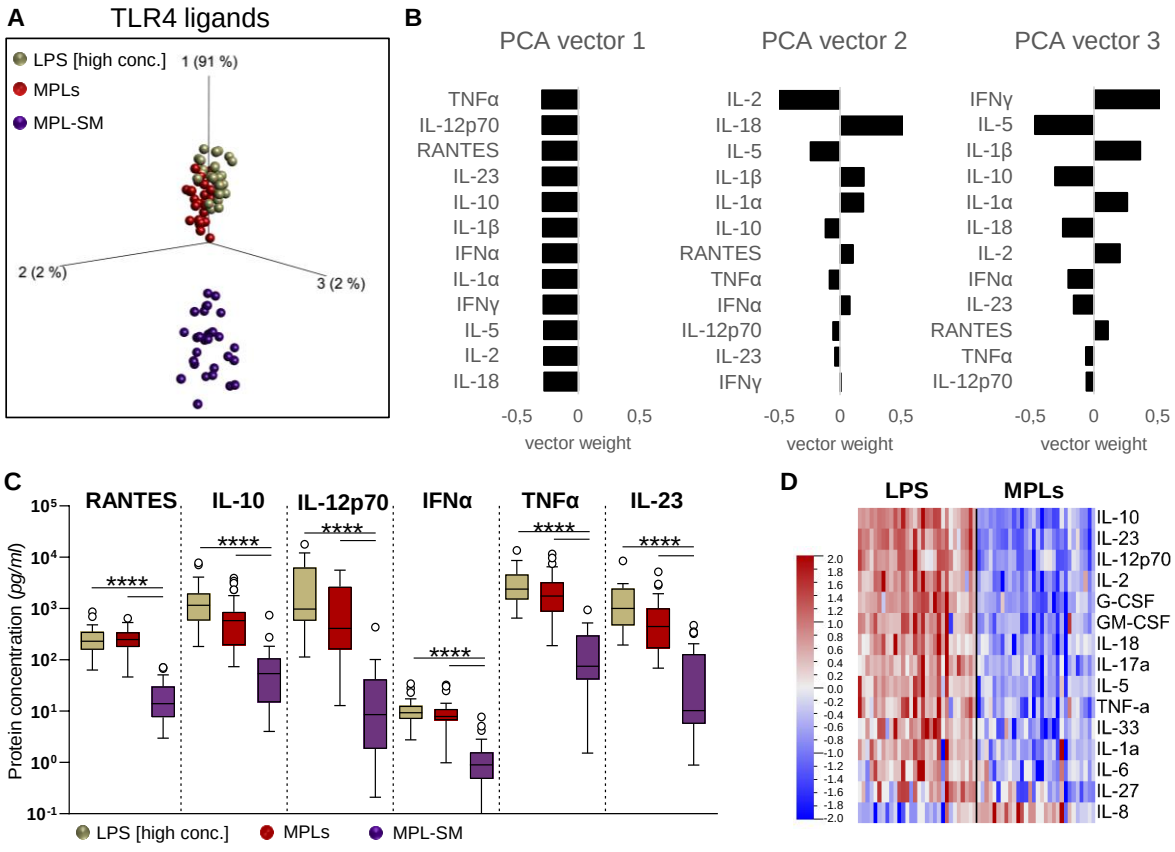

Figure 25: The TLR4 ligands MPLs, MPL-SM and LPS.
Cytokine and chemokine expression data upon stimulation with MPLs, MPL-SM and LPS of 30 donors was analyzed using (A) PCA (q-value < $1x10^{-34}$). (B) Bar graphs show cytokines, which were selected by variance and statistical filtering. Each cytokine and chemokine has different emphases on the three axis, which is depicted by the vector weight. (C) Protein concentrations of the six most differential expressed cytokines and chemokines between the TLR4 ligands are presented as raw data. Statistical comparisons was conducted using the Kruskal-Wallis test with Dunn's correction for multiple testing (* p<0.05, ** p<0.01, *** p<0.001, **** p<0.0001). (D) Expression profiles of

the 15 most differential expressed proteins between LPS and MPLs treated cells are illustrated as heat-map. Cytokines are listed according to their increasing p-value (cut-off q-value: $1x10^{-27}$).

6.4.4.2 The TLR7 ligands GARD, IMQ and R848

Another group of adjuvants that target the same receptor, are the TLR7 ligands. However, while GARD and IMQ bind solely to TLR7, R848 is a dual TLR7/8 agonist. Again, we performed PCA analysis to discover differences in the cytokine and chemokine expression profiles. We found that R848, GARD and IMQ could be segregated by PCA (Figure 26A), with PCA vectors displaying 91% of the total variance. The expression profiles of R848-treated cells are directed to PCA vector 1, indicating a potent pro-inflammatory response due to a strong contribution of TNFα, IFNγ, IL-6, IL-12p70, MIP-1α to that axis. Although PCA vector 1 dominates with 79% of the total variance, the separation of GARD and IMQ is also driven by PCA vector 2 corresponding to the differentially induced proteins IFNα, MIG and IL-1β (Figure 26B). For statistical comparison, we selected 6 proteins with the highest variance which were calculated by the software (Figure 26C). Compared to treatment with IMQ, protein levels of IFNα and MIG were significantly enhanced when cells had been stimulated with GARD, whereas IL-1β expression was reduced. R848 showed significantly higher levels of TNFα, IL-β, IFNγ, IL-18 and MIG in comparison to GARD and IMQ. However, no significant differences in the protein levels of IFNα were found between stimulations by GARD or R848. In addition, expression levels of the 15 protein analytes of Figure 26A are summarized in a heat map in Figure 26D. At a glance, the heat map demonstrates the distinct protein inductions by theTLR7 ligands GARD and IMQ with IL-1β, MIG, IFNα, RANTES and IL-10 being the most striking ones. The overall higher cytokine and chemokine induction by R848 compared to GARD and IMQ, is likely the reflection of additional TLR8 engagement and its strong ability to dimerize TLR7, resulting in the downstream activation of the pro-inflammatory transcription factors (Zhang et al., 2018).

This cytokine and chemokine analysis of 25 proteins upon adjuvant stimulation resulted in adjuvant-specific protein expression profiles, despite their classification into strong, intermediate and weak immunomodulators. Moreover, even adjuvants targeting the same TLR displayed differences in cytokine and chemokine secretion, demonstrating that subtle structural changes, can have pronounced effects.

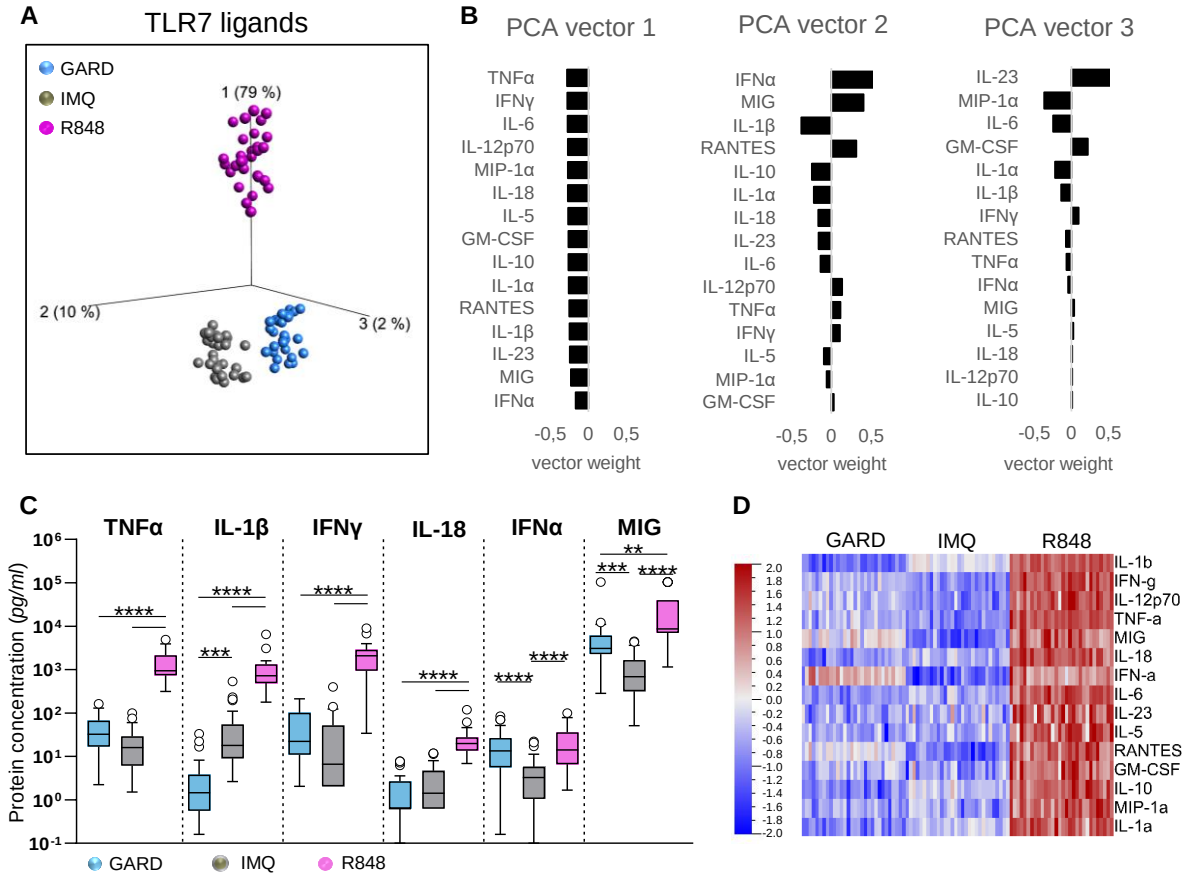

Figure 26: The TLR7 ligands GARD, IMQ and R848.
(A) PCA was performed to distinguish cluster formation due to their differential expression of cytokines and chemokines of GARD, IMQ and R848-treated cells (n=30 donors). Variance filtering and a cut-off q-value of ≤ $1x10^{-15}$ selected 15 cytokines and chemokines, which contribute differently to the three PC axis. Here, the positioning of the bars is not considered positive or negative, except in relation to the other analytes. (C) 6 Protein analytes with the highest variance were selected for statistical comparison using Kruskal-Wallis test with Dunn's correction for multiple testing (* p<0.05, ** p<0.01, *** p<0.001, **** p<0.0001). Analysis was performed on the raw data. (D) Illustration of the expression levels of 15 cytokines and chemokines selected in (A) after stimulation with GARD, IMQ and R848. The proteins are listed according to their variance in decreasing order.

6.5 The NF-κB signaling pathway is induced upon adjuvant stimulation

Transcription factor nuclear factor-kappaB (NF-κB) is a transcription factor, which plays a key role in regulating innate and adaptive immunity by controlling gene expression required for cell development, maturation, proliferation and cytokine production. The signaling pathways that lead to activation of NFκB are induced by a wide range of stimuli such as pathogens, stress signals and pro-inflammatory cytokines like TNFα and IL-1β (Li and Verma, 2002). The inhibitory factor IκBα regulates the transient activation of NF-κB. It is rapidly degraded upon receptor stimulation, and usually resynthesized within one or two hours as part of a negative feedback loop to avoid hyperactivation of NFκB. To test, whether the cytokine and chemokine production upon stimulation of Toll-Like Receptors (TLRs) with adjuvants is dependent on

NFkB activation (Kawai and Akira, 2007), we studied the turnover of IκBα after adjuvant treatment by western blot. We stimulated the DC:PBL co-culture with the adjuvants for 30, 60 and 120 min, followed by cell lysis and performing SDS page with subsequent immunoblotting. We normalized the protein amount of IκBα to the housekeeping protein α-tubulin and to the respective non-stimulated control to assess the decrease of IκBα. As control for an efficient IκBα protein reduction, LPS-stimulated DC_{solo} were taken along on each gel. We observed a decrease of IκBα of around 50% for Pam (52.39 ± 33.56%; Figure 27A), MPLs (58 ± 30.01%), MPL-SM (56. ± 25.32%), LPS (52 ± 17.48; all three Figure 27C) and R848 (59±21.42%; Figure 27D) after 60 min stimulation with the respective TLR ligand. A higher IκBα reduction was not ascertained for the co-culture, whereas IκBα levels reached a decline down to 11% (±13.06) in LPS-stimulated DC_{solo}. For Pam, MPL-s, MPL-SM, LPS and R848, we noted elevated IκBα levels again after 120 min of stimulation, indicating a re-synthetization of the protein. TDB led to a slight drop of IκBα levels to 72% (±18.15) after 120 min stimulation (Figure 27A). Stimulation with GARD, IMQ (both Figure 27D), $Al(OH)_3$, ADX and Quil (all three Figure 27B) did not reveal a remarkable decline in IκBα protein levels.

Taken together, IκB protein reduction after stimulation with Pam, TDB, LPS, MPL-s, MPL-SM and R848 demonstrated the involvement of NFκB signaling. In contrast, GARD, IMQ, $Al(OH)_3$, ADX and Quil-treated cells did not exhibit activation of NFκB signaling, suggesting the use of inappropriate time points to detect NFκB activity or the involvement of other transcription factors upon adjuvant stimulation.

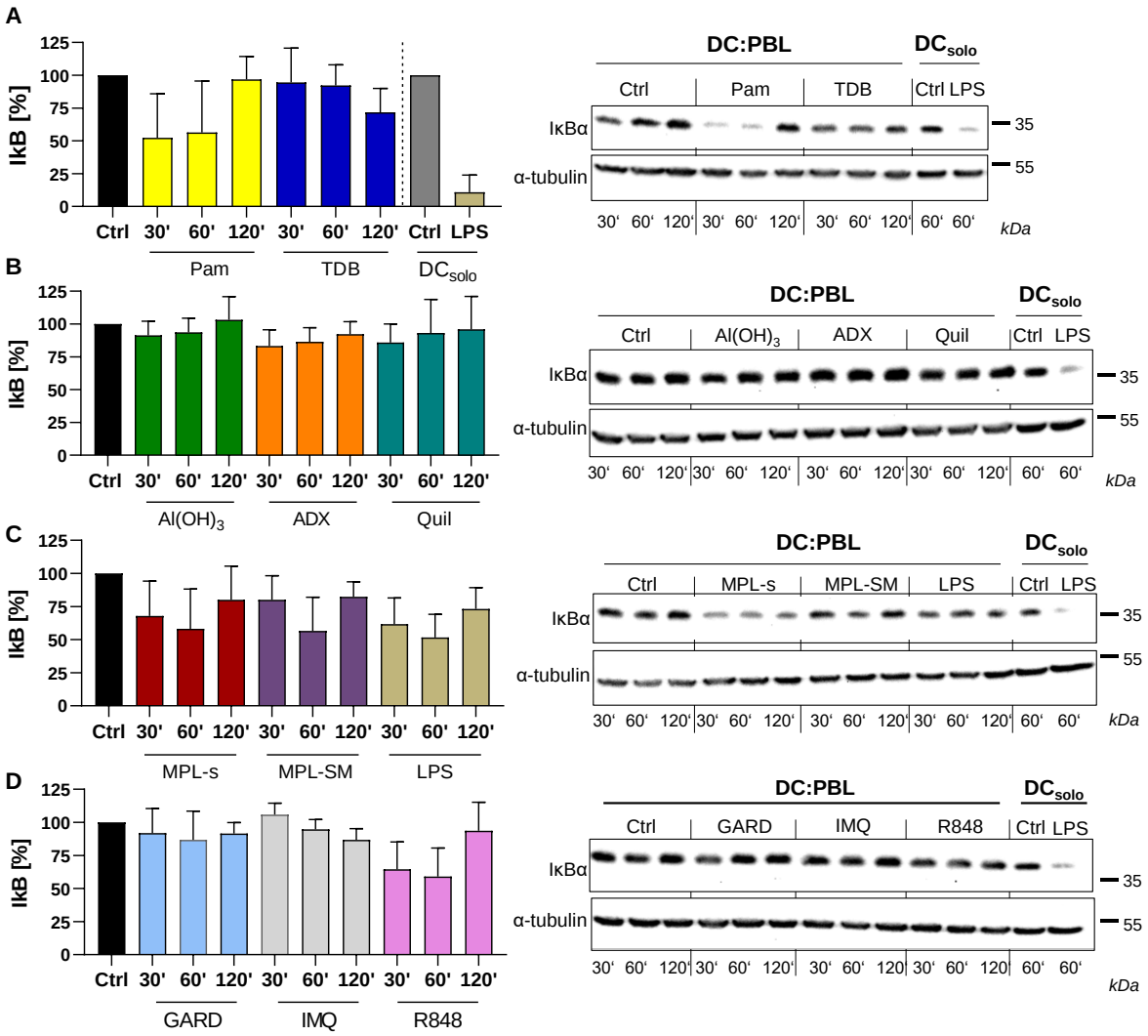

Figure 27: NF-κB is activated upon adjuvant stimulation of TLRs.
(A)-(D) DCs were harvested on day 5 or day 6 of culture. PBLs were thawed and added to the DCs at a 1:5 ratio. DC:PBL co-cultures were rested for 2 hours at 37°C and subsequently stimulated with the different adjuvants for 30, 60 or 120 minutes. Untreated controls were carried along at the indicated time points. Cell lysates were analyzed by SDS-Page and immunoblotting for IκBα and α-tubulin. Levels of IκBα and α-tubulin were determined by densitometry, followed by the normalization of IκBα to α-tubulin for each sample. To evaluate the decrease of IκBα, the ratio was normalized to its respective unstimulated control by setting the control to 100%. LPS-stimulated DC_{solo} served as control for effective IκBα reduction on each immunoblot. Data is presented as mean ± SD of at least 2 independent experiments (n=4-9 donors). Western blots are representative for one donor.

6.6 Immunomodulatory effects of adjuvants on lymphocyte proliferation

6.6.1 Adjuvants stimulate the proliferation of lymphocytes to different degrees and in an antigen-independent manner

Next, we focused on the immunomodulatory effects of the adjuvants on the adaptive immune response by investigating the proliferation of lymphocytes. For this purpose, we employed cells collected from the 30 donors that had already been used for the cytokine and chemokine

profiling. To assess the proliferation of lymphocytes, cells were labeled with CFSE followed by the stimulation of the DC:PBL co-culture with the different adjuvants for 6-7 days. Colony formation within the wells of the culture plate indicated cell proliferation and could be examined by light microscopy upon day 4 (Figure 28A). To quantify lymphocyte proliferation, viable single lymphocytes were probed by flow cytometry for transmitting a lower fluorescence intensity of the CFSE dye, which is indicative for CFSE dilution due to cell division. (Figure 28B). Firstly, by focusing on the total population of proliferating lymphocytes, we observed that all TLR ligands, except for IMQ, induced the proliferation to different degrees, with R848 being the strongest inducer of proliferation (Ctrl: 7.4 ± 3.7%; R848 high conc.: 36.5 ± 10.0%) (Figure 28C). Furthermore, we found similar levels of lymphocyte proliferation for the TLR4 ligands LPS (LPS high conc.: 22.6 ± 9.2%), MPLs (high conc.: 20.1 ± 8.8) and MPL-SM (high conc.: 20.3 ± 9.2). For TDB (high conc.: 11.3 ±5.9%), IMQ (high conc.: 4.6 ±4.1%), ADX (high conc.: 3.3 ±1.8%), Quil (high conc.: 3.6 ±2.2%) and $Al(OH)_3$ (high conc.: 5.5 ±3.1%) we noted no significant increase of proliferating lymphocytes compared to the unstimulated control.

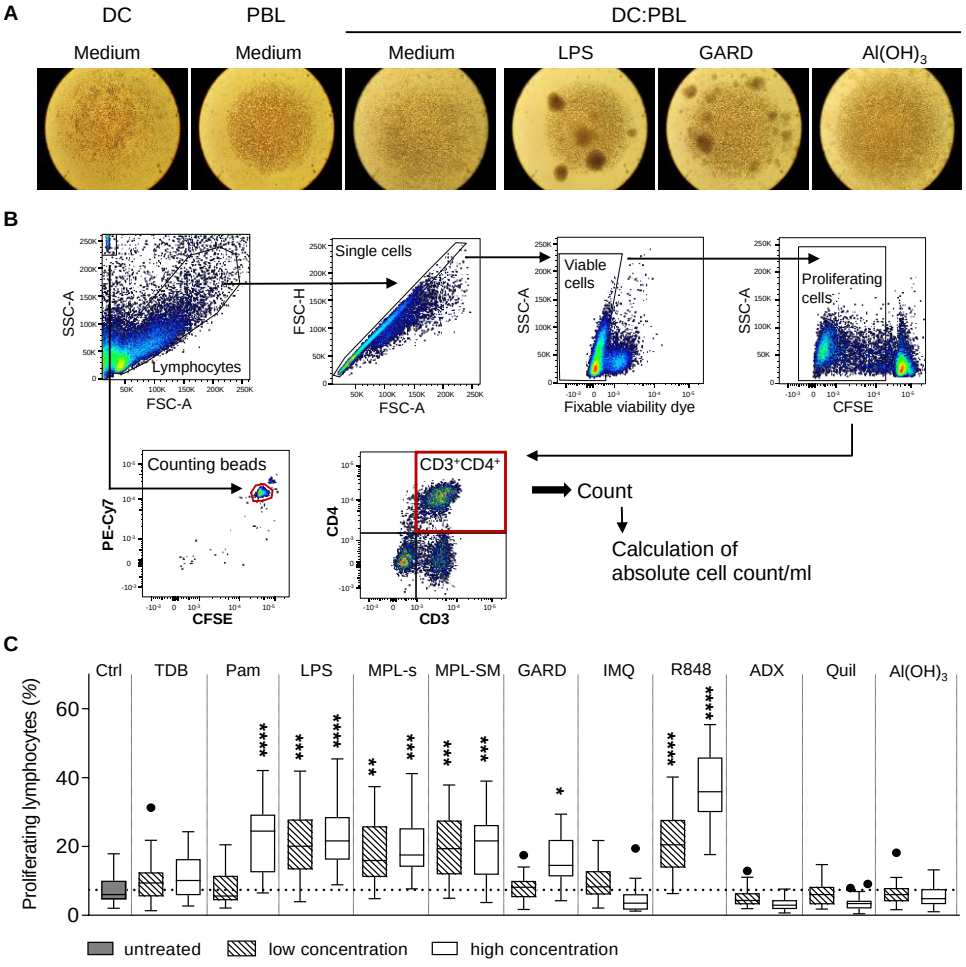

Figure 28: Adjuvants stimulate the proliferation of lymphocytes to different degrees.

CFSE-labeled DC:PBL co-cultures were stimulated with the different adjuvants for 6 days, followed by antibody staining and flow cytometry analysis. (A) Representative light microscopy pictures showing the cells within the U-bottom plate on day 6 of stimulation. (B) Gating strategy to assess the proliferation of different lymphocyte populations. Doublets and apoptotic cells were excluded. Proliferating cells were identified by exposing a lower intensity of the CFSE dye. Within the proliferating lymphocytes, various sub-populations were identified by specific antibody staining. Here, an example for $CD3^+CD4^+$ T cells is shown. Counting beads were acquired during sample analysis allowing the calculation of the absolute cell count of proliferating $CD3^+CD4^+$ T cells within the respective sample. (C) Box Whisker plots (Tukey) represent adjuvant-induced total lymphocyte proliferation. Statistical comparisons of the unstimulated control and the adjuvant was performed using the Kruskal-Wallis test with Dunn's correction (* $p<0.05$, ** $p<0.01$, *** $p<0.001$, **** $p<0.0001$) (n=24 donors). If not otherwise specified, comparison to the unstimulated control revealed no significance. Data is representative for at least three independent experiments.

6.6.2 Adjuvants induce the proliferation of different lymphocyte populations

Secondly, to further address the question whether stimulation with the different immunomodulators induce adjuvant-specific proliferation profiles, we analyzed the absolute cell count for each lymphocyte population through the use of counting beads during sample acquisition (Figure 28B). The TLR2 ligand Pam led to the proliferation of both $CD4^+$ (2.9x compared to ctrl) and $CD8^+$ T cells (3.0x) as well as NK cells ($CD3^-CD56^+$; 5.4x). The increase in cell count was only observed when stimulated with the high concentration of the adjuvant. Surprisingly, within the group of TLR4 ligands, different proliferation profiles were found. Here, LPS induced the proliferation of all examined lymphocyte populations with a significant increase in absolute cell counts ($CD4^+$: 3.5x $CD8^+$: 7.3x; NKT ($CD3^+CD56^+$): 10.6x; B ($CD3^-CD19^+$): 5.8x; NK: 10.3x). The proliferation pattern induced by MPL-s overlaped with that of LPS but differed in the induction of B cells. Here, the absolute B cell count was only slightly enhanced (Ctrl: 739 ± 766; LPS: 4283 ± 5950; MPL-s: 2928 ± 3957 [abs. cell counts]). Notably, for both LPS and MPL-s, the cell number of $CD4^+$ T cells was only significantly enhanced upon stimulation with the low concentration of both immunomodulators (LPS low: 3.5x; MPL-s low: 2.9x). Upon stimulation with the high concentrations, cell counts were only slightly increased compared to the unstimulated control, suggesting a suppressive factor being secreted under these conditions (LPS high: 1.8x; MPL-s high: 2.0x). Taking the cytokine secretion data after 24 hour stimulation into account, we found IL-10 to be highly expressed upon stimulation with the high concentration of LPS and MPL-s, but not when stimulated with the low concentration of LPS and MPL-s (Figure 30). For both concentrations of MPL-SM, we detected comparable IL-10 levels to the low concentration of LPS and MPL-s and observed significantly higher $CD4^+$ T cell counts compared to the unstimulated control (MPL-SM low: 3.4x; MPL-SM high: 3.3x). In contrast to LPS and MPL-s, NK T cell levels were elevated but not significantly different to the unstimulated control upon MPL-SM stimulation using Kruskal-Wallis test (LPS high: 12.2x; MPL-s high: 11.8x; MPL-SM high: 5.1x (Figure 29A, B).

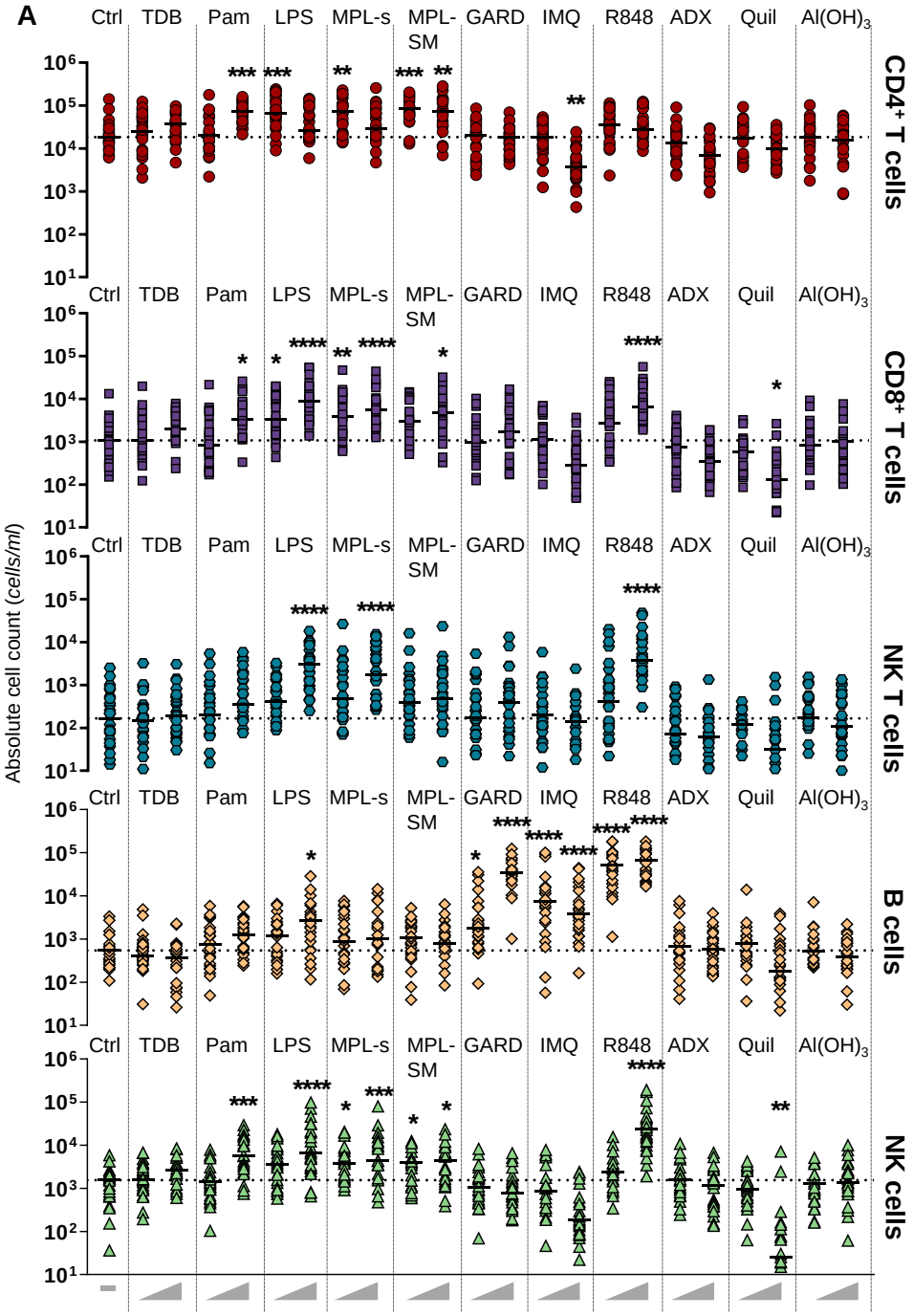

B

	TDB	Pam	LPS	MPL-s	MPL-SM	GARD	IMQ	R848	ADX	Quil	Al(OH)$_3$
CD4$^+$ T cells		+	+	+	+						
CD8$^+$ T cells		+	+	+	+			+			
NK T cells			+	+				+			
B cells			+			+	+	+			
NK cells		+	+	+	+			+			

Figure 29: Adjuvants induce the proliferation of different lymphocyte populations.
iDCs were harvested on day 5 and co-cultured with autologous PBLs at a 1:5 ratio. Both DC and PBLs were labeled with CFSE prior to seeding. Subsequently, cells were stimulated with the different adjuvants or left untreated (Ctrl). (A) After 6 days, PBLs were stained for CD3, CD4, CD8, CD19 and CD56, and proliferating cells were analyzed by flow cytometry. Counting beads were used during sample acquisition to allow the calculation of absolute cell numbers. Aligned dot plot showing the individual values and median from 26 donors. Statistical comparison of the

unstimulated control and the adjuvants was performed using the Kruskal-Wallis test with Dunn's correction (* p<0.05, ** p<0.01, *** p<0.001, **** p<0.0001). If not otherwise specified, comparison revealed no significance. Statistical significance obtained in (A) is summarized in (B): '+' displays determined statistical significance regardless of the p-value.

Furthermore, the proliferation profiles also vary between the TLR7 ligands GARD, IMQ and R848 regarding the lymphocyte populations being induced. R848 stimulation led to the proliferation of $CD8^+$ T cells, NK T cells, B cells and NK cells, but not of $CD4^+$ T cells. Remarkably, especially the induction of B, NK and NKT cell proliferation by R848 was powerful, as indicated by high absolute cell counts (B: 74738 ± 46701; NK: 40533 ± 48266; NKT: 4110 ± 4247) and exceeding the cell numbers achieved with LPS stimulation (B: 4283 ± 5950; NK: 16198 ± 23141; NKT: 8547 ± 12115). GARD and IMQ had a similar proliferation-inducing profile, with B cells being the only cell population they stimulated to proliferate. Here, the high concentration of GARD induced higher absolute cell counts compared to IMQ (GARD: 58.1x to IMQ: 11.8x). Notably, the high concentration of IMQ led to the decrease of total lymphocyte proliferation (Figure 28C) which was probably caused by the significant drop in $CD4^+$ T cell count (0.2x) compared to the unstimulated control (Figure 29A). This finding confirms Dominguez-Villar and colleagues, who described that TLR7 stimulation induces anergy in human $CD4^+$ T cells in a concentration-dependent manner (Dominguez-Villar et al., 2015). We observed a similar effect of reduced proliferation of total lymphocytes (Figure 28C) and a decrease in absolute cell counts ($CD8^+$ T cells: 0.2x and NK T cells: 0.3x, Figure 29A) when stimulating with Quil (Marty-Roix et al., 2016). Finally, for TDB, ADX and $Al(OH)_3$, we found no significant rise in absolute cell counts for any of the lymphocyte populations. All significantly increased absolute cell counts compared to the unstimulated control are summarized in Figure 29B.

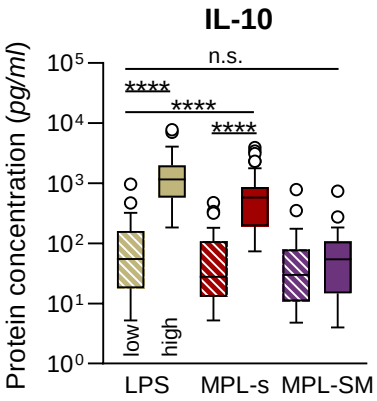

Figure 30: IL-10 as a potential suppressive factor of $CD4^+$ T cell proliferation.
The DC:PBL co-culture was stimulated at a low and a high concentration of the TLR4 ligands LPS, MPL-s and MPL-SM for 24 hours. The supernatant was analyzed for the cytokine IL-10 by Luminex xMap analysis. Data are presented as Box-Whisker plots (Tukey) and were compared by Kruskal-Wallis test with Dunn's correction (**** p< 0.0001) (n=30 donors). Data is representative for at least three independent experiments.

6.6.3 The sex, but not the age, impacts the cell count of proliferating B and NK

It is common knowledge that the immune response weakens with age. This has consequences on vaccine efficacy and demands the development of tailored vaccines that stimulate an effective immune response in elderly (Weinberger and Grubeck-Loebenstein, 2012). Furthermore, both the innate and adaptive immune response of females and males differs when stimulated, but this effect is so far not considered in vaccine design (Fink and Klein, 2015). We examined the effects of adjuvants on sex and age by separating the 30 donors according to their sex and their age class (< 40 years/ > 40 years). We did not ascertain sex or age-related effects on the innate immune response by evaluating cytokine and chemokine secretion (Figure 9B). Hence, we continued to investigate potential sex and age-related effects on the adaptive immune response by analyzing proliferating lymphocytes and associated cell type specific differences. Therefore, absolute cell counts of adjuvant-stimulated samples (Figure 29) were normalized to their respective unstimulated control, and resulting fold changes were compared between females and males, or the two age classes. We found that B cells of female donors proliferated to a significantly higher degree (115 ± 84 fold change to the unstimulated ctrl) in response to stimulation with the TLR7 ligands GARD compared to B cells of male donors (52 ± 39; Figure 31A). The same trend was observed, when B cells were stimulated with the other TLR7 ligands IMQ (F: 21 ± 13; M: 13 ± 20; Figure 31B) or TLR7/8 ligands R848 (F: 217 ± 149; M: 102 ± 41; Figure 31C). Additionally, we noted significant sex-related differences in the proliferation of NK cells. In contrast to the previous result that TLR7 ligands promoted a higher proliferation of B cells from female donors, the TLR4 ligand MPL-s led to a higher proliferation of NK cells from male donors (F: 7 ± 17; M: 18 ± 18; Figure 31D). We observed neither for proliferated B cells, nor for NK cells age class-related effects (Figure 31A-D). Comparisons between sex and age class-dependent comparisons between the other proliferating lymphocyte populations upon adjuvant stimulation revealed no further differences.

Taken together, the TLR ligands Pam, LPS, MPL-s, MPL-SM, GARD, IMQ and R848 stimulated the proliferation of distinct lymphocyte subsets in an antigen-independent context. While GARD and IMQ solely induced B cells to proliferate, at least three cell types responded with proliferation to all other TLR ligands. Surprisingly, upon R848 stimulation proliferating cells exceeded the cell count of LPS-induced proliferating cells. Additionally, we observed a sex-driven bias of B cell proliferation in female donors upon TLR7 proliferation.

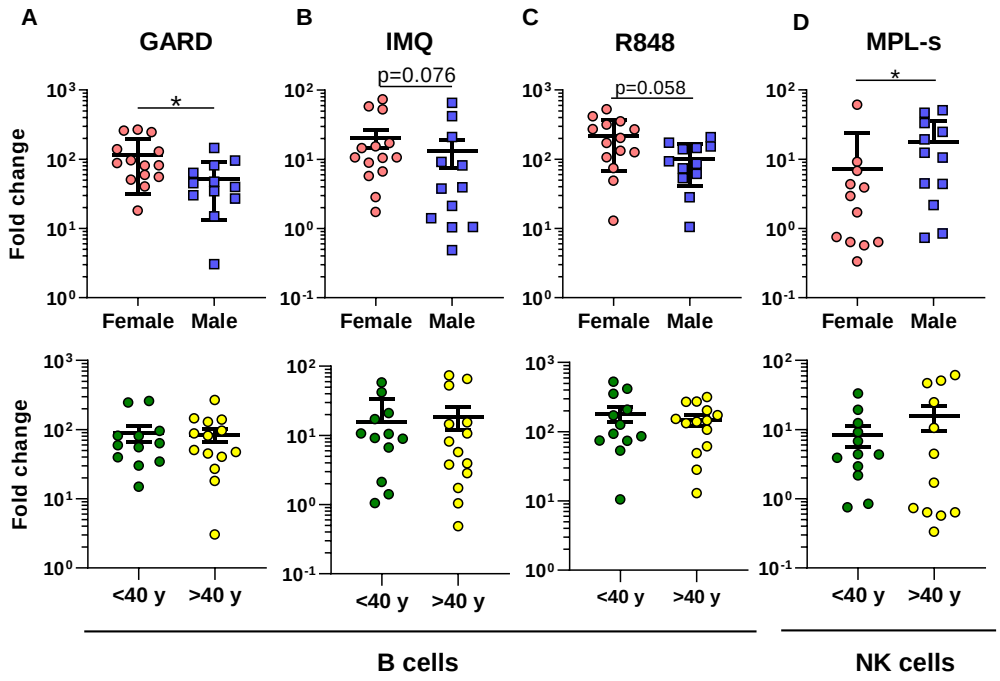

Figure 31: Sex, but not age, impacts the cell count of proliferating B and NK cells.
Data of adjuvant-induced proliferating lymphocytes (Figure 29) were compared for sex and age-related differences. Therefore, absolute cell counts were normalized to its respective unstimulated control. The resulting fold changes of 30 donors were analyzed using the Mann-Whitney test (* p< 0.05). Sex-related comparisons are shown for (A) GARD-, (B) IMQ- and (C) R848-stimulated B cells as well as (D) MPLs-stimulated NK cells. Data is presented as mean ± SD and representative for at least three independent experiments.

6.7 The proliferation of lymphocyte subpopulations can be linked to the expression of certain cytokines and chemokines

As we employed cells from the same donors for the analysis of the adjuvant-induced cytokine and chemokine signature as well as for the proliferating lymphocyte population profile, we sought to test whether the cytokine and chemokine milieu at early time points of lymphocyte proliferation (after 24 hours of adjuvant stimulation) could have had an effect on the resulting lymphocyte proliferation after 6 days of DC:PBL co-culture. For each donor, we normalized the measured values of the cytokine and chemokine data set as well as the lymphocyte proliferation data set to their respective unstimulated control. Potential influences of the individual donors, sex or age of the donor, the day of experiment, day of Luminex analysis or individual sample plates on the measured protein analytes and lymphocytes have been assessed individually using the Kruskal-Wallis test (Figure 32A). The logarithmized p-values demonstrated an expected donor dependency, with an impact especially on GM-CSF, IL-17A, IL-18, IL-2, IL-3, IL-4, IL5 concentrations and NKT cell proliferation. Interestingly, when performing a spearman correlation of protein analytes and lymphocyte proliferation we obtained an overall positive correlation (Figure 32B). Although most of the values indicated only a weak correlation (around r=0.3), the proliferation of distinct lymphocyte populations

correlated moderately (around r=0.5) to several cytokines. $CD8^+$ T cell proliferation could be linked to the increased expression of multiple cytokines such as IFNy (r=0.45), IL-10 (r=0.52), IL-12p70 (r=0.44), IL-1α/β (r=0.47/0.48), IL-6 (r=0.49), MIG (r=0.5), MIP-1α (r=0.46), RANTES (r=0.58) and TNFα (r=0.46). Also, NKT cell proliferation could be related to a cytokine pool out of IL-10 (r=0.46), IL- 23, IL-6, MIG and RANTES (all r=0.47). In contrast, the proliferation of B cells showed a moderate correlation to only two cytokines, namely IFN-α (r=0.5) and MCP-1 (r=0.46). NK cells rather correlated to RANTES (r=0.46). Strikingly, $CD4^+$ T cell proliferation and the listed cytokines and chemokines correlated only weakly in our analysis. However, given the quite early analysis of cytokine and chemokine expression and a relatively late analysis of lymphocyte proliferation in our experimental setup, there might be a stronger correlation of these two responses which we simply did not catch by the time points chosen.

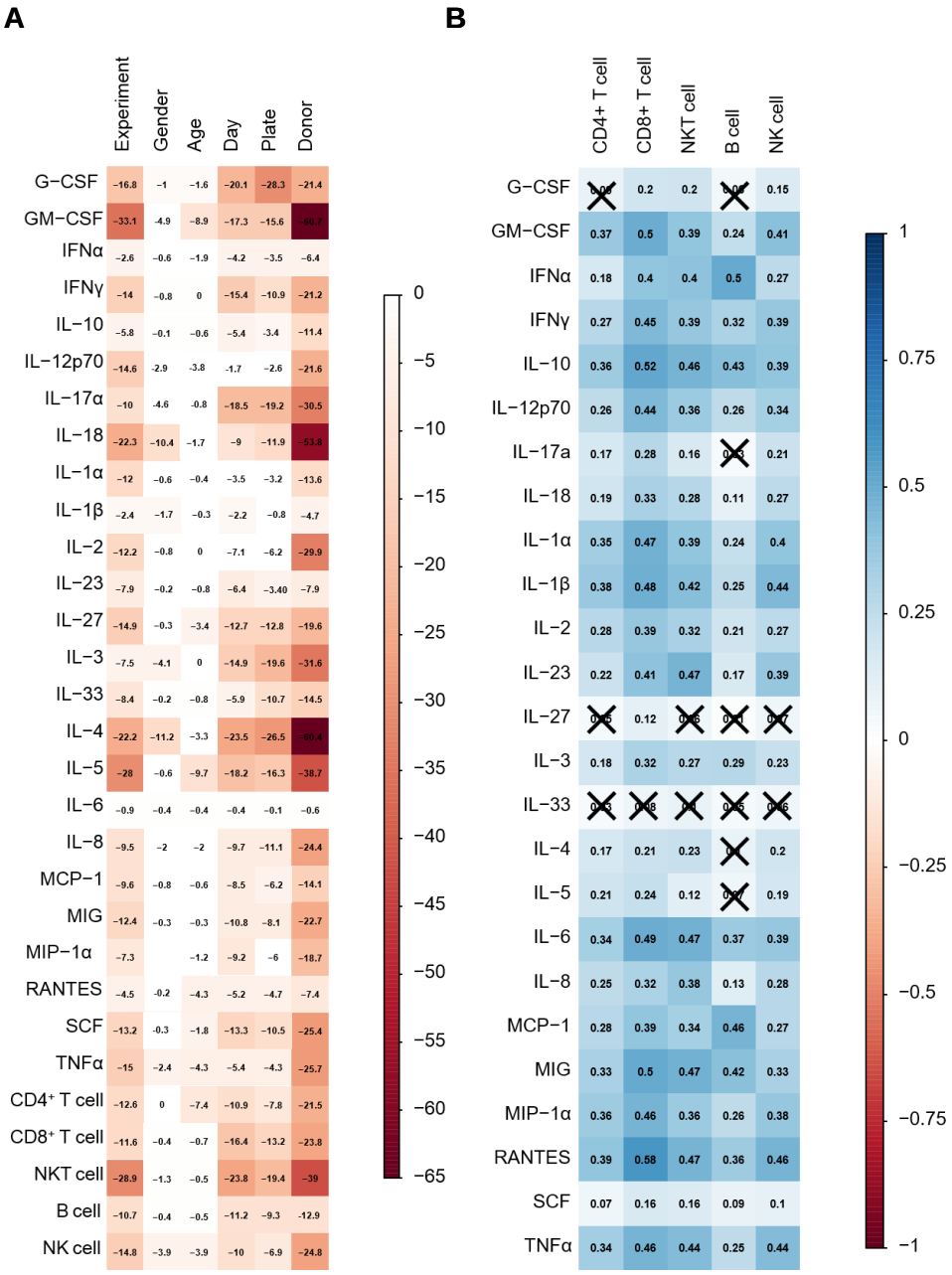

Figure 32: The proliferation of lymphocyte subpopulations can be linked to the expression of certain cytokines and chemokines.
(A) The influences of several experimental factors on measured cytokine and chemokine concentrations as well as on absolute lymphocyte count had been assessed individually by Kruskal-Wallis test. The data set used for the correlation analysis is based on sample values normalized to the unstimulated control of each donor. Presented values are the common logarithms of the p-values. Data sets of adjuvant-induced lymphocyte proliferation assessed after 6 days (Fig. 5) were linked to adjuvant-induced cytokine and chemokine secretion after 24 hours (Fig. 3, 4) using Spearman's rank correlation (B) Spearman's correlation coefficients associated with a p-value above 0.01 were crossed out. All analyses are exploratory without corrections for multiple testing.

6.8 Antigen-specific T cell modulation by adjuvants

Having revealed important effects of the adjuvants on DCs and lymphocytes in an antigen-independent manner, we were interested if the adjuvants are able to induce a directed T cell response within an antigen-specific context. For this purpose, we used short peptide

sequences of the model antigens tetanus toxoid protein p2 (TT; $p2_{829-844}$: MQYIKANSKFIGITEL) and influenza matrix protein 1 (FluM1; $FluM1_{58-66}$: GILGFVFTL) to re-stimulate antigen-specific T cells within the isolated T cell population in a so called “antigen recall assay”. The peptide sequences were loaded on the MHC molecules of DCs for the presentation to the T cells’ TCRs. T cells that recognize their antigen get activated and start to proliferate. Using fluorescently labeled peptide-specific MHC tetramers, we were able to detect antigen-specific T cells by flow cytometry, and could thus examine the impact of adjuvant stimulation on the development of the antigen-specific T cell population. In Figure 33, the gating strategy to detect antigen-specific $CD4^+$ and $CD8^+$ T cells by flow cytometry is shown. After exclusion of cell doublets and apoptotic cells, $CD3^+CD4^+$ or $CD3^+CD8^+$ double positive T cells were selected to further identify TT- or FluM1- positive T cells. As a control for functionality of these T cells, we additionally checked their proliferation.

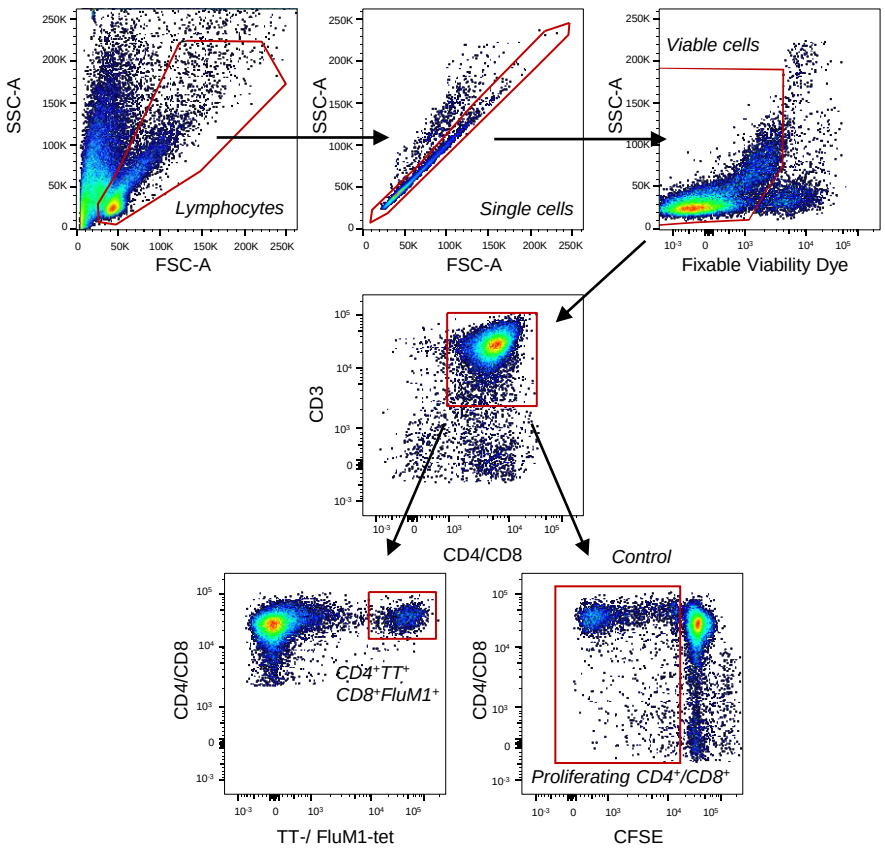

Figure 33: Gating strategy for the detection of antigen-specific $CD4^+$ and $CD8^+$ T cells by flow cytometry using MHC-tetramers.
T cells were harvested on day 6 or 7 from the DC:T cell co-culture. Total lymphocytes were gated according to their SSC/FSC properties. Apoptotic cells were excluded using a viability dye. $CD3^+CD4^+$ and $CD3^+CD8^+$ T cells were determined by staining with respective antibodies. Antigen-specific T cells (TT^+/ $FluM1^+$) were identified by fluorescently labeled MHC tetramers. Proliferating ($CFSE^{low}$) T cells served as control for T cell functionality.

6.8.1 Immunomodulators do not induce a significant increase of the TT-specific $CD4^+$ T cell population

For the analysis of antigen-specific T cells with MHC multimers, two technical requirements have to be considered: The binding of MHC multimers to antigen-specific T cells demands the same HLA characteristic. In addition, the peptide sequence of the antigen determines the

binding affinity to the MHC complex of the DCs. Thus, MHC-tetramers marketed by specified companies predefine both the HLA phenotype as well as the peptide sequence. Hence, we had to use exactly the same peptide for the stimulation of antigen-specific T cells as present within the peptide-MHC complex of the multimer. The selection of donors according to the appropriate HLA-type is described in 5.2.2.6.1 and Figure 11 (p. 66-67). For the antigen-specific $CD4^+$ T cell assay, cells were isolated from donors carrying the characteristic HLA- DRB1*11:01. Instead of PBLs, we used isolated $CD4^+$ T cells for this assay to increase the percentage of potential TT^+-specific T cells within the co-culture. The donor-specific frequency of TT^+CD4^+ T cells was ascertained by TT-tetramer staining directly after isolation of the $CD4^+$ T cell population (Figure 34A). Since all donors had been vaccinated against tetanus in the past, antigen-specific memory T cells should have been detectable (Li Causi et al., 2015). We found a frequency of TT^+CD4^+ T cells ranging from 0.023% to 0.11% within the total $CD4^+$ T cell population. $CD4^+$ T cells were co-cultured with peptide-loaded DCs at a 1:5 ratio. DCs, which had not been loaded with a peptide, served as control cells (DC^{Ctrl}). After 7 days of adjuvant stimulation, TT-specific $CD4^+$ T cells were analyzed by flow cytometry (Figure 34B, C). Representative dot plots of three donors are shown in Figure 34B. Upon stimulation of the DC^{Ctrl}:$CD4^+$ T cell co-culture with MPL-s we noted similar frequencies of TT-specific $CD4^+$ T cells as in the unstimulated control. In contrast, peptide presentation by DC^{TT} combined with MPL-s stimulation increased the frequencies of TT-specific $CD4^+$ T cells of donors Sp19-001 and Sp19-003, as exemplified in Figure 34B. However, MPL-s stimulation did not enhance the frequencies of Sp19-002's TT-specific $CD4^+$ T cells. We investigated the frequencies of TT-specific $CD4^+$ T cells after stimulation with two concentrations of each of the 10 adjuvants and the positive control LPS. Although we clearly observed a trend of enhanced frequencies of TT-specific $CD4^+$ T cells for MPL-s-treated lymphocytes (Figure 34C), it was not significant for any of the tested adjuvants. This might be partially due to the high variation between donors (Figure 34B), but also due to the quite low abundance of TT-specific $CD4^+$ T cells in some donors (0.057±0.028%; Figure 34A) and hence, higher variations in measured differences between the samples.

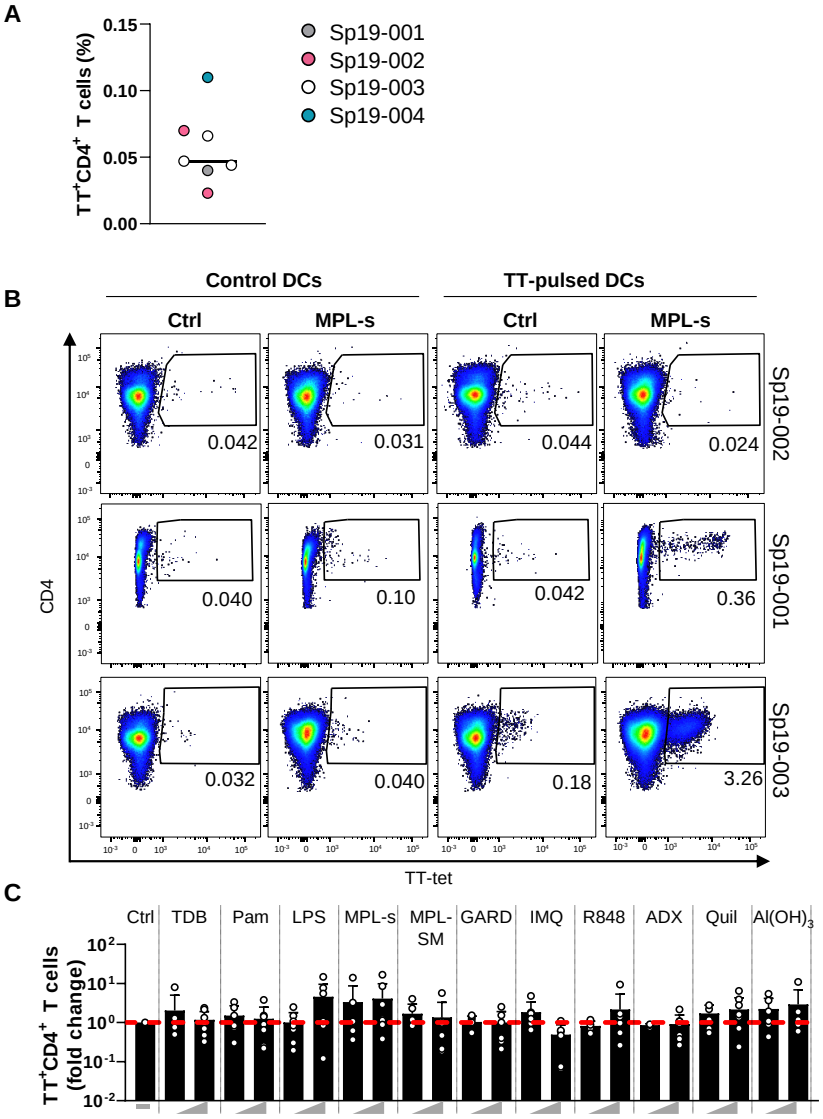

Figure 34: Immunomodulators do not induce a significant increase of the TT-specific CD4⁺ T cell population. DCs loaded with the TT $p2_{829-844}$ peptide (MQYIKANSKFIGITEL) were co-cultured with autologous CD4⁺ T cells and stimulated with the different adjuvants. The negative control was left untreated. CD4⁺ T cells were stained with a peptide-corresponding MHC class II tetramer (MQYIKANSKFIGITEL HLA-DRB1*1101-PE) and anti-CD3 and -CD4 antibodies for analysis by flow cytometry. (A) Donor-specific TT⁺CD4⁺ T cell frequencies of the CD3⁺CD4⁺ T cell population were analyzed after CD4⁺ T cell isolation. (B) Representative dot plots from three donors showing the non- or MPLs-stimulated TT⁺CD4⁺ T cell population after 7 days of co-culture with either DC^{Ctrl} or DC^{TT}. (C) TT⁺CD4⁺ T cell frequencies generated by peptide and adjuvant stimulation were analyzed on day 7 of co-culture. Frequencies were normalized to the respective unstimulated control of each donor. For pairwise comparison of the adjuvant-stimulated condition with the unstimulated control non-normalized data was used (Wilcoxon test revealed no significance; n=6-8). Data is representative for at least three independent experiments.

6.8.2 Pam, MPL-s and $Al(OH)_3$ enhance the frequency of FluM1-specific $CD8^+$ T cells

As a cytotoxic $CD8^+$ T cell response is beneficial to control infection of intracellular pathogens, we were interested if the adjuvants have the potential to enhance the antigen-specific $CD8^+$ T cell response using the HLA-A*0201 restricted influenza A matrix protein 1 peptide ($FluM1_{58-66}$: GILGFVFTL). Therefore, $CD8^+$ T cells were isolated and co-cultured with FluM1-pulsed DCs (DC^{FluM1}). DCs, which were not loaded with the FluM1-peptide served as control. After 6 to 7 days of stimulation with the different adjuvants, FluM1-specific $CD8^+$ T cells were identified and analyzed employing a peptide corresponding HLA-A2.1 tetramer. Notably, we found donor-specific baseline levels of FluM1-specific T cells ranging from 0.004% to 0.51% (mean: 0.14%) of total $CD8^+$ T cells (Figure 35A). These levels did not change upon co-culture with DC^{Ctrl} independent of adjuvant stimulation (Figure 35B). In contrast, DCs pulsed with the FluM1-peptide were able to support the development of the FluM1-specific $CD8^+$ T cell population (Figure 35B). To investigate if the immunomodulators are capable to further boost the development of FluM1-specific $CD8^+$T cells, we tested all immunomodulators in two different concentrations (Figure 35C). Despite the suppression of FluM1-specific $CD8^+$ T cells upon stimulation with the high concentration of IMQ and Quil, we found Pam, MPL-s and $Al(OH)_3$ to be able to further increase the FluM1-specific $CD8^+$ T cell population compared to the non-stimulated control (Figure 35D). The increase in the FluM1-specific $CD8^+$ T cell population upon stimulation with Pam, $Al(OH)_3$ and MPL-s was significantly higher when compared to the unstimulated control in a paired t-test, with some donors reacting stronger than others. We observed a mean fold increase of 1.7 (fold change min-max: 0.94-2.75) for Pam, 1.9 (fold change min-max: 0.80 – 4.02) for $Al(OH)_3$ and 2.5 for MPL-s (fold change min-max: 0.66-4.75).

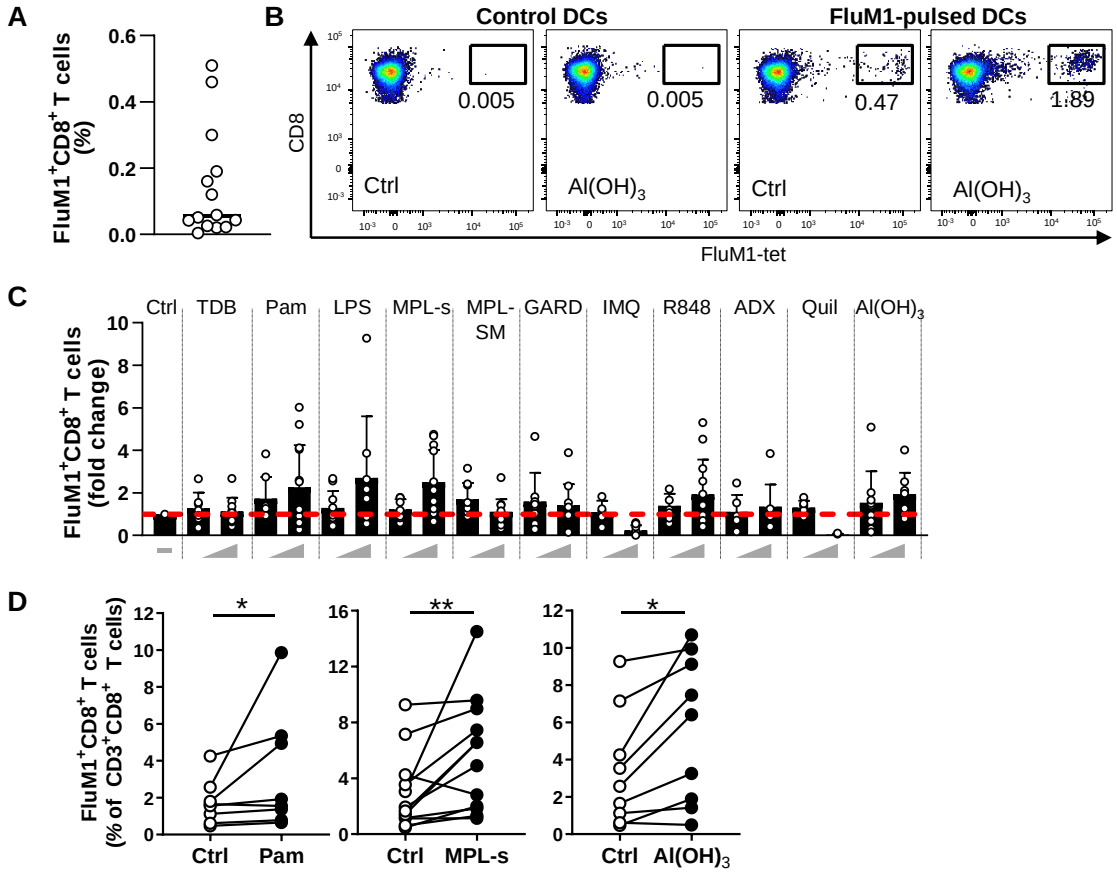

Figure 35: Pam, MPL-s and Al(OH)$_3$ enhance the FluM1-specific CD8$^+$ T cell population.
FluM1 peptide-loaded iDCs of HLA-A*0201$^+$ donors and autologous CD8$^+$ T cells were co-cultured at a 1:5 ratio and stimulated with the different adjuvants or left untreated. On day 6 or 7, CD8$^+$ T cells were stained with a peptide corresponding MHC class I tetramer (GILGFVFTL HLA-A*0201-PE) and analyzed by flow cytometry. (A) Donor individual baseline levels of FluM1-specific CD8$^+$ T cells were measured after CD8$^+$ T cell isolation (n=14). (B) Representative dot plots of the FluM1-specific CD8$^+$ T cell population on day 7 of the DC^{FluM1}:CD8$^+$ T cell co-culture, which was stimulated either with Al(OH)$_3$ or left untreated (ctrl). DCs, which were not loaded with the FluM1 peptide served as control (control DCs). (C) Adjuvant-induced FluM1-specific CD8$^+$ T cell frequencies were normalized to its respective unstimulated control (set to 1 (dashed red line); n=7-12 donors). (D) For each donor, pairwise comparison of the unstimulated control and the adjuvant-stimulated conditions Pam [100 pg/ml], MPLs [1 µg/ml] and Al(OH)$_3$ [10 µg/ml] was performed using the Wilcoxon test. Black lines connecting both conditions indicate individual donors (n=8-11).

6.8.3 Pam- or Al(OH)$_3$- but not MPL-s-expanded FluM1-specific CD8$^+$ T cells show a polyfunctional cytokine secretion profile upon a second FluM1-challenge

Polyfunctional T cells are capable of performing multiple effector functions, such as the production of several cytokines and the lysis of target cells as their effector strategy against pathogens and cancer. Thus, to assess if the adjuvant-expanded FluM1-specific CD8$^+$ T cells are polyfunctional, we analyzed their potential to secrete multiple cytokines such as IFNγ, TNFα and IL-2 (Han et al., 2012) upon a second challenge with the FluM1 peptide. Furthermore, we assessed cytotoxic degranulation indicated by the cell surface localization of the lysosomal associated protein CD107a (Lorenzo-Herrero et al., 2019). HLA*0201–positive

TAP-deficient T2 cells were loaded with the FluM1 peptide to serve as target of cytotoxic effects. T2 cells loaded with a control peptide (NY-ESO-1) were used to check the antigen-specificity of the FluM1-specific $CD8^+$ T cells. $CD8^+$ T cells were harvested from the co-culture with DCs and added to T2 cells in a 1:1 ratio. After 6 hours of co-culture, cells were stained for flow cytometric analysis. FluM1-specific $CD8^+$ T cells expanded with Pam, $Al(OH)_3$ or the non-stimulated control, secreted all three cytokines and CD107a, a marker for degranulation, was detected at the cell surface when re-stimulated with their cognate antigen (Figure 36A). The expression levels were comparable to PMA/Ionomycin stimulation, which served as non-specific activating control. Moreover, FluM1-specific $CD8^+$ T cells stimulated with Pam, $Al(OH)_3$ or the non-stimulated control did not respond to the ctrl-peptide. The expression profiles of Pam or $Al(OH)_3$ expanded FluM1-specific $CD8^+$ T cells corresponded to that of FluM1-specific $CD8^+$ T cells expanded in the ctrl-condition, indicating that both, Pam or $Al(OH)_3$ have no effect on T cell functionality. In contrast, the cytokine expression profile of MPL-s-expanded FluM1-specific $CD8^+$ T cells was different. Upon MPL-s treatment, we detected a decreased secretion of TNFα and IL-2, when stimulated with PMA/Ionomycin (Figure 36A), and a significantly lower expression of IL-2 upon re-stimulation with the FluM1-peptide, when compared to the expression levels of FluM1-specific $CD8^+$ T cells expanded in the control condition (Figure 36A, B). Furthermore, also TNFα and IFNγ levels showed a slight decline, when FluM1-specific $CD8^+$ T cells were stimulated with MPL-s. Strikingly, we found that MPL-s- expanded FluM1-specific $CD8^+$ T cells had significantly increased IFNγ and CD107a at the cell surface in conditions were no antigen recognition occured (unstimulated ctrl or ctrl- peptide condition; Figure 36A).

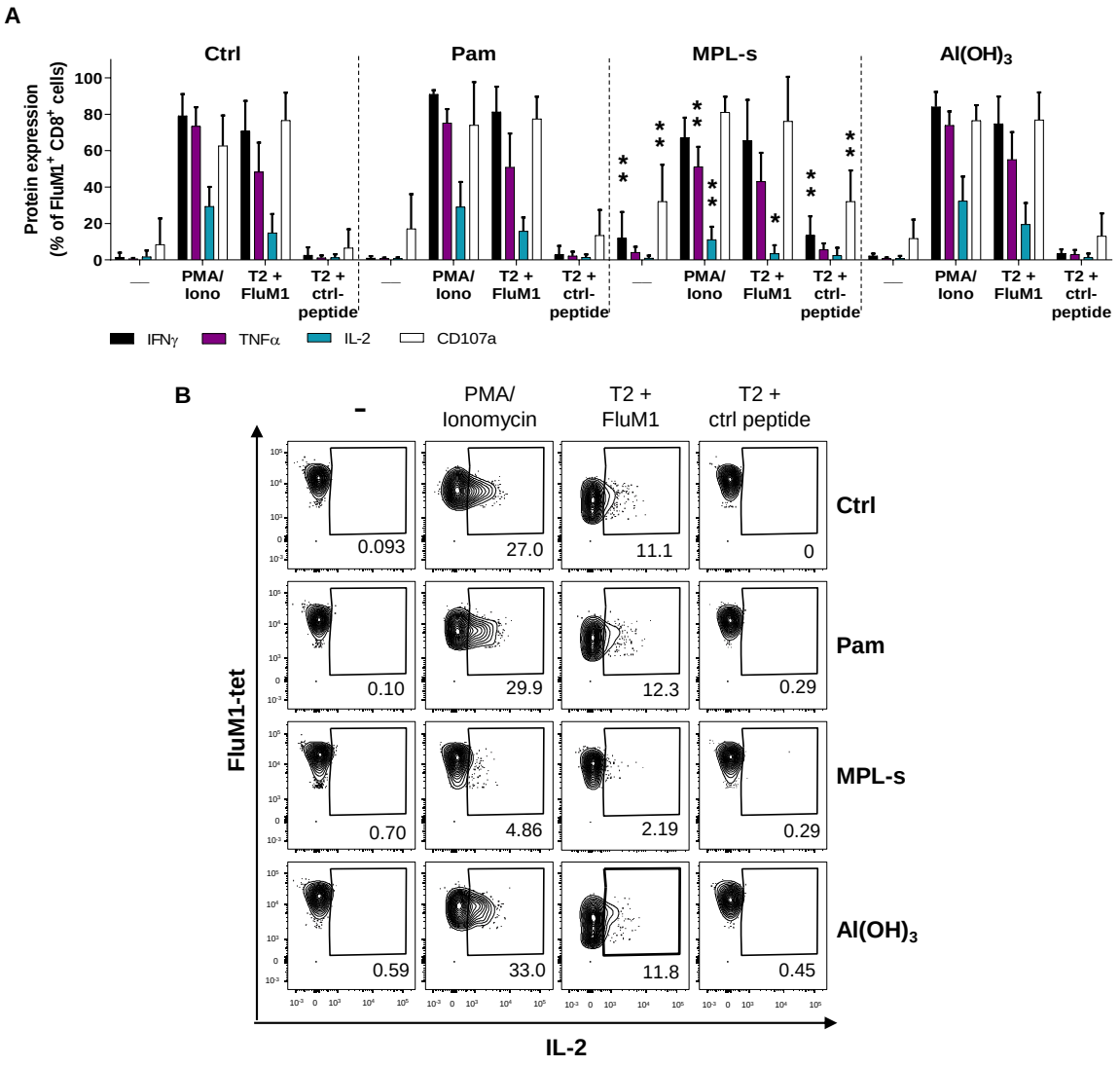

Figure 36: Pam- and Al(OH)3- but not MPL-s-expanded FluM1-specific T cells show a polyfunctional cytokine secretion profile upon a second FluM1challenge.

FluM1-specific $CD8^+$ T cells were expanded with the help of DC^{FluM1} and either Pam, MPL-s and $Al(OH)_3$ or without adjuvant for 7 days. Subsequently, FluM1-specific $CD8^+$ T cells were harvested for (A) re-stimulation using FluM1- or ctrl-peptide-loaded T2 cells, followed by staining of IFNγ, TNFα, IL-2 and CD107a. Here, PMA/Iono served as non-specific activating control. Statistical comparisons between the adjuvants and the control were performed using the Kruskal-Wallis test with Dunn's correction (* $p< 0.05$, ** $p< 0.01$). Thereby, each cytokine and stimulating condition (e.g. PMA/Iono) was analyzed seperately. (B) Dot plots of a representative donor showing the differences in IL-2 secretion when $FluM1^+CD8^+$ T cells were expanded with MPL-s compared to Pam, $Al(OH)_3$ and the unstimulated ctrl.

6.8.4 MPL-s expanded $FluM1^+CD8^+$ T cells express higher levels of inhibitory receptors compared to Pam and $Al(OH)_3$ expanded $FluM1^+CD8^+$ T cells

Exhausted T cells develop in response to chronic antigen stimulation and are characterized by a progressive loss of their effector function and high inhibitory receptor expression (McLane et al., 2019). Since a decline in cytokine synthesis could be an indicator for an exhausted phenotype (Wherry and Kurachi, 2015), we evaluated the expression of several inhibitory

receptors on ctrl-, Pam-, MPL-s- and Al(OH)$_3$-expanded FluM1-specific CD8$^+$ T cells (Figure 37A). Interestingly, we observed a significantly higher expression of LAG-3, 2B4 and CTLA-4 on MPL-s-expanded FluM1-specific CD8$^+$ T cells compared to the other conditions. In contrast, PD-1 and Tim-3 protein levels were not elevated on MPL-s-expanded FluM1-specific CD8$^+$ T cells, but on the total CD8$^+$ T cell population (Figure 37B), while all other inhibitory markers on total CD8$^+$ T cells remain inconspicuous. The mitogen PHA, which leads to polyclonal T cell activation, served here as positive control for exhausted T cells (Filippis et al., 2017).

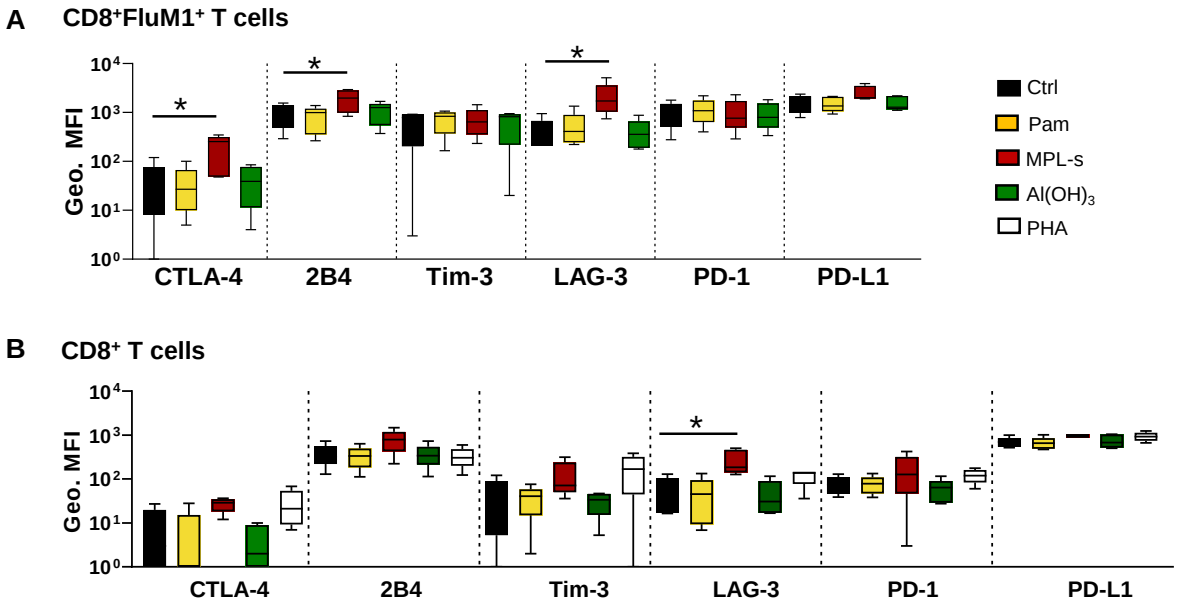

Figure 37: MPL-s expanded FluM1$^+$CD8$^+$ T cells expressed higher levels of inhibitory receptors compared to Pam and Al(OH)$_3$ expanded FluM1$^+$CD8$^+$ T cells.

Flow cytometric analysis of inhibitory ligand expression on (A) FluM1-specific CD8$^+$ T cells or (B) total CD3$^+$CD8$^+$ T cells after having been stimulated for 6-7 days with Pam, MPL-s, Al(OH)$_3$, PHA or left untreated (Ctrl). Statistical differences between the adjuvant stimulations and the unstimulated control were compared by Friedman test with Dunn's correction (n=5). A p-value of < 0.05 (*) was considered as statistically significant. Data are representative of at least three independent experiments.

6.8.5 FluM1$^+$CD8$^+$ T cells present an effector memory T cell phenotype upon peptide encountering

Memory CD8$^+$ T cells are a long-lived population providing protection by rapidly acting upon contact with their cognate antigen. Until today, several subsets of memory T cells have been described, with the most prominent being central memory (T_{CM}) and effector memory T cells (T_{EM}; (Samji and Khanna, 2017). While T_{CM} lack immediate effector function, but express lymph node homing receptors such as CCR7, T_{EM} express receptors for migration to inflamed tissue and are able to secrete IFNγ or perforin (Sallusto et al., 1999). We were interested which T cell phenotype FluM1-specific CD8$^+$ T cells have before or after recognition of the FluM1 peptide. To differentiate between naïve T cells and T_{CM} or T_{EM}, we used fluorescent antibodies

to stain the marker proteins CD45RA/ CD45RO, CCR7, CD62L and HLA-DR (Mahnke et al., 2013) for the analysis by flow cytometry. $CD8^+$ T cells were either cultured alone or in the presence of autologous DC^{FluM1} for 6 days. Subsequently, cells were harvested and prepared for flow cytometric analysis. FluM1-specific $CD8^+$ T cells were detected using the FluM1-tetramer. We noted that FluM1-specific $CD8^+$ T cells, which had not been stimulated with the peptide, generally presented a phenotype of naïve T cells ($CD45RA^+CD45RO^-CCR7^+CD62L^+HLA\text{-}DR^-$) (Figure 38). However, the expression of CD45RA and CD45RO was not stringent enough to allow a clear classification into $CD45RA^+CD45RO^-$ naïve and $CD45RA^-CD45RO^+$ memory cells. Thus, we assume that T_{CM} were also present within the FluM1-specific $CD8^+$ T cell population ($CD45RA^-CD45RO^+$ $CCR7^+CD62L^+HLA\text{-}DR^-$). In contrast, $FluM1^+CD8^+$ T cells, which were stimulated with the peptide, point to T_{EM} cells by showing a $CD45RA^-CD45RO^+CCR7^-CD62L^-HLA\text{-}DR^+$ phenotype. Although we observed clear differences in the phenotypes of $FluM1^+CD8^+$ T cells with or without peptide stimulation, further experiments with additional subset-specific markers are needed to clarify the T cell subsets being present.

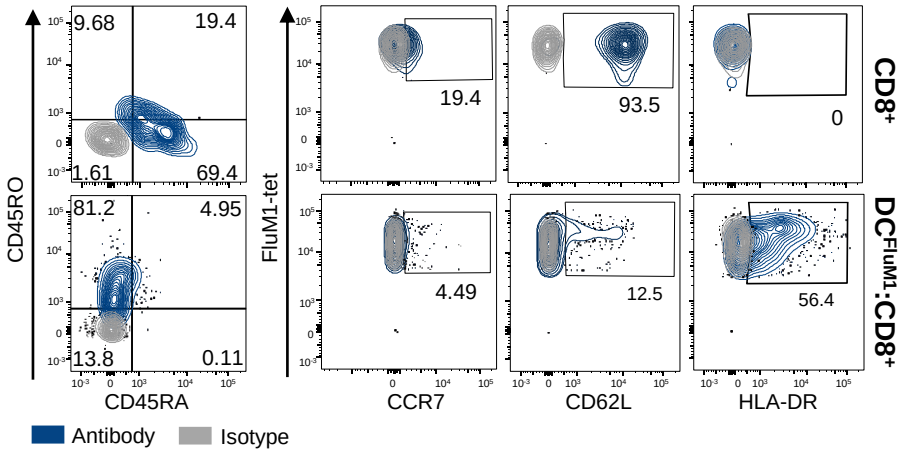

Figure 38: $FluM1^+CD8^+$ T cells present an effector memory T cell phenotype upon peptide encountering. Selected $CD8^+$ T cells from HLA-A*02:01 positive donors were cultured either alone or with FluM1-loaded DCs. After 6 days of culture, cells were harvested and stained against CD45RA, CD45RO, CCR7, CD62L and HLA- DR. Contour plots of a representative donor show the marker expression of single, viable $FluM1^+CD8^+$ T cells. Data are representative of at least two independent experiments.

6.8.6 Elucidating $Al(OH)_3$'s immunogenic potential to induce a FluM1-specific $CD8^+$ T cell response

In antigen-independent experiments, we observed only minor immunogenic effects upon $Al(OH)_3$ stimulation on DCs and lymphocytes compared to the fulminant effects induced by the other adjuvants. Except for reduced levels of MIG and elevated expression of MCP-1 (6.4.3.3), we found only weak effects on the expression of DC maturation marker and lymphocyte proliferation upon $Al(OH)_3$ stimulation. However, we noted a significant increase of antigen-

specific $CD8^+$ T cells using the model antigen FluM1. To elucidate if the peptide has an additive effect on $Al(OH)_3$-stimulated DCs, we analyzed the expression of maturation markers and compared the effects between DC_{PBL} and $DC^{FluM1}{}_{PBL}$. DCs either loaded with the FluM1 peptide (DC^{FluM1}) or left untreated, were co-cultured with autologous PBLs and remained either unstimulated or $Al(OH)_3$ was added for 24 to 72 hours. Cells were analyzed for their expression of CD40, CCR7, CD86, PD-L1 and CD80 every 24 hours by flow cytometry. For comparison between the data sets, all values were normalized to their respective control of the DC:PBL condition. We observed comparable expression levels between all conditions for CD40, CCR7, CD86 and CD80, except for PD-L1 after 24 hour of stimulation (Figure 39). Here, expression levels were significantly increased, when DCs had been loaded with FluM1. Strikingly, this effect was independent of $Al(OH)_3$ stimulation, indicating that the peptide itself led to the increased expression of PD-L1. A similar trend was observed after 48 and 72 hours, even though the differences in expression were not as pronounced (data not shown). Since we observed significantly elevated $FluM1^+CD8^+$ T cell frequencies upon $Al(OH)_3$ stimulation compared to the unstimulated control (Figure 35), the mechanism behind this effect has to be further elucidated.

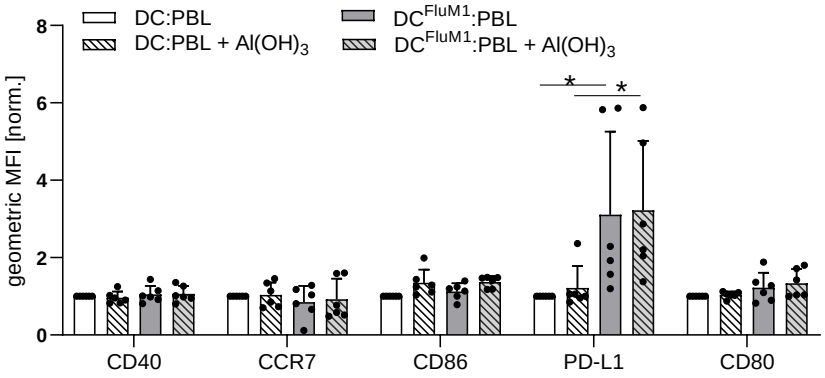

Figure 39: The FluM1 peptide's effect on PD-L1 expression of DCs.
DCs^{FluM1} and DCs were co-cultured with autologous PBLs and stimulated with $Al(OH)_3$ or left untreated. After 24 hours of stimulation, cells were stained for the maturation markers CD40, CCR7, CD86, PD-L1 and CD80 and analyzed by flow cytometry. The geo MFI of each marker was assessed on viable $CD14^-CD1a^+$ DCs. The obtained geo. MFI values were normalized to their respective control of the DC:PBL condition. The pairwise comparison was performed using Wilcoxon's signed rank test (n=6 donors). A p-value < 0.05 (*) was considered as statistically significant. Data are representative of at least three independent experiments.

Overall, we detected significantly enhanced frequencies of FluM1-specific $CD8^+$ T cells using Pam, MPL-s or $Al(OH)_3$ in comparison to the unstimulated control. These antigen-specific $CD8^+$ T cells had an effector memory cell phenotype Upon FluM1-restimulation, Pam or $Al(OH)_3$-expanded antigen-specific $CD8^+$ T cells demonstrated their polyfunctional effector functions by secreting high levels of IFNγ, followed by lower levels of TNFα and IL-2. When compared to Pam or $Al(OH)_3$, MPL-s-expanded antigen-specific $CD8^+$ T cells still secreted similar levels of IFNγ, but lower levels of TNFα and IL-2, which was accompanied with a higher expression of

the inhibitory receptors CTLA-4, 2B4 and LAG-3. Since $Al(OH)_3$ induced only weak effects on DCs and lymphocytes without antigen, we suppose a peptide/adjuvant-mediated effect for the development of antigen-specific T cells, which might be favored by enhanced PD-L1 expression on DCs. We found no significant elevated frequencies of TT-specific $CD4^+$ T cells, but this was probably due to the limited number of donors used.

7 Discussion

One of the greatest challenges of today's subunit vaccine development is the selection of a suitable adjuvant to achieve the desired immune response for long-lived protection. Thus, a deep understanding of the adjuvants' MoAs is required to predict its adjuvanticity. To validate our hypothesis that specific innate and adaptive immune responses can be linked to adjuvants' immunomodulatory MoAs, we developed a human primary immune cell-based *in vitro* assay comprised of monocyte-derived DCs and autologous PBLs to compare prototypic and established adjuvants side-by-side. The comparison revealed a profound understanding of the adjuvants' immunomodulatory MoAs and immunogenic signatures by addressing several aspects of adjuvant function on the immune cells.

DCs that encounter a stimulus sensed by their PRRs undergo a maturation process. This is a prerequisite for a key function of DCs, namely, the ability to prime naïve T cells, which is of pivotal importance for cell-mediated vaccine efficacy. Thus, we first investigated whether the adjuvants are able to activate the DCs. The maturation of DCs was induced upon stimulation with Pam, GARD, IMQ, R848, MPL-s and MPL-SM as demonstrated by enhanced expression of DC maturation marker and a reduced endocytic activity (Figure 40, ①). While minor effects were observed for TDB - $Al(OH)_3$, ADX and Quil did not affect DC maturation.

By analyzing 25 secreted cell signaling molecules in the supernatant of the DC:PBL co-culture, we generated comprehensive cytokine and chemokine profiles that displayed adjuvant-specific signatures (Figure 40, ②). Depending on the number and expression levels of these signaling molecules, they were classified into strong (R848, MPL-s), intermediate (MPL-SM, Pam, GARD, IMQ, TDB) or weak ($Al(OH)_3$, ADX, Quil) immunomodulators. Additionally, we observed that adjuvants with structure similarity and which target the same receptor, such as TLR4 (LPS, MPL-s, MPL-SM) or TLR7 ligands (GARD, IMQ, R848), have still distinct protein expression pattern. The TLR4 ligands differed most strongly in expression levels of IL-10, IL-12p70 and IL-23, while the TLR7 ligands demonstrated distinct secretion of IFNα, MIG and IL-1β.

By focusing on the adaptive immune response, we found that Pam, MPL-s, MPL-SM, GARD, IMQ and R84 stimulate antigen-independent proliferation of the co-cultured PBLs to varying degrees (Figure 40, ③). A detailed examination of proliferating $CD4^+$, $CD8^+$, NKT, B and NK cells revealed that these immunomodulators induced distinct lymphocyte populations to proliferate. We noted that GARD and IMQ induce only B cells to proliferate, whereas Pam, MPL-s, MPL-SM, MPL-s and R848 activate at least three of five cell subsets.

Using peptide epitopes of the model antigens tetanus toxoid (TT) and influenza matrix protein 1 (FluM1), we assessed the adjuvants' capability to boost antigen-specific $CD4^+$ and $CD8^+$ T cell development (Figure 40, ④). Although we observed a trend of enhanced frequencies of TT-specific $CD4^+$ T cells for MPL-s-treated lymphocytes, the difference to the

unstimulated control was not significant for any of the tested adjuvants. In contrast, we observed that Pam, MPL-s and Al(OH)$_3$ increased the FluM1-specific CD8$^+$ T cell population. Upon restimulation with the FluM1-peptide, these CD8$^+$ T cells exerted potent effector functions by degranulation as indicated by CD107a cell surface localization and by secretion of the cytokines TNFα, IFNγ and IL-2. However, MPL-s-expanded FluM1-specific CD8$^+$ T cells showed lower secretion levels of TNFα and IL-2, accompanied with enhanced expression levels of the inhibitory receptors CTLA-4, 2B4 and LAG-3. Figure 40 graphically illustrastes the obtained results of this thesis.

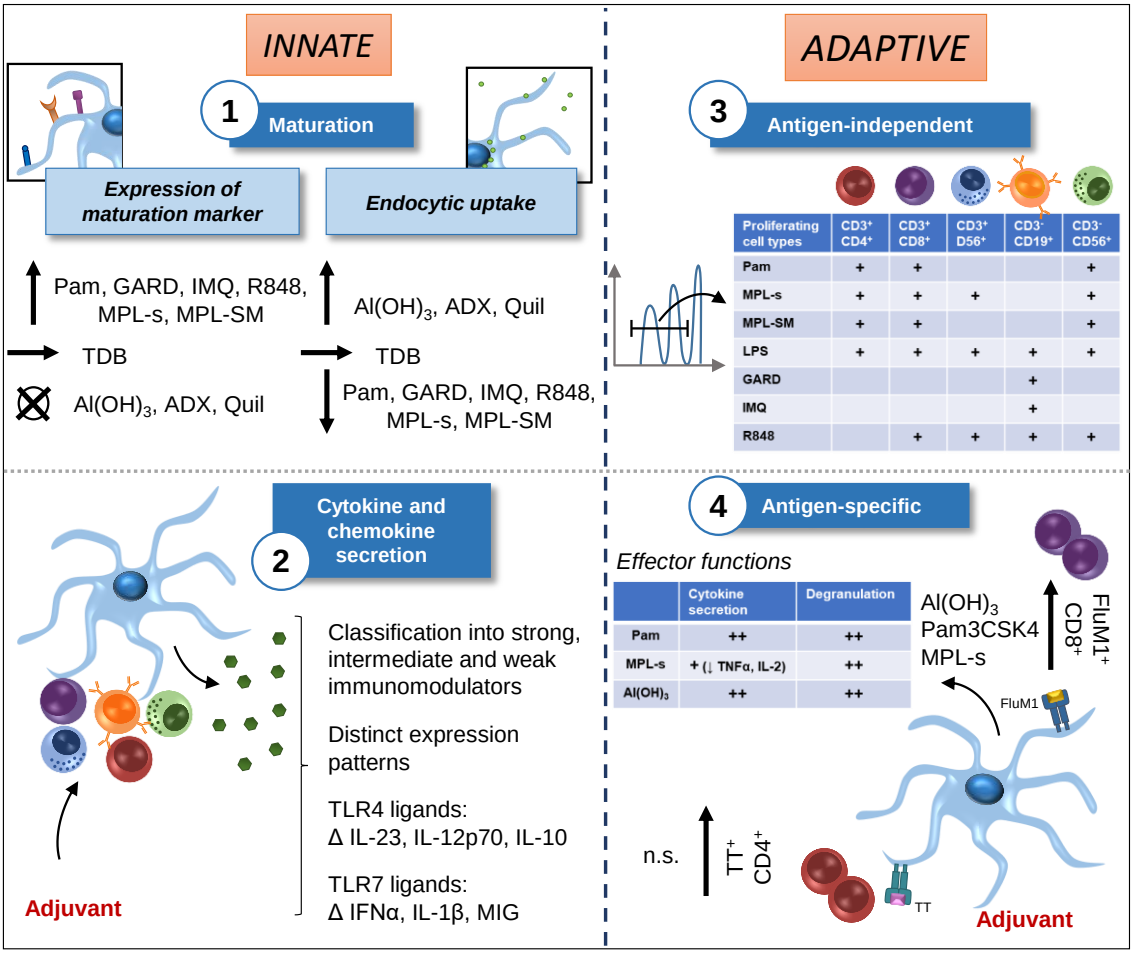

Figure 40: Summary of the obtained research data.
Our human primary immune cell-based *in vitro* assay comprising moDCs and autologous PBLs allowed us to analyze the immunomodulatory properties of ten adjuvants. (1) A full maturation of DCs on phenotypical (maturation marker expression) and functional level (endocytic capacity) was induced by Pam, GARD, IMQ, R848, MPL-s and MPL-SM. (2) Luminex multiplex analysis of 25 signaling molecules (cytokines and chemokines) after 24-hour stimulation with the different adjuvants enabled the profiling of adjuvant-specific protein signatures. (3) Adjuvants stimulated different lymphocyte populations to proliferate in an antigen-independent manner. (4) The activation of TT-specific CD4$^+$ T cells or FluM1-specific CD8$^+$ T cells was enhanced to different degrees by the tested adjuvants.

7.1 Advantages and limitations of our human primary immune cell-based assay as tool to facilitate the prognosis of adjuvant effectiveness.

The wide range of different immunomodulators necessitates the development of an *in vitro* assay, which enables the investigation and prognosis of an adjuvant's MoA. So far, the MoAs of adjuvants being used in approved vaccines are not fully understood, although inappropriate immune responses can have fatal consequences on vaccine efficacy and could cause severe adverse effects. Furthermore, the diversity of potential new candidate adjuvants has created another dimension of complexity, and we are confronted with the challenge to find the best suitable model reflecting the induced immune response in humans most accurately. Pre-clinical testing in animal models will remain indispensable, but only selected adjuvant candidates can be tested here, while *in vitro* assays could cover pre-selection processes of several potential adjuvant candidates simultaneously.

The development of protective adaptive memory responses is dependent on the potent activation of the innate immune system (Coffman et al., 2010). Thus, an *in vitro* assay system should provide information about what is required to initiate, amplify and shape a potent adaptive immune response in order to reflect the *in vivo* situation most reliably. We focused on these hallmarks in our primary immune cell assay by examining the maturation of DCs (initiation), secretion of cytokines and chemokines (amplification) and activation of lymphocytes as well as the induction of antigen-specific T cell responses (shaping). For the first time, our study compared a panel of 10 different prototypic or established adjuvants side-by-side within the same *in vitro* assay system, focusing on both, the innate and adaptive immune response of human primary immune cells.

7.1.1 Advantages

7.1.1.1 Comparison to other immunological in vitro assays

Since DCs are key players in initiating and directing adaptive immune responses (Banchereau and Steinman, 1998), moDCs set the basis of this *in vitro* assay. Co-incubated autologous PBLs gave rise to a stimulatory immune milieu, which took complex cellular interactions into account. This feature is often disregarded in several studies evaluating adjuvant or vaccine candidates in human cells by focusing only on monocytes, moDCs or cell lines (Spisek et al., 2004; Seubert et al., 2008; Zaitseva et al., 2012; Banchereau et al., 2014; Hoonakker et al., 2015; Tapia-Calle et al., 2017; Ming et al., 2019; Tapia-Calle et al., 2019). Although it was shown that moDC were promising in evaluating innate immune-potentiating capacities of vaccines (Bodewes et al., 2009; Banchereau et al., 2014; Hoonakker et al., 2015; Tapia-Calle

et al., 2017), the connection to the resulting adaptive immune response was still missing. However, adjuvant-induced cellular and humoral immune responses represent a causal link to vaccine efficacy. As a proof of concept, with their *in vitro* autologous moDC:$CD4^+$ T cell assay, Moser and colleagues demonstrated the utility to screen vaccine candidates, using the formulated yellow fever vaccine YF-VAX®. They showed $CD4^+$ T cell polarization and memory T cell development as functional consequence of potent DC maturation (Moser et al., 2010; Vandebriel and Hoefnagel, 2012). While PBMC-based *in vitro* assays were also used to address influenza vaccine-dependent T cell-mediated immune response (Tapia-Calle et al., 2019), moDC-based *in vitro* assays provided a higher potency of T cell stimulation (Moser et al., 2010). In contrast to the defined number of moDCs employed here, the reduced T cell-stimulatory capacity in PBMC assays is probably due to the lower and varying cell number of cDCs (Osugi et al., 2002). This might also apply to whole blood assays (WBA). Although WBAs are inexpensive, technically easy, allow a quick handling and reflect a physiological relevant condition (Brookes et al., 2014), the cell concentration is not controlled. This could lead to variations in secreted cytokine levels between individuals and might result in wrong conclusions (Deenadayalan et al., 2013). Furthermore, the presence of anticoagulants might affect the immune response (Strobel and Johswich, 2018).

The use of *in vitro*-generated moDCs is discussed controversially because of their comparison to cDCs and the accompanied consequent functional differences (Osugi et al., 2002). However, by transcriptomic analysis, *in vitro*-generated moDCs were recently shown to resemble *in vivo* inflammatory DCs (Sander et al., 2017). Inflammatory DCs differentiate from monocytes at the site of inflammation, are able to migrate to the lymph node and to stimulate potent $CD4^+$ and $CD8^+$ T cell responses (Segura and Amigorena, 2013). Since most vaccines are applied intramuscularly, DC subsets within the muscle include cDCs as well as moDCs (Langlet et al., 2012). Thus, moDCs provide a good and alternative source for studying T cell-mediated immune responses. Although natural occurring DCs such as cDCs or pDCs are of high physiological relevance, their low occurrence in human peripheral blood prevent the investigation of several adjuvants in parallel.

The *in vitro* testing of adjuvants or candidate vaccine formulation on cell lines, even on MUTZ- 3 cells, resembling moDCs most closely (Larsson et al., 2006), omit an important point in vaccination: the naturally occurring variation of the immune response in a healthy population. Recently, the *Milieu Intérieur* consortium analyzed the activation of innate immune cells of healthy donors after stimulation with 28 different conditions comprising different pathogens, adjuvants, cytokines and T cell activators using a WBA and a multiplex cytokine read-out. They suggested that the detected variations of the innate immune response explain the differential

response to therapeutic intervention (Duffy et al., 2014). Variation in vaccine efficacy within the population is known for several vaccines against e.g. influenza, hepatitis B as well as measles and can be ascribed to several intrinsic (immunogenetics, age, gender) and environmental factors affecting the individual's immune response (Thomas and Moridani, 2010; Posteraro et al., 2014; White et al., 2014). Thus, the evaluation of variation in immune response upon adjuvant stimulation is of urgent importance in pre-clinical testing. When using primary immune cells isolated from peripheral blood of different donors in contrast to cell lines, the variation of the immune response is taken into account including gender and age-specific differences (see 7.2.3). Consequently, adjuvants could be selected for candidate vaccines on the basis of inducing only low variations in the immune response of various individuals.

7.1.1.2 The cell composition of our in vitro assay provides the basis for the stimulation with ligands for TLR1-9

Another advantage of our primary immune cell-based *in vitro* assay is the complete covering of TLR1-9 expression on the immune cells included in the assay, despite existing cell type-restricted TLR expression patterns (Hornung et al., 2002; Karlsen et al., 2017). That this is of enormous importance became clear, when we compared the maturation of DCs upon adjuvant stimulation, cultured either alone (DC_{solo}) or in the co-culture with PBLs (DC_{PBL}). Strikingly, DC_{solo} were not affected by the TLR7 ligands GARD and IMQ (Hemmi et al., 2002), while both ligands contributed to the maturation of DC_{PBL}. This result demonstrates that the maturation of TLR7-negative DCs was only possible due to an indirect activation through cellular or soluble interactions in the DC:PBL co-culture. The *in vitro* study by Ma and colleagues, assessing the immunopotency of TLR agonists in a tissue-engineered immunological model revealed a similar result (Ma et al., 2010b). In contrast to purified myeloid cells, pDCs as part of the PBMC population contributed to the immune-responsiveness to TLR7 ligand GARD including the maturation of moDCs and specific antibody production. The presence of pDCs within the PBL fraction in our *in vitro* assay could be an explanation for the TLR7 ligand-mediated effects in the DC:PBL co-culture (Gibson et al., 2002), however, we did not investigate this phenomenon in more detail. Nonetheless, our human primary cell-based *in vitro* assay enabled the comparisons of adjuvants targeting distinct TLRs. Thus, it provides the feasibility to investigate adjuvant formulations comprising several TLR ligands as recently described in (Sato-Kaneko et al., 2020).

7.1.1.3 Antigen-independent analyses allows the investigation of the adjuvants' own adjuvanticity

Despite the fact that adjuvants are mainly applied to individuals as part of an antigen-containing vaccine, several factors brought us to the decision to study the immunogenicity of adjuvants antigen-independently. First, antigens can vary in their inherent immunogenicity between individuals (Davis, 2008). Second, the understanding of inter- relationship between antigen and adjuvant and their potential compensation for each other is of great importance in subunit vaccine design. The antigen dose determined with adjuvant A may be suboptimal with adjuvant B (Davis, 2008). Third, antigens have the inherent potential to influence the immune response. A transcriptomic analysis of iDCs pulsed with the human papillomavirus (HPV) E7 peptide ascertained 52 peptide-modulated genes, which differed to the control peptide, indicating peptide-specific effects (Yang et al., 2014). Furthermore, another study demonstrates the modulation of the immune response by peptides. Here, the phenol-soluble modulin (PSM) peptide of Staphylococcus aureus induced the generation of tolerogenic DCs independently of simultaneous TLR stimulation. The consequent priming of regulatory T cells prevented immune activation (Armbruster et al., 2016; Richardson et al., 2018) Similarly, when we investigated the adjuvants' potential of enhancing an antigen-directed immune response, we noted that the FluM1 peptide had intrinsic effects on DCs (6.8.6, p. 115) by increasing PD-L1 expression on DCs. Consequences of this effect regarding changes in frequencies of FluM1-specific $CD8^+$ T cells will be discussed below (7.2.3). Due to the possible intrinsic peptide or antigen effects, we decided to compare adjuvant effects mainly in absence of an antigen in our study. The adjuvant-specific MoAs described in this thesis shall facilitate the adjuvant selection to achieve the desired immune response for a certain indication. Nevertheless, the combination of adjuvant and antigen has to be tested again to exclude changes of the induced immune response due to their possible inter-relationship.

7.1.2 Limitations

7.1.2.1 Comparison to in vivo models

Despite several advantages of our human primary immune cell assay, there are also some limitations in reconstructing the immune response upon vaccination. These limitations are not exclusively concerning our assay, but *in vitro* assays in general. Adjuvants' MoAs such as cell recruitment to the injection site, local tissue responses, APC migration to the draining lymph node, but also other factors influencing vaccine efficacy and safety such as antigen and adjuvant distribution, route of administration, adverse reactions as well as the longevity of the memory response can only be studied *in vivo*. Animal models are essential during vaccine

development to acquire data specifically to the mentioned points before. Nevertheless, extrapolating results from animal models to human is challenging (Davis, 2008): Species-specific differences such as ligand recognition, receptor expression and its restriction to certain cell types or the diverse distribution in tissue, complicates the selection of an appropriate animal model, especially for adjuvants targeting TLRs. For instance, murine TLR8 does not recognize human TLR8 ligands (Barrat, 2018), and TLR9 is expressed on several cell types in mice but restricted to B cells and pDCs in humans (Hornung et al., 2002). While previously, pre-clinical investigations in animal models provided information about immediate adverse events such as fever or rash at the injection site, potential fever reactions can now be tested *in vitro* with the monocyte activation test (MAT, (European Pharmacopoeia, 10th edition, English, 2019); Monograph 2.6.30). Prior to the analysis of adjuvant-induced immune responses, we tested all adjuvants at their defined concentrations in the MAT, followed by the cytokine read-out of IL-1β (6.2.2, p. 76) and IL-6 (data not shown). Except for the high concentrations of LPS, MPL-s and MPL-SM, all other concentrations of the different adjuvants did not reach the fever-inducing threshold (0.5 EU/ml LPS). Zaitseva and colleagues demonstrated in their *in vitro* assay using MonoMac6 cells that Pam exceeded the safety threshold, while MPL-SM did not. However, in their study, they applied lower or higher concentrations, respectively, than we used in our study (Zaitseva et al., 2012). These varieties might be attributed to differences in several factors such as the cells which were used for this assay, the adjuvant source, solvent, purity of adjuvant and solvent as well as cell the culture media, which all can influence the biologic activity of adjuvants (Okemoto et al., 2008).

Although, animal models cannot reflect serious adverse events (SAE) such as the potential development of autoimmune diseases (Ahmed et al., 2011), broad immunoprofiling by *in vitro* and *in vivo* testing in combination with machine learning methods will enable a reliable immune signature of adjuvants and minimize the risk of SAEs (Chaudhury et al., 2018). Furthermore, the understanding of a clear immune signature ensures a good starting point for clinical studies, including the characterization of the MoAs, evaluation of safety and the examination of relevance in terms of susceptibility to infection and its resolution (Boucher, 2017).

7.1.3 I. Interim conclusion

Our human primary immune cell-based *in vitro* assay is an artificial system with a cell composition, which does not reflect the primary response to a vaccine within the lymph node, but which approaches the situation upon the secondary response within the tissue. Since we were able to discriminate distinct immunogenic profiles of the ten tested adjuvants, the assay has the potential to investigate adjuvants' MoAs such as DC maturation, cytokine and

chemokine response as well as the activation of lymphocytes by simultaneously giving an overview of the natural variation of the immune response due to distinct donors. Further, the assay provides the potential to more closely assess the humoral immune response by investigating e.g. B cell activation, antibody secretion and antibody class switch - important aspects of long-term immunity which are not yet addressed by this study.

7.2 What is generally expected from adjuvants in prophylactic vaccines? Do the adjuvants tested in this thesis fulfill the requirements?

Adjuvants should provide the potential to elicit, to amplify and to shape the immune response for the generation of a potent and protective immune response against the antigens of pathogen. Since DCs are required for the priming of an immune response, we investigated the adjuvants' capability to activate and mature DCs as an initial step. Subsequently, the amplification of the immune response is facilitated by cytokine and chemokine secretion. To elucidate differences between the adjuvants, we performed a comprehensive profiling of 25 potential induced cytokine and chemokines. Conclusively, the shaping of the immune response is executed by the activation of lymphocytes, which are responsible for fulfilling the protective memory response. To characterize the adjuvants' inherent potential to activate lymphocytes, we characterized the proliferation of several lymphocyte subsets

7.2.1 Elicitation of the immune response

Since the process of DC maturation is important for a directed adaptive immune response, we tested the adjuvants for their capability to mature DCs including the phenotypical and functional differentiation. In contrast to TDB, $Al(OH)_3$, Quil and ADX, all of the tested TLR ligands namely Pam (Deifl et al., 2014), MPL-s/ MPL-SM (García-González et al., 2013), GARD (Ma et al., 2010b), IMQ, R848 (Hackstein et al., 2011) induced a proper DC maturation with at least two significantly enhanced expressed maturation marker and a strong reduction of the endocytic capacity within the DC:PBL co-culture. Although not as pronounced as the TLR ligands, TDB increased the expression of CD86 and HLA-DR on DCs (Ostrop et al., 2015; Kodar et al., 2020), and reduced DC's endocytosis slightly. We already discussed before (7.1.1.2) that the TLR7 ligands GARD and IMQ induce the maturation of the DC only when co-cultured with PBLs. The differentiation can be mediated either directly by TLR7 stimulation in pre-activated and TLR sensitized DCs (Severa et al., 2007) or indirectly by creating an pro-inflammatory milieu through stimulation of TLR7-expressing cells within the DC:PBL co-culture (Ma et al., 2010b). In contrast, the dual TLR7/8 ligand R848 activates DCs directly through binding to TLR8 (Hackstein et al., 2011). On the contrary, we did not observe significant effects of ADX,

Quil or $Al(OH)_3$ on DC maturation. In contrast to PRR ligand adjuvants, the receptors for these three adjuvants remain unidentified until today (Gad, 2011). $Al(OH)_3$ and ADX (MF-59) were described to act mainly on macrophages and monocytes rather than on DCs *in vitro* (Seubert et al., 2008). Although MF-59 drives the differentiation of monocytes to moDCs and the activation *in vivo* (Cioncada et al., 2017), these results might explain the adjuvants' weak effects on DC's maturation in our *in vitro* assay due to the missing target cells. In contrast, Quil is described to act on DCs *in vitro*. While we observed only slight increased levels of CD86, another study demonstrated that the effect was more pronounced, when Quil was formulated in cholesterol containing liposomes, which were endocytosed by DCs in a cholesterol dependent manner and leading to their activation due to lysosomal destabilization (Welsby et al., 2016). This hints to possible differences of effectiveness due to an altered route of application or, more precisely, a better uptake of the adjuvant into the APC.

Regarding the adjuvant-induced DC maturation, we can conclude that the stimulation with adjuvants targeting PRR in our primary immune cell *in vitro* assay reflect the observations of other studies. The results we obtained with $Al(OH)_3$, ADX and Quil differ to other studies and might be a result of differing adjuvant formulations (Quil) or varying cell compositions between the assays.

7.2.2 Amplification of the immune response

Cytokines and chemokines are important amplifying mediators of an immune response by activating other immune cells. Using Luminex *x*Map analysis, we examined the adjuvant-specific cytokine and chemokine response after 24-hour stimulation. By determining the protein levels of 25 cytokines and chemokines, we provided a comprehensive overview of the differential expression patterns induced by the adjuvants. Although such studies are valuable to uncover the adjuvants' MoAs, our study is indeed the first one that compares the cytokine and chemokine secretion induced by 10 different adjuvants within the same *in vitro* assay system and comprised of cells derived from 30 donors. In the study by Duffy and colleagues of the *Milieu Intérieur* Consortium, the adjuvants GARD and R848 as well as LPS were also analyzed in such a broad protein analyte screening using a WBA (Duffy et al., 2014). In line with their results, we demonstrated that LPS (and MPL- s in our study) are unique inducers of IL-23 with LPS stimulating higher levels compared to MPL-s. Furthermore, we can confirm that GARD and R848 secrete a similar pro-inflammatory protein signature, but with overall higher levels of protein analytes (IL-12p70, IL-1β, TNFα) in response to R848. Furthermore, we dissected the differences in protein induction by the TLR7 ligands R848, GARD and IMQ in more detail. Here, R848's strong pro-inflammatory effects can be explained by the dual binding of TLR7 and TLR8 with a strong IL-12p70 secretion as exemplified TLR8 activity (Bekeredjian-

Ding et al., 2006; Berger et al., 2009; Marcken et al., 2019), while varied protein levels of GARD and IMQ such as IFNα, IL-1β and MIG might be attributed to a different binding affinity to TLR7. TLR7 dimerizes upon ligand binding, bringing the cytoplasmic Toll/interleukin- 1 receptor (TIR) domain in close proximity, which consequently initiates the MyD88-dependent signal transduction (Petes et al., 2017). As reported by Zhang et al., the protein-ligand interaction by hydrophobic bonds is important for the binding affinity. In contrast to GARD and R848, IMQ lacks the interaction with the hydrophobic pocket due to structural differences, resulting in a weak binding to TLR7 followed by a weak dimerization of TLR7. (Zhang et al., 2018). It is assumed that the level of dimerization is linked to the strength of the transcriptional response, which might explain the lower expression of IFNα induced by IMQ in contrast to GARD and R848.

Moreover, we observed a characteristic TLR7-mediated induction of IFNα (Saitoh et al., 2017), whereas IFNα protein levels had not been detected in the study by Duffy et al. (Duffy et al., 2014). R848 induced high levels of IFNα, which has been shown to be essential for its adjuvanticity to stimulate a protective adaptive immune response (Kastenmüller et al., 2011; Caproni et al., 2012).

All TLR4 ligands in our study induced a strong DC maturation and also a potent pro-inflammatory cytokine response dominated by TNFα, IL-6, IL-1β and IFNγ, confirming the earlier results obtained by the MAT. We observed that LPS and MPL- s are very similar in their induced cytokine and chemokine profile, with enhanced levels of IL-23 (Duffy et al., 2014), IL-10 and IL-12p70. In contrast, we noted that MPL-SM had general lower protein levels with protein reductions spanning up to 100-fold for IL-12p70 (Ismaili et al., 2002; Schülke et al., 2015). Similar results were obtained in a study by van Haren et al., showing that glucopyranosyl lipid adjuvant (GLA; equal to MPL-s) is more potent and effective than MPLA (equal to MPL-SM) in inducing cytokines such as IL-10, IL-1β, IL-6 and IL-12 in a WBA (van Haren et al., 2016). Strikingly, direct comparisons between LPS and the detoxified variants of naturally derived MPL- SM and synthetic MPL-s are limited. Most studies focused on complex adjuvant formulations or performed general basic *in vivo* analysis. Based on the existing data, we cannot explain why MPL-s has similar effects on cytokine secretion as LPS, although being structurally different and detoxified.

TDB demonstrated to induce IL-6, IL-8, MCP-1 and MIP-1α according to literature (Ostrop et al., 2015), while we additionally found TNFα and IL-1β to be up-regulated. Our observation that Pam-stimulated donors separated into ‘low’ and ‘high’ responders according to their cytokine expression profiles, is potentially contributed by a TLR2 single nucleotide polymorphism influencing the expression of pro-inflammatory cytokines such as TNFα and IL-1β (Mandala et al., 2020).

Again, our results are in line with observations made in several other studies. However, our dataset covering the analysis of adjuvant-induced expression of 25 cytokines and chemokines by multianalyte profiling strongly exceeds the amount of information with respect to potential dependencies or correlations compared to much smaller previously published studies.

7.2.3 Shaping of the immune response

We evaluated the activation of lymphocyte subsets in response to the different adjuvants using a cell proliferation assay. Since antigens can already have intrinsic influences on the resulting immune response (see 7.1.1.3), we chose to investigate the activation of lymphocytes in an antigen-independent context. In our experiments, the proliferation of lymphocytes was strongly induced by TLR agonists. As our previous results demonstrates, TLR signaling drives DC maturation and cytokine responses and is also known to stimulate cell proliferation (Li et al., 2010). Several studies showed that memory cells can directly get activated by TLR ligands or that TLR stimulation functions as co-stimulus which lowers the antigen threshold required for activation of T cells (Sieg et al., 2005; Salerno et al., 2019). While this was not in our focus to investigate, our human primary immune cell-based *in vitro* assay confirmed that different TLR immunomodulators induce proliferation of distinct lymphocyte subsets.

In line with other studies, Pam induced the proliferation of NK cells (Smith et al., 2017), $CD4^+$ (Caron et al., 2005), and $CD8^+$ T cells (Cottalorda et al., 2009). Furthermore, as assumed by their similar cytokine signature, LPS and MPL-s both equally stimulated $CD4^+$, $CD8^+$, NKT and NK cells to proliferate (Caramalho et al., 2003; Salio et al., 2007; Mian et al., 2010). The only difference in their proliferation profiles was the observed minor B cell proliferation upon LPS stimulation. Since TLR4 is absent in human B cells (Bourke et al., 2003), this effect is potentially due to the activation of bystander cells (Jasiulewicz et al., 2015) or consequential higher IL-12 levels triggering the activation of B cells (Durali et al., 2003). Strikingly, the TLR4 ligand MPL-SM did not stimulate NKT cell proliferation compared to LPS and MPL-s (Salio et al., 2007). Here, we found significant lower levels of IL-18 and IL-12p70 at the beginning of proliferation (24 hours), which were both shown to be critical inducers of NKT cell activation (Nagarajan and Kronenberg, 2007).

Although the TLR7 ligands GARD and IMQ reveal differences in their induced protein expression signatures, they both stimulated only B cell proliferation, which has previously been attributed to the expansion of IgM^+ memory B cells (Hanten et al., 2008; Agrawal and Gupta, 2011; Simchoni and Cunningham-Rundles, 2015).

In response to R848, we observed high proliferation of $CD8^+$ T cells (Salerno et al., 2016), NKT cells (Salio et al., 2007), B cells and NK cells (Lu et al., 2012). Remarkable was the induction of R848-induced B, NK and NKT cell proliferation with respect to absolute cell counts, as it

exceeded even the numbers achieved with LPS stimulation. However, it is doubtful if such a strong antigen-independent polyclonal activation allows antigen-specific development when antigen is present.

Interestingly, we observed a higher B cell proliferation in cells obtained from female donors compared to male donors upon TLR7 stimulation. Since TLR7 ligands were shown to increase the differentiation of B cells to antibody-secreting cells (Simchoni and Cunningham-Rundles, 2015), the observed higher proliferation might point to an elevated antibody production. Recently, it was shown that female mice have a higher expression and activity of TLR7 on B cells, resulting in a greater antibody response to influenza vaccination compared to male mice (Fink et al., 2018). Sex-based differences in the immune response are important for vaccine developers, but need further investigation.

The induction of a directed memory cell-mediated immune response is of highest interest for vaccines aiming to provide protection especially against intracellular pathogens. In this thesis, we examined the adjuvant's potential to boost the antigen-specific $CD8^+$ and $CD4^+$ T cell response to the peptide epitopes $FluM1_{58-66}$ and TT ($p2_{829-844}$; (Panina-Bordignon et al., 1989) respectively. Although we observed a trend of MPL-s-induced TT-specific $CD4^+$ T cell expansion, this was not proven to be statistically significant. The result might be explained by two important factors: For this assay, we were dependent on blood donations from donors carrying the HLA-DRB1*11:01 allele, but out of all tested volunteers, only 5 donors were tested positive for the required allele. This low number of different donors, the high donor-dependent variability in the immune response and the overall low frequencies of antigen-specific T cells made it difficult to reliably detect differences upon adjuvant stimulation. Additionally, we found a high inter-variability of baseline TT-specific $CD4^+$ T cell levels between these donors, which was probably linked to the length of the period after the last vaccination against TT.

In contrast to this and in line with other studies, we observed that Pam, MPL-s and $Al(OH)_3$ boosted the expansion of antigen-specific $CD8^+$ T cells (Cottalorda et al., 2006; Mercier et al., 2009; Rhee et al., 2010; Jayakumar et al., 2011; MacLeod et al., 2011; Zom et al., 2014; Horrevorts et al., 2018; Zahm et al., 2018; Salerno et al., 2019). Strikingly, we noted that most of the data regarding an increase of the antigen-specific $CD8^+$ T cell population upon adjuvant treatment originate from *in vivo* mouse studies. Hence, we were pleased to see that we can mimic the *in vivo* situation within our *in vitro* assay for these immunomodulators. However, the TLR7 ligands did not consistently enhance the antigen-specific $CD8^+$ T cell population as observed by others (Pufnock et al., 2011; Zahm et al., 2018). We found that around half of the donors responded to GARD and R848 with increasing frequencies of $FluM1^+CD8^+$ T cells, while the other half did not. Whether this result is linked to the TLR7 sex-based phenomenon has to be elucidated.

Intriguingly, we neither measured an antigen-independent $Al(OH)_3$-induced maturation of DCs (Sun et al., 2003), nor a drastic effect of $Al(OH)_3$ on the cytokine response or on lymphocyte proliferation, but we detected an increase of the FluM1-specific $CD8^+$ T cell population upon stimulation with $Al(OH)_3$, when the FluM1 peptide was presented by DCs. Although it is common knowledge that aluminium salts induce the differentiation of Th2 and T_{FH} cells and thus mediate a humoral response (Hogenesch, 2012), antigen-specific $CD8^+$ T cell responses boosted by aluminium salts were shown in mice in several studies (Dillon et al., 1992; McKee et al., 2009; MacLeod et al., 2011; Wang et al., 2015). So far, $Al(OH)_3$ is included in formulation of AS04 and AS01, but induced Th1 or cytotoxic T cell responses were only attributed to the adjuvants counterparts MPL or QS-21 (Garçon and Di Pasquale, 2017). Interestingly, in our experiments, we noted an increased expression of PD-L1 on DCs after FluM1-peptide pulsing. PD-L1 is known as inhibitory receptor of T cell activation. However, we observed the expansion of FluM1-specific $CD8^+$ T cells, when FluM1-loaded DCs were present. Additional stimulation with $Al(OH)_3$ significantly increased the frequencies of FluM1-specific $CD8^+$ T cells compared to the unstimulated condition with FluM1-loaded DCs only. These results are in line with Goto et al., who demonstrated that PD-L1 expression on APCs facilitates the induction of cytomegalovirus (CMV)-specific cytotoxic T cells, while blocking of PD-L1 resulted in less efficient induction (Goto et al., 2016). This observation was confirmed for the induction of HIV-specific $CD8^+$ T cells, too (Garcia-Bates et al., 2019). The mechanism behind this is still unclear, but other studies support the hypothesis of PD-L1's dual role in co-inhibition and co-stimulation of T cells (Rowe et al., 2008; Lee et al., 2010). Due to the minor antigen-indepent effects of $Al(OH)_3$, we cannot explain the mechanism behind the $Al(OH)_3$-induced increase of the FluM1-specific $CD8^+$ T cell population, but we assume a FluM1 peptide/ $Al(OH)_3$ synergism in our assay. Despite the observed intrinsic effect of the FluM1-peptide on PD-L1 expression, aluminium salts are described to mediate their immunogenicity by inducing cell death, which causes the release of DAMPs such as host DNA and uric acid (Kool et al., 2008b; Marichal et al., 2011; McKee et al., 2013). Since we observed cell death of 24.5% upon stimulation with 10 µg/ml $Al(OH)_3$ (6.2.1; p. 75), this might be an additional factor contributing to the expansion of FluM1-specific $CD8^+$ T cells, which has not been explored in this thesis.
It is still questionable, if $Al(OH)_3$ would also favor the development of antigen-specific $CD8^+$ T cells in naïve individuals *in vivo*, since we investigated the expansion of memory $CD8^+$ T cells in an antigen recall assay (van de Sandt et al., 2015).

T cell-mediated protection against pathogens is linked to their cytokine polyfunctionality (Panagioti et al., 2018). Thus, we examined if the adjuvant-expanded FluM1-specific $CD8^+$ T cells are still able to secrete the cytokines TNFα, IFNγ and IL-2 upon re-stimulation with the FluM1 peptide. $Al(OH)_3$ and Pam-expanded FluM1-specific T cells secreted all these

three cytokines to similar levels as non-adjuvanted control cells. In contrast, MPL-s-expanded FluM1-specific T cells showed lower levels of IL-2 and TNFα, while IFNγ levels remained normal. It is described that an early sign of T cell exhaustion is the loss of IL- 2, while the ability to secrete IFNγ persists longer (Wherry et al., 2003). The step-wise progressive loss of T cells' functions results in unresponsiveness to infections and thus, is not desired upon vaccination (Yi et al., 2010). IL- 10 has been associated with T cell exhaustion as its neutralization increased the virus-specific T cells in chronic *lymphocytic choriomeningitis mammarenavirus (*LCMV) infection again (Maris et al., 2007; Brooks et al., 2008). In contrast to Pam or $Al(OH)_3$ stimulation, MPL-s induced a pronounced pro-inflammatory cytokine response with high levels of IL-10 in our *in vitro* assay. So far, there are no studies showing the induction of exhausted T cells upon MPL stimulation. Since we did not observe the exhaustion characteristic of highly expressed PD-1 levels on FluM1-specific T cells, further investigations are needed to clarify the impairment of polyfunctionality of MPL-s-expanded antigen-specific T cells.

Collectively, the antigen-independent shaping of the lymphocyte subsets was favored by TLR ligands. The distinct proliferation signatures induced by the adjuvants were in accordance with several other studies. However, for the first time, we showed a comprehensive analysis of $CD4^+$, $CD8^+$, NK T cells, B and NK cells responding to ten adjuvants and thus, provide an attractive *in vitro* tool for adjuvant comparing studies. The investigations with regard to adjuvant-dependent antigen-specific T cell expansion gave a first insight which adjuvants might favor a certain development towards an antigen-specific immune response. But more antigens have to be tested to draw the conclusion whether Pam, MPL-s and $Al(OH)_3$ induce antigen-specific $CD8^+$ T cell development in general.

7.2.4 II. Interim conclusion

As a summary, we can conclude that some of the tested adjuvants, namely TDB, Pam, MPL-s, MPL-SM, GARD, IMQ and R848, fulfill the critical steps in initiating, amplifying and shaping the immune response. In contrast, within our experimental setup, the adjuvants ADX, $Al(OH)_3$ and Quil did not fully exhibit their immunogenic signature in absence of an antigen in our *in vitro* assay system. Caproni and colleagues showed that *in vitro* stimulation of splenocytes with MF-59 (similar to ADX) was ineffective, while strong transcriptional changes at the injection site were found (Caproni et al., 2012). Eventually, ATP release by muscle cells was required for adjuvanticity of MF-59 (Vono et al., 2013). This demonstrates that the MoA cannot be elucidated *in vitro* for all adjuvants.

7.2.5 Undesired effects in response to adjuvants

Serious adverse advents (SAEs), such as the incident of increased narcolepsy cases, being linked to an adjuvanted vaccine against H1N1 swine flu (Nohynek et al., 2012; Partinen et al., 2012; Miller et al., 2013) or adverse events (AE) such as fever, lymphadenopathy and generalized rash (Di Pasquale et al., 2016), are of high concern and diminish the acceptance for vaccines and vaccination within the population. The prediction of vaccine safety and response is of high interest (Ahmed et al., 2012). It is known that certain immunogenetic factors or inflammatory mediators can promote AEs (Stanley et al., 2007; Williams et al., 2018). Several vaccines are suspected as trigger contributing to the development of autoimmune diseases in individuals with a genetic predisposition (Vadalà et al., 2017). How these develop is still under debate but a potential risk factor includes the polyclonal activation of lymphocytes (Guimarães et al., 2015). Polyclonal B cell activation is stimulated by several pathogens independently of BCR specificity and might be essential for the early host defense by providing a broad antibody repertoire to conserved microbial structures or the maintenance of memory B cells (Montes et al., 2007). In contrast, polyclonal B cell activation can also result in hypergammaglobulinemia, lymphoproliferation and non-specific and autoreactive antibody production (Reina-San-Martín et al., 2000; Ramos et al., 2005). Adjuvants are of special concern here, due to their potential to non-specifically activate the immune system. We and others observed very strong antigen-independent B cell proliferation upon TLR7 stimulation associated with early IFNα production (Bekeredjian-Ding et al., 2005; Caproni et al., 2012). Despite the demonstrated adjuvanticity of R484, TLR7-mediated secretion of IFNα has also been implicated in the pathogenesis of inflammatory and autoimmune disorders (Crow, 2010). Nonetheless, Bekeredjian-Ding and colleagues showed that R848 is unable to differentiate naïve B cells to IgG-producing plasma cells, which might limit the autoreactive potential of R848 (Bekeredjian-Ding et al., 2005). As recently published, combined TLR7/ IFNα stimulation of B cells from healthy individuals can promote IgM^+ autoantibody secretion. However, the authors commented that these autoantibodies might be protective as it is the case for natural antibodies ameliorating autoimmune disease (Simchoni and Cunningham-Rundles, 2015). To draw a conclusion of the potential risk of antigen-independent polyclonal B cell activation by adjuvants and potential autoantibody development, in depth analysis of B cell differentiation during antigen-dependent adjuvant stimulation is required.

Our analysis also revealed pronounced to strong proliferation of NK cells in response to Pam, LPS, MPL-s, MPL-SM or R848 respectively. In regard of vaccination, the activation of NK cells was not linked to adverse events, but to vaccine efficacy. In a systems vaccinology approach to identify correlates of protection to RTS,S malaria vaccination in humans, the researchers detected a strong negative correlation to antibody titers and protection (Kazmin et al., 2017) In

accordance with these results, earlier investigations showed that B cell immunity is impaired by NK cells through their suppressive mechanisms on $CD4^+$ and T_{FH} cells (Cook et al., 2015; Rydyznski et al., 2015). In contrast, several other studies highlight the importance of NK cells for the humoral response or vaccine efficacy (Satoskar et al., 1999; Albarran et al., 2005; Krebs et al., 2009; Gao et al., 2011). Thus, further research is needed to clarify the consequences of the adjuvant-induced strong activation of NK cells.

Cytokine expression and secretion by immune cells is tightly controlled due to their function as signaling amplifiers and inflammatory mediators. Upon vaccination and consequent stimulation of the immune response, imbalances of pro- and anti-inflammatory cytokines might occur (Stratton et al., 2011). The MAT is an example of how fever-inducing cytokines such as IL-1β, IL-6 and TNFα induced by pyrogenic contaminants can already be detected in parenteral drugs before their application and thus prevent potentially developing AEs ((Schindler et al., 2009). After application of the vaccine, serum cytokines could function as early predictive "biomarkers" for an adverse event, as already mentioned for IFNα. Several studies investigated the serum cytokine levels after smallpox vaccination. SCF, G-SCF, IL-10, MIG, ICAM-1, IFNγ, Eotaxin, TIMP-2 and IP-10 were found to contribute to adverse events such as fever, generalized rash and lymphadenopathy (Rock et al., 2004; McKinney et al., 2006; Reif et al., 2009). We did not investigate predictive biomarkers for adjuvant-induced adverse events, but identified MPL-s and R848 in our cytokine and chemokine analysis as strong immunomodulators with high levels of IL-1β, IL-6, TNFα, IFNγ and IL-10. Furthermore, measured SCF and G-SCF levels were higher as compared to the other adjuvants. Due to their additional potent immunogenicity on DCs and lymphocytes, we expect them to be more reactogenic compared to the other adjuvants. To identify predictive biomarkers correlating to adverse events, system vaccinology approaches which are already used to prospectively determine vaccine efficacy might be helpful (Querec et al., 2009; Li et al., 2014; Haks et al., 2015; Kazmin et al., 2017).

7.3 Concluding remarks

Overall, this study provides an *in vitro* model of human primary cells that allows the side-by-side comparison of different adjuvants in order to analyze DC maturation, cytokine and chemokine secretion, the activation of several lymphocyte subsets as well as antigen-specific T cell development. In-depth analysis of these four parts resulted in distinct immunogenic signatures and potencies of the ten prototypic and established adjuvants. Further investigations of areas regarding naïve B and T cell differentiation, memory development of T, B and NK cells, the use of different antigens and many more would be feasible in this assay

and are required to sufficiently understand the adjuvants' MoAs. While we were able to fully reflect the immunogenicity of PRR adjuvants *in vitro*, we found only minor effects on the immune response by $Al(OH)_3$, ADX and Quil, when compared to *in vivo* data. This demonstrates that the analysis of cellular and soluble mediators in combined *in vitro* and *in vivo* studies comprising vaccine-relevant areas such as tissue at the injection site, draining lymph nodes and blood is an important approach to elucidate all MoAs of adjuvants independent of the compound class (McKay et al., 2019).

The next level of complexity has been achieved by combining different adjuvants within a formulation. The goal is to overcome inherent limitations of distinct immune responses which are attributed to single adjuvants by the combination with another adjuvant comprising a complementary immunogenic profile. While this might result in a synergistic immune reaction, concerns about a stronger activation of the immune response will require rigorous safety assessment (Mutwiri et al., 2011). Nonetheless, the characterization of a reliable immune signature of adjuvants will reduce the risk of adjuvant-related AEs and moreover, is of highest importance for the rapid development of highly efficient vaccines especially during a pandemic as illustrated in present times by the COVID-19 outbreak. Thus, our results provide a comprehensive compilation of the immunogenic effects of prototypic candidates and established adjuvants on human primary immune cells and may contribute to facilitate the progression of tailored vaccines.

8 Appendix

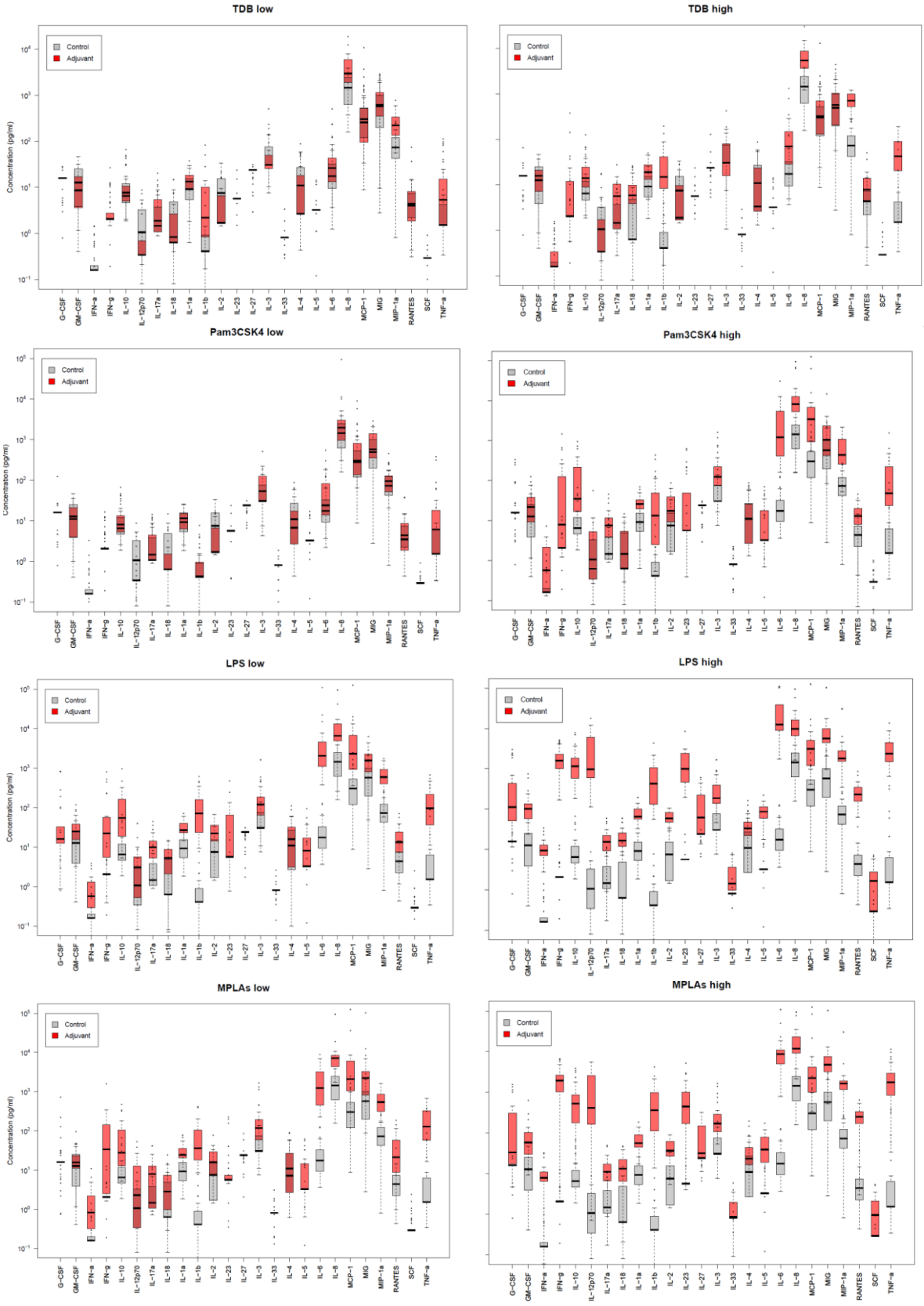
TDB low
TDB high
Pam3CSK4 low
Pam3CSK4 high
LPS low
LPS high
MPLAs low
MPLAs high
Control
Adjuvant
Concentration (pg/ml)
G-CSF
GM-CSF
IFN-a
IFN-g
IL-10
IL-12p70
IL-17a
IL-18
IL-1a
IL-1b
IL-2
IL-23
IL-27
IL-3
IL-33
IL-4
IL-5
IL-6
IL-8
MCP-1
MIG
MIP-1a
RANTES
SCF
TNF-a

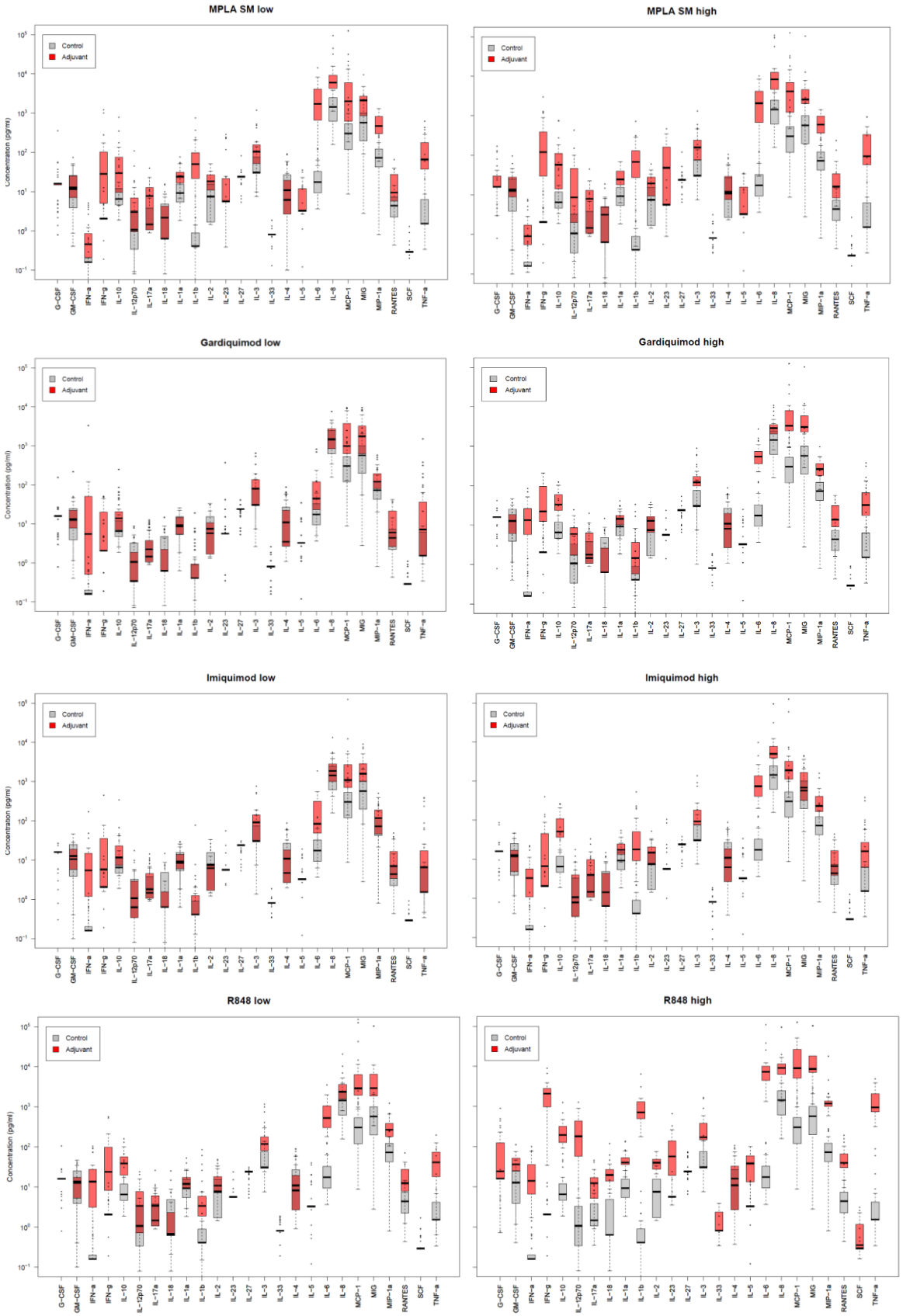
MPLA SM low
MPLA SM high
Gardiquimod low
Gardiquimod high
Imiquimod low
Imiquimod high
R848 low
R848 high
Control
Adjuvant
Concentration (pg/ml)
G-CSF
GM-CSF
IFN-a
IFN-g
IL-10
IL-12p70
IL-17a
IL-18
IL-1a
IL-1b
IL-2
IL-23
IL-27
IL-3
IL-33
IL-4
IL-5
IL-6
IL-8
MCP-1
MIG
MIP-1a
RANTES
SCF
TNF-a

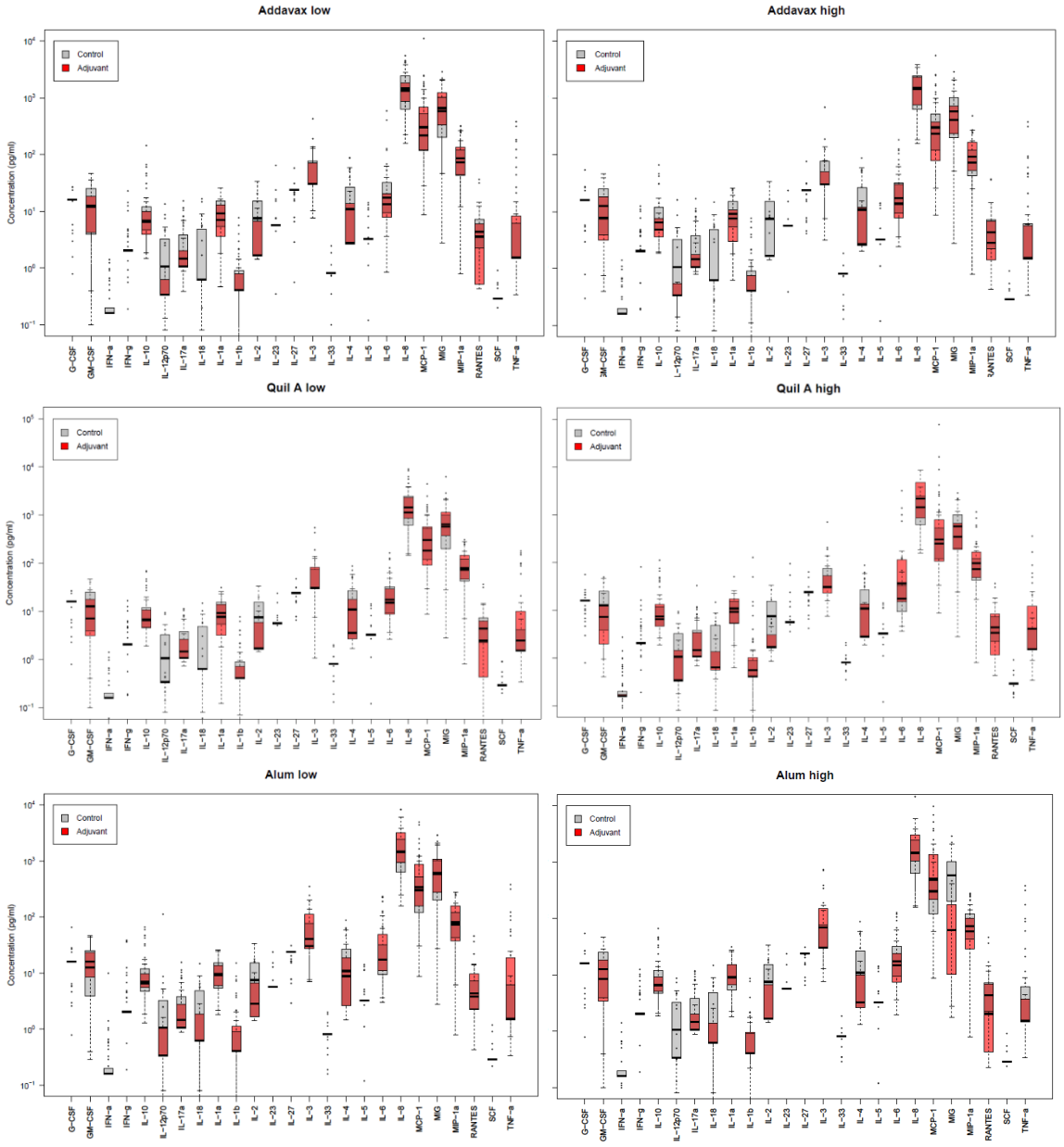
Addavax low
Addavax high
Quil A low
Quil A high
Alum low
Alum high
Control
Adjuvant
Concentration (pg/ml)
G-CSF
GM-CSF
IFN-a
IFN-g
IL-10
IL-12p70
IL-17a
IL-18
IL-1a
IL-1b
IL-2
IL-23
IL-27
IL-3
IL-33
IL-4
IL-5
IL-6
IL-8
MCP-1
MIG
MIP-1a
RANTES
SCF
TNF-a

References

Agnandji, S.T., Lell, B., Soulanoudjingar, S.S., Fernandes, J.F., Abossolo, B.P., Conzelmann, C., Methogo, B.G.N.O., Doucka, Y., Flamen, A., and Mordmüller, B., et al. (2011). First results of phase 3 trial of RTS,S/AS01 malaria vaccine in African children. The New England journal of medicine *365*, 1863-1875.

Agrawal, S., and Gupta, S. (2011). TLR1/2, TLR7, and TLR9 signals directly activate human peripheral blood naive and memory B cell subsets to produce cytokines, chemokines, and hematopoietic growth factors. Journal of clinical immunology *31*, 89-98.

Ahmed, S.S., Black, S., and Ulmer, J. (2012). New developments and concepts related to biomarker application to vaccines. Microbial biotechnology *5*, 233-240.

Ahmed, S.S., Plotkin, S.A., Black, S., and Coffman, R.L. (2011). Assessing the safety of adjuvanted vaccines. Science translational medicine *3*, 93rv2.

Akira, S., Uematsu, S., and Takeuchi, O. (2006). Pathogen recognition and innate immunity. Cell *124*, 783-801.

Akondy, R.S., Fitch, M., Edupuganti, S., Yang, S., Kissick, H.T., Li, K.W., Youngblood, B.A., Abdelsamed, H.A., McGuire, D.J., and Cohen, K.W., et al. (2017). Origin and differentiation of human memory CD8 T cells after vaccination. Nature *552*, 362-367.

Albarran, B., Goncalves, L., Salmen, S., Borges, L., Fields, H., Soyano, A., Montes, H., and Berrueta, L. (2005). Profiles of NK, NKT cell activation and cytokine production following vaccination against hepatitis B. APMIS : acta pathologica, microbiologica, et immunologica Scandinavica *113*, 526-535.

Alderson, M.R., Tough, T.W., Davis-Smith, T., Braddy, S., Falk, B., Schooley, K.A., Goodwin, R.G., Smith, C.A., Ramsdell, F., and Lynch, D.H. (1995). Fas ligand mediates activation-induced cell death in human T lymphocytes. The Journal of experimental medicine *181*, 71-77.

Allie, N., Grivennikov, S.I., Keeton, R., Hsu, N.-J., Bourigault, M.-L., Court, N., Fremond, C., Yeremeev, V., Shebzukhov, Y., and Ryffel, B., et al. (2013). Prominent role for T cell-derived tumour necrosis factor for sustained control of Mycobacterium tuberculosis infection. Scientific reports *3*, 1809.

Armbruster, N.S., Richardson, J.R., Schreiner, J., Klenk, J., Günter, M., and Autenrieth, S.E. (2016). Staphylococcus aureus PSM peptides induce tolerogenic dendritic cells upon treatment with ligands of extracellular and intracellular TLRs. International journal of medical microbiology : IJMM *306*, 666-674.

Awate, S., Babiuk, L.A., and Mutwiri, G. (2013). Mechanisms of action of adjuvants. Frontiers in immunology *4*, 114.

Aylward, B., and Tangermann, R. (2011). The global polio eradication initiative: lessons learned and prospects for success. Vaccine *29 Suppl 4*, D80-5.

Bachmann, M.F., and Jennings, G.T. (2010). Vaccine delivery: a matter of size, geometry, kinetics and molecular patterns. Nature reviews. Immunology *10*, 787-796.

Banchereau, J., and Steinman, R.M. (1998). Dendritic cells and the control of immunity. Nature *392*, 245-252.

Banchereau, R., Baldwin, N., Cepika, A.-M., Athale, S., Xue, Y., Yu, C.I., Metang, P., Cheruku, A., Berthier, I., and Gayet, I., et al. (2014). Transcriptional specialization of human dendritic cell subsets in response to microbial vaccines. Nature communications *5*, 5283.

Banzhoff, A., Gasparini, R., Laghi-Pasini, F., Staniscia, T., Durando, P., Montomoli, E., Capecchi, P.L., Capecchi, P., Di Giovanni, P., and Sticchi, L., et al. (2009). MF59-adjuvanted H5N1 vaccine

induces immunologic memory and heterotypic antibody responses in non-elderly and elderly adults. PloS one *4*, e4384.

Barrat, F.J. (2018). TLR8: No gain, no pain. The Journal of experimental medicine *215*, 2964-2966.

Bekeredjian-Ding, I., Roth, S.I., Gilles, S., Giese, T., Ablasser, A., Hornung, V., Endres, S., and Hartmann, G. (2006). T cell-independent, TLR-induced IL-12p70 production in primary human monocytes. Journal of immunology (Baltimore, Md. : 1950) *176*, 7438-7446.

Bekeredjian-Ding, I.B., Berkeredjian-Ding, I.B., Wagner, M., Hornung, V., Giese, T., Schnurr, M., Endres, S., and Hartmann, G. (2005). Plasmacytoid dendritic cells control TLR7 sensitivity of naive B cells via type I IFN. Journal of immunology (Baltimore, Md. : 1950) *174*, 4043-4050.

Bekker, L.-G., Moodie, Z., Grunenberg, N., Laher, F., Tomaras, G.D., Cohen, K.W., Allen, M., Malahleha, M., Mngadi, K., and Daniels, B., et al. (2018). Subtype C ALVAC-HIV and bivalent subtype C gp120/MF59 HIV-1 vaccine in low-risk, HIV-uninfected, South African adults: a phase 1/2 trial. The Lancet HIV *5*, e366-e378.

Belloc, F., Dumain, P., Boisseau, M.R., Jalloustre, C., Reiffers, J., Bernard, P., and Lacombe, F. (1994). A flow cytometric method using Hoechst 33342 and propidium iodide for simultaneous cell cycle analysis and apoptosis determination in unfixed cells. Cytometry *17*, 59-65.

Berek, C., and Ziegner, M. (1993). The maturation of the immune response. Immunology Today *14*, 400-404.

Berger, M., Ablasser, A., Kim, S., Bekeredjian-Ding, I., Giese, T., Endres, S., Hornung, V., and Hartmann, G. (2009). TLR8-driven IL-12-dependent reciprocal and synergistic activation of NK cells and monocytes by immunostimulatory RNA. Journal of immunotherapy (Hagerstown, Md. : 1997) *32*, 262-271.

Blasius, A.L., and Beutler, B. (2010). Intracellular toll-like receptors. Immunity *32*, 305-315.

Bodewes, R., Geelhoed-Mieras, M.M., Heldens, J.G.M., Glover, J., Lambrecht, B.N., Fouchier, R.A.M., Osterhaus, A.D.M.E., and Rimmelzwaan, G.F. (2009). The novel adjuvant CoVaccineHT increases the immunogenicity of cell-culture derived influenza A/H5N1 vaccine and induces the maturation of murine and human dendritic cells in vitro. Vaccine *27*, 6833-6839.

Bonam, S.R., Partidos, C.D., Halmuthur, S.K.M., and Muller, S. (2017). An Overview of Novel Adjuvants Designed for Improving Vaccine Efficacy. Trends in pharmacological sciences *38*, 771-793.

Boucher, P.E. (2017). A Framework for Evaluating Nonclinical Safety of Novel Adjuvants and Adjuvanted Preventive Vaccines. In Immunopotentiators in Modern Vaccines (Elsevier), pp. 445–476.

Bourke, E., Bosisio, D., Golay, J., Polentarutti, N., and Mantovani, A. (2003). The toll-like receptor repertoire of human B lymphocytes: inducible and selective expression of TLR9 and TLR10 in normal and transformed cells. Blood *102*, 956-963.

Boyle, J., Eastman, D., Millar, C., Camuglia, S., Cox, J., Pearse, M., Good, J., and Drane, D. (2007). The utility of ISCOMATRIX adjuvant for dose reduction of antigen for vaccines requiring antibody responses. Vaccine *25*, 2541-2544.

Brandt, K.J., Fickentscher, C., Kruithof, E.K.O., and Moerloose, P. de (2013). TLR2 ligands induce NF-κB activation from endosomal compartments of human monocytes. PloS one *8*, e80743.

Brewitz, A., Eickhoff, S., Dähling, S., Quast, T., Bedoui, S., Kroczek, R.A., Kurts, C., Garbi, N., Barchet, W., and Iannacone, M., et al. (2017). CD8+ T Cells Orchestrate pDC-XCR1+ Dendritic Cell Spatial and Functional Cooperativity to Optimize Priming. Immunity *46*, 205-219.

Brookes, R.H., Hakimi, J., Ha, Y., Aboutorabian, S., Ausar, S.F., Hasija, M., Smith, S.G., Todryk, S.M., Dockrell, H.M., and Rahman, N. (2014). Screening vaccine formulations for biological activity using fresh human whole blood. Human vaccines & immunotherapeutics *10*, 1129-1135.

Brooks, D.G., Lee, A.M., Elsaesser, H., McGavern, D.B., and Oldstone, M.B.A. (2008). IL-10 blockade facilitates DNA vaccine-induced T cell responses and enhances clearance of persistent virus infection. The Journal of experimental medicine *205*, 533-541.

Brugnolo, F., Sampognaro, S., Liotta, F., Cosmi, L., Annunziato, F., Manuelli, C., Campi, P., Maggi, E., Romagnani, S., and Parronchi, P. (2003). The novel synthetic immune response modifier R-848 (Resiquimod) shifts human allergen-specific CD4+ TH2 lymphocytes into IFN-gamma-producing cells. The Journal of allergy and clinical immunology *111*, 380-388.

Calabro, S., Tortoli, M., Baudner, B.C., Pacitto, A., Cortese, M., O'Hagan, D.T., Gregorio, E. de, Seubert, A., and Wack, A. (2011). Vaccine adjuvants alum and MF59 induce rapid recruitment of neutrophils and monocytes that participate in antigen transport to draining lymph nodes. Vaccine *29*, 1812-1823.

Calabro, S., Tritto, E., Pezzotti, A., Taccone, M., Muzzi, A., Bertholet, S., Gregorio, E. de, O'Hagan, D.T., Baudner, B., and Seubert, A. (2013). The adjuvant effect of MF59 is due to the oil-in-water emulsion formulation, none of the individual components induce a comparable adjuvant effect. Vaccine *31*, 3363-3369.

Cantisani, R., Pezzicoli, A., Cioncada, R., Malzone, C., Gregorio, E. de, D'Oro, U., and Piccioli, D. (2015). Vaccine adjuvant MF59 promotes retention of unprocessed antigen in lymph node macrophage compartments and follicular dendritic cells. Journal of immunology (Baltimore, Md. : 1950) *194*, 1717-1725.

Caproni, E., Tritto, E., Cortese, M., Muzzi, A., Mosca, F., Monaci, E., Baudner, B., Seubert, A., and Gregorio, E. de (2012). MF59 and Pam3CSK4 boost adaptive responses to influenza subunit vaccine through an IFN type I-independent mechanism of action. Journal of immunology (Baltimore, Md. : 1950) *188*, 3088-3098.

Caramalho, I., Lopes-Carvalho, T., Ostler, D., Zelenay, S., Haury, M., and Demengeot, J. (2003). Regulatory T cells selectively express toll-like receptors and are activated by lipopolysaccharide. The Journal of experimental medicine *197*, 403-411.

Caron, G., Duluc, D., Frémaux, I., Jeannin, P., David, C., Gascan, H., and Delneste, Y. (2005). Direct stimulation of human T cells via TLR5 and TLR7/8: flagellin and R-848 up-regulate proliferation and IFN-gamma production by memory CD4+ T cells. Journal of immunology (Baltimore, Md. : 1950) *175*, 1551-1557.

Cerundolo, V., Alexander, J., Anderson, K., Lamb, C., Cresswell, P., McMichael, A., Gotch, F., and Townsend, A. (1990). Presentation of viral antigen controlled by a gene in the major histocompatibility complex. Nature *345*, 449-452.

Chaudhury, S., Duncan, E.H., Atre, T., Storme, C.K., Beck, K., Kaba, S.A., Lanar, D.E., and Bergmann-Leitner, E.S. (2018). Identification of Immune Signatures of Novel Adjuvant Formulations Using Machine Learning. Scientific reports *8*, 17508.

Chiang, C.-Y., Engel, A., Opaluch, A.M., Ramos, I., Maestre, A.M., Secundino, I., Jesus, P.D. de, Nguyen, Q.T., Welch, G., and Bonamy, G.M.C., et al. (2012). Cofactors required for TLR7- and TLR9-dependent innate immune responses. Cell host & microbe *11*, 306-318.

Cioncada, R., Maddaluno, M., Vo, H.T.M., Woodruff, M., Tavarini, S., Sammicheli, C., Tortoli, M., Pezzicoli, A., Gregorio, E. de, and Carroll, M.C., et al. (2017). Vaccine adjuvant MF59 promotes the intranodal differentiation of antigen-loaded and activated monocyte-derived dendritic cells. PloS one *12*, e0185843.

codecademy (2020). Normalization. www.codecademy.com/articles/normalization. 14.07.2020.

Coffey, F., Alabyev, B., and Manser, T. (2009). Initial clonal expansion of germinal center B cells takes place at the perimeter of follicles. Immunity *30*, 599-609.

Coffman, R.L., Sher, A., and Seder, R.A. (2010). Vaccine adjuvants: putting innate immunity to work. Immunity *33*, 492-503.

Coler, R.N., Bertholet, S., Moutaftsi, M., Guderian, J.A., Windish, H.P., Baldwin, S.L., Laughlin, E.M., Duthie, M.S., Fox, C.B., and Carter, D., et al. (2011). Development and characterization of synthetic glucopyranosyl lipid adjuvant system as a vaccine adjuvant. PloS one *6*, e16333.

Coler, R.N., Day, T.A., Ellis, R., Piazza, F.M., Beckmann, A.M., Vergara, J., Rolf, T., Lu, L., Alter, G., and Hokey, D., et al. (2018). The TLR-4 agonist adjuvant, GLA-SE, improves magnitude and quality of immune responses elicited by the ID93 tuberculosis vaccine: first-in-human trial. NPJ vaccines *3*, 34.

Collin, M., and Bigley, V. (2018). Human dendritic cell subsets: an update. Immunology *154*, 3-20.

Cook, K.D., Kline, H.C., and Whitmire, J.K. (2015). NK cells inhibit humoral immunity by reducing the abundance of CD4+ T follicular helper cells during a chronic virus infection. Journal of leukocyte biology *98*, 153-162.

Cottalorda, A., Mercier, B.C., Mbitikon-Kobo, F.M., Arpin, C., Teoh, D.Y.L., McMichael, A., Marvel, J., and Bonnefoy-Bérard, N. (2009). TLR2 engagement on memory CD8(+) T cells improves their cytokine-mediated proliferation and IFN-gamma secretion in the absence of Ag. European journal of immunology *39*, 2673-2681.

Cottalorda, A., Verschelde, C., Marçais, A., Tomkowiak, M., Musette, P., Uematsu, S., Akira, S., Marvel, J., and Bonnefoy-Berard, N. (2006). TLR2 engagement on CD8 T cells lowers the threshold for optimal antigen-induced T cell activation. European journal of immunology *36*, 1684-1693.

Crow, M.K. (2010). Type I interferon in organ-targeted autoimmune and inflammatory diseases. Arthritis research & therapy *12 Suppl 1*, S5.

Dalsgaard, K. (1974). Saponin adjuvants. Archiv f Virusforschung *44*, 243-254.

Davis, H.L. (2008). Novel vaccines and adjuvant systems: the utility of animal models for predicting immunogenicity in humans. Human vaccines *4*, 246-250.

Deenadayalan, A., Maddineni, P., and Raja, A. (2013). Comparison of whole blood and PBMC assays for T-cell functional analysis. BMC research notes *6*, 120.

Deifl, S., Kitzmüller, C., Steinberger, P., Himly, M., Jahn-Schmid, B., Fischer, G.F., Zlabinger, G.J., and Bohle, B. (2014). Differential activation of dendritic cells by toll-like receptors causes diverse differentiation of naïve CD4+ T cells from allergic patients. Allergy *69*, 1602-1609.

Desel, C., Werninghaus, K., Ritter, M., Jozefowski, K., Wenzel, J., Russkamp, N., Schleicher, U., Christensen, D., Wirtz, S., and Kirschning, C., et al. (2013). The Mincle-activating adjuvant TDB induces MyD88-dependent Th1 and Th17 responses through IL-1R signaling. PloS one *8*, e53531.

Di Pasquale, A., Bonanni, P., Garçon, N., Stanberry, L.R., El-Hodhod, M., and Tavares Da Silva, F. (2016). Vaccine safety evaluation: Practical aspects in assessing benefits and risks. Vaccine *34*, 6672-6680.

Di Pasquale, A., Preiss, S., Tavares Da Silva, F., and Garçon, N. (2015). Vaccine Adjuvants: from 1920 to 2015 and Beyond. Vaccines *3*, 320-343.

Dillon, S.B., Demuth, S.G., Schneider, M.A., Weston, C.B., Jones, C.S., Young, J.F., Scott, M., Bhatnaghar, P.K., LoCastro, S., and Hanna, N. (1992). Induction of protective class I MHC-

restricted CTL in mice by a recombinant influenza vaccine in aluminium hydroxide adjuvant. Vaccine *10*, 309-318.

Dominguez-Villar, M., Gautron, A.-S., Marcken, M. de, Keller, M.J., and Hafler, D.A. (2015). TLR7 induces anergy in human CD4(+) T cells. Nature immunology *16*, 118-128.

Draper, E., Bissett, S.L., Howell-Jones, R., Waight, P., Soldan, K., Jit, M., Andrews, N., Miller, E., and Beddows, S. (2013). A randomized, observer-blinded immunogenicity trial of Cervarix(®) and Gardasil(®) Human Papillomavirus vaccines in 12-15 year old girls. PloS one *8*, e61825.

Duffy, D., Rouilly, V., Libri, V., Hasan, M., Beitz, B., David, M., Urrutia, A., Bisiaux, A., Labrie, S.T., and Dubois, A., et al. (2014). Functional analysis via standardized whole-blood stimulation systems defines the boundaries of a healthy immune response to complex stimuli. Immunity *40*, 436-450.

Dupuis, M. (1999). Distribution of adjuvant MF59 and antigen gD2 after intramuscular injection in mice. Vaccine *18*, 434-439.

Durali, D., Goër Herve, M.-G. de, Giron-Michel, J., Azzarone, B., Delfraissy, J.-F., and Taoufik, Y. (2003). In human B cells, IL-12 triggers a cascade of molecular events similar to Th1 commitment. Blood *102*, 4084-4089.

Duthie, M.S., Windish, H.P., Fox, C.B., and Reed, S.G. (2011). Use of defined TLR ligands as adjuvants within human vaccines. Immunological reviews *239*, 178-196.

Enama, M.E., Ledgerwood, J.E., Novik, L., Nason, M.C., Gordon, I.J., Holman, L., Bailer, R.T., Roederer, M., Koup, R.A., and Mascola, J.R., et al. (2014). Phase I randomized clinical trial of VRC DNA and rAd5 HIV-1 vaccine delivery by intramuscular (i.m.), subcutaneous (s.c.) and intradermal (i.d.) administration (VRC 011). PloS one *9*, e91366.

(2019). European Pharmacopoeia, 10th edition, English. Subscription to Main volume + Supplement 1 + Supplement 2 (Stuttgart: Deutscher Apotheker Verlag).

Farber, D.L., Yudanin, N.A., and Restifo, N.P. (2014). Human memory T cells: generation, compartmentalization and homeostasis. Nature reviews. Immunology *14*, 24-35.

Fenner, F., Henderson, D.A., Arita, I., Jezek, Z., Ladnyi, I.D. and World Health Organization (1988). Smallpox and its eradication (Geneva: World Health Organization) *no. 6.* https://apps.who.int/iris/handle/10665/39485.

Filippis, C., Arens, K., Noubissi Nzeteu, G.A., Reichmann, G., Waibler, Z., Crauwels, P., and van Zandbergen, G. (2017). Nivolumab Enhances In Vitro Effector Functions of PD-1+ T-Lymphocytes and Leishmania-Infected Human Myeloid Cells in a Host Cell-Dependent Manner. Frontiers in immunology *8*, 1880.

Fink, A.L., Engle, K., Ursin, R.L., Tang, W.-Y., and Klein, S.L. (2018). Biological sex affects vaccine efficacy and protection against influenza in mice. Proceedings of the National Academy of Sciences of the United States of America *115*, 12477-12482.

Fink, A.L., and Klein, S.L. (2015). Sex and Gender Impact Immune Responses to Vaccines Among the Elderly. Physiology (Bethesda, Md.) *30*, 408-416.

Foged, C., Hansen, J., and Agger, E.M. (2012). License to kill: Formulation requirements for optimal priming of CD8(+) CTL responses with particulate vaccine delivery systems. European journal of pharmaceutical sciences : official journal of the European Federation for Pharmaceutical Sciences *45*, 482-491.

Fontes, M., and Soneson, C. (2011). The projection score--an evaluation criterion for variable subset selection in PCA visualization. BMC bioinformatics *12*, 307.

Frey, S.E., Reyes, M.R.A.-D.L., Reynales, H., Bermal, N.N., Nicolay, U., Narasimhan, V., Forleo-Neto, E., and Arora, A.K. (2014). Comparison of the safety and immunogenicity of an MF59®-adjuvanted with a non-adjuvanted seasonal influenza vaccine in elderly subjects. Vaccine *32*, 5027-5034.

Fujii, S.-I., Liu, K., Smith, C., Bonito, A.J., and Steinman, R.M. (2004). The linkage of innate to adaptive immunity via maturing dendritic cells in vivo requires CD40 ligation in addition to antigen presentation and CD80/86 costimulation. The Journal of experimental medicine *199*, 1607-1618.

Gad, S.C. (2011). Development of Therapeutic Agents Handbook (Wiley).

Gao, N., Jennings, P., Guo, Y., and Yuan, D. (2011). Regulatory role of natural killer (NK) cells on antibody responses to Brucella abortus. Innate immunity *17*, 152-163.

Garcia-Bates, T.M., Palma, M.L., Shen, C., Gambotto, A., Macatangay, B.J.C., Ferris, R.L., Rinaldo, C.R., and Mailliard, R.B. (2019). Contrasting Roles of the PD-1 Signaling Pathway in Dendritic Cell-Mediated Induction and Regulation of HIV-1-Specific Effector T Cell Functions. Journal of virology *93*.

García-González, P., Morales, R., Hoyos, L., Maggi, J., Campos, J., Pesce, B., Gárate, D., Larrondo, M., González, R., and Soto, L., et al. (2013). A short protocol using dexamethasone and monophosphoryl lipid A generates tolerogenic dendritic cells that display a potent migratory capacity to lymphoid chemokines. Journal of translational medicine *11*, 128.

Garçon, N., Chomez, P., and van Mechelen, M. (2007). GlaxoSmithKline Adjuvant Systems in vaccines: concepts, achievements and perspectives. Expert review of vaccines *6*, 723-739.

Garçon, N., and Di Pasquale, A. (2017). From discovery to licensure, the Adjuvant System story. Human vaccines & immunotherapeutics *13*, 19-33.

Garçon, N., and Tavares Da Silva, F. (2017). Development and Evaluation of AS04, a Novel and Improved Adjuvant System Containing 3-O-Desacyl-4′- Monophosphoryl Lipid A and Aluminum Salt. In Immunopotentiators in Modern Vaccines (Elsevier), pp. 287–309.

Geijtenbeek, T.B.H., Torensma, R., van Vliet, S.J., van Duijnhoven, G.C.F., Adema, G.J., van Kooyk, Y., and Figdor, C.G. (2000). Identification of DC-SIGN, a Novel Dendritic Cell–Specific ICAM-3 Receptor that Supports Primary Immune Responses. Cell *100*, 575-585.

Ghimire, T.R. (2015). The mechanisms of action of vaccines containing aluminum adjuvants: an in vitro vs in vivo paradigm. SpringerPlus *4*, 181.

Ghimire, T.R., Benson, R.A., Garside, P., and Brewer, J.M. (2012). Alum increases antigen uptake, reduces antigen degradation and sustains antigen presentation by DCs in vitro. Immunology letters *147*, 55-62.

Gibson, S.J., Lindh, J.M., Riter, T.R., Gleason, R.M., Rogers, L.M., Fuller, A.E., Oesterich, J.L., Gorden, K.B., Qiu, X., and McKane, S.W., et al. (2002). Plasmacytoid dendritic cells produce cytokines and mature in response to the TLR7 agonists, imiquimod and resiquimod. Cellular Immunology *218*, 74-86.

Gilliet, M., Cao, W., and Liu, Y.-J. (2008). Plasmacytoid dendritic cells: sensing nucleic acids in viral infection and autoimmune diseases. Nature reviews. Immunology *8*, 594-606.

Gorden, K.B., Gorski, K.S., Gibson, S.J., Kedl, R.M., Kieper, W.C., Qiu, X., Tomai, M.A., Alkan, S.S., and Vasilakos, J.P. (2005). Synthetic TLR agonists reveal functional differences between human TLR7 and TLR8. Journal of immunology (Baltimore, Md. : 1950) *174*, 1259-1268.

Gordon, S. (2002). Pattern Recognition Receptors. Cell *111*, 927-930.

Goto, T., Nishida, T., Takagi, E., Miyao, K., Koyama, D., Sakemura, R., Hanajiri, R., Watanabe, K., Imahashi, N., and Terakura, S., et al. (2016). Programmed Death-Ligand 1 on Antigen-presenting

Cells Facilitates the Induction of Antigen-specific Cytotoxic T Lymphocytes: Application to Adoptive T-Cell Immunotherapy. Journal of immunotherapy (Hagerstown, Md. : 1997) *39*, 306-315.

Guimarães, L.E., Baker, B., Perricone, C., and Shoenfeld, Y. (2015). Vaccines, adjuvants and autoimmunity. Pharmacological research *100*, 190-209.

Guy, B. (2007). The perfect mix: recent progress in adjuvant research. Nature reviews. Microbiology *5*, 505-517.

Hackstein, H., Knoche, A., Nockher, A., Poeling, J., Kubin, T., Jurk, M., Vollmer, J., and Bein, G. (2011). The TLR7/8 ligand resiquimod targets monocyte-derived dendritic cell differentiation via TLR8 and augments functional dendritic cell generation. Cellular Immunology *271*, 401-412.

Haks, M.C., Goeman, J.J., Magis-Escurra, C., and Ottenhoff, T.H.M. (2015). Focused human gene expression profiling using dual-color reverse transcriptase multiplex ligation-dependent probe amplification. Vaccine *33*, 5282-5288.

Han, Q., Bagheri, N., Bradshaw, E.M., Hafler, D.A., Lauffenburger, D.A., and Love, J.C. (2012). Polyfunctional responses by human T cells result from sequential release of cytokines. Proceedings of the National Academy of Sciences of the United States of America *109*, 1607-1612.

Hanten, J.A., Vasilakos, J.P., Riter, C.L., Neys, L., Lipson, K.E., Alkan, S.S., and Birmachu, W. (2008). Comparison of human B cell activation by TLR7 and TLR9 agonists. BMC immunology *9*, 39.

He, X.-S., Holmes, T.H., Zhang, C., Mahmood, K., Kemble, G.W., Lewis, D.B., Dekker, C.L., Greenberg, H.B., and Arvin, A.M. (2006). Cellular immune responses in children and adults receiving inactivated or live attenuated influenza vaccines. Journal of virology *80*, 11756-11766.

Hemmi, H., Kaisho, T., Takeuchi, O., Sato, S., Sanjo, H., Hoshino, K., Horiuchi, T., Tomizawa, H., Takeda, K., and Akira, S. (2002). Small anti-viral compounds activate immune cells via the TLR7 MyD88-dependent signaling pathway. Nature immunology *3*, 196-200.

Hémont, C., Neel, A., Heslan, M., Braudeau, C., and Josien, R. (2013). Human blood mDC subsets exhibit distinct TLR repertoire and responsiveness. Journal of leukocyte biology *93*, 599-609.

Hogenesch, H. (2012). Mechanism of immunopotentiation and safety of aluminum adjuvants. Frontiers in immunology *3*, 406.

Holzmann, H., Hengel, H., Tenbusch, M., and Doerr, H.W. (2016). Eradication of measles: remaining challenges. Medical microbiology and immunology *205*, 201-208.

Hoonakker, M.E., Verhagen, L.M., Hendriksen, C.F.M., van Els, C.A.C.M., Vandebriel, R.J., Sloots, A., and Han, W.G.H. (2015). In vitro innate immune cell based models to assess whole cell Bordetella pertussis vaccine quality: a proof of principle. Biologicals : journal of the International Association of Biological Standardization *43*, 100-109.

Hornung, V., Rothenfusser, S., Britsch, S., Krug, A., Jahrsdörfer, B., Giese, T., Endres, S., and Hartmann, G. (2002). Quantitative expression of toll-like receptor 1-10 mRNA in cellular subsets of human peripheral blood mononuclear cells and sensitivity to CpG oligodeoxynucleotides. Journal of immunology (Baltimore, Md. : 1950) *168*, 4531-4537.

Horrevorts, S.K., Duinkerken, S., Bloem, K., Secades, P., Kalay, H., Musters, R.J., van Vliet, S.J., García-Vallejo, J.J., and van Kooyk, Y. (2018). Toll-Like Receptor 4 Triggering Promotes Cytosolic Routing of DC-SIGN-Targeted Antigens for Presentation on MHC Class I. Frontiers in immunology *9*, 1231.

Huppa, J.B., and Davis, M.M. (2003). T-cell-antigen recognition and the immunological synapse. Nature reviews. Immunology *3*, 973-983.

Ikeno, D., Kimachi, K., Kino, Y., Harada, S., Yoshida, K., Tochihara, S., Itamura, S., Odagiri, T., Tashiro, M., and Okada, K., et al. (2010). Immunogenicity of an inactivated adjuvanted whole-virion influenza A (H5N1, NIBRG-14) vaccine administered by intramuscular or subcutaneous injection. Microbiology and immunology *54*, 81-88.

Ilyinskii, P.O., Roy, C.J., O'Neil, C.P., Browning, E.A., Pittet, L.A., Altreuter, D.H., Alexis, F., Tonti, E., Shi, J., and Basto, P.A., et al. (2014). Adjuvant-carrying synthetic vaccine particles augment the immune response to encapsulated antigen and exhibit strong local immune activation without inducing systemic cytokine release. Vaccine *32*, 2882-2895.

Ismaili, J., Rennesson, J., Aksoy, E., Vekemans, J., Vincart, B., Amraoui, Z., van Laethem, F., Goldman, M., and Dubois, P.M. (2002). Monophosphoryl lipid A activates both human dendritic cells and T cells. Journal of immunology (Baltimore, Md. : 1950) *168*, 926-932.

Jameson, S.C., and Masopust, D. (2018). Understanding Subset Diversity in T Cell Memory. Immunity *48*, 214-226.

Janeway, C.A. (1989). Approaching the asymptote? Evolution and revolution in immunology. Cold Spring Harbor symposia on quantitative biology *54 Pt 1*, 1-13.

Jasiulewicz, A., Lisowska, K.A., Pietruczuk, K., Frąckowiak, J., Fulop, T., and Witkowski, J.M. (2015). Homeostatic 'bystander' proliferation of human peripheral blood B cells in response to polyclonal T-cell stimulation in vitro. International immunology *27*, 579-588.

Jayakumar, A., Castilho, T.M., Park, E., Goldsmith-Pestana, K., Blackwell, J.M., and McMahon-Pratt, D. (2011). TLR1/2 activation during heterologous prime-boost vaccination (DNA-MVA) enhances CD8+ T Cell responses providing protection against Leishmania (Viannia). PLoS neglected tropical diseases *5*, e1204.

Jiang, W., Swiggard, W.J., Heufler, C., Peng, M., Mirza, A., Steinman, R.M., and Nussenzweig, M.C. (1995). The receptor DEC-205 expressed by dendritic cells and thymic epithelial cells is involved in antigen processing. Nature *375*, 151-155.

Jo, E.-K., Kim, J.K., Shin, D.-M., and Sasakawa, C. (2016). Molecular mechanisms regulating NLRP3 inflammasome activation. Cellular & molecular immunology *13*, 148-159.

Joffre, O.P., Segura, E., Savina, A., and Amigorena, S. (2012). Cross-presentation by dendritic cells. Nature reviews. Immunology *12*, 557-569.

Johnson, T.R., Rao, S., Seder, R.A., Chen, M., and Graham, B.S. (2009). TLR9 agonist, but not TLR7/8, functions as an adjuvant to diminish FI-RSV vaccine-enhanced disease, while either agonist used as therapy during primary RSV infection increases disease severity. Vaccine *27*, 3045-3052.

Jordan, M.B., Mills, D.M., Kappler, J., Marrack, P., and Cambier, J.C. (2004). Promotion of B cell immune responses via an alum-induced myeloid cell population. Science (New York, N.Y.) *304*, 1808-1810.

Jung, S., Unutmaz, D., Wong, P., Sano, G.-I., los Santos, K. de, Sparwasser, T., Wu, S., Vuthoori, S., Ko, K., and Zavala, F., et al. (2002). In Vivo Depletion of CD11c+ Dendritic Cells Abrogates Priming of CD8+ T Cells by Exogenous Cell-Associated Antigens. Immunity *17*, 211-220.

Jurk, M., Heil, F., Vollmer, J., Schetter, C., Krieg, A.M., Wagner, H., Lipford, G., and Bauer, S. (2002). Human TLR7 or TLR8 independently confer responsiveness to the antiviral compound R-848. Nature immunology *3*, 499.

Kang, S., Brown, H.M., and Hwang, S. (2018). Direct Antiviral Mechanisms of Interferon-Gamma. Immune network *18*, e33.

Kapsenberg, M.L. (2003). Dendritic-cell control of pathogen-driven T-cell polarization. Nature reviews. Immunology *3*, 984-993.

Karlsen, M., Jakobsen, K., Jonsson, R., Hammenfors, D., Hansen, T., and Appel, S. (2017). Expression of Toll-Like Receptors in Peripheral Blood Mononuclear Cells of Patients with Primary Sjögren's Syndrome. Scandinavian journal of immunology *85*, 220-226.

Kastenmüller, K., Wille-Reece, U., Lindsay, R.W.B., Trager, L.R., Darrah, P.A., Flynn, B.J., Becker, M.R., Udey, M.C., Clausen, B.E., and Igyarto, B.Z., et al. (2011). Protective T cell immunity in mice following protein-TLR7/8 agonist-conjugate immunization requires aggregation, type I IFN, and multiple DC subsets. The Journal of clinical investigation *121*, 1782-1796.

Kawai, T., and Akira, S. (2007). Signaling to NF-kappaB by Toll-like receptors. Trends in molecular medicine *13*, 460-469.

Kawai, T., and Akira, S. (2010). The role of pattern-recognition receptors in innate immunity: update on Toll-like receptors. Nature immunology *11*, 373-384.

Kawai, T., and Akira, S. (2011). Toll-like receptors and their crosstalk with other innate receptors in infection and immunity. Immunity *34*, 637-650.

Kazmin, D., Nakaya, H.I., Lee, E.K., Johnson, M.J., van der Most, R., van den Berg, R.A., Ballou, W.R., Jongert, E., Wille-Reece, U., and Ockenhouse, C., et al. (2017). Systems analysis of protective immune responses to RTS,S malaria vaccination in humans. Proceedings of the National Academy of Sciences of the United States of America *114*, 2425-2430.

Kensil, C.R., Patel, U., Lennick, M., and Marciani, D. (1991). Separation and characterization of saponins with adjuvant activity from Quillaja saponaria Molina cortex. Journal of immunology (Baltimore, Md. : 1950) *146*, 431-437.

Kensil, C.R., Wu, J.Y., and Soltysik, S. (1995). Structural and immunological characterization of the vaccine adjuvant QS-21. Pharmaceutical biotechnology *6*, 525-541.

Kerfoot, S.M., Yaari, G., Patel, J.R., Johnson, K.L., Gonzalez, D.G., Kleinstein, S.H., and Haberman, A.M. (2011). Germinal center B cell and T follicular helper cell development initiates in the interfollicular zone. Immunity *34*, 947-960.

Khurana, S., Verma, N., Yewdell, J.W., Hilbert, A.K., Castellino, F., Lattanzi, M., Del Giudice, G., Rappuoli, R., and Golding, H. (2011). MF59 adjuvant enhances diversity and affinity of antibody-mediated immune response to pandemic influenza vaccines. Science translational medicine *3*, 85ra48.

Kodar, K., McConnell, M.J., Harper, J.L., Timmer, M.S., and Stocker, B.L. (2020). The coadministration of trehalose dibehenate and monosodium urate crystals promotes an antitumor phenotype in human-derived myeloid cells. Immunology and cell biology *98*, 411-422.

Kommareddy, S., Singh, M., and O'Hagan, D.T. (2017). MF59: A Safe and Potent Adjuvant for Human Use. In Immunopotentiators in Modern Vaccines (Elsevier), pp. 249–263.

Kool, M., Pétrilli, V., Smedt, T. de, Rolaz, A., Hammad, H., van Nimwegen, M., Bergen, I.M., Castillo, R., Lambrecht, B.N., and Tschopp, J. (2008a). Cutting edge: alum adjuvant stimulates inflammatory dendritic cells through activation of the NALP3 inflammasome. Journal of immunology (Baltimore, Md. : 1950) *181*, 3755-3759.

Kool, M., Soullié, T., van Nimwegen, M., Willart, M.A.M., Muskens, F., Jung, S., Hoogsteden, H.C., Hammad, H., and Lambrecht, B.N. (2008b). Alum adjuvant boosts adaptive immunity by inducing uric acid and activating inflammatory dendritic cells. The Journal of experimental medicine *205*, 869-882.

Krammer, P.H., Arnold, R., and Lavrik, I.N. (2007). Life and death in peripheral T cells. Nature reviews. Immunology *7*, 532-542.

Krebs, P., Barnes, M.J., Lampe, K., Whitley, K., Bahjat, K.S., Beutler, B., Janssen, E., and Hoebe, K. (2009). NK-cell-mediated killing of target cells triggers robust antigen-specific T-cell-mediated and humoral responses. Blood *113*, 6593-6602.

Kruit, W.H.J., Suciu, S., Dreno, B., Mortier, L., Robert, C., Chiarion-Sileni, V., Maio, M., Testori, A., Dorval, T., and Grob, J.-J., et al. (2013). Selection of immunostimulant AS15 for active immunization with MAGE-A3 protein: results of a randomized phase II study of the European Organisation for Research and Treatment of Cancer Melanoma Group in Metastatic Melanoma. Journal of clinical oncology : official journal of the American Society of Clinical Oncology *31*, 2413-2420.

Kurosaki, T., Kometani, K., and Ise, W. (2015). Memory B cells. Nature reviews. Immunology *15*, 149-159.

Laidlaw, B.J., Craft, J.E., and Kaech, S.M. (2016). The multifaceted role of CD4(+) T cells in CD8(+) T cell memory. Nature reviews. Immunology *16*, 102-111.

Lal, H., Cunningham, A.L., Godeaux, O., Chlibek, R., Diez-Domingo, J., Hwang, S.-J., Levin, M.J., McElhaney, J.E., Poder, A., and Puig-Barberà, J., et al. (2015). Efficacy of an adjuvanted herpes zoster subunit vaccine in older adults. The New England journal of medicine *372*, 2087-2096.

Langlet, C., Tamoutounour, S., Henri, S., Luche, H., Ardouin, L., Grégoire, C., Malissen, B., and Guilliams, M. (2012). CD64 expression distinguishes monocyte-derived and conventional dendritic cells and reveals their distinct role during intramuscular immunization. Journal of immunology (Baltimore, Md. : 1950) *188*, 1751-1760.

Larsson, K., Lindstedt, M., and Borrebaeck, C.A.K. (2006). Functional and transcriptional profiling of MUTZ-3, a myeloid cell line acting as a model for dendritic cells. Immunology *117*, 156-166.

Lee, S.-J., O'Donnell, H., and McSorley, S.J. (2010). B7-H1 (programmed cell death ligand 1) is required for the development of multifunctional Th1 cells and immunity to primary, but not secondary, Salmonella infection. Journal of immunology (Baltimore, Md. : 1950) *185*, 2442-2449.

Lemaitre, B., Nicolas, E., Michaut, L., Reichhart, J.-M., and Hoffmann, J.A. (1996). The Dorsoventral Regulatory Gene Cassette spätzle/Toll/cactus Controls the Potent Antifungal Response in Drosophila Adults. Cell *86*, 973-983.

Levie, K., Gjorup, I., Skinhøj, P., and Stoffel, M. (2002). A 2-dose regimen of a recombinant hepatitis B vaccine with the immune stimulant AS04 compared with the standard 3-dose regimen of Engerix-B in healthy young adults. Scandinavian journal of infectious diseases *34*, 610-614.

Li, Q., and Verma, I.M. (2002). NF-kappaB regulation in the immune system. Nature reviews. Immunology *2*, 725-734.

Li, Q., Yan, Y., Liu, J., Huang, X., Zhang, X., Kirschning, C., Xu, H.C., Lang, P.A., Dittmer, U., and Zhang, E., et al. (2019). Toll-Like Receptor 7 Activation Enhances CD8+ T Cell Effector Functions by Promoting Cellular Glycolysis. Frontiers in immunology *10*, 2191.

Li, S., Rouphael, N., Duraisingham, S., Romero-Steiner, S., Presnell, S., Davis, C., Schmidt, D.S., Johnson, S.E., Milton, A., and Rajam, G., et al. (2014). Molecular signatures of antibody responses derived from a systems biology study of five human vaccines. Nature immunology *15*, 195-204.

Li, X., Jiang, S., and Tapping, R.I. (2010). Toll-like receptor signaling in cell proliferation and survival. Cytokine *49*, 1-9.

Li Causi, E., Parikh, S.C., Chudley, L., Layfield, D.M., Ottensmeier, C.H., Stevenson, F.K., and Di Genova, G. (2015). Vaccination Expands Antigen-Specific CD4+ Memory T Cells and Mobilizes Bystander Central Memory T Cells. PloS one *10*, e0136717.

Lieberman, J. (2003). The ABCs of granule-mediated cytotoxicity: new weapons in the arsenal. Nature reviews. Immunology *3*, 361-370.

Lindblad, E.B., and Duroux, L. (2017). Mineral Adjuvants∗∗The present chapter is an updated version of the chapter “Mineral Adjuvants,” published in Immunopotentiators in Modern Vaccines, p. 217–233. Ed. Virgil Schijns & Derek O'Hagan, Elsevier Science Publishers (2005). In Immunopotentiators in Modern Vaccines (Elsevier), pp. 347–375.

Lindt, K.-A. (2017). Untersuchung der immunmodulatorischen Eigenschaften von Adjuvantien auf Zellen des angeborenen und adaptiven Immunsystems. Bachelorarbeit zur Erlangung des Grades Bachelor of Science (Hochschule Fresenius University of Applied Sciences).

Lofano, G., Mancini, F., Salvatore, G., Cantisani, R., Monaci, E., Carrisi, C., Tavarini, S., Sammicheli, C., Rossi Paccani, S., and Soldaini, E., et al. (2015). Oil-in-Water Emulsion MF59 Increases Germinal Center B Cell Differentiation and Persistence in Response to Vaccination. Journal of immunology (Baltimore, Md. : 1950) *195*, 1617-1627.

Lombardi, V., van Overtvelt, L., Horiot, S., Moussu, H., Chabre, H., Louise, A., Balazuc, A.-M., Mascarell, L., and Moingeon, P. (2008). Toll-like receptor 2 agonist Pam3CSK4 enhances the induction of antigen-specific tolerance via the sublingual route. Clinical and experimental allergy : journal of the British Society for Allergy and Clinical Immunology *38*, 1819-1829.

Lorenzo-Herrero, S., Sordo-Bahamonde, C., Gonzalez, S., and López-Soto, A. (2019). CD107a Degranulation Assay to Evaluate Immune Cell Antitumor Activity. Methods in molecular biology (Clifton, N.J.) *1884*, 119-130.

Lu, H., Dietsch, G.N., Matthews, M.-A.H., Yang, Y., Ghanekar, S., Inokuma, M., Suni, M., Maino, V.C., Henderson, K.E., and Howbert, J.J., et al. (2012). VTX-2337 is a novel TLR8 agonist that activates NK cells and augments ADCC. Clinical cancer research : an official journal of the American Association for Cancer Research *18*, 499-509.

Lund, F.E., and Randall, T.D. (2010). Effector and regulatory B cells: modulators of CD4+ T cell immunity. Nature reviews. Immunology *10*, 236-247.

Ma, F., Zhang, J., Zhang, J., and Zhang, C. (2010a). The TLR7 agonists imiquimod and gardiquimod improve DC-based immunotherapy for melanoma in mice. Cellular & molecular immunology *7*, 381-388.

Ma, Y., Poisson, L., Sanchez-Schmitz, G., Pawar, S., Qu, C., Randolph, G.J., Warren, W.L., Mishkin, E.M., and Higbee, R.G. (2010b). Assessing the immunopotency of Toll-like receptor agonists in an in vitro tissue-engineered immunological model. Immunology *130*, 374-387.

MacLeod, M.K.L., McKee, A.S., David, A., Wang, J., Mason, R., Kappler, J.W., and Marrack, P. (2011). Vaccine adjuvants aluminum and monophosphoryl lipid A provide distinct signals to generate protective cytotoxic memory CD8 T cells. Proceedings of the National Academy of Sciences of the United States of America *108*, 7914-7919.

Mahnke, Y.D., Brodie, T.M., Sallusto, F., Roederer, M., and Lugli, E. (2013). The who's who of T-cell differentiation: human memory T-cell subsets. Eur. J. Immunol. *43*, 2797-2809.

Mandala, J.P., Ahmad, S., Pullagurla, A., Thada, S., Joshi, L., Ansari, M.S.S., Valluri, V.L., and Gaddam, S.L. (2020). Toll-like receptor 2 polymorphisms and their effect on the immune response to ESAT-6, Pam3CSK4 TLR2 agonist in pulmonary tuberculosis patients and household contacts. Cytokine *126*, 154897.

Månsson, A., Adner, M., Höckerfelt, U., and Cardell, L.-O. (2006). A distinct Toll-like receptor repertoire in human tonsillar B cells, directly activated by PamCSK, R-837 and CpG-2006 stimulation. Immunology *118*, 539-548.

Marcken, M. de, Dhaliwal, K., Danielsen, A.C., Gautron, A.S., and Dominguez-Villar, M. (2019). TLR7 and TLR8 activate distinct pathways in monocytes during RNA virus infection. Science signaling *12*.

Marichal, T., Ohata, K., Bedoret, D., Mesnil, C., Sabatel, C., Kobiyama, K., Lekeux, P., Coban, C., Akira, S., and Ishii, K.J., et al. (2011). DNA released from dying host cells mediates aluminum adjuvant activity. Nature medicine *17*, 996-1002.

Maris, C.H., Chappell, C.P., and Jacob, J. (2007). Interleukin-10 plays an early role in generating virus-specific T cell anergy. BMC immunology *8*, 8.

Marrack, P., McKee, A.S., and Munks, M.W. (2009). Towards an understanding of the adjuvant action of aluminium. Nature reviews. Immunology *9*, 287-293.

Marty-Roix, R., Vladimer, G.I., Pouliot, K., Weng, D., Buglione-Corbett, R., West, K., MacMicking, J.D., Chee, J.D., Wang, S., and Lu, S., et al. (2016). Identification of QS-21 as an Inflammasome-activating Molecular Component of Saponin Adjuvants. The Journal of biological chemistry *291*, 1123-1136.

Mata-Haro, V., Cekic, C., Martin, M., Chilton, P.M., Casella, C.R., and Mitchell, T.C. (2007). The vaccine adjuvant monophosphoryl lipid A as a TRIF-biased agonist of TLR4. Science (New York, N.Y.) *316*, 1628-1632.

Matzinger, P. (1994). Tolerance, danger, and the extended family. Annual review of immunology *12*, 991-1045.

Mbow, M.L., Gregorio, E. de, Valiante, N.M., and Rappuoli, R. (2010). New adjuvants for human vaccines. Current opinion in immunology *22*, 411-416.

McKay, P.F., Cizmeci, D., Aldon, Y., Maertzdorf, J., Weiner, J., Kaufmann, S.H., Lewis, D.J., van den Berg, R.A., Del Giudice, G., and Shattock, R.J. (2019). Identification of potential biomarkers of vaccine inflammation in mice. eLife *8*.

McKee, A.S., Burchill, M.A., Munks, M.W., Jin, L., Kappler, J.W., Friedman, R.S., Jacobelli, J., and Marrack, P. (2013). Host DNA released in response to aluminum adjuvant enhances MHC class II-mediated antigen presentation and prolongs CD4 T-cell interactions with dendritic cells. Proceedings of the National Academy of Sciences of the United States of America *110*, E1122-31.

McKee, A.S., Munks, M.W., MacLeod, M.K.L., Fleenor, C.J., van Rooijen, N., Kappler, J.W., and Marrack, P. (2009). Alum induces innate immune responses through macrophage and mast cell sensors, but these sensors are not required for alum to act as an adjuvant for specific immunity. Journal of immunology (Baltimore, Md. : 1950) *183*, 4403-4414.

McKinney, B.A., Reif, D.M., Rock, M.T., Edwards, K.M., Kingsmore, S.F., Moore, J.H., and Crowe, J.E. (2006). Cytokine expression patterns associated with systemic adverse events following smallpox immunization. The Journal of infectious diseases *194*, 444-453.

McLane, L.M., Abdel-Hakeem, M.S., and Wherry, E.J. (2019). CD8 T Cell Exhaustion During Chronic Viral Infection and Cancer. Annual review of immunology *37*, 457-495.

Mercier, B.C., Cottalorda, A., Coupet, C.-A., Marvel, J., and Bonnefoy-Bérard, N. (2009). TLR2 engagement on CD8 T cells enables generation of functional memory cells in response to a suboptimal TCR signal. Journal of immunology (Baltimore, Md. : 1950) *182*, 1860-1867.

Mian, M.F., Lauzon, N.M., Andrews, D.W., Lichty, B.D., and Ashkar, A.A. (2010). FimH can directly activate human and murine natural killer cells via TLR4. Molecular therapy : the journal of the American Society of Gene Therapy *18*, 1379-1388.

Miller, E., Andrews, N., Stellitano, L., Stowe, J., Winstone, A.M., Shneerson, J., and Verity, C. (2013). Risk of narcolepsy in children and young people receiving AS03 adjuvanted pandemic A/H1N1 2009 influenza vaccine: retrospective analysis. BMJ (Clinical research ed.) *346*, f794.

Ming, M., Bernardo, L., Williams, K., Kolattukudy, P., Kapoor, N., Chan, L.G., Pagnon, A., Piras, F., Su, J., and Gajewska, B., et al. (2019). An in vitro functional assay to measure the biological activity of TB vaccine candidate H4-IC31. Vaccine *37*, 2960-2966.

Montag, T., Spreitzer, I., Löschner, B., Unkelbach, U., Flory, E., Sanzenbacher, R., Schwanig, M., and Schneider, C.K. (2007). Safety testing of cell-based medicinal products: opportunities for the monocyte activation test for pyrogens. ALTEX *24*, 81-89.

Montes, C.L., Acosta-Rodríguez, E.V., Merino, M.C., Bermejo, D.A., and Gruppi, A. (2007). Polyclonal B cell activation in infections: infectious agents' devilry or defense mechanism of the host? Journal of leukocyte biology *82*, 1027-1032.

Morefield, G.L., Sokolovska, A., Jiang, D., Hogenesch, H., Robinson, J.P., and Hem, S.L. (2005). Role of aluminum-containing adjuvants in antigen internalization by dendritic cells in vitro. Vaccine *23*, 1588-1595.

Mort, M., Destefano, F., Giududu, J., Vellozzi, C., Mehta, U., Pless, R., Abdoellah, S.A., Yosephine, P. and Karolina, S. (2020). Vaccine Safety Basics. e-learning course. https://vaccine-safety-training.org/. 24.07.2020.

Moser, J.M., Sassano, E.R., Leistritz, D.C., Eatrides, J.M., Phogat, S., Koff, W., and Drake, D.R. (2010). Optimization of a dendritic cell-based assay for the in vitro priming of naïve human CD4+ T cells. Journal of immunological methods *353*, 8-19.

Moyer, T.J., Zmolek, A.C., and Irvine, D.J. (2016). Beyond antigens and adjuvants: formulating future vaccines. The Journal of clinical investigation *126*, 799-808.

Mueller, S.N., Gebhardt, T., Carbone, F.R., and Heath, W.R. (2013). Memory T cell subsets, migration patterns, and tissue residence. Annual review of immunology *31*, 137-161.

Murphy, K.M., and Weaver, C. (2017). Janeway's immunobiology (New York, London: GS Garland Science Taylor & Francis Group).

Mutwiri, G., Gerdts, V., van Drunen Littel-van den Hurk, S., Auray, G., Eng, N., Garlapati, S., Babiuk, L.A., and Potter, A. (2011). Combination adjuvants: the next generation of adjuvants? Expert review of vaccines *10*, 95-107.

Nagarajan, N.A., and Kronenberg, M. (2007). Invariant NKT cells amplify the innate immune response to lipopolysaccharide. Journal of immunology (Baltimore, Md. : 1950) *178*, 2706-2713.

Newman, M.J., Wu, J.Y., Gardner, B.H., Munroe, K.J., Leombruno, D., Recchia, J., Kensil, C.R., and Coughlin, R.T. (1992). Saponin adjuvant induction of ovalbumin-specific CD8+ cytotoxic T lymphocyte responses. Journal of immunology (Baltimore, Md. : 1950) *148*, 2357-2362.

Nizzoli, G., Krietsch, J., Weick, A., Steinfelder, S., Facciotti, F., Gruarin, P., Bianco, A., Steckel, B., Moro, M., and Crosti, M., et al. (2013). Human CD1c+ dendritic cells secrete high levels of IL-12 and potently prime cytotoxic T-cell responses. Blood *122*, 932-942.

Nohynek, H., Jokinen, J., Partinen, M., Vaarala, O., Kirjavainen, T., Sundman, J., Himanen, S.-L., Hublin, C., Julkunen, I., and Olsén, P., et al. (2012). AS03 adjuvanted AH1N1 vaccine associated with an abrupt increase in the incidence of childhood narcolepsy in Finland. PloS one *7*, e33536.

Nolan, T., Bravo, L., Ceballos, A., Mitha, E., Gray, G., Quiambao, B., Patel, S.S., Bizjajeva, S., Bock, H., and Nazaire-Bermal, N., et al. (2014). Enhanced and persistent antibody response against homologous and heterologous strains elicited by a MF59-adjuvanted influenza vaccine in infants and young children. Vaccine *32*, 6146-6156.

O'Hagan, D.T., and Gregorio, E. de (2009). The path to a successful vaccine adjuvant--'the long and winding road'. Drug discovery today *14*, 541-551.

O'Hagan, D.T., Ott, G.S., van Nest, G., Rappuoli, R., and Giudice, G.D. (2013). The history of MF59(®) adjuvant: a phoenix that arose from the ashes. Expert review of vaccines *12*, 13-30.

Okada, T., Miller, M.J., Parker, I., Krummel, M.F., Neighbors, M., Hartley, S.B., O'Garra, A., Cahalan, M.D., and Cyster, J.G. (2005). Antigen-engaged B cells undergo chemotaxis toward the T zone and form motile conjugates with helper T cells. PLoS biology *3*, e150.

Okemoto, K., Hanada, K., Nishijima, M., and Kawasaki, K. (2008). The preparation of a lipidic endotoxin affects its biological activities. Biological & pharmaceutical bulletin *31*, 1952-1954.

Ostrop, J., Jozefowski, K., Zimmermann, S., Hofmann, K., Strasser, E., Lepenies, B., and Lang, R. (2015). Contribution of MINCLE-SYK Signaling to Activation of Primary Human APCs by Mycobacterial Cord Factor and the Novel Adjuvant TDB. Journal of immunology (Baltimore, Md. : 1950) *195*, 2417-2428.

Osugi, Y., Vuckovic, S., and Hart, D.N.J. (2002). Myeloid blood CD11c(+) dendritic cells and monocyte-derived dendritic cells differ in their ability to stimulate T lymphocytes. Blood *100*, 2858-2866.

Ozinsky, A., Underhill, D.M., Fontenot, J.D., Hajjar, A.M., Smith, K.D., Wilson, C.B., Schroeder, L., and Aderem, A. (2000). The repertoire for pattern recognition of pathogens by the innate immune system is defined by cooperation between toll-like receptors. Proceedings of the National Academy of Sciences of the United States of America *97*, 13766-13771.

Panagioti, E., Klenerman, P., Lee, L.N., van der Burg, S.H., and Arens, R. (2018). Features of Effective T Cell-Inducing Vaccines against Chronic Viral Infections. Frontiers in immunology *9*, 276.

Panina-Bordignon, P., Tan, A., Termijtelen, A., Demotz, S., Corradin, G., and Lanzavecchia, A. (1989). Universally immunogenic T cell epitopes: promiscuous binding to human MHC class II and promiscuous recognition by T cells. European journal of immunology *19*, 2237-2242.

Partinen, M., Saarenpää-Heikkilä, O., Ilveskoski, I., Hublin, C., Linna, M., Olsén, P., Nokelainen, P., Alén, R., Wallden, T., and Espo, M., et al. (2012). Increased incidence and clinical picture of childhood narcolepsy following the 2009 H1N1 pandemic vaccination campaign in Finland. PloS one *7*, e33723.

Petes, C., Odoardi, N., and Gee, K. (2017). The Toll for Trafficking: Toll-Like Receptor 7 Delivery to the Endosome. Frontiers in immunology *8*, 1075.

Plotkin, S. (2014). History of vaccination. Proceedings of the National Academy of Sciences of the United States of America *111*, 12283-12287.

Pockros, P.J., Guyader, D., Patton, H., Tong, M.J., Wright, T., McHutchison, J.G., and Meng, T.-C. (2007). Oral resiquimod in chronic HCV infection: safety and efficacy in 2 placebo-controlled, double-blind phase IIa studies. Journal of hepatology *47*, 174-182.

Posteraro, B., Pastorino, R., Di Giannantonio, P., Ianuale, C., Amore, R., Ricciardi, W., and Boccia, S. (2014). The link between genetic variation and variability in vaccine responses: systematic review and meta-analyses. Vaccine *32*, 1661-1669.

Pufnock, J.S., Cigal, M., Rolczynski, L.S., Andersen-Nissen, E., Wolfl, M., McElrath, M.J., and Greenberg, P.D. (2011). Priming CD8+ T cells with dendritic cells matured using TLR4 and TLR7/8 ligands together enhances generation of CD8+ T cells retaining CD28. Blood *117*, 6542-6551.

Pujol, J.-L., Vansteenkiste, J.F., Pas, T.M. de, Atanackovic, D., Reck, M., Thomeer, M., Douillard, J.-Y., Fasola, G., Potter, V., and Taylor, P., et al. (2015). Safety and Immunogenicity of MAGE-A3

Cancer Immunotherapeutic with or without Adjuvant Chemotherapy in Patients with Resected Stage IB to III MAGE-A3-Positive Non-Small-Cell Lung Cancer. Journal of thoracic oncology : official publication of the International Association for the Study of Lung Cancer *10*, 1458-1467.

Querec, T.D., Akondy, R.S., Lee, E.K., Cao, W., Nakaya, H.I., Teuwen, D., Pirani, A., Gernert, K., Deng, J., and Marzolf, B., et al. (2009). Systems biology approach predicts immunogenicity of the yellow fever vaccine in humans. Nature immunology *10*, 116-125.

Qureshi, N., Takayama, K., and Ribi, E. (1982). Purification and structural determination of nontoxic lipid A obtained from the lipopolysaccharide of Salmonella typhimurium. The Journal of biological chemistry *257*, 11808-11815.

Ramos, O.P., Silva, E.E.C., Falcão, D.P., and Medeiros, B.M.M. de (2005). Production of autoantibodies associated with polyclonal activation in Yersinia enterocolitica O: 8-infected mice. Microbiology and immunology *49*, 129-137.

Rappuoli, R. (2000). Reverse vaccinology. Current Opinion in Microbiology *3*, 445-450.

Rappuoli, R. (2007). Bridging the knowledge gaps in vaccine design. Nature biotechnology *25*, 1361-1366.

Rappuoli, R. (2014). Vaccines: science, health, longevity, and wealth. Proceedings of the National Academy of Sciences of the United States of America *111*, 12282.

Rappuoli, R., Bottomley, M.J., D'Oro, U., Finco, O., and Gregorio, E. de (2016). Reverse vaccinology 2.0: Human immunology instructs vaccine antigen design. The Journal of experimental medicine *213*, 469-481.

Reed, S.G., Bertholet, S., Coler, R.N., and Friede, M. (2009). New horizons in adjuvants for vaccine development. Trends in immunology *30*, 23-32.

Reed, S.G., Orr, M.T., and Fox, C.B. (2013). Key roles of adjuvants in modern vaccines. Nature medicine *19*, 1597-1608.

Reif, D.M., Motsinger-Reif, A.A., McKinney, B.A., Rock, M.T., Crowe, J.E., and Moore, J.H. (2009). Integrated analysis of genetic and proteomic data identifies biomarkers associated with adverse events following smallpox vaccination. Genes and immunity *10*, 112-119.

Reina-San-Martín, B., Cosson, A., and Minoprio, P. (2000). Lymphocyte Polyclonal Activation: A Pitfall for Vaccine Design against Infectious Agents. Parasitology Today *16*, 62-67.

Reis e Sousa, C., Stahl, P.D., and Austyn, J.M. (1993). Phagocytosis of antigens by Langerhans cells in vitro. The Journal of experimental medicine *178*, 509-519.

Rhee, E.G., Kelley, R.P., Agarwal, I., Lynch, D.M., La Porte, A., Simmons, N.L., Clark, S.L., and Barouch, D.H. (2010). TLR4 ligands augment antigen-specific CD8+ T lymphocyte responses elicited by a viral vaccine vector. Journal of virology *84*, 10413-10419.

Richardson, J.R., Armbruster, N.S., Günter, M., Henes, J., and Autenrieth, S.E. (2018). Staphylococcus aureus PSM Peptides Modulate Human Monocyte-Derived Dendritic Cells to Prime Regulatory T Cells. Frontiers in immunology *9*, 2603.

Rock, M.T., Yoder, S.M., Talbot, T.R., Edwards, K.M., and Crowe, J.E. (2004). Adverse events after smallpox immunizations are associated with alterations in systemic cytokine levels. The Journal of infectious diseases *189*, 1401-1410.

Römer, P.S., Berr, S., Avota, E., Na, S.-Y., Battaglia, M., Berge, I. ten, Einsele, H., and Hünig, T. (2011). Preculture of PBMCs at high cell density increases sensitivity of T-cell responses, revealing cytokine release by CD28 superagonist TGN1412. Blood *118*, 6772-6782.

Rowe, J.H., Johanns, T.M., Ertelt, J.M., and Way, S.S. (2008). PDL-1 blockade impedes T cell expansion and protective immunity primed by attenuated Listeria monocytogenes. Journal of immunology (Baltimore, Md. : 1950) *180*, 7553-7557.

RTS, S.C.T.P. (2015). Efficacy and safety of RTS,S/AS01 malaria vaccine with or without a booster dose in infants and children in Africa: final results of a phase 3, individually randomised, controlled trial. Lancet (London, England) *386*, 31-45.

Rueckert, C., and Guzmán, C.A. (2012). Vaccines: from empirical development to rational design. PLoS pathogens *8*, e1003001.

Ryan, A.A., Nambiar, J.K., Wozniak, T.M., Roediger, B., Shklovskaya, E., Britton, W.J., Fazekas de St Groth, B., and Triccas, J.A. (2009). Antigen load governs the differential priming of CD8 T cells in response to the bacille Calmette Guerin vaccine or Mycobacterium tuberculosis infection. Journal of immunology (Baltimore, Md. : 1950) *182*, 7172-7177.

Rydyznski, C., Daniels, K.A., Karmele, E.P., Brooks, T.R., Mahl, S.E., Moran, M.T., Li, C., Sutiwisesak, R., Welsh, R.M., and Waggoner, S.N. (2015). Generation of cellular immune memory and B-cell immunity is impaired by natural killer cells. Nature communications *6*, 6375.

Sabbaghi, A., Miri, S.M., Keshavarz, M., Zargar, M., and Ghaemi, A. (2019). Inactivation methods for whole influenza vaccine production. Reviews in medical virology *29*, e2074.

Saitoh, S.-I., Abe, F., Kanno, A., Tanimura, N., Mori Saitoh, Y., Fukui, R., Shibata, T., Sato, K., Ichinohe, T., and Hayashi, M., et al. (2017). TLR7 mediated viral recognition results in focal type I interferon secretion by dendritic cells. Nature communications *8*, 1592.

Salerno, F., Freen-van Heeren, J.J., Guislain, A., Nicolet, B.P., and Wolkers, M.C. (2019). Costimulation through TLR2 Drives Polyfunctional CD8+ T Cell Responses. Journal of immunology (Baltimore, Md. : 1950) *202*, 714-723.

Salerno, F., Guislain, A., Cansever, D., and Wolkers, M.C. (2016). TLR-Mediated Innate Production of IFN-γ by CD8+ T Cells Is Independent of Glycolysis. Journal of immunology (Baltimore, Md. : 1950) *196*, 3695-3705.

Salio, M., Speak, A.O., Shepherd, D., Polzella, P., Illarionov, P.A., Veerapen, N., Besra, G.S., Platt, F.M., and Cerundolo, V. (2007). Modulation of human natural killer T cell ligands on TLR-mediated antigen-presenting cell activation. Proceedings of the National Academy of Sciences of the United States of America *104*, 20490-20495.

Sallusto, F., Cella, M., Danieli, C., and Lanzavecchia, A. (1995). Dendritic cells use macropinocytosis and the mannose receptor to concentrate macromolecules in the major histocompatibility complex class II compartment: downregulation by cytokines and bacterial products. The Journal of experimental medicine *182*, 389-400.

Sallusto, F., and Lanzavecchia, A. (1994). Efficient presentation of soluble antigen by cultured human dendritic cells is maintained by granulocyte/macrophage colony-stimulating factor plus interleukin 4 and downregulated by tumor necrosis factor alpha. The Journal of experimental medicine *179*, 1109-1118.

Sallusto, F., Lenig, D., Förster, R., Lipp, M., and Lanzavecchia, A. (1999). Two subsets of memory T lymphocytes with distinct homing potentials and effector functions. Nature *401*, 708-712.

Sallusto, F., Schaerli, P., Loetscher, P., Schaniel, C., Lenig, D., Mackay, C.R., Qin, S., and Lanzavecchia, A. (1998). Rapid and coordinated switch in chemokine receptor expression during dendritic cell maturation. Eur. J. Immunol. *28*, 2760-2769.

Samji, T., and Khanna, K.M. (2017). Understanding memory CD8+ T cells. Immunology letters *185*, 32-39.

Sander, J., Schmidt, S.V., Cirovic, B., McGovern, N., Papantonopoulou, O., Hardt, A.-L., Aschenbrenner, A.C., Kreer, C., Quast, T., and Xu, A.M., et al. (2017). Cellular Differentiation of Human Monocytes Is Regulated by Time-Dependent Interleukin-4 Signaling and the Transcriptional Regulator NCOR2. Immunity *47*, 1051-1066.e12.

Sandle, T. (2016). Endotoxin and pyrogen testing. In Pharmaceutical Microbiology (Elsevier), pp. 131–145.

Sato-Kaneko, F., Yao, S., Lao, F.S., Shpigelman, J., Messer, K., Pu, M., Shukla, N.M., Cottam, H.B., Chan, M., and Chu, P.J., et al. (2020). A Novel Synthetic Dual Agonistic Liposomal TLR4/7 Adjuvant Promotes Broad Immune Responses in an Influenza Vaccine With Minimal Reactogenicity. Frontiers in immunology *11*, 1207.

Satoskar, A.R., Stamm, L.M., Zhang, X., Okano, M., David, J.R., Terhorst, C., and Wang, B. (1999). NK cell-deficient mice develop a Th1-like response but fail to mount an efficient antigen-specific IgG2a antibody response. Journal of immunology (Baltimore, Md. : 1950) *163*, 5298-5302.

Schindler, S., Aulock, S. von, Daneshian, M., and Hartung, T. (2009). Development, validation and applications of the monocyte activation test for pyrogens based on human whole blood. ALTEX *26*, 265-277.

Schindler, S., Spreitzer, I., Löschner, B., Hoffmann, S., Hennes, K., Halder, M., Brügger, P., Frey, E., Hartung, T., and Montag, T. (2006). International validation of pyrogen tests based on cryopreserved human primary blood cells. Journal of immunological methods *316*, 42-51.

Schoenberger, S.P., Toes, R.E., van der Voort, E.I., Offringa, R., and Melief, C.J. (1998). T-cell help for cytotoxic T lymphocytes is mediated by CD40-CD40L interactions. Nature *393*, 480-483.

Schülke, S., Flaczyk, A., Vogel, L., Gaudenzio, N., Angers, I., Löschner, B., Wolfheimer, S., Spreitzer, I., Qureshi, S., and Tsai, M., et al. (2015). MPLA shows attenuated pro-inflammatory properties and diminished capacity to activate mast cells in comparison with LPS. Allergy *70*, 1259-1268.

Schwarz, T.F., Horacek, T., Knuf, M., Damman, H.-G., Roman, F., Dramé, M., Gillard, P., and Jilg, W. (2009). Single dose vaccination with AS03-adjuvanted H5N1 vaccines in a randomized trial induces strong and broad immune responsiveness to booster vaccination in adults. Vaccine *27*, 6284-6290.

Schwickert, T.A., Victora, G.D., Fooksman, D.R., Kamphorst, A.O., Mugnier, M.R., Gitlin, A.D., Dustin, M.L., and Nussenzweig, M.C. (2011). A dynamic T cell-limited checkpoint regulates affinity-dependent B cell entry into the germinal center. The Journal of experimental medicine *208*, 1243-1252.

Segura, E., and Amigorena, S. (2013). Inflammatory dendritic cells in mice and humans. Trends in immunology *34*, 440-445.

Serre, K., Mohr, E., Toellner, K.-M., Cunningham, A.F., Bird, R., Khan, M., and MacLennan, I.C.M. (2009). Early simultaneous production of intranodal CD4 Th2 effectors and recirculating rapidly responding central-memory-like CD4 T cells. Eur. J. Immunol. *39*, 1573-1586.

Seubert, A., Monaci, E., Pizza, M., O'Hagan, D.T., and Wack, A. (2008). The adjuvants aluminum hydroxide and MF59 induce monocyte and granulocyte chemoattractants and enhance monocyte differentiation toward dendritic cells. Journal of immunology (Baltimore, Md. : 1950) *180*, 5402-5412.

Severa, M., Remoli, M.E., Giacomini, E., Annibali, V., Gafa, V., Lande, R., Tomai, M., Salvetti, M., and Coccia, E.M. (2007). Sensitization to TLR7 agonist in IFN-beta-preactivated dendritic cells. Journal of immunology (Baltimore, Md. : 1950) *178*, 6208-6216.

Shakya, A.K., Chowdhury, M.Y.E., Tao, W., and Gill, H.S. (2016). Mucosal vaccine delivery: Current state and a pediatric perspective. Journal of controlled release : official journal of the Controlled Release Society *240*, 394-413.

Sieg, S.F., Rodriguez, B., Asaad, R., Jiang, W., Bazdar, D.A., and Lederman, M.M. (2005). Peripheral S-phase T cells in HIV disease have a central memory phenotype and rarely have evidence of recent T cell receptor engagement. The Journal of infectious diseases *192*, 62-70.

Simchoni, N., and Cunningham-Rundles, C. (2015). TLR7- and TLR9-responsive human B cells share phenotypic and genetic characteristics. Journal of immunology (Baltimore, Md. : 1950) *194*, 3035-3044.

Sittig, S.P., Bakdash, G., Weiden, J., Sköld, A.E., Tel, J., Figdor, C.G., Vries, I.J.M. de, and Schreibelt, G. (2016). A Comparative Study of the T Cell Stimulatory and Polarizing Capacity of Human Primary Blood Dendritic Cell Subsets. Mediators of inflammation *2016*, 3605643.

Smith, J.G., Levin, M., Vessey, R., Chan, I.S.F., Hayward, A.R., Liu, X., Kaufhold, R.M., Clair, J., Chalikonda, I., and Chan, C., et al. (2003). Measurement of cell-mediated immunity with a Varicella-Zoster Virus-specific interferon-gamma ELISPOT assay: responses in an elderly population receiving a booster immunization. Journal of medical virology *70 Suppl 1*, S38-41.

Smith, S.G., Kleinnijenhuis, J., Netea, M.G., and Dockrell, H.M. (2017). Whole Blood Profiling of Bacillus Calmette-Guérin-Induced Trained Innate Immunity in Infants Identifies Epidermal Growth Factor, IL-6, Platelet-Derived Growth Factor-AB/BB, and Natural Killer Cell Activation. Frontiers in immunology *8*, 644.

Soema, P.C., Kompier, R., Amorij, J.-P., and Kersten, G.F.A. (2015). Current and next generation influenza vaccines: Formulation and production strategies. European journal of pharmaceutics and biopharmaceutics : official journal of Arbeitsgemeinschaft fur Pharmazeutische Verfahrenstechnik e.V *94*, 251-263.

Spisek, R., Brazova, J., Rozkova, D., Zapletalova, K., Sediva, A., and Bartunkova, J. (2004). Maturation of dendritic cells by bacterial immunomodulators. Vaccine *22*, 2761-2768.

Stanley, S.L., Frey, S.E., Taillon-Miller, P., Guo, J., Miller, R.D., Koboldt, D.C., Elashoff, M., Christensen, R., Saccone, N.L., and Belshe, R.B. (2007). The immunogenetics of smallpox vaccination. The Journal of infectious diseases *196*, 212-219.

Steinman, R.M., Pack, M., and Inaba, K. (1997). Dendritic cells in the T-cell areas of lymphoid organs. Immunological reviews *156*, 25-37.

Stinchcombe, J.C., Majorovits, E., Bossi, G., Fuller, S., and Griffiths, G.M. (2006). Centrosome polarization delivers secretory granules to the immunological synapse. Nature *443*, 462-465.

Stratton, K., Ford, A., Rusch, E. and Clayton, E.W. (2011). Adverse Effects of Vaccines: Evidence and Causality (Washington (DC)).

Strobel, L., and Johswich, K.O. (2018). Anticoagulants impact on innate immune responses and bacterial survival in whole blood models of Neisseria meningitidis infection. Scientific reports *8*, 10225.

Stuber, E., Strober, W., and Neurath, M. (1996). Blocking the CD40L-CD40 interaction in vivo specifically prevents the priming of T helper 1 cells through the inhibition of interleukin 12 secretion. The Journal of experimental medicine *183*, 693-698.

Sun, H., Pollock, K.G.J., and Brewer, J.M. (2003). Analysis of the role of vaccine adjuvants in modulating dendritic cell activation and antigen presentation in vitro. Vaccine *21*, 849-855.

Supersaxo, A., Hein, W.R., and Steffen, H. (1990). Effect of molecular weight on the lymphatic absorption of water-soluble compounds following subcutaneous administration. Pharmaceutical research *7*, 167-169.

Swiecki, M., and Colonna, M. (2015). The multifaceted biology of plasmacytoid dendritic cells. Nature reviews. Immunology *15*, 471-485.

Takayama, K., Ribi, E., and Cantrell, J.L. (1981). Isolation of a nontoxic lipid A fraction containing tumor regression activity. Cancer research *41*, 2654-2657.

Takeda, K., Takeuchi, O., and Akira, S. (2002). Recognition of lipopeptides by Toll-like receptors. Journal of endotoxin research *8*, 459-463.

Takeuchi, O., and Akira, S. (2010). Pattern recognition receptors and inflammation. Cell *140*, 805-820.

Tapia-Calle, G., Born, P.A., Koutsoumpli, G., Gonzalez-Rodriguez, M.I., Hinrichs, W.L.J., and Huckriede, A.L.W. (2019). A PBMC-Based System to Assess Human T Cell Responses to Influenza Vaccine Candidates In Vitro. Vaccines *7*.

Tapia-Calle, G., Stoel, M., Vries-Idema, J. de, and Huckriede, A. (2017). Distinctive Responses in an In Vitro Human Dendritic Cell-Based System upon Stimulation with Different Influenza Vaccine Formulations. Vaccines *5*.

Teunissen, M.B.M., and Zehrung, D. (2015). Cutaneous vaccination - Protective immunization is just a skin-deep step away. Vaccine *33*, 4659-4662.

Thomas, C., and Moridani, M. (2010). Interindividual variations in the efficacy and toxicity of vaccines. Toxicology *278*, 204-210.

Tivol, E.A., Borriello, F., Schweitzer, A.N., Lynch, W.P., Bluestone, J.A., and Sharpe, A.H. (1995). Loss of CTLA-4 leads to massive lymphoproliferation and fatal multiorgan tissue destruction, revealing a critical negative regulatory role of CTLA-4. Immunity *3*, 541-547.

Trombetta, E.S., and Mellman, I. (2005). Cell biology of antigen processing in vitro and in vivo. Annual review of immunology *23*, 975-1028.

Vadalà, M., Poddighe, D., Laurino, C., and Palmieri, B. (2017). Vaccination and autoimmune diseases: is prevention of adverse health effects on the horizon? The EPMA journal *8*, 295-311.

van de Sandt, C.E., Hillaire, M.L.B., Geelhoed-Mieras, M.M., Osterhaus, A.D.M.E., Fouchier, R.A.M., and Rimmelzwaan, G.F. (2015). Human Influenza A Virus-Specific CD8+ T-Cell Response Is Long-lived. The Journal of infectious diseases *212*, 81-85.

van Dissel, J.T., Joosten, S.A., Hoff, S.T., Soonawala, D., Prins, C., Hokey, D.A., O'Dee, D.M., Graves, A., Thierry-Carstensen, B., and Andreasen, L.V., et al. (2014). A novel liposomal adjuvant system, CAF01, promotes long-lived Mycobacterium tuberculosis-specific T-cell responses in human. Vaccine *32*, 7098-7107.

van Haren, S.D., Ganapathi, L., Bergelson, I., Dowling, D.J., Banks, M., Samuels, R.C., Reed, S.G., Marshall, J.D., and Levy, O. (2016). In vitro cytokine induction by TLR-activating vaccine adjuvants in human blood varies by age and adjuvant. Cytokine *83*, 99-109.

Vandebriel, R., and Hoefnagel, M.M.N. (2012). Dendritic cell-based in vitro assays for vaccine immunogenicity. Human vaccines & immunotherapeutics *8*, 1323-1325.

Vasilakos, J.P., Smith, R.M., Gibson, S.J., Lindh, J.M., Pederson, L.K., Reiter, M.J., Smith, M.H., and Tomai, M.A. (2000). Adjuvant activities of immune response modifier R-848: comparison with CpG ODN. Cellular Immunology *204*, 64-74.

Vermes, I., Haanen, C., Steffens-Nakken, H., and Reutellingsperger, C. (1995). A novel assay for apoptosis Flow cytometric detection of phosphatidylserine expression on early apoptotic cells using fluorescein labelled Annexin V. Journal of immunological methods *184*, 39-51.

Vetter, V., Denizer, G., Friedland, L.R., Krishnan, J., and Shapiro, M. (2018). Understanding modern-day vaccines: what you need to know. Annals of medicine *50*, 110-120.

Villadangos, J.A., and Young, L. (2008). Antigen-presentation properties of plasmacytoid dendritic cells. Immunity *29*, 352-361.

Vogelzang, A., McGuire, H.M., Di Yu, Sprent, J., Mackay, C.R., and King, C. (2008). A fundamental role for interleukin-21 in the generation of T follicular helper cells. Immunity *29*, 127-137.

Vono, M., Taccone, M., Caccin, P., Gallotta, M., Donvito, G., Falzoni, S., Palmieri, E., Pallaoro, M., Rappuoli, R., and Di Virgilio, F., et al. (2013). The adjuvant MF59 induces ATP release from muscle that potentiates response to vaccination. Proceedings of the National Academy of Sciences of the United States of America *110*, 21095-21100.

Wagner, T.L., Ahonen, C.L., Couture, A.M., Gibson, S.J., Miller, R.L., Smith, R.M., Reiter, M.J., Vasilakos, J.P., and Tomai, M.A. (1999). Modulation of TH1 and TH2 cytokine production with the immune response modifiers, R-848 and imiquimod. Cellular Immunology *191*, 10-19.

Walsh, K.P., and Mills, K.H.G. (2013). Dendritic cells and other innate determinants of T helper cell polarisation. Trends in immunology *34*, 521-530.

Wang, B., Wang, X., Wen, Y., Fu, J., Wang, H., Ma, Z., Shi, Y., and Wang, B. (2015). Suppression of established hepatocarcinoma in adjuvant only immunotherapy: alum triggers anti-tumor CD8+ T cell response. Scientific reports *5*, 17695.

Weeks, C.E., and Gibson, S.J. (1994). Induction of interferon and other cytokines by imiquimod and its hydroxylated metabolite R-842 in human blood cells in vitro. Journal of interferon research *14*, 81-85.

Wei, M.L., and Cresswell, P. (1992). HLA-A2 molecules in an antigen-processing mutant cell contain signal sequence-derived peptides. Nature *356*, 443-446.

Weinberger, B., and Grubeck-Loebenstein, B. (2012). Vaccines for the elderly. Clinical microbiology and infection : the official publication of the European Society of Clinical Microbiology and Infectious Diseases *18 Suppl 5*, 100-108.

Welsby, I., Detienne, S., N'Kuli, F., Thomas, S., Wouters, S., Bechtold, V., Wit, D. de, Gineste, R., Reinheckel, T., and Elouahabi, A., et al. (2016). Lysosome-Dependent Activation of Human Dendritic Cells by the Vaccine Adjuvant QS-21. Frontiers in immunology *7*, 663.

Welters, M.J.P., Bijker, M.S., van den Eeden, S.J.F., Franken, K.L.M.C., Melief, C.J.M., Offringa, R., and van der Burg, S.H. (2007). Multiple CD4 and CD8 T-cell activation parameters predict vaccine efficacy in vivo mediated by individual DC-activating agonists. Vaccine *25*, 1379-1389.

Werninghaus, K., Babiak, A., Gross, O., Hölscher, C., Dietrich, H., Agger, E.M., Mages, J., Mocsai, A., Schoenen, H., and Finger, K., et al. (2009). Adjuvanticity of a synthetic cord factor analogue for subunit Mycobacterium tuberculosis vaccination requires FcRgamma-Syk-Card9-dependent innate immune activation. The Journal of experimental medicine *206*, 89-97.

Wherry, E.J., Blattman, J.N., Murali-Krishna, K., van der Most, R., and Ahmed, R. (2003). Viral persistence alters CD8 T-cell immunodominance and tissue distribution and results in distinct stages of functional impairment. Journal of virology *77*, 4911-4927.

Wherry, E.J., and Kurachi, M. (2015). Molecular and cellular insights into T cell exhaustion. Nature reviews. Immunology *15*, 486-499.

White, M.T., Bejon, P., Olotu, A., Griffin, J.T., Bojang, K., Lusingu, J., Salim, N., Abdulla, S., Otsyula, N., and Agnandji, S.T., et al. (2014). A combined analysis of immunogenicity, antibody kinetics and vaccine efficacy from phase 2 trials of the RTS,S malaria vaccine. BMC medicine *12*, 117.

Whitney, J.B., and Ruprecht, R.M. (2004). Live attenuated HIV vaccines: pitfalls and prospects. Current opinion in infectious diseases *17*, 17-26.

Williams, S.A., Murthy, A.C., DeLisle, R.K., Hyde, C., Malarstig, A., Ostroff, R., Weiss, S.J., Segal, M.R., and Ganz, P. (2018). Improving Assessment of Drug Safety Through Proteomics: Early Detection and Mechanistic Characterization of the Unforeseen Harmful Effects of Torcetrapib. Circulation *137*, 999-1010.

Yang, A.X., Chong, N., Jiang, Y., Catalano, J., Puri, R.K., and Khleif, S.N. (2014). Molecular characterization of antigen-peptide pulsed dendritic cells: immature dendritic cells develop a distinct molecular profile when pulsed with antigen peptide. PloS one *9*, e86306.

Yi, J.S., Cox, M.A., and Zajac, A.J. (2010). T-cell exhaustion: characteristics, causes and conversion. Immunology *129*, 474-481.

Youngblood, B., Hale, J.S., and Ahmed, R. (2013). T-cell memory differentiation: insights from transcriptional signatures and epigenetics. Immunology *139*, 277-284.

Zahm, C.D., Colluru, V.T., McIlwain, S.J., Ong, I.M., and McNeel, D.G. (2018). TLR Stimulation during T-cell Activation Lowers PD-1 Expression on CD8+ T Cells. Cancer immunology research *6*, 1364-1374.

Zaitseva, M., Romantseva, T., Blinova, K., Beren, J., Sirota, L., Drane, D., and Golding, H. (2012). Use of human MonoMac6 cells for development of in vitro assay predictive of adjuvant safety in vivo. Vaccine *30*, 4859-4865.

Zehrung, D., Jarrahian, C., and Wales, A. (2013). Intradermal delivery for vaccine dose sparing: overview of current issues. Vaccine *31*, 3392-3395.

Zhang, J.-G., Czabotar, P.E., Policheni, A.N., Caminschi, I., Wan, S.S., Kitsoulis, S., Tullett, K.M., Robin, A.Y., Brammananth, R., and van Delft, M.F., et al. (2012). The dendritic cell receptor Clec9A binds damaged cells via exposed actin filaments. Immunity *36*, 646-657.

Zhang, L., Wang, W., and Wang, S. (2015). Effect of vaccine administration modality on immunogenicity and efficacy. Expert review of vaccines *14*, 1509-1523.

Zhang, Z., Ohto, U., Shibata, T., Taoka, M., Yamauchi, Y., Sato, R., Shukla, N.M., David, S.A., Isobe, T., and Miyake, K., et al. (2018). Structural Analyses of Toll-like Receptor 7 Reveal Detailed RNA Sequence Specificity and Recognition Mechanism of Agonistic Ligands. Cell reports *25*, 3371-3381.e5.

Zom, G.G., Khan, S., Britten, C.M., Sommandas, V., Camps, M.G.M., Loof, N.M., Budden, C.F., Meeuwenoord, N.J., Filippov, D.V., and van der Marel, G.A., et al. (2014). Efficient induction of antitumor immunity by synthetic toll-like receptor ligand-peptide conjugates. Cancer immunology research *2*, 756-764.

Zou, B.-B., Wang, F., Li, L., Cheng, F.-W., Jin, R., Luo, X., Zhu, L.-X., Geng, X., and Zhang, S.-Q. (2015). Activation of Toll-like receptor 7 inhibits the proliferation and migration, and induces the apoptosis of pancreatic cancer cells. Molecular medicine reports *12*, 6079-6085.

Acknowledgements

Declaration of Authorship

I hereby certify that I have written the present dissertation with the title

In-depth immunological analysis of prototypic adjuvants for vaccine formulations

independently, using no other aids then those I have cited. I have clearly mentioned the source of the passages that are taken word for word or paraphrased from other works.

The presented thesis has not been submitted in this or any other form to another faculty or examination institution.

Eidesstattliche Versicherung

Hiermit versichere ich, dass ich die vorgelegte Dissertation mit dem Titel

In-depth immunological analysis of prototypic adjuvants for vaccine formulations

Selbstständig verfasst habe und keine anderen als die angegeben Quellen und Hilfsmittel verwendet habe. Die Stellen der Dissertation, die anderen Werken oder Veröffentlichungen dem Wortlaut oder dem Sinn nach entnommen wurden, sind durch Quellenangaben gekennzeichnet.

Diese Dissertation wurde in der jetzigen oder in ähnlicher Form noch an keiner anderen Hochschule eingereicht und hat noch keinen sonstigen Prüfungszwecken gedient.

Darmstadt, 30.07.2020

Laura Roßmann

Curriculum Vitae